Selective delivery of arsenic trioxide to HPV positive cervical cancer cells with targeted liposomes

A thesis submitted to Middlesex University in partial fulfilment of the requirements for the degree of Doctor of Philosophy

Anam Akhtar

M00505770

B.Tech Biotechnology, Adv. P.G. diploma Nanotechnology,
MSc Bionanotechnology

School of Science & Technology, Department of Natural Science,
Middlesex University, The Burroughs, Hendon, London. NW4 4BT. UK

September 2018

This thesis is dedicated to my Mother

With deepest thanks and love for all her invaluable support

Selective delivery of arsenic trioxide to HPV positive cervical cancer cells with targeted liposomes

Anam Akhtar

Abstract

Infection with high risk human papilloma viruses (HPVs) is directly associated with the occurrence and development of cervical cancer, however, currently there is no specific anti-HPV drug available for cancer treatment. Arsenic trioxide (ATO) has been shown to induce apoptosis in HPV-infected cervical cancer cells *in vitro* but its wider clinical applications have been compromised by its toxicity and poor pharmacokinetics. This research explores an optimized drug delivery system for ATO using liposomal nanotechnology with the aim of enhancing its potential as a cervical cancer treatment. The size and surface charge of liposomes were optimised and 100nm neutral liposomes demonstrated maximum stability, least intrinsic toxicity and highest loading efficiency among all the tested formulations. Furthermore, both free and chosen liposomal-ATO were exposed to two cervical cancer cell lines (HeLa and HT-3, with and without HPV) and control cells. Liposomal-ATO was most effective in inducing toxic response in HPV+ ve HeLa cells, followed by HT-3 and control cells. These cells were then screened for different surface markers in order to identify the best ligand for selectively targeting HPV positive cells. Folate receptor (FR) was found as the most abundantly expressed receptor on HeLa cells, therefore, folic acid (FA) was chosen as the targeting ligand. FA-liposomal-ATO were synthesised by linking liposomal-ATO to FA using 5000kDa PEG spacer, which was shown to be most efficient and specific in enhancing the cellular uptake of ATO in FR positive cells. Finally, FA-liposomal-ATO were examined for their effectiveness in reducing HPV oncogenes and the possible mechanisms. Results showed that FA-liposomal-ATO induced higher cell death in HPV cells than free ATO per unit arsenic and also demonstrated higher selectivity and efficiency in inducing cell apoptosis, downregulating oncogenes and upregulating the tumour suppressors in HPV positive cells. These findings provide a promising therapeutic strategy in managing HPV-associated cancers.

Acknowledgements

Alhamdulillahi rabbil alamin. All praises due to Allah, the most gracious, the most merciful.

Firstly, I would like to express my most sincere gratitude to my supervisor Dr. Xuesong Wen for her continuous support of my PhD study, for her never-ending patience, motivation, and immense knowledge. Song gave me the freedom to do whatever I wanted, at the same time continuing to contribute valuable feedback, advice, and encouragement. Her guidance helped me throughout the time of research and writing of this thesis, her selfless time and care was sometimes all that kept me going. I simply could not have imagined having a better advisor and mentor for my PhD study. I thank her a lot.

I would also like to express my heart-felt gratitude to Dr. Celia Bell, who has long been an inspiring figure for me. Being the outstanding educator that she is, without her constant support, boundless enthusiasm and encouragement, this thesis would not have been possible. I am deeply thankful to Dr. Lucy Ghali, not only for her insightful comments, but also for the hard questions which motivated me to widen my research from various perspectives.

I am deeply indebted to my adviser Dr. Scarlet Wang for her fundamental role in my doctoral work. Scarlet provided me with every bit of guidance, assistance, and expertise that I needed during my first year and before she left to welcome her little baby in this world, she equipped me with the knowledge and confidence to venture into research on my own and branch out into new research areas. My supervisory team was the best anyone could have wished for and I am very grateful to them.

I would like to thank the Natural Science faculty at Middlesex University. I am particularly thankful to Nick Kassouf, without whose precious support, this research could not have been possible. I would also like to extend my sincere thanks to Manika

Chowdhary, Leonardo Pantoja Munoz and Alejandra Gonzales for their unwavering help. I thank my fellow lab mates for the stimulating discussions and fun we have had in the last four years while sharing the highs and lows that come with PhD life.

Finally, I would like to thank my family: my mother Rizwana Jamshed, father Jamshed Akhtar and brother Dr. Feroz Akhtar for always being my pillar of support and encouragement all my life. They have always given me reasons never to give up even when the going gets tougher. My biggest appreciation is for my husband, Saif Alam, it's been a long and tough journey, and he has never wavered from his support and motivation and has made me a stronger woman. Last but never the least; to my little angel Alzia, the research journey can never be complete without the mention of her name. I thank her for being the best baby and letting mum get her work done when she had to.

Table of Contents

List of Figures

List of Abbreviations

Acronym/ Symbol	Definition
%	percentage
$\Delta\psi_m$	membrane potential
µg	microgram
µl	microliter
µM	micromolar
µm	Micrometre
η	Dynamic viscosity
2D	Two dimensional
3D	Three dimensional
A549	Human lung epithelial cancer cell line
ABC	Avidin - biotin complex method
Abraxane	Paclitaxel albumin bound nanoparticles
AIDS	Acquired immunodeficiency syndrome
AIF	Apoptosis inducing factor
AP 1	Activating protein 1
Apaf-1	Apoptosis protease activating factor-1
APL	Acute promyelocytic leukemia
ARF	ADP ribosylation factor; tumour suppressor protein

As	Arsenic
$As(OH)_3$	Arsenic hydroxide
ATO	Arsenic Trioxide
ATRA	All-*trans* retinoic acid
Bak	Bcl2 homologous antagonist killer
BSA	Bovine serum albumin
C	Centigrade
C33-A	Human cervical epithelial cells (HPV negative)
C-terminal	Amino acid chain terminating by a free carboxyl group (-COOH)
CaSki	Human cervical epithelial cells
CBP	CREB binding protein
CCD	Charged coupled devices
Chol	Cholesterol
CIN	Cervical intraepithelial neoplasia
CLSM	Confocal laser scanning microscopy
cm	centimetre
CML	Chronic myelogenous leukemia
Co	Cobalt
CRL-1790	Normal human colon epithelial cells
CV	Coefficient of variation

cys	cysteine
D	Translational self-diffusion coefficient
Da	Dalton
DAB	3'-Diaminobenzidine
DAPI	4′,6-diamidino-2-phenylindole
DaunoXome	Liposomal daunorubicin
DDAB	Didodecyldimethylammonium bromide
DepoCyt	Liposomal cytarabine
DiIC18(3)-DS	1,1'-Dioctadecyl-3,3,3',3'-Tetramethylindocarbocyanine-5,5'-Disulfonic Acid
DLS	Dynamic Light Scattering
DMEM	Dulbecco's Modified Eagle's medium
DMSO	Dimethyl sulfoxide
DNA	Deoxy ribonucleic acid
DSPE-PEG2000	Methoxypolyethyleneglycol-distearoyl-phosphatidylethanolamine with mPEG MW2000Da
DSPE-PEG2000-Folate	1,2-distearoyl-sn-glycero-3-phosphoethanolamine-N-folate(polyethylene glycol)-2000 with mPEG MW2000Da
DSPE-PEG5000-Folate	1,2-distearoyl-sn-glycero-3-phosphoethanolamine-N-folate(polyethylene glycol)-5000 with mPEG MW5000Da
DSPG	1,2-distearoyl-*sn*-glycero-3-phospho-(1'-*rac*-glycerol) (sodium salt)
ECL	Enhanced chemiluminescence

EDTA	Ethylenediaminetetraacetic acid
EGFR	Epidermal growth factor receptor
EPR	Enhanced Permeability and Retention effect
FA	Folic acid
FACS	Fluorescence activated cell sorting
FADD	Fas associated protein with death domain
FBS	Fetal Bovine Serum
FCS	Fetal Calf Serum
FDA	Food and Drug Administration
FITC	Fluorescein isothiocyanate
FR	Folate receptor
FSC	Forward scatter signal
Ga	Gallium
gm	gram
h	Hour(s)
H_2O	water
H_2O_2	Hydrogen peroxide
HB-EGF	Heparin binding EGF
HCE-16/3 cells	Human corneal endothelial cells
HeLa	Human cervical epithelial cells of adenocarcinoma
HK	Primary human epidermal keratinocytes

HPV	Human Papilloma Virus
HRP	Horse-radish peroxidase
HT-3	Human cervical cancer cell line (HPV negative)
hTERT	Human telomerase reverse transcriptase
IARC	International Agency for Research on Cancer
IC50	Half maximal inhibitory concentration of a substance
ICC	Immunocytochemistry
ICP-MS	Inductively coupled plasma-mass spectrometer
ICP-OES	Inductively coupled plasma-optical emission spectrometer
IgG	Immunoglobulin G
IV	intravenous
JNK phosphatase	c-Jun N-terminal kinase phosphatase
k	Boltzmann's constant
K	Kelvin
KB	Human nasopharyngeal cell line contaminated with HeLa cells
kDa	kilodalton
LEEP	Loop electrosurgical excision procedure
Lipo	Liposome
LLETZ	Large loop excision of the transformation zone
mAb	Monoclonal antibody
ME-180	Human cervical epithelial cells (HPV-18 positive)

min	Minute(s)
mm	Millimetre
mM	Millimolar
mol	Molarity
MPP2	Palmitoylated membrane protein 2
MPS	Mononuclear phagocytic system
mRNA	Messenger RNA
MTD	Maximal tolerated dose
MTT	3-(4, 5-dimethylthiazolyl-2)-2, 5-diphenyltetrazolium bromide
mV	millivolt
MW	Molecular weight
NADH	Nicotinamide adenine dinucleotide
NADPH	Nicotinamide adenine dinucleotide phosphate
NaH_2PO_4	Sodium dihydrogen phosphate
Na_2HPO_4	Disodium Hydrogen Phosphate
NC	Nitrocellulose
NF 1	Nuclear factor 1
Ni	Nickle
$Ni(OAc)_2$	Nickle acetate
nm	nanometre
NuMa	Nuclear mitotic apparatus protein

$O_2.^-$	Superoxide
$OH^·$	Hydroxyl
P	Phospholipids
p21	Potent cyclin-dependent kinase inhibitor 1
p27	Cyclin-dependent kinase inhibitor 1B
p53	Tumour suppressor protein p53
pAb	Polyclonal antibody
PAG	Polyacrylamide gel
PAGE	Polyacrylamide gel electrophoresis
PAE	Early polyadenylation site
PAL	Late polyadenylation site
Pap test	Papanicolaou test
PBS	Phosphate buffered saline
PBS-T	Phosphate buffered saline with Tween-20
PC	Phosphatidyl choline
PCS	Photon correlation spectroscopy
PDGF	Platelet derived growth factor
PDZ	Structural domain named after PSD95, DlgA and Zo-1 proteins
PE	Phosphatidyl ethanolamine
PEG	Polyethylene glycol
PHPMA	Poly(N-(2-hydroxypropyl)methacrylamide)

PI	Propidium iodide
PML-RARα	Promyelocytic leukemia-retinoic acid receptor α
PMT	Photomultiplier tube
ppt	Parts per trillion
pRb	Retinoblastoma tumour suppressor protein
PS	Phosphatidylserine
Pt	Platinum
PTPC	Permeability transition pore complex
PVDF	Polyvinylidene difluoride
r	Radius
RES	Reticuloendothelial system
RF	Radiofrequency
RIPA buffer	Radioimmunoprecipitation assay buffer
ROS	Reactive oxygen species
rpm	Revolutions per minute
SD	Standard deviation
SDS	Sodium dodecyl substrate
SiHa	Human cervical epithelial cells
SOP	Standard operating procedure
SSC	Side scatter signal
STD	Sexually transmitted disease

T	Absolute temperature
TBP	TATA binding protein
TBS-T	Tris buffered saline-Tween 20
TEMED	Tetramethylenediamine
Tf	Transferrin
TfR	Transferrin receptor
TGF-α	Transforming growth factor-α
TNF-α	Tumour necrosis factor α
TSA	Tyramide signal amplification
Tyk 2	Tyrosine kinase 2
UK	United Kingdom
URR	Upstream regulatory region
USA	United States of America
VDAC	Voltage dependent anion channel
VEGF	Vascular endothelial growth factor
VLP	Virus like particles
v/v	Volume by volume
w/v	Weight/volume

Chapter 1

INTRODUCTION AND BACKGROUND

1.1 INTRODUCTION

Cervical cancer is responsible for 14% of all gynaecological related cancers in women (Lorusso et al., 2014). Although it is a theoretically preventable disease with effective screening programs in place for an early identification at its pre-cancerous stage, once the cancer progresses to metastatic or recurrent stage, the prognosis is appalling with one year survival rate between 15 and 20 percent and mortality rate reaches as high as 50 percent (Lorusso et al., 2014). Moreover the lack of efficient screening programs or affordable treatment options in developing countries has resulted in cervical cancer being the most prevalent disease among women worldwide and with highest morbidity (Appleby et al., 2007). Cervical cancer is caused by an infection with HPV, its high risk types HPV-16 and HPV-18 accounting for 70% of all cervical cancers. Viral oncogenes E6 and E7 have been established to be the main contributors to the HPV induced cervical cancer as their protein products deregulate cell cycle machinery resulting in uncontrolled proliferation (Schiffman et al., 2007).

During the early stages of invasive cancer, the most common treatment is surgery with chemoradiotherapy. This combination treatment of pelvic irradiation accompanied with weekly dose of cisplatin has the potential to treat 80-90% of women, albeit with some serious side effects (Ordikhani et al., 2016). Along with the debilitating effects of radiation, patients taking cisplatin suffers from the usual limitations of chemotherapeutic drugs including development of tumour resistance, bone marrow depression and haematological toxicity which leads to neutropenia, thrombocytopenia, neurotoxicity, nephrotoxicity and anaemia (Ordikhani et al., 2016). This necessitates the

need to explore the efficacy of other drugs to treat cervical cancer and a means of increasing their therapeutic index *in vivo* by delivering the drug specifically to the target cells sparing normal cells.

As HPV has been established as the causal agent of cervical cancer, our main aim was to specifically explore an anti-HPV agent (Schiffman et al., 2007). Among the drugs, it has been reported that ATO downregulates HPV E6 oncoprotein and reduces survival of HPV-18 HeLa cells (Wen et al, 2012). ATO is a broad spectrum anti-cancer drug with its therapeutic applications dating back to more than 2400 years when it was used in traditional Chinese medicine (Evens, Tallman and Gartenhaus, 2004). Discovery of its anti-leukemic properties is fairly recent which was initiated by a group of Chinese physicians from Harbin Medical University and Shanghai Second Medical University. Through careful clinical trials, they tested its effectiveness on patients of acute promyelocytic leukemia (APL). The highly positive results, duplicated with the success in United States, led to the approval of ATO by Food and Drug Administration (FDA) as the front line therapy for APL in 2000 (Antman, 2001). Similar clinical successes were subsequently translated for other haematological malignancies. However, when its efficacy was tested for solid tumours, ATO did not exhibit appreciable clinical success on human patients. Rapid clearance of arsenic and its products from the blood by reticuloendothelial system limits the therapeutic dose reaching the tumour site (Swindell et al., 2013). Escalating arsenic dosage could not be an alternative as it led to systemic toxicities such as long term memory damage, liver failure, cardiac failure and peripheral neuropathy (Swindell et al., 2013). Hence, to utilise its considerable anti-cancer properties for solid tumours, specifically cervical cancer, it was crucial to increase the drug's therapeutic index while sparing the surrounding healthy tissues from arsenic toxicity. Such an alluring goal seemed possible with the application of nanotechnology in the field of drug delivery.

Nanotechnology based drug delivery systems can specifically target cancer cells while avoiding direct contact with their healthy neighbours. In addition, they can prevent rapid clearance of the drug from the body and hence considerably increase the drug's therapeutic index (Bosch et al., 2002; Ordikhani et al., 2016). Among the many nanocarriers discovered till date, the oldest and most commonly employed nanoparticles are liposomes. Liposomes are spherical vesicles of phospholipid bilayer with an

aqueous core; the core can encapsulate water soluble drugs and the bilayer has the potential to entrap lipid soluble drugs (Narisawa-Saito et al., 2007). Achieved with the capacity to passively target tumour tissue and ease of surface modification where ligands can be attached complimentary to cancer cell specific receptors on their surface, liposomes can prove to be the ideal candidates to entrap anti-cancer drugs and target tumour tissue (Doorbar, 2005).

In this study, I have applied nanoparticulate formation process to encapsulate ATO in robust, pH responsive, targeted liposomes to deliver ATO specifically to HPV infected cervical cancer cells *in vitro*. The specificity and efficacy of the formulated nano-carrier on target cells have been examined and compared with the free drug. Additionally, by elucidating the molecular mechanism involved behind the action of ATO delivered via these different routes, the best delivery method has been selected for ATO to target HPV positive cervical cancer cells *in vitro*.

1.2 LITERATURE REVIEW

1.2.1 **Cervical Cancer**

1.2.1.1 Epidemiology

Cervical cancer is the second most common cancer among women worldwide (Bosch et al., 2002). It was responsible for half a million reported incidence cases and 266,000 consequent deaths worldwide in 2012 (Ferlay et al., 2015). Although this cancer can potentially be prevented by efficient routine screening programs and treatment of pre-cancerous lesions, it is still the most prevalent female cancer in developing countries, where 80% of the cases occur (International Collaboration of Epidemiological Studies of Cervical Cancer, 2006). The principle cause of this high mortality is attributed to the lack of screening and available treatment options in low-resource countries along with extremely low survival rates of women diagnosed with advanced cancer (Ordikhani et al., 2016).

During the 1990's, it was established with undisputed epidemiological studies, augmented by molecular technology, that cervical cancer is caused by an infection of certain mucosatropic strains of HPV (Bosch et al., 2002; Walboomers et al., 1999). This association was assessed under all sets of causality criteria and the presence of universally consistent results eliminated alternative hypothesis for aetiology of cervical cancer (Bosch et al., 2002; Walboomers et al., 1999). This proved to be a major discovery as HPV was proposed to be the first ever described "essential cause" of human cancer and its association as significant as that between Hepatitis B or C virus infection with the risk of liver cancer or cigarette smoking with lung cancer development (Bosch et al., 2002). Clinical and epidemiological investigations imply cervical cancer to exhibit the profile of a sexually transmitted disease (STD) where the cancer develops several years after HPV infection (Bosch et al., 2002).

Owing to its principle role in virtually all cases of cervical cancer, HPV is now essentially regarded as its necessary though insufficient cause (Schiffman et al., 2011). Over the decades, many factors were attributed to the aetiology of cervical cancer including infectious agents for STD such as syphilis, gonorrhoea and type-2 herpes simplex virus (Bosch et al., 2002). The establishment of HPV as the necessary cause of cervical cancer eliminated their possibility of being causal agents along with certain previously ill-defined behavioural and demographic factors including low socio-economic status of women, smoking, multi-parity and use of oral contraceptives, which are now recognised as pertinent co-factors that may be relevant only in the presence of HPV DNA (Bosch et al., 2002; International Collaboration of Epidemiological Studies of Cervical Cancer, 2006; Smith et al., 2003).

1.2.1.2 Human papilloma virus

HPV primarily infects epithelial cells and can be responsible for a variety of epithelial lesions including common warts, genital condyloma, verrucas and laryngeal papillomas (Doorbar, 2007). The HPV family includes more than 100 HPV types and 40 of them can infect the cervix (Doorbar, 2007). Most of them belong to alpha and beta genus with the two groups having noticeably different biology and life cycle patterns (Bosch et al. 2002; Doorbar, 2007). Of them, the alpha PVs infect humans and primates and are divided into cutaneous and mucosal types (Doorbar et al., 2012). These mucosal types are further subdivided into high risk and low risk types according to their presence in the malignant lesions of cervix, with the high risk types linked to almost 95% of cervical cancer cases (Bosch et al. 2002; Doorbar, 2007; Munoz et al., 2003; Narisawa-Saito and Kiyono, 2007). HPV-16 and HPV-18 account for 50% and 20% respectively of the viral types involved in invasive cancer (Doorbar, 2007). In addition to these, International Agency for Research on Cancer has classified HPV type- 31, 33, 35, 39, 45, 51, 52, 56, 58 and 59 as human carcinogens (Bosch et al. 2002; Munoz et al., 2003). Fundamentally, all HPV types produce warty lesions but for them to progress into invasive cancer, infection with high risk HPV type is essential (Bosch et al. 2002). Substantial evidence suggests the involvement of HPV in considerable other cancers of

genital tract (such as penis, anal canal, vulva, vagina and perianal skin) and cancers of skin and oropharyngeal tract (Bosch et al. 2002). Continuous presence and expression of high-risk HPV is found to be essential for development, maintenance and progression of invasive cervical cancer (Bosch et al. 2002).

1.2.1.3 Fundamentals of HPV virology

HPV has a single stranded, circular DNA of 8000 base pairs encoding 8 genes E1, E2, E4-E7, L1 and L2 (Fig 1.2.1) (Schiffman et al., 2007). The E and L designation is according to their expression during the early or late stage of epithelium differentiation (Schiffman et al., 2007). L1and L2 proteins assemble to form icosahedral viral capsid whereas the early proteins are responsible for viral DNA replication and virus assembly (Doorbar, 2007; Munoz et al., 2006; Schiffman et al., 2007). There is an upstream regulatory region (URR) of around 1000bp separating both the gene sets which has binding sites for transcriptional activators and repressors, such as activating protein 1 (AP 1) and nuclear factor 1 (NF 1), necessary for gene expression, replication and packaging into virus particles (Munoz et al., 2006; Soliman, Slomovitz and Wolf, 2004).

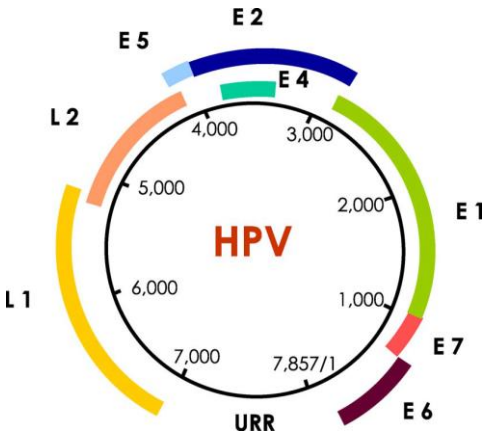

Fig 1.2.1: Schematic representation of HPV genome, displaying the arrangement of early and late (E and L) genes along with upstream regulatory region (Munoz et al., 2006).

The life cycle of HPV is perfectly adapted to its host cell biology (Narisawa-Saito and Kiyono, 2007). The basal layer of normal squamous epithelium divides like stem cells, where one of the daughter cells migrates upward and starts to undergo terminal differentiation (Narisawa-Saito and Kiyono, 2007). The other daughter stays in the basal layer and gives rise to a slow-cycling population (Narisawa-Saito and Kiyono, 2007). HPV virus establishes its infection at the basal layer of epithelium where it enters into the cells through micro-wounds (Munoz et al., 2006). Infecting an epithelial stem cell is hypothesised to be crucial for maintaining the infection (Doorbar, 2005). During the initial phase of HPV cell cycle, genome is maintained by expression of early proteins E1 and E2, in low episomal copy numbers, i.e. 25-50 genome copies per cell (Bosch et al. 2002; Munoz et al., 2006; Schiffman et al., 2007). As the basal epithelium differentiates and is propelled to the suprabasal compartment, there is a shift in the viral genome expression from early to late genes with viral life cycle subsequently going through successive stages of amplification, virus assembly and release (Schiffman et al., 2007). The release of viral progenies into the environment re-initiating the infection makes use of the natural disintegration of epithelial cells at the superficial layers (Fig 1.2.2) (Munoz et al., 2006).

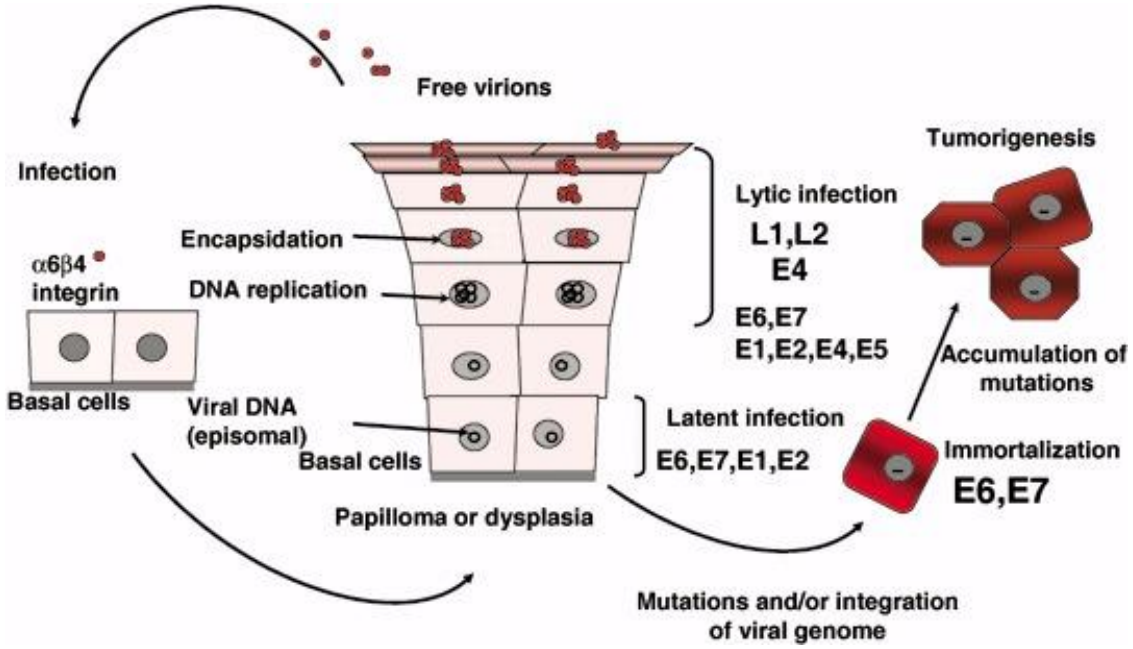

Fig 1.2.2: Infection of HPV virus and the role of the encoded genes in carcinogenesis. Initially, HPV infects basal cells of the tissue where replication of viral DNA takes place without the formation of virions. In the upper layer when the cells differentiate, capsid proteins formation co-ordinates with the viral genome replication leading to formation of virus particles that are released to infect new host cells (Narisawa-Saito and Kiyono, 2007).

1.2.1.4 Carcinogenesis of HPV E6 and E7 oncoproteins

The critical molecules responsible for HPV oncogenesis are viral proteins, E6 and E7 (Schiffman et al., 2007). These viral proteins of the high risk types are capable of inactivating two key cell cycle regulatory molecules, namely p53 and retinoblastoma tumour suppressor protein (pRb) respectively, hence overcoming the safeguard arrest response (Bosch et al. 2002; Magaldi et al., 2012; Narisawa-Saito and Kiyono, 2007; Schiffman et al., 2007). Inactivation of p53 by E6 results in apoptosis inhibition and pRb deactivation by E7 abrogates cell cycle arrest (Schiffman et al., 2007). Together, they are known to cause polyploidy in cells and deregulation of genes responsible for

G2/M phase transition in cell cycle and consequent progression to mitosis (Fig 1.2.3) (Narisawa-Saito and Kiyono, 2007)

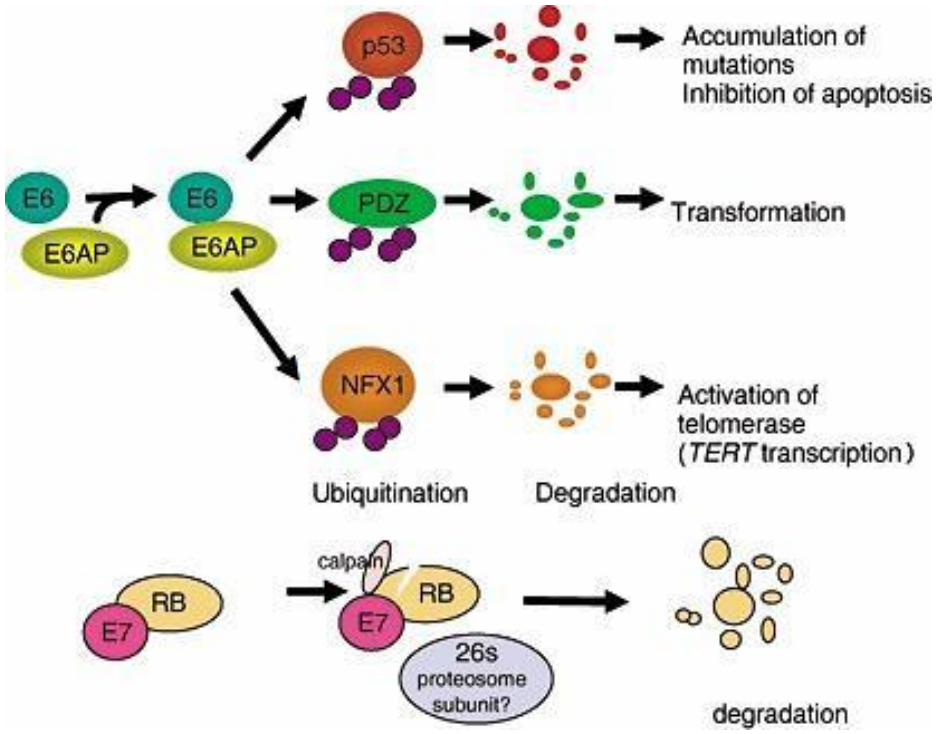

Fig 1.2.3: Carcinogenesis of E6 and E7 oncoproteins (Narisawa-Saito and Kiyono, 2007).

The primary transforming activity of E7 lies in its binding to pRb and disrupting its association with E2F family of transcription factors (Doorbar, 2007). The E2F subsequently gets released and activates host cell and viral DNA synthesis (Bosch et al. 2002). E7 also binds and activates cyclin complexes such as cyclin A and E which are responsible for cell cyclin progression (Bosch et al. 2002). Other molecules that E7 is known to associate with and inhibit are cyclin dependent kinase inhibitors p21 and p27 which are known to stall the cells in a pre-S phase and hence prevent the E7 mediated cell proliferation (Doorbar, 2007).

Another crucial cell cycle negative regulatory molecule is a tumour suppressor protein p53, which is activated upon phosphorylation by DNA damage sensing proteins (Bosch et al. 2002; Werness, Levine and Howley, 1990). Upon activation, it arrests the cell

cycle in G_1-phase and DNA repair is induced (Narisawa-Saito and Kiyono, 2007). However on encountering heavy DNA damage, p53 may induce the cell apoptotic pathways (Bosch et al. 2002). E6 is responsible for the ubiquitin mediated proteasome dependent degradation of p53 and therefore, its deactivation compromises the cellular DNA damage response, causing secondary mutations to accumulate as a result (Doorbar, 2007). It also interferes with other pro-apoptotic proteins including pro-caspase 8, Bak and FADD (Narisawa-Saito and Kiyono, 2007).

Even in the absence of E7, E6 might mediate cell proliferation by binding to PDZ structural domain through its C-terminal leading to its degradation (Doorbar, 2007). Proteins in the PDZ domain are involved in a variety of cellular functions including cellular adhesion and cell signalling (Narisawa-Saito and Kiyono, 2007). This binding disrupts the normal cell to cell contact as a result of the loss of cell polarity, eventually leading to the development of metastatic tumours (Doorbar, 2007).

Another important molecule which is activated by E6 and eventually plays a significant role in the immortalisation of HPV infected cells is telomerase (Bosch et al. 2002; Doorbar, 2007). Human telomerase is a ribonucleoprotein whose function is to stabilise telomere length and hence suppress senescence (ageing) (Narisawa-Saito and Kiyono, 2007). Shortening of telomere below a certain critical length triggers cell death (Bosch et al. 2002). Since telomerase is not active in normal somatic cells, telomeres shorten with each cell generation and eventually senescence is induced due to incomplete lagging DNA strand synthesis and end-processing events (Narisawa-Saito and Kiyono, 2007). E6 activates the catalytic subunit of telomerase hTERT (human telomerase reverse transcriptase) which induces the addition of hexamer repeats to the telomeric ends, henceforth maintaining and stabilising telomere length, causing the cells to continue dividing indefinitely (Bosch et al. 2002; Doorbar, 2007).

There are several other cellular proteins which have been reported to be targets of HPV E6 and E7 oncoproteins including AP-1, p21, p27, p600, p300/CBP, Tyk 2, Bak, c-myc, hAda3, Mi2, MPP2, NuMa, Epoc-1 and TBP (Peralta-Zaragosa et al., 2012). Hence, apart from the cell cycle control deregulation and apoptosis inhibition, E6 and E7 exert their influence on immune response escape, angiogenesis associated and independent cell proliferation processes (Peralta-Zaragosa et al., 2012). Together, this results in HPV

effectively immortalising human keratinocytes and transforming them into malignant phenotypes (Peralta-Zaragosa et al., 2012).

1.2.1.5 Development of cervical cancer

Cervical cancer is primarily the culmination of decade long process which starts with an infection with carcinogenic HPV virus (Schiffman et al., 2011). The initial phase is referred to as Stage 0, when abnormal cells with potential to become cancerous can be found in the innermost lining of the cervix (also called cervical intraepithelial neoplasia CIN) (McConville, 2015). Left untreated it can progress to Stage 4, where cancer finally spreads to bladder or other parts of the body (McConville, 2015). In its final stages, it is marked by persistent high risk HPV type infection, upregulated viral gene expression leading to uncontrolled cell proliferation and poor DNA damage control with mutations accumulating in the infected cells (Doorbar et al., 2012).

Cervical cancer develops while progressing through four primary stages: 1) HPV infection at the ring of squamous metaplastic epithelium referred to as the cervical transformation zone, 2) persistence of the infection, 3) progression of infected epithelium to precancer and 4) invasive cancer as the final stage (Schiffman et al., 2007). The cervical transformation zone is the site where stratified non-keratinising squamous cells of ectocervix meet the columnar cells of endocervix (Doorbar, 2007). This is the most significant cytological and colposcopic site as it is highly susceptible for high risk HPV infections and is where more than 90% of genital neoplasia arise (Fig 1.2.4) (Narisawa-Saito and Kiyono, 2007).

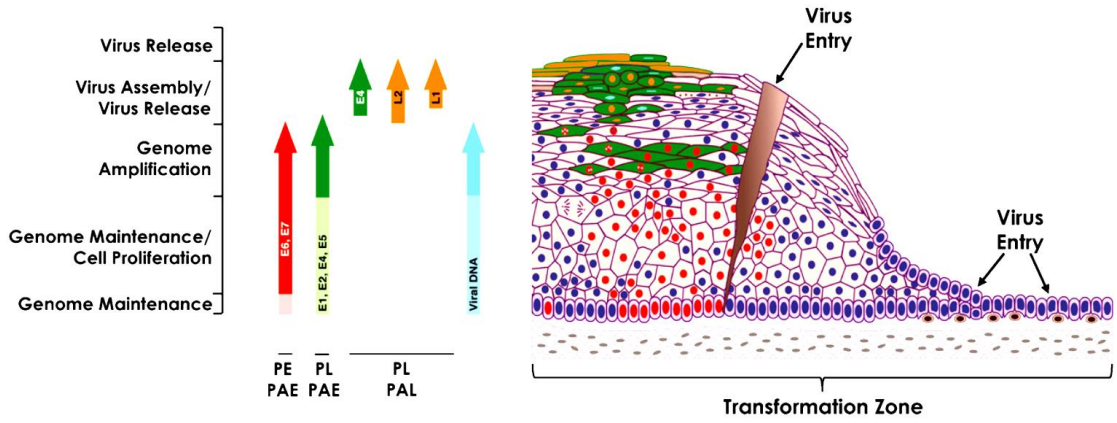

Fig 1.2.4: Life Cycle of High risk HPV (Doorbar, 2007). The six early open reading frames (E1, E2, E4, E5, E6 and E7) are expressed from early P97 (PE) or late P670 (PL) promoters during epithelial cell differentiation. The late open reading frames (L1 and L2) are also expressed from PL. This is followed from a shift in polyadenylation site usage (from early polyadenylation site PAE to late polyadenylation site (PAL).

At the site of erosion, the virions enter the basal and parabasal cells and viral DNA enters the cellular nuclei (Bosch et al., 2002). Molecular studies suggest that in many HPV associated cancers, there is an evidence of integration of HPV DNA into the cellular DNA (Bosch et al., 2002). In addition to the integrated form, HPV-16 can also be found episomally (Bosch et al., 2002; Cullen et al., 1991). Integration of viral DNA with cellular DNA results in constant levels of E6 and E7 proteins expressed via stabilisation of mRNA (Munoz et al., 2006). The consequence might be a deep-rooted presence of viral genome in the cells, the resulting infection persisting for even decades (Munoz et al., 2006; Schiffman et al., 2007). In such cases, it has an increased chance to develop into invasive cancer (Bosch et al. 2002). Although mostly, continued transcription of HPV oncogenes, instead of genome integration, is necessary for cancer development (Schiffman et al., 2007).

Long persistent infection with high risk HPV types give rise to cervical dysplasia or CIN which develops into cervical cancer (Narisawa-Saito and Kiyono, 2007). CIN I and CIN II lesions exhibit mild and moderate dysplasia respectively where the viral DNA is mostly in the episomal conformation whereas CIN III lesions displaying severe dysplasia develop when HPV DNA integrates into host DNA and this stage might

represent carcinoma *in situ* (Narisawa-Saito and Kiyono, 2007; Peralta-Zaragosa et al., 2012).

Although there is a high risk of HPV infections in approximately 80% of productive women, most HPV infections clear within 1-2 years of exposure by cell mediated immunity (Schiffman et al., 2007). The persistence of infection decreases the probability of its subsequent clearance over a period of time and thereby, increases the risk of cancer development (Fig 1.2.5) (Schiffman et al., 2007). *In-vitro* experiments have revealed that as the HPV infection progresses to cervical neoplasia, there is a reduced ability in such women to mount a T-helper cell type immune response against HPV-16 E6 and E7 peptides (Bosch et al. 2002).

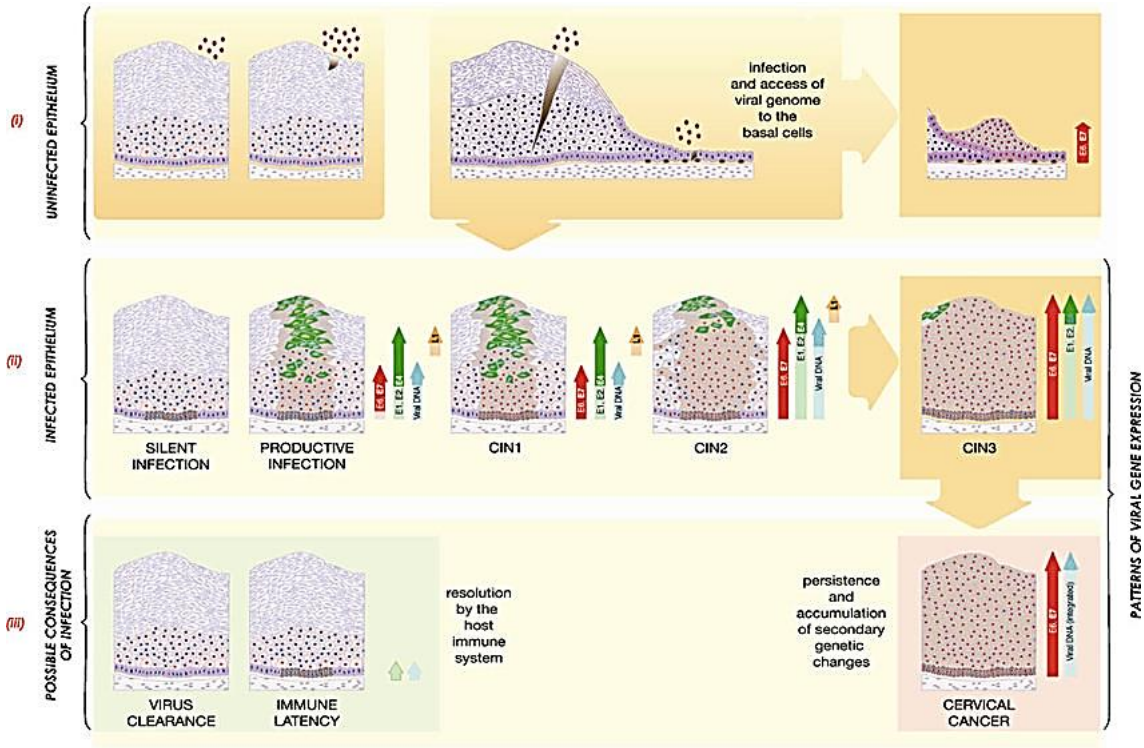

Fig 1.2.5: HPV infection and its possible consequence (Doorbar et al., 2012)

1.2.1.6 Prevention

The primary prevention of cervical cancer which could reduce incidence of the disease at population level could be in the form of health education programs promoting abstinence before marriage or stringent use of condom (Schiffman et al., 2007). However, the issue of practicality with such measures necessitate the importance of developing other techniques. In developed countries, there are currently two primary methods to prevent cervical cancer: 1, administration of HPV vaccines to prevent adolescent girls from getting infected and 2, screening for abnormal cells in cervix which can potentially be pre-cancerous (McConville, 2015).

(i) **Vaccines:** A major breakthrough in formulating vaccines against HPV infection was the development of HPV L1 virus like particles (VLP) vaccines (Harro et al., 2001). When self-assembled L1 protein in non-infectious capsid containing no genomic material was injected intra-muscularly, it induced the formation of fifty times higher titres of neutralising antibody than in normal infection (Harro et al., 2001). This could lead to protection against subsequent infections (Soliman, Slomovitz and Wolf, 2004). Two VLP prophylactic vaccines, Gerdasil (Merck and Co, USA) and Cervarix (GlaxoSmithKline, Belgium) have been developed targeting HPV-16 and HPV-18 and are commercially available (Inglis, Shaw and Koenig, 2006). Apart from VLP based vaccines, other forms of HPV vaccines formulated and tested in clinical and preclinical trials are peptide based vaccines, proteins based vaccines, DNA based vaccines, cell based vaccines and vector based vaccines (Soliman, Slomovitz and Wolf, 2004). However, current HPV vaccines do not treat existing HPV infections or lesions (Schiffman et al., 2007). Moreover, the very high costs associated with the vaccines have precluded their introduction to low-resource countries (Arbyn et al., 2011).

(ii) **Screening:** The various procedures employed for screening for HPV induced lesions are: direct visual inspection, visual inspection employing 3%-5% acetic acid, visual inspection using acetic acid and magnification, visual inspection using Lugol's iodine, cervical cytology, HPV DNA screening and speculoscopy (Aggarwal, 2014). The two most commonly used screening procedures are described below.

Cervical cytology with Papanicolaou (Pap) Tests: The major screening target for cervical cancer is treatable CIN II or CIN III lesions, rather than invasive cancer where the morbidity is high and chances to succeed are low (Schiffman et al., 2011). In this approach, exfoliated cells are analysed for presence of any biomarkers suggesting an underlying risk of cancer (Schiffman et al., 2011). Unfortunately, the sensitivity of Pap test is as low as 50-60% with an implication that a single negative Pap test is not definitive in itself but requires repeated rounds of screening to detect developing CIN lesions (Schiffman et al., 2011). Despite this fact, a negative smear does indicate a substantially lowered risk of cervical cancer for multiple years (Gustaffson et al., 1997; Schiffman et al., 2011). These cytology based cervical cancer screening for detecting and treating pre-cancerous lesions at early stage have considerably reduced the incidence and mortality associated with this disease (Schiffman et al., 2007). There is still an increasing demand to have stronger reassurance of safety when detecting the risk of cervical cancer, calling for other screening techniques (Schiffman et al., 2011).

HPV DNA Screening: Screening for carcinogenic HPV DNA has proven to be more cost effective and sensitive in detecting pre-cancerous lesions than cytology-based methods where the results might be equivocal (Schiffman et al., 2007). Moreover, testing negative for HPV DNA is a conclusive evidence of no risk of developing cervical cancer (Schiffman et al., 2007). Currently there are two methods primarily employed to detect carcinogenic HPV: 1) genome amplification using polymerase chain reaction (HPV DNA Nested Polymerase Chain Reaction Detection Kit™) and 2) hybridisation with signal amplification (Digene Hybrid Capture 2 High Risk HPV DNA Test™; Cervista HPV HR Test™) (Aggarwal, 2014; Schiffman et al., 2011). A major trade-off with HPV testing is while it has high sensitivity, it is limited on specificity (Aggarwal, 2014). It does not have the analytical specificity to decide which lesion would develop in cancer and which infection would regress taking its usual route (Aggarwal, 2014).

1.2.1.7 Treatment:

Cervical cancer is treated according to its stage of progression (Ordikhani et al., 2016). The women who are screened positive for pre-cancerous lesions have their entire transformation zone excised that is thought to contain CIN III lesions (Schiffman et al., 2011). Usually, fertility sparing treatments such as cryotherapy and cone shaped excision are employed instead of hysterectomy (Schiffman et al., 2007). A small amount of cervical stroma is removed with loop electrosurgical excision procedure (LEEP) or large loop excision of the transformation zone (LLETZ) in an outpatient setting with local anaesthesia (Schiffman et al., 2007). In the situation where a larger tissue section has to be excised, cold knife cone is employed (Schiffman et al., 2007). In low-resources areas, cryotherapy is preferred as it does not require anaesthesia or electricity and the use of carbon dioxide instead of nitrous oxide can further reduce the expenses (Schiffman et al., 2007). However, blockage of equipment and poor depth of tissue necrosis are few of the technical issues that need to be addressed for this technique to be employed effectively (Schiffman et al., 2007). Moreover, colposcopically guided biopsy and histological diagnosis suffer from poor performance as they typically concentrate on removing the most obvious lesion on visual inspection (Schiffman et al., 2011). This practice might fail to remove more than one third of the HPV positive CIN III lesion (Schiffman et al., 2011). Photodynamic therapy using photosensitising drug 5-aminolaevulinic acid was employed to treat cervical intraepithelial neoplasia in clinical trials; however it proved to be unsuccessful (Barnett et al., 2003).

For the treatment of invasive cancers, radical hysterectomy has been the preferred treatment (Schiffman et al., 2007). However, for tumours smaller than 2cm size, two modalities are most commonly employed for younger women where future pregnancy is desired: radical vaginal trachelectomy with laparoscopic lymphadenectomy or sentinel lymph node biopsy and radical abdominal trachelectomy with pelvic lymphadenectomy (Downs, 2011; Schiffman et al., 2007). Early stage cancer is mostly treated with surgery and chemoradiotherapy which has the potential to cure 80-90% of women (Peralta-Zaragosa et al., 2012). Initially, pelvic radiation was the standard treatment for advanced cancer as the principle cause of death among women was the uncontrolled

disease within the pelvis (Thomas, 1999). However, radiation dose was a severe limiting factor due to numerous late complications with this treatment (Thomas, 1999). For this reason, strategies involving combination therapy, particularly pelvic irradiation with concurrent chemotherapy was considered and that proved to be very effective for locally advanced stage cancer patients, with the mean survival rate increasing from 58 percent to 73 percent (Ordikhani et al., 2016).

Typically pelvic tumours are treated with weekly dose of cisplatin administered intravenously along with external beam irradiation and brachytherapy, the latter profiting from the easy accessibility of cervix where implants for brachytherapy can be placed non-invasively (Kang et al., 2015; McConville, 2015; Thomas, 1999). Among the chemotherapeutic drugs including cisplatin, paclitaxel, carboplatin, ifosfamide and toptecan employed for the treatment of advanced cervical tumour, cisplatin with response rate ranging from 20-30% and overall survival of 7 months, is documented to be the most active and effective drug (Downs Jr et al., 2011; Katanyoo et al., 2011; Leisching et al., 2015; Muderspach et al., 2001; Wang et al., 2015). Cisplatin is known to directly interact with DNA forming adducts, consequently inhibiting its transcription along with inducing oxidative stress and apoptosis in cancer cells (Ordikhani et al., 2016). However, it suffers from the usual limitations of platinum containing chemotherapeutic drugs such as development of tumour resistance along with serious side effects, essentially bone marrow depression and haematological toxicity which leads to neutropenia, thrombocytopenia, neurotoxicity, nephrotoxicity and anaemia (Jones, 2009; Ordikhani et al., 2016).

To increase the efficacy of the treatment, paclitaxel was used together with cisplatin and this combination treatment was better than the cisplatin monotherapy in terms of progression free survival and response rate (45-50%) although not overall survival (Cadron et al., 2007; Moore et al., 2004). When compared with other cisplatin combinations with Gemcitabine, Topotecan and Vinorelbine, none of them were as effective as the one with paclitaxel (Lorusso et al., 2014). However, prior to this could be routinely used as the new standard of care in advanced cervical cancer patients, the related toxicity and the discomfort associated with giving paclitaxel as a 24 h infusion made this combination impractical to be used as the cancer treatment (Lorusso et al., 2014). Some studies suggested that in this context, carboplatin, with its better toxicity

profile, higher tolerance, and with the ability to administer it in outpatient settings, made this a suitable substitute to cisplatin in combination treatments (Lorusso et al., 2014). Some studies have shown that cisplatin and gemtabicine acts synergistically on cancer cells both *in vitro* and *in vivo* and some demonstrate that combination of topotecan and cisplatin improves the overall survival to 9.4 months (Cadron et al., 2007). However, the lack of detailed toxicity data, quality of life data and many other factors, which are still unknown issues, could affect the clinical outcomes of cervical patients (Lorusso et al., 2014).

In cases where metastasis has not yet taken places, localised delivery of chemotherapeutic drugs holds several benefits such as less drug waste, diminished side effects and transport of high dose of drug at the active site of cervix (Ordikhani et al., 2016). Localised delivery of chemotherapeutics is possible due to the accessible location of cervix through the vagina (Ordikhani et al., 2016). Different drug formulations, gels, fibres, rings and tablets, delivered through vagina to treat bacterial or fungal infections or STDs are also being studied to deliver chemotherapeutic drugs to the cervix (McConville, 2015; Ordikhani et al., 2016). Such a localised delivery system may help the patient to recover more quickly, have a better control over the dosage delivered and reduce the burden on hospitals and overall global healthcare costs (Ordikhani et al., 2016). When the cancer progresses to metastatic stage or becomes recurrent however, the survival rate becomes extremely low and is a major cause of high mortality (Peralta-Zaragosa et al., 2012). Therefore much effort is being directed on developing new drugs or searching for alternative approaches such as gene therapy or nanotechnology which would treat cervical cancer in cases where traditional approaches fail.

1.2.1.8 Limitations:

The incidence of procuring an HPV infection and consequent development into cervical cancer depends on the average societal age of first sexual intercourse and the efficiency of screening programs. The young age at death, where women are still raising their families, further accentuates the importance of detecting/ treating this disease (Schiffman et al., 2007).

Among other cancers, the screening program for cervical cancer is most effective (International Collaboration of Epidemiological Studies of Cervical Cancer, 2006). However, cytology based cervical cancer screening requires skilled human resources, an infrastructure in place and quality assurance, which are mostly not available in developing countries (Arbyn et al., 2011). Due to this inadequate or non-existent screening and unaffordable or absent standard treatment options, the mortality rate is the highest among women with cervical cancer (Schiffman et al., 2007). VLP vaccines are not a viable form of treatment for women who are already exposed to and infected with HPV (Duncan, Eckert and Clawson, 2009). Moreover, these vaccines are still not available or affordable in less developed countries where this vaccine is most needed (Duncan, Eckert and Clawson, 2009). Another problem with screening for HPV-16 and HPV-18 lies with the fact that these two accounts for only 70% of cervical cancer cases and at least 13 other high risk HPV types exist (Duncan, Eckert and Clawson, 2009). Therefore, despite the progress made in the field, persistent HPV infections still pose a serious health problem stipulating the importance of research in finding alternative treatment/ preventative options (Duncan, Eckert and Clawson, 2009).

There are other points of concern for the available screening programs. Since the site of pre-cancer might not necessarily be the exact site of subsequent cancer development, the commonly performed biopsies of colposcopically derived tissues might inaccurately give negative histopathological results rejecting the presence of a possible pre-cancer (Schiffman et al., 2007). Moreover, unlike HPV-16, HPV-18 mostly doesn't produce the high-grade squamous intraepithelial lesions which might be a reason of poor screening performance for endocervical and glandular lesions with an increased

incidence of HPV-18 related adenocarcinomas as a consequence (Schiffman et al., 2007).

With the treatment strategies available as well, the most prevalent treatment of surgery and chemoradiotherapy results in serious side effects, including bone marrow depression and haematological toxicity along with development of tumour resistance to the drug. Moreover, radiation therapy has its own limiting drawbacks and when the cancer develops to an advanced stage and metastasizes, the mortality rate becomes insurmountably high. For these reasons, there is a necessity of exploring the efficacy of other established drugs against cervical cancer and a means of increasing their therapeutic index *in vivo* by delivering the drug specifically to the target cells sparing normal cells. ATO is one such drug that has established itself as a broad spectrum anti-cancer drug and has also shown efficacy against cervical cancer cell lines by downregulating HPV E6 oncogenes and reducing the survival of cancer cells. Equipping it with nanotechnology based drug carriers presents us with an attractive approach in our quest for finding a novel, non-invasive, affordable and fertility sparing treatment option for cervical cancer.

1.2.2 Arsenic Trioxide

Arsenic is a naturally occurring metalloid found as a trace element in the earth's crust (Shen et al., 2013). Instead of being present in its elemental state; it exists as highly toxic arsenates of metals like calcium, sodium and potassium or as oxides and sulphides. Among its three inorganic forms of red, yellow and white arsenic, the latter is ATO which is industrially produced as a by-product while roasting arsenic containing ores and purifying the smoke (Fig 1.2.6) (Miller et al., 2002). The rise of ATO from its reputation of "king of poisons" to a "broad spectrum anti-cancer drug" is among the most exciting transformation stories in clinical oncology.

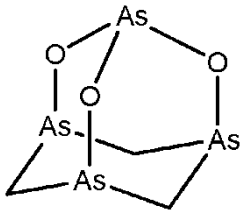

Fig 1.2.6: structure of ATO (Platanias, 2009)

Despite being the mainstay of *materia medica* for over 2400 years, arsenic faced a decline in its use as a therapeutic agent in the twentieth century due to an increasing awareness of its toxicity (Evens, Tallman and Gartenhaus, 2004). The resurgence of ATO transpired when a group of Chinese physicians realised its presence in ancient Chinese medicine as the main anti-leukemic agent and decided to evaluate its potency on patients with APL, a subtype of acute myeloid leukemia. The following clinical trials of ATO on APL patients as a single agent or in combination with conventional chemotherapy yielded highly encouraging results. ATO was consequently approved by FDA as a frontline therapy for APL in 2000 (Antman, 2001). The same kind of clinical success was translated for other haematological malignancies as well although not for the solid tumours. Rapid clearance of arsenic and its products from the blood by reticuloendothelial system limits the therapeutic dose reaching the tumour site. Escalating arsenic dosage could not be an alternative as it led to systemic toxicities such as long term memory damage, liver failure, cardiac failure and peripheral neuropathy (Swindell et al., 2013).

The enigma of arsenic with its carcinogenic and anti-carcinogenic effects may very well be related to the length (chronic vs acute), level (high dose vs low dose) and type (arsenite/ arsenate/ methylated species) of arsenic exposure. Several attempts have been carried out to utilise arsenic's significant anti-cancer properties for treating solid tumours by reducing its administered dosage while increasing its bioavailability and specificity. This includes employing ATO with other conventional chemotherapeutic agents to explore their synergistic actions, sensitising the cells prior to ATO treatment or employing nanotechnology to increase bioavailability of arsenic while reducing its systemic toxicity (Akhtar et al., 2017).

1.2.2.1 Arsenic history: renown, decline and resurgence

Arsenic presents a rich history in medicine with its therapeutic applications dating back to more than 2400 years (Waxman and Anderson, 2001). Nicknamed as the "therapeutic mule" for its widespread use in a variety of ailments, the tenacity of it being used despite the inconsistent toxicity associated with this compound, arsenic remains one of the most popular drugs of the *material medica* (Miller et al., 2002).

For thousands of years, arsenic has been used in traditional Chinese medicine to treat syphilis, psoriasis, rheumatism and to devitalise inflamed pulp tissue of the diseased teeth prior to dental work (Waxman and Anderson, 2001). Hippocrates used arsenic sulphides, orpiment (As_2S_3) and realgar (As_4S_4), as escharotics to treat ulcers and skin and breast cancers while Dioscorides administered orpiment as a depilatory (Waxman and Anderson, 2001). Centuries later, Angelus Salva administered arsenic against plague, Jean de Gorris used it as a sudorific and Lentilius recommended it as a cure for malaria (Miller et al., 2002). Arsenides and salts, observed to be more therapeutic than the pure, metallic arsenic, found diverse uses as anti-spasmodics, anti-pyretics, anti-periodics, caustics, sedatives, hematinics and tonics (Haller, 1981). Among the 60 different therapeutic preparations of arsenic in the course of its illustrious history, twenty were still prevalent at the turn of 19th century including Andrew's tonic, Arsenauro, Aiken's Tonic Pills and Gross's neuralgia pills (Haller, 1981).

Until the 17th century, the application of arsenic salts and sulphides was generally external. However, physicians soon found that boiling arsenous acid with an alkali gave water soluble solution could be administered internally. In 1780's, Thomas Fowler became intrigued with the "Tasteless Ague Drops" which was a popular anti-periodic remedy of the time and decided to imitate the preparation (Haller, 1981). The resulting solution of ATO in potassium bicarbonate (1%w/v), named Fowler's solution, quickly earned great fame for its efficacy in treating rheumatism, Hodgkins disease, pernicious anaemia, psoriasis, epilepsy, eczema, paralysis, heart palpitations, convulsions, syphilis, ulcers and cancer (Miller et al., 2002; Waxman and Anderson, 2001). Paul Ehlrich, founder of chemotherapy, further experimented with properties of arsenic and in 1910, discovered arsphenamine, an organic arsenical (Miller et al., 2002). Also popularly

known as Salvarsan or compound 606, it remained the mainstay treatment for syphilis for 40 years before being replaced by penicillin (Miller et al., 2002). It was also used to treat African trypanosomiasis, the sleeping sickness (Aronson, 1994).

Although arsenic and its anti-cancer properties were known way back in the empirical era of therapeutics, its anti-leukemic activity was first reported in 1878. ATO in the form of Fowler's solution caused a drastic decline in white blood counts in a patient with "leucocythemia" and also in two normal individuals (Kwong and Todd, 1997). The discontinuation of the therapy resulted in a progressive increase in the white blood count in the patient until the therapy had to be re-instated. Its efficacy against chronic myelogenous leukemia (CML) and other forms of cancer resulted in arsenic being the dominant anti-leukemic treatment until it was superseded by radiation therapy (Kwong and Todd, 1997).

Arsenic was not always explored for its medicinal purposes only. The women peasants of Syria and Austria habitually consumed arsenic to attain a healthy pallor with blushed cheeks and a plumper appearance, a habit which was later adopted by Victorian women. The men peasants consumed it as it gave them a better digestion, appetite, muscular and nervous functions (Haller, 1981). Moreover, when ATO was dissolved in an aqueous solution, the colourless and odourless arsenous acid formed was termed as the "king of poisons", because it was virtually undetectable with its symptoms being easily mistaken for natural disorders like haemorrhagic gastroenteritis, psychiatric disorders or cardiac arrhythmias (Antman, 2001).

Gradually, as the awareness of the toxicity of arsenic spread, its medicinal use declined until by the turn of twentieth century, arsenic acquired the reputation of a toxic compound and a carcinogen (Antman, 2001). In one study, all of the patients developed palmar and plantar keratosis after long-term ingestion of Fowler's solution, though the minimum onset of the disease was 15 years from the beginning of the treatment (Jackson and Grainge, 1975). A majority of the patients procured basal cell carcinoma around the same time. Some other manifestations were squamous cell carcinoma, colon carcinoma and breast adenocarcinoma which developed around 28-63 years after arsenic exposure (Jackson and Grainge, 1975). Acute arsenic poisoning caused gastrointestinal distress, headaches, and cardiac arrhythmias along with liver and renal failure (Swindell et al., 2013).

Chronic exposure to environmental arsenic also became a serious cause of concern in some parts of the world. In Bangladesh, contamination of arsenic in ground water caused severe health problems for millions of people (Antman, 2001). The most common side effects included hyperpigmentation of the skin, in some severe cases, bladder, lung, kidney and prostate cancers along with neuropathy, encephalopathy, leucopenia and diabetes were also reported (Swindell et al., 2013). Arsenic induces cell transformation and promotes tumour formation *in vitro* according to some experimental studies depending on the dose administered (Meng and Meng, 2000). In one study, rat epithelial cell line (TRL 1215) was exposed to 0.5µM arsenite for a period of 18 weeks. This chronic exposure induced malignant transformation of the cell lines and produced tumours which metastasized on being injected to the nude mice (Morikawa, 2000). Therefore, despite its reported anti-leukemic and medicinal properties and lack of direct experimental proof of its carcinogenicity in humans, the International Agency for Research on Cancer (IARC) declared arsenic to be in the category one of carcinogens in 1979 (Waxman and Anderson, 2001).

The resurgence of arsenic in recent times owes the credit to its long history of use in Chinese medicine as mentioned preciously (Shen et al., 1997). In 1990s, after an initial study at Harbin Medical University of the anti-leukemic properties of arsenic in traditional Chinese medicine, a group of physicians at Shanghai Second Medical University tried its efficacy on leukemic patients. In a careful clinical trial, they administered very low doses of intravenous ATO and observed remarkable results in patients with relapsed and refractory APL (Zhang, 1996). It was a finding of major importance because 20-30% of patients with APL relapsed after treatment with all-trans retinoic acid (ATRA) and anthracycline based chemotherapy and died (Waxman and Anderson, 2001). The major course of therapy then used to be bone marrow transplantation (Waxman and Anderson, 2001).

Further reports from China suggested that ATO alone induced and maintained complete remission in 9 out of 10 patients with relapsed APL without any myeloid suppression and lesser toxic side effects (Shen et al., 1997). At low doses, Chen et al. observed that ATO caused differentiation in APL cells, while at higher doses; it induced apoptosis (Chen et al., 1997). The findings, which were later successfully replicated in United States, proved to be a major breakthrough and led to the approval of ATO (Trisenox^{TM}) by FDA as a frontline drug for relapsed and refractory APL in Sept, 2000 (Antman,

2001). The intravenous administration of ATO doses, while being very effective and well tolerated, do show some side effects of cardiotoxicity with a prolonged QT_c as measured on an electrocardiogram (Swindell et al., 2013).

Till recently, the maximum success of ATO therapy has been observed in haematological cancers, where the therapeutic dosage administered is low, hence the commonly reported side effects are low grade and reversible after ceasing the ATO therapy (Swindell et al., 2013). However, the same kind of clinical success has not been translated for solid cancers in humans despite positive results in experimental animal models. This is primarily due to the rapid clearance of arsenic and its metabolites from the blood by reticuloendothelial system (RES). This limits the therapeutic dose of arsenic reaching the tumour site and hence a requirement arises for escalating arsenic dosage which might, in turn, lead to systemic toxicities associated with high arsenic concentration in blood, such as peripheral neuropathy, cardiac and liver failure (Swindell et al., 2013). Arsenic toxicity also leads to long-term memory damage and hormonal imbalance (Platanias, 2009).

1.2.2.2 Mechanism of action for solid tumours

Following the huge clinical success of ATO therapy on APL and later in other haematological malignancies such as multiple myeloma and myeloma dysplastic syndrome, the mechanism of its action on blood cancers has been carefully elucidated and reviewed (Evens, Tallman and Gartenhaus, 2004). Although promising results are shown on the experimental models, therapy by ATO on solid tumours remains limited as mentioned earlier. There have been several ongoing clinical trials to investigate its efficacy on a variety of solid tumours such as lung cancer, hepatocellular carcinoma, malignant glioma, endometrial cancer, basal skin cancer, liver cancer, germ cell tumours, colorectal cancer, pancreatic cancer, breast cancer, kidney, ovarian and cervical cancers, albeit without appreciable clinical success in human patients (Murgo, 2001). (http://www.clinicaltrials.gov) This brings to our attention the crucial need for understanding the chemistry of arsenic and identification of its potential molecular targets in different solid tumours leading to a successful treatment along with analysing

other possible ways of increasing the bioavailability of arsenic without raising its dosage.

Oxidation state of arsenic ranges from -3 in AsH_3 to +5 in arsenic acid (Chen et al., 2015). Most of the common arsenicals found in nature are either pentavalent or trivalent, out of which trivalent arsenicals are more relevant to our study as they have a high binding affinity for thiols (sulfhydryl groups) (Evens, Tallman and Gartenhaus, 2004). The interaction is rapid, energetically favoured and reversible (Swindell et al., 2013). Since in a protein, cysteine is the only naturally occurring amino acid which can be the source of accessible thiol group attachments, it is a major target for arsenic binding (Lu et al., 2008). One arsenic molecule is known to form different trigonal pyramidal complexes with three cysteine molecules in proteins (Fig 1.2.7). This interaction results in conformational changes and the consequent loss of function of the enzyme. It might also affect its interaction with other functional proteins. It has also been recently reported that arsenic has the capability to distort a polypeptide to reorganise its structure where maximum number of thiols are exposed to arsenic for coordination (Shen et al., 2013). For instance, in APL, arsenic directly binds to the cysteine residues in the zinc fingers of promyelocytic leukemia fusion protein (PML-RARα). This initiates a cascade of events like its oligomerisation, attachment to small ubiquitin like modifier protein and finally degradation by ubiquitination (Evens, Tallman and Gartenhaus, 2004).

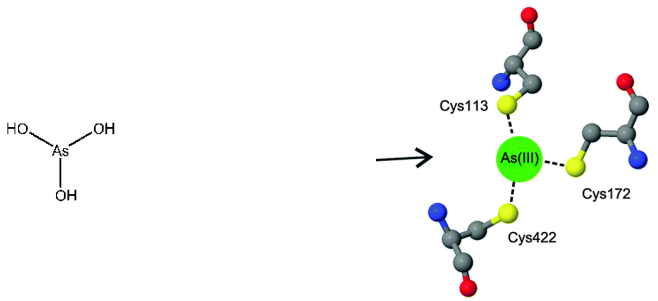

Fig 1.2.7: Trivalent arsenic binds to the residues Cys172, Cys 422 and Cys 113 of a polypeptide (Evens, Tallman and Gartenhaus, 2004).

Besides sulfhydryl groups, hydroxyl groups have also been reported to be another target for arsenic binding, making serine to be the other target for arsenic ligation (Shen et al., 2013). Hence, identifying oncoproteins for various solid tumours might be a fruitful approach in developing arsenic compounds and delivery systems for effective therapy. Some enzymes are commonly known to be inhibited by arsenic include glutathione peroxidase, glutathione reductase, glutathione S-transferase, protein tyrosine phosphatase, DNA ligase and JNK phosphatase (Shen et al., 2013). Mechanisms of its anti-cancer actions are proposed as following.

1.2.2.2.1 **Induction of apoptosis**

Inarguably, the most plausible mode of action of ATO is its ability to induce apoptosis in the cancer cells. Apoptosis or the programmed cell death however, might result from a multitude of factors such as mitochondrial damage and oxidative stress to the cell (Emadi and Gore, 2010). The key molecular enzymes in initiating apoptosis are caspases which are intracellular cysteine proteases. They cleave crucial cellular proteins which bring about the morphological features characteristic of apoptosis, i.e. nuclear condensation and fragmentation. Pro-apoptotic stimuli or mitochondrial membrane damage leads to the release of cytochrome c from the intra-membrane space of mitochondria into the cytosol where it binds to apoptosis protease activating factor (Apaf-1). This binding activates pro-caspase-9 to caspase-9 which cleaves pro-caspase 3, leading to its activation of Caspase 3. Caspase-3 eventually initiates other sub cellular events culminating in apoptosis of the cell (Emadi and Gore, 2010).

1.2.2.2.2 **Mitochondrial toxicity**

ATO is believed to bind to the thiol groups in the permeability transition pore complex (PTPC) in mitochondrial membrane, permeabilising it and decreasing membrane potential $\Delta\psi_m$ as a consequence (Larochette et al., 1999). The subsequent release of soluble intermembrane proteins (SIMPS) is responsible for the biochemical and morphological manifestations of apoptosis (Kroemer and de The, 1999). For instance,

cytochrome c, as mentioned earlier, activates pro-caspase-9; apoptosis inducing factor (AIF) causes wide spread DNA fragmentation after relocating to nucleus and activation of other pro-caspases ultimately results in proteolytic degradation of major cellular proteins (Kroemer and de The, 1999).

1.2.2.2.3 **Generation and accumulation of ROS**

Reactive oxygen species (ROS), including free radicals such as superoxide ($O_2.^-$) and hydroxyl ($OH^{\cdot}$) and molecules such as hydrogen peroxide (H_2O_2) are damaging to the cell's molecular machinery (Emadi and Gore, 2010). ROS are generated due to the accumulation of electrons, which in turn might happen when there is a mutation in the genes encoding for the mitochondrial electron transport chain. Arsenic interferes with the activity of redox sensitive signalling molecules, for instance, AP-1, p53, p21 and s-nitrothiols which changes the signalling pathways and consequently alters the gene function. The hydrogen peroxide or other ROS generated effectuate apoptosis though multiple pathways, one of which includes aggregation of mitochondria (Miller et al., 2002).

Redox capacity of many proteins depends on the sulfhydryl groups on cysteine, which detoxify the cells by binding to ROS generated by normal mitochondrial metabolism. When arsenic binds to these thiol groups instead, the capacity of these proteins to bind to ROS is compromised, leading to oxidative stress.

Intracellular redox reactions which protect the cells from oxidative stress damage are regulated by thioredoxin system of the cell which includes enzymes like NADPH, thioredoxin and thioredoxin reductase (Platanias, 2009). Other anti-oxidant enzymes involved in protecting the cell against ROS are glutathione, glutathione peroxidase, superoxide dismutase and catalase. Many of them possess vicinal thiols, and so are susceptible to arsenic action (Emadi and Gore, 2010). Arsenic blocks or intervenes in their enzymatic activity, which might account for its pro-apoptotic effect (Platanias, 2009).

Along with direct binding of arsenic with PTPC in the mitochondrial membrane, accumulation of H_2O_2 due to generation of ROS from arsenic action, is hypothesised to be another factor responsible for lowering of mitochondrial membrane potential and

consequent release of cytochrome c in the cytosol, leading to apoptosis (Fig 1.2.8) (Miller et al., 2002).

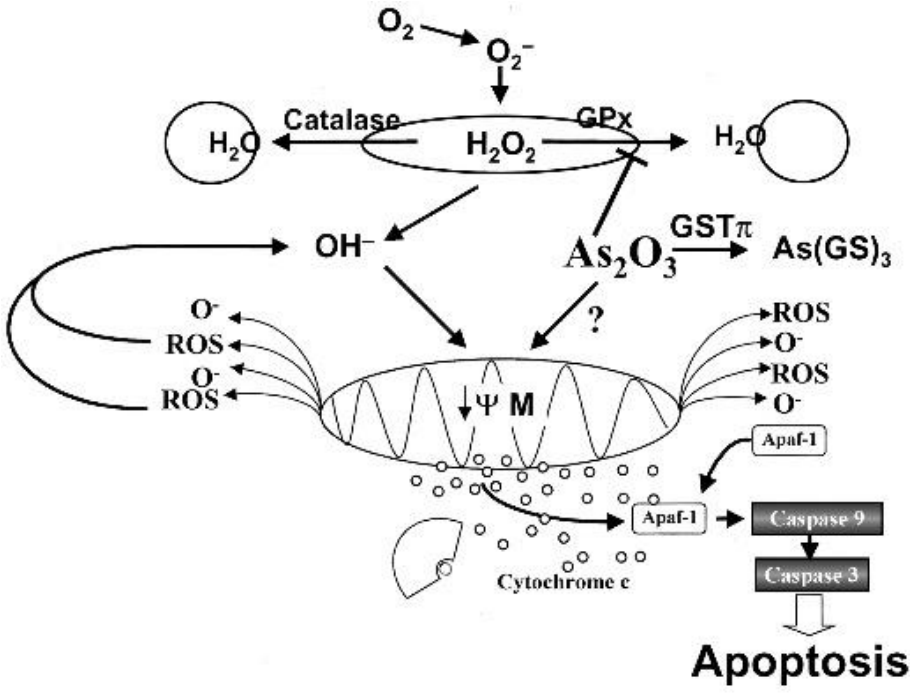

Fig 1.2.8: Pathways of apoptosis induction by ATO treatment via mitochondrial membrane destabilisation owing to increased accumulation of ROS (Platanias, 2009).

ATO enters the mammalian cells in the form of arsenous acid either via diffusion or by neutral solute transporter proteins of aquaporin family (Yang et al., 2012). Once inside, it binds to numerous available thiol residues of proteins and effectuate its anti-cancer response. Besides the abovementioned modes of arsenic action, it also interferes in other cellular events, for instance, tubulin polymerisation, DNA repair or cell cycle progression (Kroemer and de The, 1999). It inhibits the transcription of the telomerase transcriptase subunit of human telomerase *hTERT* gene, which leads to genomic instability and cancer cell death, as telomerase is essential for maintaining chromosomal ends' length which shorten after every cell division and is responsible for senescence after the chromosomal ends are reduced below a certain threshold (Chou et al., 2001).

ATO also inhibits proliferation of carcinogenic cells and is also observed to inhibit tumour angiogenesis by either down-regulating vascular endothelial growth factor (VEGF) or inducing apoptosis in endothelial cells (Miller et al., 2002).

1.2.2.2.4 **Mode of action of ATO for cervical cancer treatment**

There have been few studies investigating ATO's mode of action, specifically for cervical cancer treatment. A study demonstrated that ATO causes G2/M phase arrest, caspase-9 activity and mitochondrial destabilisation on a range of cervical cancer cell lines including HeLa, C33a, SiHa and Caski cells (Yu et al., 2007). For mitochondrial destabilisation, ATO induced homodimerisation of voltage dependent anion channel (VDAC) proteins, an abundant protein in the outer mitochondrial membrane, leading to the formation of a channel through which cytochrome c migrates from the mitochondria to the cytosol, causing apoptosis (Yu et al., 2007). In a separate study, ATO was shown to cause the translocation of Apaf-1, a mitochondrial intermembrane flavoprotein, to the nucleus which resulted in DNA fragmentation and chromatin condensation (Kang et al., 2004).

Cervical cancer cell lines were also tested for their attachment and migration ability after the treatment with ATO as tumour cell migration and metastasis are highly interlinked processes (Yu et al., 2007). The crucial proteins here are E-cadherin which enhances intercellular adhesion and inhibits tumourigenecity and invasiveness of epithelial tumour cells (Vleminckx et al., 1991); β-catenin which links E-cadherin to actin cytoskeleton (Rimm et al., 1995); and Caveolin-1 which targets or anchors proteins to their specific site of action (Yu et al., 2007). ATO treatment was observed to upregulate caveolin-1 and E-cadherin and downregulate β-catenin which enhanced the cell-cell contact and invasion suppression of tumour cells (Yu et al., 2007).

Cervical cancer cells potentially offer a unique environment as unlike other carcinomas, they have HPV as the major etiologic agent for carcinogenesis and the critical molecules responsible for HPV oncogenesis are viral E6 and E7 oncoproteins (Yu et al., 2007). Hence, downregulating their expression might provide an effective form of anti-cancer therapy. ATO downregulated viral E7 gene expression which is closely associated with the apoptosis induction in HPV-16 DNA immortalised HCE-16/3 cells

(Zheng et al., 1999). The results were consistent with another set of findings by Um et al. (2002) where they observed a downregulation of HPV E6 and E7 oncogene expression in ATO-treated HeLa cells. This downregulation was hypothesised to be due to the repressing of the activity of AP-1 transcriptional factor in HPV-18 URR (Um et al., 2002). This led to the inhibition of growth, induction of apoptosis and increased levels of p53 in human cervical cancer cells (Um et al., 2002).

As evidenced above, ATO demonstrates significant efficacy against cervical cancer cell lines. However, chemotherapy is always riddled with serious side effects due to the toxicity to the surrounding normal tissue. A truly desirable treatment would be one where the therapeutic index of the drug is made considerably higher to selectively target cancer cells. This would overcome the side effects arising from systemic toxicities which are common with chemotherapeutic treatments. The advent of nanotechnology in the field of drug delivery has given us the possibility to realise such an ideal treatment for a variety of problematic cancers including cervical cancer.

1.2.3 **Nanotechnology in drug delivery**

Utilising traditional chemotherapeutic drugs including ATO to treat cervical cancer is riddled with challenges currently. One of the major issues in cancer therapeutics is tissue selectivity (Danhier, Feron and Preat, 2010). Limited dose reaching the solid tumour causes problems of suboptimal treatment and excessive toxicities, which further result in poor quality of life of the patient and low overall survival (Danhier, Feron and Preat, 2010). The same issue has plagued the utilisation of ATO for treatment of solid cancers, like cervical cancer. The typical limitations of commercial drugs are their poor solubility, low bioavailability, high toxicity, non-specific delivery, short circulation times and *in vivo* degradation (Orive et al., 2003). In general, therapeutic potential of any anti-cancer drug can be improved if its toxic side effects to the healthy surrounding tissue could be reduced and it could be delivered specifically to the cancer cells. In

essence, in the current scenario, the field of drug delivery presents itself as a major impediment to pharmaceutical and biotechnology industries requiring to be mastered in order to fully utilise the plethora of new and old therapeutics that are hampered by their poor delivery and toxicity issues (Sahoo, Misra and Parveen, 2017).

One of the most effective steps in the direction of addressing this issue is the implementation of nanotechnology in the field of drug delivery. As per the National Nanotechnology Initiative (http://www.nano.gov), nanotechnology is defined as the controlled development and utilisation of structures, devices and systems at atomic, molecular and or macromolecular scale approximately in the 1-100nm size range in at least one dimension (Zamboni et al., 2012; Farokhzad and Langer, 2009). This technology is increasingly being applied to healthcare and drug delivery is one of its most rapidly developing fields of research which attempts to deliver a bioactive agent to its therapeutic site of action at a predetermined rate (Sahoo, Misra and Parveen, 2017).

The advent of nanotechnology has already changed the landscape of drug delivery. It focusses on formulating therapeutic agents by encapsulating drugs in biocompatible nanocarriers such as nanoparticles, dendrimers, micelles or nanocapsules (Sahoo, Misra and Parveen, 2017). Encapsulating chemotherapeutic drugs in nanocarriers promises considerable benefits including: protecting the drug from chemical and biological degradation in the blood stream, improving bioavailability and stability of the drug, eliminating the toxic side effects of the free form, providing the possibility for encapsulating both hydrophilic and hydrophobic drugs and the option of targeted drug delivery (Sahoo, Misra and Parveen, 2017), (Bulbake et al., 2017). Nanocarriers also are known to increase drug specificity, improve absorption rates, and overcome multi-drug resistance phenomenon and penetrate cellular barriers like blood brain barrier among others (Zamboni et al., 2012; Bulbake et al., 2017). They can provide sustained release of the drug at a predetermined rate for specified time (Bulbake et al., 2017). They can reduce the need for repeated drug administration, which could lead to increased patient's compliance and reduced healthcare costs (Sahoo, Misra and Parveen, 2017). The biggest advantage, however, in employing nanotechnology is the possibility of achieving targeted drug delivery either through passive targeting or active targeting (Sahoo, Misra and Parveen, 2017).

1.2.3.1 Types of targeting

1.2.3.1.1 **Passive targeting**

When solid tumours are smaller than $2mm^3$, they are dependent on their microenvironment for oxygen and nutrients, which easily diffuses to the core of the tumour (Malam, Loizidou and Seifalian, 2009). However, when tumour reaches the size of $2mm^3$ and beyond, the cells at the centre get hypoxic initiating angiogenesis (Malam, Loizidou and Seifalian, 2009). Hypoxia instigates a cascade of events which lead to the upregulation of pro-angiogenic proteins such as VEGF, platelet derived growth factor (PDGF) or tumour necrosis factor α (TNF-α) (Malam, Loizidou and Seifalian, 2009). Consequently, new blood vessels are formed but the immature vasculature undergoes rigorous remodelling aided by pericytes and smooth muscles cells (Danhier, Feron and Preat, 2010). This process remains incomplete leading to the formation of dilated and irregular shaped tumour vessels lacking in integrity (Danhier, Feron and Preat, 2010).

The creation of long circulating "stealth nanoparticles" which could evade immune response by having a polyethylene glycol (PEG) layer grafted on their surface allow an opportune exploitation of the above mentioned structural changes in vascular pathophysiology (Danhier, Feron and Preat, 2010). The tumour blood vessels are abnormal with decreased number of pericytes lining the rapidly multiplying endothelial cells and an aberrant basement membrane formation with pores in the range of 10nm-1000nm (Torchilin, 2000; Haley and Frenkel, 2008). This is in stark contrast with the tight endothelial junctions of normal blood vessels (Haley and Frenkel, 2008). Hence, nanoparticles in the size range of 20-200 nm can extravasate from this "leaky vasculature" into the interstitial spaces of tumour tissue but not through a healthy blood vessel of a surrounding normal tissue (Fig 1.2.9) (Danhier, Feron and Preat, 2010). Moreover, lymphatic vessels in tumour tissue are either absent or non-functional

leading to a poor lymphatic drainage (Danhier, Feron and Preat, 2010). The nanoparticles leaking through the pores are hence not removed leading to their accumulation within the interstitial space of the tumour (Danhier, Feron and Preat, 2010). This phenomenon was discovered by Matsumura and Maeda in 1986 and they termed it as Enhanced Permeability and Retention (EPR) effect (Matsumura and Maeda, 1986).

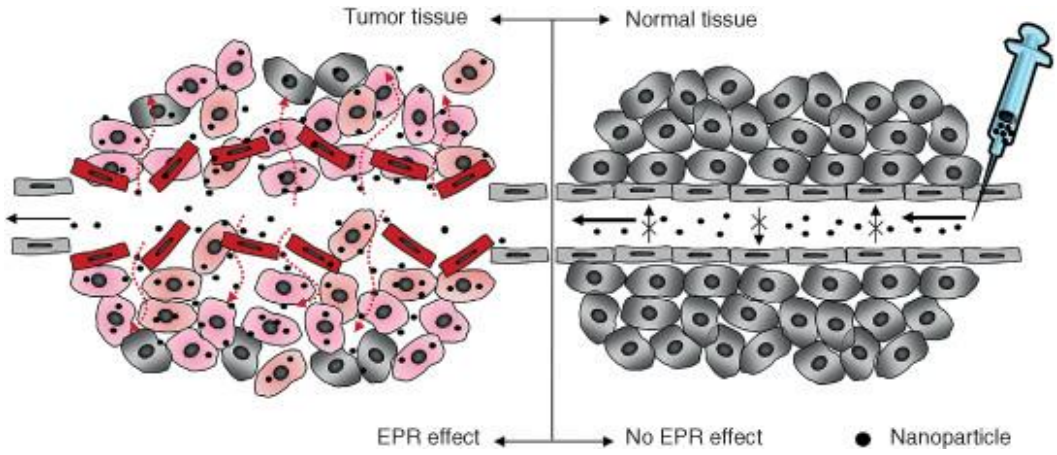

Fig 1.2.9: Differences between the tumour and normal blood vessels which explain the passive accumulation of nanoparticles via EPR effect. (Park and Na, 2015)

The inefficient lymphatic drainage has another beneficial effect from using nanoparticles carrying chemotherapeutic drug over their free molecular counterpart. It causes a high osmotic pressure in tumours, which is highest at its centre while fading away at the periphery (Jain, 1987). This results in a mass flow of fluid away from the centre so the drug molecules are unable to penetrate the inside of tumour resulting in an inefficient treatment (Danhier, Feron and Preat, 2010). For this reason, conventional drugs have a poor pharmacokinetic profile with an implication that they are distributed non-specifically in the body leading to debilitating and systemic toxicities (Danhier, Feron and Preat, 2010). However, the larger sized nanoparticles are less resisted by this

high tumour interstitial fluid pressure, resulting in their overcoming of these barriers and successful accumulation within the tumour (Danhier, Feron and Preat, 2010). Another relevant characteristic of tumour environment that facilitates the release of active drug molecule from nanocarrier once it has accumulated within the tumour is the presence of lower pH in tumours than normal tissues (Van Sluis et al., 1999). The extracellular pH of normal tissues is 7.4, whereas the average extracellular tumour pH is between 6 and 7 (Van Sluis et al., 1999). The lower pH destabilises the nanocarrier which might release the drug in the vicinity of the cancer cells expediting their uptake (Danhier, Feron and Preat, 2010).

EPR effect is a technique that has been greatly exploited to deliver the therapeutics to their site of action. Also, the transport of nanocarriers through the leaky vasculature into the tumour interstitium via EPR effect is popularly termed as passive targeting (Danhier, Feron and Preat, 2010). This targeting is only conceivable when the nanocarriers carrying the drug payload can escape the immune surveillance and circulate for a longer period of time (Danhier, Feron and Preat, 2010). To this end, nanoparticle's surface is grafted with polyethylene glycol PEG layer, as mentioned above, which acts as a brush and prevents opsonisation and immune clearance by reticuloendothelial system (RES) (Danhier, Feron and Preat, 2010).

One of the first sterically stabilised PEGylated liposome (lipid nanoparticles) encapsulating a chemotherapeutic drug, doxorubicin, approved by FDA was Doxil (Gullotti and Yeo, 2009). Doxil displayed a good retention time in its liposomal formulation, a better circulation time *in vivo* and was almost 6 times as effective as the parent drug (Gullotti and Yeo, 2009). Relying on EPR mechanism, it proved a success in shrinking tumour size both in animal models and patients (Maeda, Bharate and Daruwalla, 2009). Consequently, it was approved for the treatment of chemotherapy refractory AIDS related Kaposi's sarcoma, advanced ovarian cancer and metastatic breast cancer (Gullotti and Yeo, 2009). Currently, there are apparently fifteen approved liposomal formulations including liposomal cytarabine (DepoCyt), paclitaxel albumin bound nanoparticles (Abraxane) and liposomal daunorubicin (DaunoXome) (Fig 1.2.10) (Bulbake et al., 2017; Chang and Yeh, 2012; Zamboni et al., 2012).

Fig 1.2.10: FDA approved liposomal formulations and their therapeutic areas (Bulbake et al., 2017).

1.2.3.1.2 **Active targeting**

Passive targeting has limitations owing to differential susceptibility of different tumour tissues to the EPR effect (Federman and Denny, 2010). Consequently, passive targeting may bring the nanoparticle in close proximity to the tumour tissue but not guarantee its entry within the tumour cells (Federman and Denny, 2010). To achieve the latter, the approach of active targeting is employed (Federman and Denny, 2010). Active targeting is accomplished when a receptor specific ligand is conjugated to the nanocarrier encapsulating therapeutic drug to stimulate site specific targeting (Sahoo, Misra and Parveen, 2017). This receptor mediated binding of nanoparticles to the surface receptors expressed on tumour cells leads to a preferential accumulation of drug at the diseased site (Sahoo, Misra and Parveen, 2017), (Zamboni et al., 2012). These ligand-liposomal complexes are then internalised by tumour cells via receptor mediated endocytosis (Fig 1.2.11) (Kirpotin, 2006). The success of active targeting relies on few factors: 1, the targeting ligand should have a high affinity and high specificity for the surface receptors, 2 be amenable to surface modifications to permit conjugation, 3 surface

receptor and ligand should be abundant to increase the chances of conjugation between them (Sahoo, Misra and Parveen, 2017).

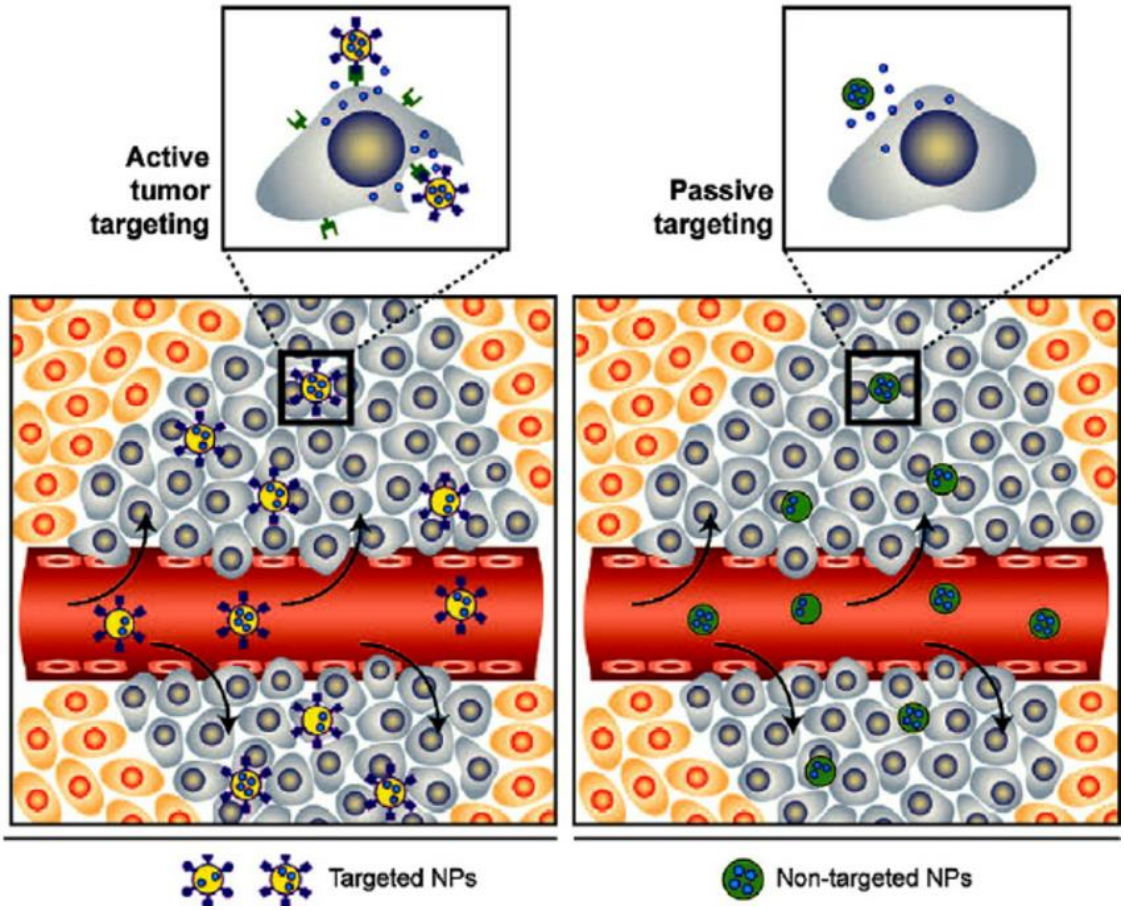

Fig 1.2.11: Passive targeting vs active targeting (Farokhzad and Langer, 2009)

The optimum size of nanoparticles and the ability to conjugate ligands complementary to diseased cell's receptors facilitates overcoming of the physiological barriers followed by efficient uptake and cellular internalisation (Sahoo, Misra and Parveen, 2017). Hence, drug encapsulated in nanocarriers have a greater opportunity to accumulate in cancerous tissue than its free form (Sahoo, Misra and Parveen, 2017). Targeting ligand acts as a "homing device" for nanocarriers and increases their specificity to target specific tissues and cells (Danhier, Feron and Preat, 2010). Despite proving their

efficacy in preclinical models, only three actively targeted nanocarriers have reached clinical trials till now: transferrin conjugated liposome containing oxaliplatin, galactosamine targeted PHPMA doxorubicin and GAH conjugated liposome containing doxorubicin (Danhier, Feron and Preat, 2010).

1.2.3.2 Liposomes

Many types of nanoparticles have been employed for the purpose of drug delivery in medicine including dendrimers, micelles, nanospheres, nanocapsules, fullerenes, nanotubes, polymer nanoparticles and liposomes (Fig 1.2.12) (Haley and Frenkel, 2008). Our main interest however is in liposomes which were first described in 1960 by Alec Bangham and colleagues (Bangham, Standish and Watkins, 1965). In 1971, Gregory Gregoriadis established the utility of liposomes in encapsulating drugs (Gregoriadis and Ryman, 1971). Since then, liposomes have been the object of immense research and directed effort to improve their efficacy as drug delivery vehicles. A myriad of drugs have been incorporated in liposomes, including anti-cancer or anti-microbial drugs, proteins, peptides, hormones, genetic material, chelating agents and vaccines, to achieve selective delivery to target cells for therapeutic applications (Chang and Yeh, 2012). Liposomes have gained increased interest among other nanoparticles due to their good biocompatibility, easy control over their compositions and properties and cost-effective production costs (Zamboni et al., 2012).

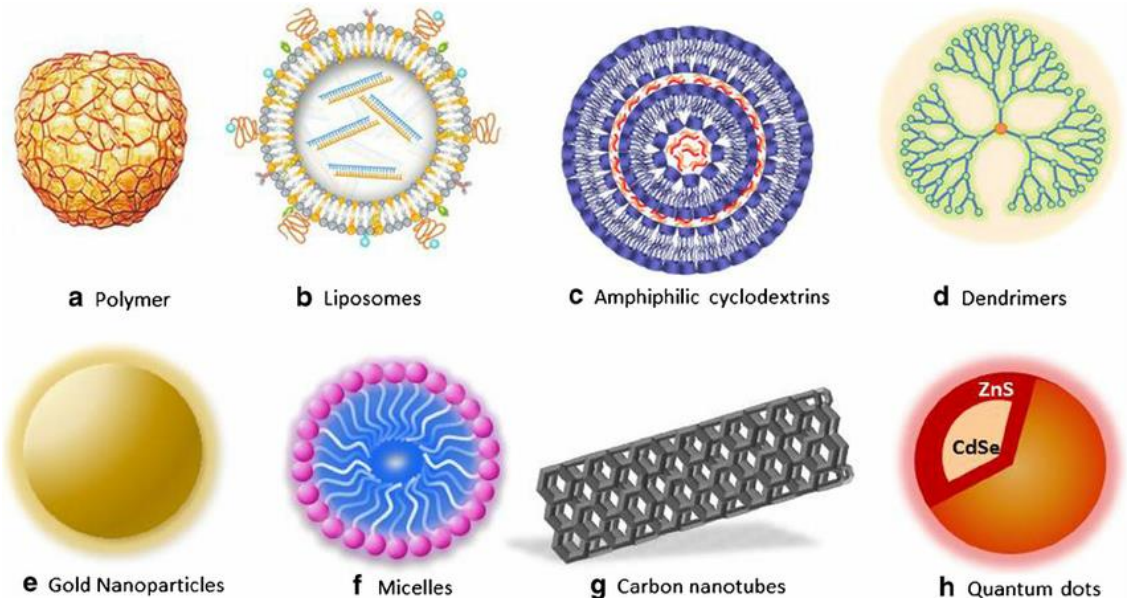

Fig 1.2.12: Different types of nanoparticles commonly employed in biomedical applications of drug delivery (Mc Carthy et al., 2015)

Liposomes are spherical vesicles composed of phospholipid bilayers surrounding an aqueous core (Malam, Loizidou and Seifalian, 2009). The aqueous core can be utilised to encapsulate hydrophilic drug molecules whereas the lipid bilayer can entrap lipid soluble drugs (Haley and Frenkel, 2008). The "first generation" liposomes suffered from a major drawback of rapidly getting opsonised soon after an intravenous injection and consequent clearance by RES (Haley and Frenkel, 2008). They were taken up the cells of mononuclear phagocytic system (MPS), particularly spleen and liver leading to their inactivation along with causing toxicity to the MPS organs involved (Allen and Cullis, 2013). Liposomes were further rendered vulnerable from electrostatic, van der Waal's and hydrophobic forces which could lead to their disintegration (Haley and Frenkel, 2008). This warranted a need for steric stabilisation of liposomes which could be attained by coating their surface with an inert polymer (Lasic, 1996). PEG surface coating could provide this steric stabilisation and render the particle invisible to the opsonins, subsequently preventing their clearance by immune system (Haley and Frenkel, 2008). This "stealth" technology utilising "second generation" liposomes, first described in 1987, had much longer circulation times, better bio-distribution and dose dependent pharmacokinetics as they had a higher opportunity to accumulate within

tumour tissue via EPR effect (Allen and Chonn, 1987; Allen and Cullis, 2013; Haley and Frenkel, 2008).

When a targeting ligand is attached to the PEG layer of liposomal surface, the resulting nanoparticle is classified as a "third generation" liposome (Farokhzad and Langer, 2009). In 1987, Heath et al. showed that targeting the liposome with an antibody complimentary to receptors on cancer cell surface could indeed enhance the selectivity of the liposomal anti-cancer drug in cultures (Heath et al., 1983). Both the targeted and non-targeted liposomes have similar distribution in the cancerous tissue via EPR effect, however in the vicinity of the target cells; conjugated liposomes might exhibit an increased uptake due to receptor mediated endocytosis (Allen and Cullis, 2013). However both the targeted liposomes and passively targeted liposomes should have an appreciable content retention and an appropriate release rate to increase their therapeutic index (Allen and Cullis, 2013).

1.2.3.2.1 **Considerations of liposomal design**

Despite the fact that liposomes are biocompatible and biodegradable systems, on entering the blood stream, they are susceptible to destabilisation after opsonisation and consequent immune response in the form of MPS or the complement system (Vonarbourg et al., 2006). The phospholipid component of the liposomal composition is a strong activator of the complement system (Vonarbourg et al., 2006). Hence, a careful consideration is required to design the liposomal surface in a way that its circulation time is increased to allow the EPR effect to take place, to make active targeting possible by conjugating ligands specific to the target cancer cells' receptors, to have a scope of sustained release of drug when in the vicinity of the tumour or inside cancer cells and also have a good drug encapsulation efficiency with a high, specific uptake by target cells (fig 1.2.13). To that effect, soy lecithin (phosphatidyl choline PC or phosphatidyl ethanolamine PE) is added to the liposomal composition as their choline and phosphate groups impart hydrophilic properties to the surface and henceforth, inhibit complement activation (Mosqueira et al., 2001). A few other factors which have an inhibitory effect on the complement activation are the presence of a low surface charge, smaller size, rigid membrane and cholesterol (Vonarbourg et al., 2006). Cholesterol has been

reported to increase the mechanical strength, membrane elasticity, reduce the membrane surface defects and hence remove the potential adsorption sites for blood proteins which destabilise liposomes (Magarkar et al., 2014; Semple, Chonn and Cullis, 1998).

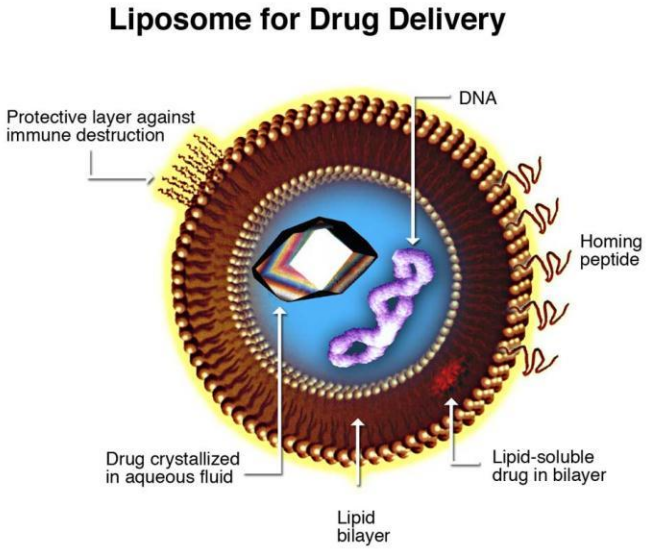

Fig 1.2.13: Liposomal design for drug delivery (Torchilin, 2006)

The introduction of hydrophilic polymer chain such as PEG at the nanoparticle surface is a very effective way to make the surface hydrophilic and reduce hydrophobic interactions (Van Oss, 1975). These PEG chains, with a high affinity for water molecules, create a 'water cloud' around the nanoparticle, leading to repulsion from the environmental proteins (Coleman, Gregonis and Andrade, 1982). PEG is uncharged and non-immunogenic in nature and can be easily grafted or incorporated on the nanoparticle surface, increasing the latter's biocompatibility (Vonarbourg et al., 2006). Moreover, the presence of two terminal hydroxyl groups allows functionalisation and covalent coupling to ligands to achieve active targeting (Vonarbourg et al., 2006). However, the PEG's capacity to prevent opsonisation depends largely on the optimisation of various parameters including its molecular weight, flexibility, density

and conformation of the chains (Gref, 1995). It has been reported that the efficient molecular weight is around 1500-3000 Da and the presence of PEG chains of mixed lengths can have an advantage of long chains providing accessibility for ligands for endocytosis and smaller lengths providing the coating necessary for longer circulation (Pavey and Olliff, 1999). In addition, the more flexible and dense the chain is, the more efficient it is in improving circulation profile (Vonarbourg et al., 2006).

1.2.3.2.2 **Liposomes and cervical cancer**

With its growing prowess, researchers have started using liposomal technology to specifically treat cervical cancer (Casagrande et al., 2013; Saengkrit et al., 2014; Saini et al., 2014). The conventional drug for treating cervical cancer, cisplatin, was encapsulated in liposomes and the resultant formulation was termed lipoplatin (Casagrande et al., 2013). Lipoplatin showed similar efficacy as the parent drug with associated reduced toxicities on metastatic breast cancer, head and neck and pancreatic cancers (Casagrande et al., 2013). It was recently tested for cervical cancer and lipoplatin displayed appreciable anti-tumour activity on cisplatin resistant cervical cancer cell lines and was able to induce apoptosis and inhibit migration and invasion (Casagrande et al., 2013). Other drugs that have been encapsulated in liposomes for treating cervical cancer are bleomycin sulphate and curcumin (Saengkrit et al., 2014; Saini et al., 2014). Similarly, ATO along with few other organic arsenicals has also been encapsulated in nanoparticles and their efficacy investigated and verified, although not for cervical cancer.

Owing to the immense potential of liposomes in the field of clinical medicine and research, there is no doubt that they can be fittingly envisioned as the future of drug delivery technology along with other nanoparticles (Sahoo, Misra and Parveen, 2017). Nanomedicines are the answer to an increasingly efficient cancer therapy and an improved patient's quality of life, holding the potential to radically change the way in which we diagnose, image and treat cancer. However, massive challenge still remains to specifically tailor the nanocarrier and optimise its design to treat a specific tumour. Liposomal size, charge, cholesterol content, PEG density to be used and loading techniques of the drug are only few of the parameters among many that need an arduous

and careful optimisation before they can be employed as carriers of ATO for effective treatment of cervical cancer. The specific aims for the undertaken research are enumerated in the following section to optimise the liposomal ATO carrier to display a most effective anti-cancer response towards HPV positive cervical cancer cells.

1.3 Aims

The overall aims of this project were to selectively deliver ATO to HPV positive cervical cancer cells *in vitro* via an optimized liposomal carrier. The effectiveness of delivered ATO via the formulated drug delivery system by targeting identified surface markers on target cancer cells was evaluated. The molecular mechanisms of ATO action delivered through this route including changes in cancer cell apoptosis and the expression of HPV oncogenes along with tumour suppressor proteins were then examined and compared with free ATO, which was tested on HPV positive cervical cancer cell lines along with control cell lines.

The aims were achieved from the following steps:

1.3.1 *Optimising physical parameters (mainly, size and charge) of drug encapsulating liposomes to increase their efficacy as nano-carriers of ATO to HPV positive cervical cancer cells.*

Specific objectives were:

i. To synthesise ATO encapsulating liposomes and to optimise their physico-chemical and biological properties (loading efficiency, stability and inherent cytotoxicity) in terms of best **size** and **charge**, specifically for HPV positive cervical cancer cells;
ii. To compare any differences seen in liposomal uptake, cellular toxicity and apoptosis induction in the cancer lines towards the optimised liposomal treatment based on the presence or absence of HPV oncogenes.
iii. To investigate their toxicity towards non-cancerous normal cells.

1.3.2 *Selecting the best ligand for liposomal conjugation to actively target HPV positive cervical cancer cells*.

Specific objectives were:

i. To screen for surface markers (EGFR, folate receptor and transferrin) on cervical cancer cells (both HPV positive and HPV negative)

ii. To identify a surface marker which is abundantly expressed on HPV positive cervical cancer cells (HeLa cells) and negligibly expressed in HPV negative cervical cancer cells (HT-3 cells), in order to find the best targeting **ligand** for liposomes targeting specifically the HPV positive cervical cancer cells.

1.3.3 *Designing targeted ATO liposomes and optimising their physical parameters (mainly, ligand-PEG spacer length and ligand density) to attain highly specific cellular uptake in HPV positive cells.*

Specific objectives were:

i. To design **targeted,** PEGylated liposomes conjugated with the chosen ligand;

ii. To optimise their parameters including PEG spacer length of conjugated ligand for better selectivity and uptake to receptor positive cell lines (preferably HPV positive cells) and evaluate their physico-chemical properties and biological responses (including cellular uptake and *in vitro* cytotoxicity).

1.3.4 *Selecting the best delivery method for ATO to HPV positive cervical cancer cells by investigating and comparing the molecular mechanism of ATO delivered free or encapsulated in (both targeted and non-targeted) liposomes.*

Specific objectives were:

(i) To investigate the **mechanism** of ATO action delivered via the three routes: free form and liposomally (both non-targeted and targeted approach) by examining the induction of apoptosis, downregulation of oncogenes E6 and E7 and upregulation of tumour suppressor proteins p53/ pRb.

(ii) To investigate which delivery method is the most selective and effective for treating HPV positive cervical cancer cells.

Chapter 2

MATERIALS AND METHODS

2.1 MATERIALS

2.1.1 Major Equipment

PLATE READER	FLUOStar Omega BMG Plate Reader, BMG LABTECH Ltd., Bucks, UK
FLOW CYTOMETER	BD FACSCalibur, BD BioSciences, Oxford, UK
FLOW CYTOMETER SOFTWARE	Cell Quest Pro software, BD BioSciences, Oxford, UK
WESTERN BLOT IMAGING SYSTEM	Licor Odyssey Fc Imaging system, LICOR BioSciences, Cambridge, UK

WESTERN BLOT IMAGING SOFTWARE	Image Studio Lite ver. 4.0, LICOR BioSciences, Cambridge, UK
WESTERN BLOT TRANSFER EQUIPMENT	Trans-Blot® Turbo™ Transfer System, Bio-Rad Laboratories Ltd., Hertfordshire, UK
GEL ELECTROPHORESIS TANK	Mini-PROTEAN® Tetra Vertical Electrophoresis Cell, Bio-Rad Laboratories Ltd., Hertfordshire, UK
GEL ELECTROPHORESIS TANK POWER SUPPLY	Mini Trans-Blot® Module and PowerPac™ HC Power Supply, Bio-Rad Laboratories Ltd., Hertfordshire, UK
EPPENDORF THERMOSTAT HEATING BLOCK	Eppendorf ThermoStat plus, Fisher Scientific, Leicestershire, UK
DYNAMIC LIGHT SCATTERING (DLS) INSTRUMENT	Zetasizer Nano ZS, Malvern Instruments Ltd, Malvern, UK
INDUCTIVELY COUPLED PLASMA-MASS SPECTROMETER (ICP-MS)	X Series 2, Thermo Scientific, Paisley, UK
INDUCTIVELY COUPLED PLASMA-OPTICAL EMISSION SPECTROMETER	iCAP 6500 - ICP-OES CID Spectrometer, Thermo Scientific, Paisley, UK

CONFOCAL MICROSCOPE	Leica Mircosystems, Milton Keynes, UK
0.4µm, 0.2µm and 0.1µm SYRINGE FILTERS	Whatman Anotop Filters, Sigma-Aldrich Company Ltd., Dorset, UK
DIALYSIS TUBING	Dialysis tubing (MW 20kDa), Sigma-Aldrich Company Ltd., Dorset, UK
MINI DIALYSIS DEVICES	Slide-A-Lyzer™ MINI Dialysis Device, 20K MWCO Fisher Scientific, Leicestershire, UK
CELL CULTURE HOODS	Mars Class 2 Cabinets Labogene, Thistle Scientific Ltd., UK
CO_2 INCUBATOR	Binder CO_2 incubator, Series C, BINDER GmbH – Headquarters, Germany
WATER BATH	Grant SUB Aqua 5 digital water bath, Laboratory Analysis Ltd., Exeter, UK
DIONISED WATER PURIFIER	Purite Select Fusion Water Purification System, Camlab Limited, Cambridge, UK

ICE MACHINE	Scotsman AF200 Ice flaker, Hubbard Systems, Suffolk, UK
pH METER	Jenway 3505 pH meter, Camlab Limited Cambridge, UK
AUTOCLAVE	BioCote, Coventry, UK
BALANCES	Acculab ALC-110.4, Fisher Scientific, Leicestershire, UK
CENTRIFUGES (1)	Eppendorf Centrifuge 5430 R, Fisher Scientific, Leicestershire, UK
CENTRIFUGES (2)	Sigma 4-16K centrifuge, SciQuip Ltd., Shropshire, UK
HEATING BLOCK	Techne Dri-Block DB.3, Cole-Parmer, Staffordshire, UK
VORTEX	Vortex Genie-2T, Scientific Industries, New York, USA

ROTATOR	Rotator Variable Speed Stuart SB3, Camlab Limited Cambridge, UK
ROLLER MIXERS (1)	Thermo Denley Spiramix 5, Thermo Scientific, Paisley PA4 9RF, UK
ROLLER MIXERS (2)	Roller Stuart roller mixer SRT6D, Cole-Parmer, Staffordshire, UK
ROCKER	Rocker 35 EZ Large Capacity Lab Rocker Labnet International Inc., Edison, NJ
MAGNETIC STIRRER (1)	L-71 R Labinco, The Netherlands
MAGNETIC STIRRER (2)	Hot Plate Magnetic Stirrer FB15001 Fisher Scientific, Leicestershire, UK

2.1.2 Minor equipment

PIPETTES, PIPETTE TIPS,	Gilson Pipettes Starlab UK Ltd., Milton Keynes, UK
VORTEX MIXERS	Stuart Vortex Mixers SA8 Cole-Parmer, Staffordshire, UK
GAS 95% O_2; 5% CO_2; NITROGEN	BOC Group Plc., Surrey, UK
PIPETTE TIPS, 5000ML, 2000ML AND 1000ML GRADUATED BEAKERS, GRADUATED PIPETTES, EPPENDORF TUBES, CORNING™ FALCON™ ROUND-BOTTOM POLYSTYRENE TUBES, GLASSWARE, STARSTEDT 96, 24, 12 AND 6 WELL PLATES, GLOVES, 1.5 ML, 4ML AND 7ML GLASS VIALS, BD PLASTIPAK SYRINGES, WYPALL ABSORBENT PAPER TOWEL, MENZEL GLASER COVERSLIPS	Fisher Scientific, Leicestershire, UK
HAEMOCYTOMETER	Neubauer haemocytometer Paul Marienfeld GmbH & Co. KG, Germany
MICROSCOPIC SLIDES	Superfrost Microscopic Slides VWR International Ltd, Leicestershire

2.1.3 Reagents

2.1.3.1 Cell culture

Cell Lines: Two human cervical cancer cell lines, HeLa (HPV positive) and HT-3 (HPV negative) along with two normal cell lines, human epidermal keratinocytes HK and human colon epithelial cells CRL-1790, were used in the first part of the study. For the liposomal conjugation studies, nasopharyngeal cell line KB and lung cancer cell line A549 were also included as controls along with the cervical cancer cell lines. All the cancer cell lines were used till passage number 40 or below, while the normal cell lines were used between passage numbers 3 and 12.

- HeLa (ATCC® CCL-2™, UK) is a human cervical epithelial cancer cell line of adenocarcinoma. HeLa cells have been reported to contain HPV-18 sequences.
- HT-3 (ATCC® HTB-32™, UK) is also a human cervical cancer cell line of epithelial origin which is negative for HPV DNA or RNA.
- HK (Fisher Scientific, UK) cells are primary human epidermal keratinocytes which are isolated from neonatal foreskin.
- CRL-1790 (ATCC, UK) cells are normal human colon epithelial cells.
- KB (ATCC® CCL-17™, UK) cell line was originally derived from an epidermal carcinoma of the mouth but was later contaminated with HeLa cell line. Hence, it has been reported to contain HPV-18 DNA sequences. It is highly positive for folate receptor expression.
- A549 (ATCC® CCL-185™, UK) cells are human lung epithelial cancer cells. They have been reported to be negative for folate receptor expression.

Culture media:

- RPMI media-1640 (Gibco, Thermo Fisher Scientific, UK)
- DMEM Media - GlutaMAX™ (Thermo Fisher, UK)
- Folate free RPMI-1640 media (Fisher Scientific, UK)

- Gibco McCoy's 5A (Modified) medium (Fisher Scientific, UK)
- Ham's F-10 Nutrient Mix (Thermo Fisher Scientific, UK).
- Fetal Bovine Serum (Invitrogen Life Technologies, Fisher Scientific, UK)
- Penicillin-Streptomycin (5000U/ml) (Invitrogen Life Technologies, Fisher Scientific, UK)
- EpiLife® Medium, with 60 µM calcium (Fisher Scientific, UK)
- Human Keratinocyte Growth Supplement (Fisher Scientific, UK)
- Trypsin-EDTA (Fisher Scientific, UK)
- DMSO (Sigma, UK)
- Trypan Blue (Fisher Scientific, UK)

Toxicity and apoptosis studies:

- *Thiazolyl blue tetrazolium bromide powder* (Sigma, UK), which is dissolved in serum free media at a concentration of 2.5mg/ml immediately before use.
- Isopropanol (Fisher Scientific, UK)
- Sheath Fluid, BD^{TM} FACSClean, BD^{TM} FACS Rinse (BD Biosciences, UK).
- *Annexin V FITC apoptosis detection kit* (Abcam, UK) has 500µl Annexin V-FITC, 500µl Propidium iodide and 50ml binding buffer.

2.1.3.2 Liposome studies

Synthesis: The lipids were purchased from Avanti Polar Lipids (AL, USA) unless mentioned specifically,

- Soy phosphatidylcholine (PC)
- Methoxypolyethyleneglycol-distearoyl- phosphatidylethanolamine (DSPE-PEG2000; with mPEG MW2000Da)
- 1,2-distearoyl-sn-glycero-3-phosphoethanolamine-N-folate(polyethylene glycol)-2000 (DSPE-PEG2000- Folate; with mPEG MW2000Da)

- 1,2-distearoyl-sn-glycero-3-phosphoethanolamine-N-folate(polyethylene glycol)-5000 (DSPE-PEG5000- Folate; with mPEG MW5000Da)
- 1,2-distearoyl-*sn*-glycero-3-phospho-(1'-*rac*-glycerol) (sodium salt) (DSPG)
- Cholesterol (Chol)
- Didodecyldimethylammonium bromide (DDAB) (Sigma, UK)
- Nickel acetate (Sigma, UK)
- ATO (Sigma, UK)
- Methanol (Fisher Scientific, UK)
- Dichloromethane (Fisher Scientific, UK)
- 1,1'-Dioctadecyl-3,3,3',3'-Tetramethylindocarbocyanine-5,5'-Disulfonic Acid (DiIC18(3)-DS) (Invitrogen, ThermoFisher Scientific, UK).
- Sodium dihydrogen phosphate, NaH_2PO_4 (Fisher Scientific, UK)
- Disodium Hydrogen Phosphate, Na_2HPO_4 (Fisher Scientific, UK)
- *Dialysis buffer* (0.01M NaH_2PO_4/Na_2HPO_4 pH 7): Dissolve 1.2gm NaH_2PO_4 and 4.26gm Na_2HPO_4 in 4 lit dH_2O.

Characterisation: All the chemicals were purchased from Fisher Scientific (UK),

- Nitric acid
- Hydrogen chloride
- Sodium hydroxide
- Calibration standards for arsenic, nickel and phosphorus
- Oxoid Phosphate Buffered Saline Tablets

2.1.3.3 Protein expression studies

Antibodies: All the antibodies were supplied by Abcam (UK) unless stated otherwise,

- β-actin antibody (ab119716, rabbit polyclonal to beta actin);

- transferrin antibody (ab84036, rabbit pAb to transferrin receptor);
- EGFR antibody (ab137660, rabbit pAb to EGFR N-terminal);
- Active caspase-3 antibody: (ab32042, rabbit mAb to active caspase-3) and (ab2302, rabbit pAb to active caspase-3);
- Rb antibody: (ab24, mouse mAb to Rb) and (ab181616, rabbit mAb to Rb);
- HPV18 E7 antibody: (ab100953, mouse mAb to HPV-18 E7);
- p53 antibody: (ab28, mouse mAb to p53), (ab26, mouse mAb to p53) and (ab131442, rabbit pAb to p53);
- E6 antibody: (ab70, mouse mAb to HPV-16+Anti-HPV18 E6);
- Caspase 3 antibody: (ab32351, rabbit mAb to caspase-3) and (ab13847, rabbit pAb to caspase-3);
- Rabbit FOLR1 Polyclonal Antibody (Fisher Scientific UK);
- Goat Anti-rabbit IgG FITC Conjugate (Fisher Scientific UK);
- Mouse mAb to HPV18 E6 (Santa Cruz Biotechnology, UK).

Immunocytochemistry/ Immunofluorescence cytochemistry:

- Haematoxylin (Sigma, UK)
- Paraformaldehyde (Fisher Scientific, UK)
- Triton X-100 (Sigma, UK)
- Immunomount (Fisher Scientific, UK)
- Hydrogen peroxide 30% (v/v) (Thermo Fisher Scientific, UK)
- VECTASHIELD Hard Set Mounting Media with DAPI (Vector Labs, UK)
- *Pierce™ DAB Substrate Kit* (Thermo Fisher Scientific, UK) has 25ml of 10X DAB solution and 250ml of stable Peroxide Substrate Buffer. The working solution must be prepared immediately before use by combining 2.5mL of DAB with 22.5mL of the Stable Peroxide Substrate Buffer and mixing thoroughly.
- *TSA™ Cyanine 5 System*, for 50-150 Slides (Perkin Elmer, USA) has 15 ml of 1X Plus Amplification Diluent and Cyanine 5 Plus Amplification Reagent (2 tubes, to which 150 µL DMSO has to be added). To prepare working solution for this stock, before each procedure, TSA Plus Stock Solution is diluted in the ratio of 1:50 in 1X Amplification Diluent.

- *TSA™ Fluorescein System* (Perkin Elmer, USA) has similar 15ml of 1X Plus Amplification Diluent and Fluorescein Plus Amplification Reagent (2 tubes where 150µl of DMSO has to be added in each tube). Working solution is prepared in the same way as TSA™ Cyanine 5 System.
- *VECTASTAIN Elite ABC HRP Kit* (Vector Labs, UK) contains 3 ml Blocking Serum (Normal Serum), 1 ml biotinylated, affinity-purified anti-Immunoglobulin, 2 ml Reagent A (Avidin DH) and 2ml and Reagent B (Biotinylated Horseradish Peroxidase H). Biotinylated Antibody is prepared by added 150µl of normal blocking serum stock to 10ml of PBS along with 50 µl of biotinylated antibody stock. For VectaStain ABC reagent, 100 µl Reagent A and Reagent B are added to 5ml of PBS and allowed to stand for 30 min before use.

Western blot:

- Halt Protease Inhibitor Cocktail (100X) (Fisher Scientific, UK)
- Halt Phosphatase Inhibitor Cocktail (100X) (Fisher Scientific, UK).
- Pierce RIPA buffer (ThermoScientific, UK).
- Bradford Reagent (Sigma-Aldrich, UK)
- 2x Laemmli Sample Buffer (Biorad, UK)
- PageRuler Prestained Protein Ladder 10-180kDa (ThermoFisher, UK)
- Trizma Base (Sigma-Aldrich, UK)
- Ethylenediaminetetraacetic acid EDTA (Sigma-Aldrich, UK)
- Glycine (Fisher Scientific, UK)
- Mini-PROTEAN® TGX™ Precast Gels (Biorad, UK)
- Trans-Blot® Turbo™ Mini Nitrocellulose Transfer Packs (Biorad, UK)
- REVERT Total Protein Stain (Licor, UK).
- Tween-20 (Fisher Scientific, UK)
- Skimmed Milk Powder (Sigma-Aldrich, UK)
- Restore Western Blot Stripping buffer (Fisher Scientific, UK)
- *Running buffer*: 10X running buffer is prepared by dissolving 30.0 g of Tris base, 144.0 g of glycine, and 10.0 g of SDS in 1000 ml of H_2O. The pH of

the buffer should be 8.3 and no pH adjustment is required. The running buffer is stored at room temperature and diluted to 1X before use.

- *Washing buffer*: 0.3% Tween 20 in PBS, pH 7.2-7.4
- *Blocking buffer*: 5% skimmed milk in PBS- 0.1%Tween 20
- *Antibody solution*: Antibody is dissolved in appropriate dilution in blocking buffer.
- *Pierce ECL Western Blotting Substrate* (Fisher Scientific, UK) has substrate A and substrate B which are mixed in equal proportion just before the development of the blot and around 75-100µl is sufficient for one membrane.

2.2 METHODS

2.2.1 Cell culture

2.2.1.1 Growing conditions

All cells were grown at 37°C in a humidified atmosphere of 5% CO_2, usually in T-75 flasks with a volume of 12 ml of media. Media was renewed two to three times per week. HeLa was grown in RPMI media-1640, HT-3 in McCoy's 5A (modified) media, HK in EpiLife® Medium and CRL-1790 in DMEM Media - GlutaMAX™. For folate conjugation studies, HeLa and KB cell lines were grown in folate free RPMI-1640 media for a minimum of three weeks before experiments' commencement and A549 cell lines in Ham's F-10 Nutrient Mix. All these media (except for HK's EpiLife® media, which was supplemented with Human Keratinocyte Growth Supplement) had 10% Fetal Bovine Serum –FBS and 1% Penicillin-Streptomycin (5000U/ml) added to them. Freezing media for each cell line was additionally supplemented with 10% DMSO. Cells were detached from their surface using Trypsin-EDTA and counted employing Trypan Blue on haemocytometer to distinguish between viable and non-viable cell population.

2.2.1.2 Storage of cells

For long term storage, cells were harvested from the confluent flask using dissociating agent Trypsin-EDTA and centrifuged at 1500 g-force for 3 min. The pellet was re-suspended in freezing medium such that there were 2 million cells/ ml and transferred to

cryogenic vials (Nunc). The vials were stored at -80°C overnight and then transferred to liquid nitrogen tanks.

2.2.1.3 Passaging of cells

The cells were allowed to reach 80% confluence before splitting them in 1:3 ratios. After passage, the cells were transferred to new culture flasks with fresh media.

2.2.1.4 Cell counting

For counting, each flask was firstly washed with 1 ml PBS, followed by adding 2 ml of 0.25% Trypsin – 0.53mM EDTA and incubating at 37 ºC for 2-5 minutes. To stop trypsin action, media supplemented with FCS (volume 3ml) were added to flasks. The trypsin with media was then aspirated into 15ml Falcon tubes and centrifuged for 3 minutes at 1500 rpm. To count the cells, 2 ml of medium was added to the cell pellet and resuspended thoroughly. 20µl of cell suspension was then mixed with 20µl of 0.4% Trypan blue with the help of a vortex in a 1ml centrifuge tube and 20µl of the obtained mix was used for counting on a haemocytometer.

2.2.2 Liposome synthesis and conjugation

Liposomes were composed of soy PC, cholesterol, and methoxypolyethyleneglycol-di-stearoyl-phosphatidylethanolamine at a molar ratio of 53:45:2 mol %. Liposomes were prepared as described elsewhere with slight modifications (Chen et al., 2006). Briefly, the lipids were dissolved in methanol: dichloromethane 1:2 (v/v) at room temperature. The lipid mixtures were deposited on the side wall of the rotary glass vial by removing the solvent with nitrogen. The dried lipid films were hydrated in 730 mM nickel acetate ($Ni(OAc)_2$) aqueous solutions for 1 h with gentle rotation. This process led to the spontaneous formation of multilamellar PEGylated liposomes. The liposome suspension was subsequently subjected to 10 freeze-and-thaw cycles (freezing in liquid nitrogen for 3 min and thawing in 37 °C water bath for 3 min). For different sizes, the liposomes were downsized by passing through 0.1, 0.2 and 0.4-μm Anotop filters (Whatman, UK). Extruded liposomes were dialysed overnight against 10 mM sodium phosphate buffer at pH 7 to get rid of unencapsulated $Ni(OAc)_2$. The nickel acetate encapsulated liposomes were then incubated with 20mM ATO solution at room temperature with gentle rolling for 5 h. The unencapsulated ATO was further removed by dialysis overnight.

Liposomes of different charges were prepared as described above with the exception of positive liposome composition to be PC/Chol/DSPE-PEG_{2000}/DDAB at a molar ratio of 50/33/1/16 and negative liposome composition to be PC/Chol/DSPE-PEG_{2000}/DSPG at molar ratio of 50/33/1/16. The positive and negative liposomes were extruded with 0.1μm Anotop filters. Similarly for conjugated liposomes with PEG-ligand spacer length of 2000MW and 5000MW, PC/Chol/mPEG-DSPE /DSPE-PEG_{2000}-FA and PC/Chol/mPEG-DSPE /DSPE-PEG_{5000}-FA were taken respectively at a ratio of 53/45/1.9/0.1mol% and passed through 0.1μm Anotop filters. Rest of the procedure was the same as the one described above.

2.2.3 Liposome characterisation

The mean sizes and zeta potential of synthesised liposomes were obtained through dynamic light scattering on a Zetasizer-Nano ZS. The concentrations of phospholipids (P), encapsulated arsenic (As) and nickel (Ni) in the liposomes were determined by ICP-OES.

2.2.3.1 Size and zeta potential measurement by Zetasizer

Principle

***Size*:** Zetasizer makes use of DLS technique to determine the size distribution profile of nanoparticles in liquid (Fig 2.2.1) (Pecora, 2000). Also referred to as photon correlation spectroscopy (PCS), it is based on the fact that when light hits small particles, with the particles' sizes comparable to the wavelength of the incident light, it scatters in all directions (Reyleigh scattering). Since small particles in suspension undergo random thermal motion referred to as Brownian motion, the light scattered from a dispersion of such particles interferes (constructively or destructively) on the surface of a square-law detector (Goldburg, 1999). This interference defines the scattering angle and intensity of the scattered beam. The positions of the particles in the medium relative to the incoming and scattering beams determine the phases obtained at the detector. Since, the position constantly changes as a result of Brownian motion, the scattered light also fluctuates (Goldburg, 1999). These intensity fluctuations are used to calculate time correlation function and from that, translational self-diffusion coefficient D of the nanoparticle is calculated (Chu, 2008).

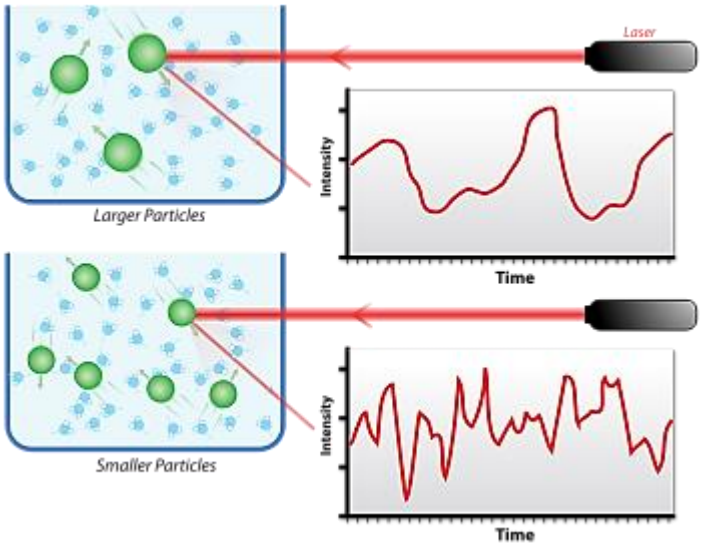

Fig 2.2.1: Hypothetical fluctuations of scattered light from larger and smaller particles; with larger particles generating higher intensity than smaller particles (Kim et al., 2014).

For spherical particles in a dilute dispersion, the obtained translational self-diffusion coefficient D can be used to calculate particle radius R using Stoke-Einstein equation, which is,

$$D = \frac{kT}{6\pi\eta R}$$

where, k is the Boltzmann's constant, T absolute temperature and η is the dynamic viscosity of the dispersing medium (Schmitz and Phillies, 1991). When nanoparticles are polydisperse, as is usually the case, then particles have different self-diffusion translation coefficients. In those instances, a cumulant method is used to calculate the sum of exponentials, which provides a size distribution range of the particles (Goldburg, 1999).

Zeta Potential: Apart from the hydrodynamic size, Zetasizer can also calculate zeta potential of the particles in suspension. Zeta potential is the net electric charge of a particle in dispersion within a region bound by the slipping plane (Fig 2.2.2)

(Bhattacharjee, 2016). Briefly, a charged particle in a suspension attracts oppositely charged ions, the closer ones are tightly bound by the particle, while the farther ones are loosely bound, forming a Diffuse Layer. Theoretically, any ions within this boundary are liable to move with the particle while the ions outside will stay where they are. This notional boundary is called Slipping Plane (Bhattacharjee, 2016). The potential at the Slipping Plane is called the zeta potential, which is indicative of the charge of the particle. Zeta Potential is determined using a combination of two techniques: Laser Doppler Velocimetry and Electrophoresis which measures velocity of a particle in a liquid when electric field is applied (Bhattacharjee, 2016).

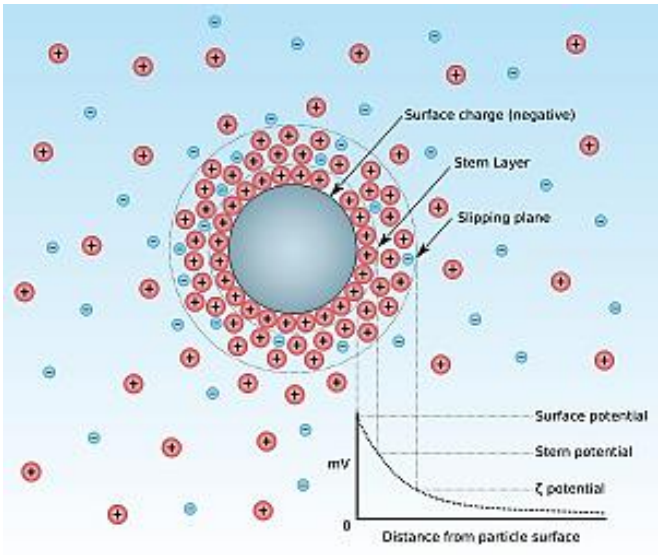

Fig 2.2.2: Illustration of potential difference and ionic concentration as a function of distance from the charged surface of the particle dispersed in a medium (Contributors, 2018).

Zeta potential is a key indicator of stability of colloidal dispersions (Bhattacharjee, 2016). High zeta potential (positive or negative) values are indicative of high electrostatic repulsion between adjacent, similarly charged particles in dispersion. If the zeta potential values are low, the repulsive forces may be weak and easily overcome by

the attractive forces, leading to the coagulation of the particles in the colloid (Bhattacharjee, 2016).

Instrumentation

A typical Zetasizer installation has the following components as depicted in Fig 2.2.3 (a). The optical set up for DLS is shown in Fig 2.2.3 (b). After the light illuminates the sample from a laser source, it gets scattered which is collected, either at a 90 degree (right angle) or 173 degree (back angle) scattering angle. Only liquid refractive index and viscosity needs to be known for interpreting the measurement results.

(a)

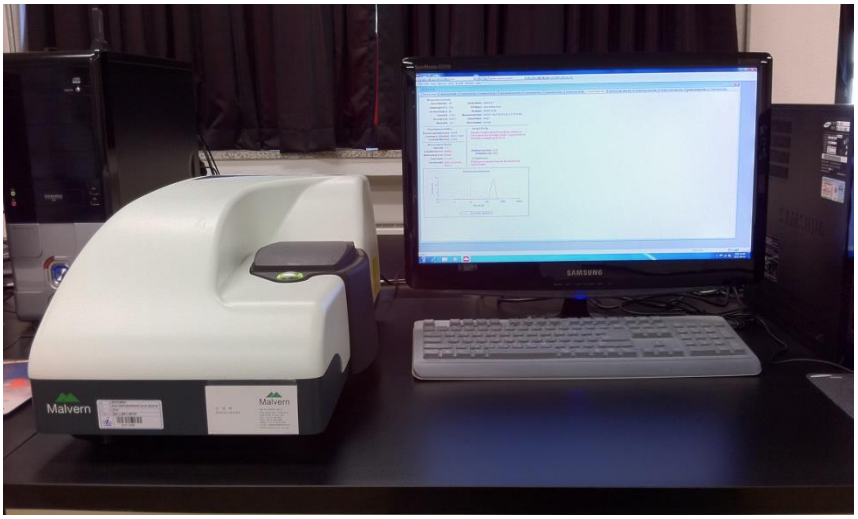

(b)

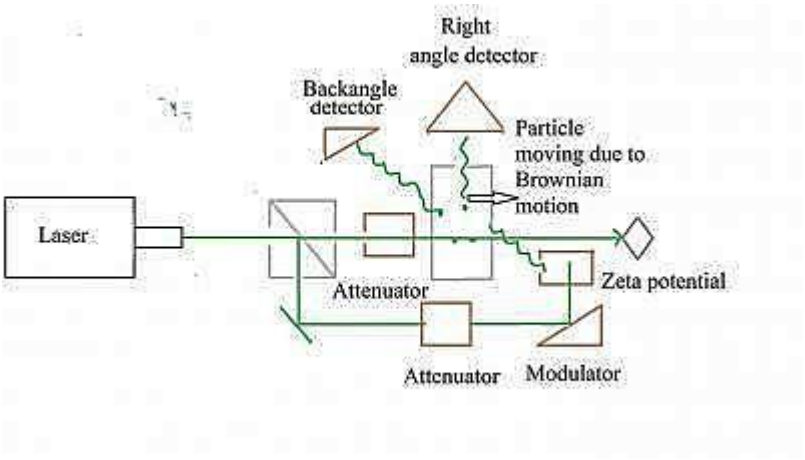

Fig 2.2.3: (a) Representation of a typical DLS instrument, (b) Optical setup for DLS nanoparticle size and zeta potential analyser (Bose, 2016).

Protocol

The process of taking a measurement from Zetasizer is very straightforward. The sample is introduced in the optical unit in a clear cuvette and then the Zetasizer software can be used to either run a manual or standard operating procedure (SOP) measurement. However, care should be taken for sample preparation. The particle concentration should not be too low in case that scattered light will not be picked up by the detector. The concentration should also not be high to avoid multiple scattering (Bhattacharjee, 2016). For size measurements, the liposomes diluted in PBS with 1:100 ratio gives the appropriate reading with 500µl total volume. The PBS needs to be filtered to remove dust particles which might give additional peaks and interfere with the results. For zeta potential, liposomes need to be diluted in the same ratio in deionised water to get the readings in 1ml final volume.

2.2.3.2 Loading efficiency of arsenic and time/ pH stability studies of liposomes by ICP-OES

Principle

ICP-OES is a versatile analytical technique for the detection of trace metals. It is a type of emission spectroscopy that utilises inductively coupled plasma to generate excited atoms or ions which emit electromagnetic radiation at wavelength characteristic to the particular element (Principle of ICP Optical Emission Spectrometry (ICP-OES), 2018). The excitation temperatures are generated using inert gas Argon using flame technique which generates a temperature of 5000K to 7000K, capable of exciting many elements.

This optical emission spectroscopy is based on the principle that when a sample is imparted plasma energy, its individual components (atoms) are excited and while returning to their low energy state, they emit radiations of wavelength specific to the element, which is measured and analysed. The radiation's intensity corresponds to the amount of each element present in the sample.

Instrumentation

A typical schematic representation of ICP-OES is shown in the Fig 2.2.4.

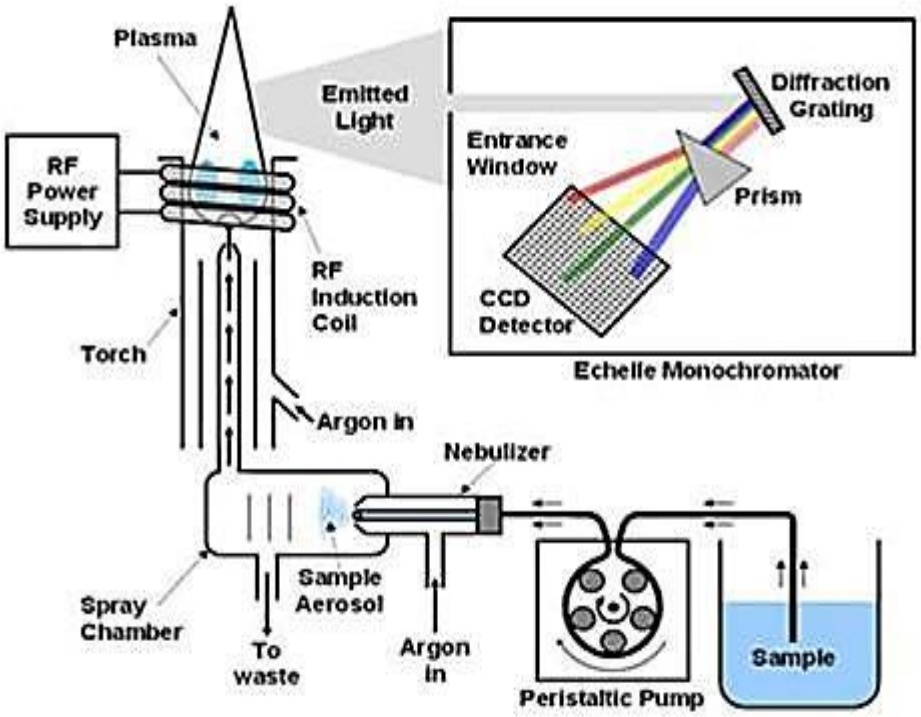

Fig 2.2.4: Diagram representing the various components of ICP-OES including torch generating plasma, nebuliser, peristaltic pump and spray chamber (Haung and Hieftje, 1989)

According to its name, ICP-OES has two principle components, ICP torch and optical spectrometer. The ICP torch consists of three concentric quartz glass tubes, around which the work coil of radiofrequency (RF) generator is wound (Rezaaiyaan et al., 1982). When the torch is turned on, high frequency electric current flows through the work coil at the tip of the torch tube which generates electromagnetic field (Principle of ICP Optical Emission Spectrometry (ICP-OES), 2018). To this torch coil, argon gas is applied which get ionised, generating plasma of high electron density and temperature of the magnitude of 10000K as a consequence of inelastic collisions between charged ions and neutral argon atoms (Haung and Hieftje, 1989). This energy is used in the

excitation-emission of the sample. A peristaltic pump introduces the solution samples into a spray chamber through an analytical nebuliser where the sample is turned into mist and fed to the plasma torch (Haung and Hieftje, 1989). The high temperatures cause the individual molecules to be broken down to their respective atoms and lose electrons and when they recombine, they give off radiation in the wavelength characteristic of the element (Fig 2.2.4) (Haung and Hieftje, 1989). The emitted light is focussed on a diffraction grating, where it is separated into its individual component wavelengths in the optical spectrometer. The separated wavelengths fall upon an array of semiconductor photodetectors such as charged coupled devices (CCD) which are capable of measuring the intensities of all the wavelengths simultaneously, allowing the samples to be analysed very quickly. The intensities are then compared to the intensities of known concentration of the elements and the unknown concentrations are then calculated based on the extrapolation along calibration graph (Charles and Freeden, 1997).

Protocol

Liposome samples were acidified in 2% nitric acid and delivered in 15 ml falcon tubes to the ICP-OES instrument. The concentrations of phospholipids (P), encapsulated arsenic (As) and nickel (Ni) in the liposomes were determined. The molar ratios of As/ P were calculated and used to determine loading efficiency. Liposomal stability over time was determined by checking the As/ P ratio over a period of 4 weeks when liposomes were stored at 4°C in buffers of pH 7.4. Drug leakage at different pH was studied by dialysing liposomes in buffers of pH 4, pH 7 and pH 10 and assessing their loading efficiency at a period of 1, 2, 4, 6 and 24 h by measuring the As/P ratio of the samples by ICP-OES.

2.2.4 MTT toxicity analysis

Principle

Cytotoxicity of various liposomal formulations of ATO was determined by an MTT Assay as described previously (Lee and Low, 1995). This *in vitro* assay is based on the principle that tetrazolium salts can be reduced to a different coloured formazan in living cells. Metabolically active cells reduce the yellow tetrazolium salt MTT by the action of dehydrogenase enzymes to generate reducing equivalents such as NADH and NADPH. The resulting intracellular purple formazan is solubilized and quantified by spectrophotometric means. Through this assay, a linear relationship between cell number and optical density signal produced is established, which allows an accurate quantification of changes in the rate of cell proliferation.

Protocol

Briefly, the experiments were set up in 96 well plates, where the toxicity of control empty and ATO encapsulating liposomes of varying sizes, charges and compositions were investigated. Around 30,000 cells were seeded per well in 100µl media and allowed to attach overnight. Next day, the cells were treated with liposomes in varying dilutions for different time periods and at the end of the treatment, the spent media was removed carefully and 50µl of MTT solution was added per well. Cells were further incubated for 30 minutes at 37°C with 95% O_2 and 5% CO_2. MTT solution was then removed and 100µl propanol was added per well for at least 30 minutes incubation at 37°C to dissolve crystals. The absorbance of this coloured solution was quantified by measuring at a wavelength of 570 nm from BMG LabTech FLUOstar Omega Plate Reader.

2.2.5 Flow Cytometry studies for apoptosis, cellular protein expression and liposomal uptake

Principle

Flow cytometry is a popular biophysical technique that employs laser technology to count, sort and profile cells in a heterogeneous fluid mixture. In a flow cytometer, the cells in a liquid stream pass in a single file through a laser light beam and their interaction with the light is detected by a detector either as light scatter or fluorescence intensity (Vladimir et al., 2007). It is also a quantitative technique as when a fluorescent label is bound to a cellular component, the fluorescent intensity detected, represents the concentration of that particular component.

Flow cytometry is a powerful tool because it allows simultaneous multiparametric analysis of the physical and chemical characteristics of up to thousands of particles per second. This makes it a rapid and quantitative method for the analysis of cells in suspension. In a conventional flow cytometry, forward-scatter, side-scatter, and fluorescent signal are detected from different filters and electronical data are collected. The diagram below illustrates the general procedure of a typical flow cytometry set up (Fig 2.2.5).

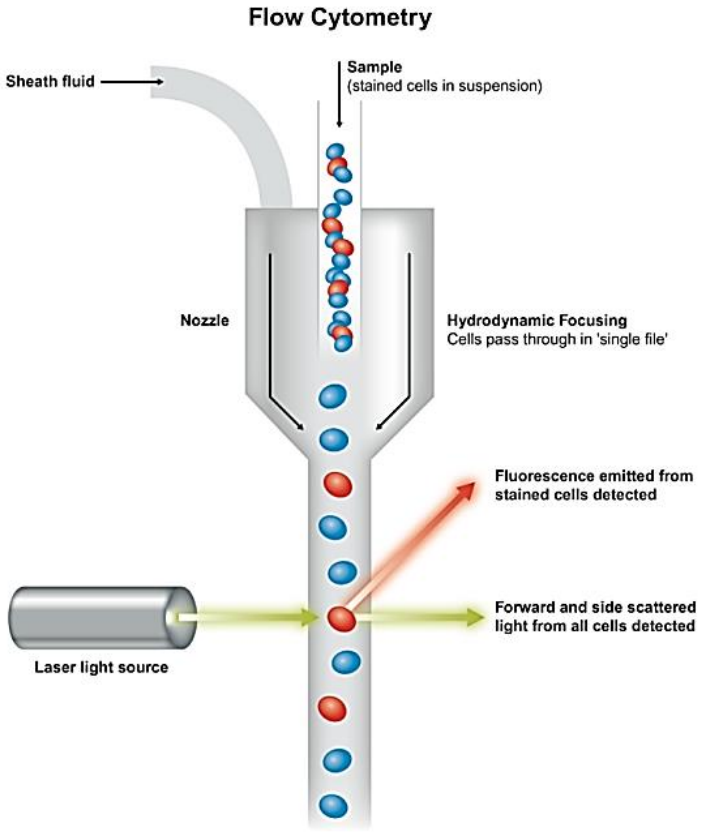

Fig 2.2.5: Illustration of a flow cytometry experimental set up (Flow cytometry, no date.)

This technique is especially useful when specific biomarkers presented on the cellular surface, the expression of proteins and apoptosis induced in the cells after a certain treatment need to be determined.

Apoptosis analysis

Apoptosis is genetically programmed cell death in eukaryotes which is crucial during embryogenesis, in immune response development, maintenance of homeostasis and tumour regression (Wyllie, 1997). During the early stages of apoptosis, certain signals activate a family of proteins known as caspases in the cells. These enzymes cleave key cellular substrates necessary for cellular functions such as nuclear proteins and structural proteins in cytoskeleton (Riccardi and Nicoletti, 2006). This brings about a number of morphological and distinct biophysical changes in the cells such as plasma

membrane blebbing or its loss of plasma membrane symmetry, nuclear condensation and internucleosomal DNA cleavage (Arends, Morris and Wyllie, 1990). In essence, the loss of plasma membrane symmetry is one of the earliest hallmarks of apoptosis. During the induction of apoptosis, the membrane phospholipid phosphatidylserine (PS) which is usually present in the inner leaflet of the plasma membrane translocates to the outer side, exposing itself to the external cellular environment (van Heerde et al., 2007). Annexin V is a 35-36 kDa phospholipid-binding protein which has a high affinity for PS. Hence, Annexin V binds to the exposed apoptotic cell surface PS (Vermes et al., 1995). Annexin V is usually conjugated with fluorochromes (for instance, FITC) and hence, it can serve as a sensitive probe for flow cytometric analysis of early apoptotic cells (van Heerde et al., 2007).

PS translocation is usually followed by a loss of membrane integrity either from apoptotic or necrotic processes. Hence, another dye such as propidium iodide (PI) is used in conjunction with Annexin V to distinguish between cellular populations undergoing early or late apoptosis. Viable cells undergoing early apoptosis have intact membranes, so they bind to Annexin V but exclude PI, whereas the membranes of damaged cells are permeable to PI. Therefore, viable cells are both Annexin V and PI negative, early apoptotic cells are Annexin V positive but PI negative and late apoptotic or necrotic cells are both Annexin V and PI positive (van Heerde et al., 2007). This process is illustrated in the fig 2.2.6.

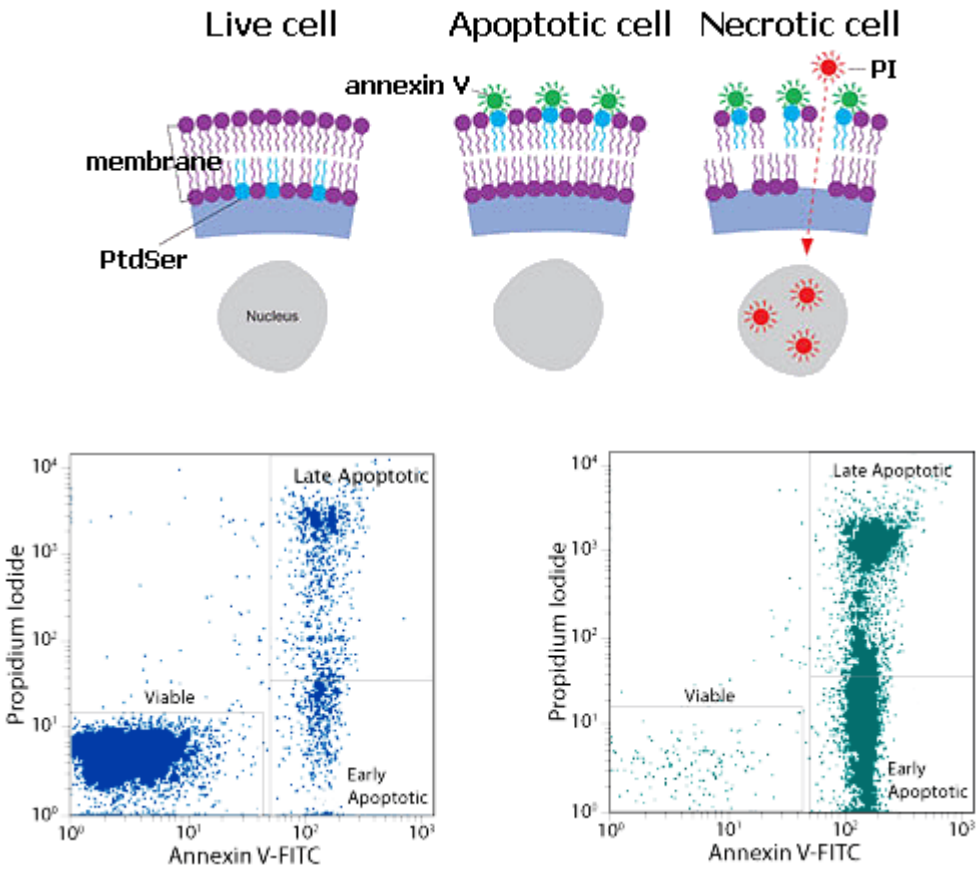

Fig 2.2.6: Illustration showing healthy and apoptotic cells with markers for detection of apoptosis and flow cytometric analysis of such cell populations before and after the apoptosis inducing treatment (Apoptosis, no date).

Protein analysis

It works on the principle that when antibodies are conjugated to fluorescent dyes, they can bind to specific proteins either on the cell surface or intracellularly. When such fluorescently labelled cells pass through the laser, the fluorescent molecules are excited to higher energy state, which emit radiations upon returning to their ground state, capable of being detected at specific filters (Shapiro, H. M., & Darzynkiewicz, Z., 1995).

Cellular uptake studies of fluorescent liposomes

Labelling liposomes by coupling a fluorescent dye with their membrane component or encapsulating a fluorescent compound within their lumen can allow us to analyse the amount of fluorescent liposomes taken up by the cells through flow cytometry (Ducat et al., 2007). Following laser excitation, each cell emits fluorescence characteristic of the dye used to label the liposomes, allowing for the analysis of fluctuations in brightness (Cram, 2003).

Instrumentation:

A flow cytometer has three main components: fluidics, optics and electronics (Ãlvarez-Barrientos, 2000). The first component has a flow cell where the sample fluid is injected. The sheath fluid carries and aligns the cells in a single file through a narrow channel where it can be intercepted with the laser beam. The optics component has a laser light source and various filters and light detectors. Lasers are available at different wavelengths ranging from ultraviolet to far red and have a variable range of power levels. The interaction with the laser light causes a compatible fluorophore to excite and then fluoresce at a certain wavelength. The detector in the front measures forward scatter (FSC) while the detectors to the side measure side scatter signals (SSC). Fluorescence detectors measure the fluorescence intensity from the positively stained cells. These light signals are converted to data by the electronics system that can be visualized and interpreted by software (Adanet al., 2017). The diagram below illustrates the parts and setup of a typical flow cytometer instrument BD FACSCalibur (Fig 2.2.7).

Fig 2.2.7: Representation of a BD FACSCalibur flow cytometer

Protocol

Apoptosis analysis

Cells from different cell lines were seeded at 5×10^5/ml in six-well culture plates and grown overnight for the cell attachment. Desired treatments were applied to the cells. After appropriate time interval, the cells were washed twice with PBS, trypsinized, washed again by PBS twice and then collected into 15-ml centrifuge tubes for further staining. The cells were re-suspended in 500µl Annexin-V binding buffer before incubating them with 5µl FITC- conjugated Annexin-V and 5µl PI according to the protocol described for the product. All samples were analysed within 1 h of PI staining using FACSCalibur. Excitation was done at 488 nm and the emission filters used were 350nm FL1 detector (Annexin V-FITC) and FL3 detector for PI. A minimum of 10000 cells per sample were analysed. Electronic compensation was used to eliminate bleed through of fluorescence. Data analysis was performed with the standard CellQuest Pro software where percentages of events in each quadrant were calculated from the scatterplot to analyse the cellular population undergoing early or late apoptosis.

Protein expression analysis

Cells were grown in T-75 flasks till they attained confluency. After being treated for the intended duration of time, they were harvested with trypsin followed by centrifugation to collect them. The obtained cell pellet was resuspended in media and counted to collect around two million cells in separate Eppendorf tubes. The tubes were again centrifuged at 1500rpm for 3 min and resuspended in 4% formaldehyde at 37°C for 10 min to fix the cells. The tubes with the cell pellets were chilled on ice for 1 minute. The cells were pelleted by centrifugation, the fixative removed and resuspended in 90% methanol for 30 min on ice to permeabilise the cells. The cells are centrifuged and washed once with incubation buffer containing 0.5% BSA in PBS. The cells are blocked in the same incubation buffer for 10 minutes at room temperature. Primary antibody is added to each assay tube at an appropriate dilution and incubated for 1 hour at room temperature. After washing the cells in the incubation buffer once, the cells are incubated with fluorochrome- conjugated secondary antibody diluted in incubation buffer, for 30 minutes at room temperature. The cells are washed once with incubation buffer, resuspended in 0.5 ml PBS and analysed on flow cytometer. The fluorescence intensity observed by flow cytometry corresponds to the amount of proteins present in the sample. A histogram of the fluorescence intensity was plotted and the percentage total of cells staining for the protein for each cell type was compared.

Cellular uptake of fluorescent liposomes analysis

Briefly, the experiments were set up in 6 well plates, where the cellular uptake of non-targeted and targeted liposomes of varying ligand PEG spacers were investigated. Around 1 million cells were seeded per well in 1 ml media and allowed to attach overnight. The cells were drugged with 9μM liposomes for 2 h, 6 h and 24 h and were washed twice with PBS. The cells were trypsinised and the cell pellet obtained was washed again. The cells were centrifuged to obtain a pellet which was resuspended in 500μl ice cold PBS and analysed. The fluorescence intensity of the samples were analysed and the histograms obtained of targeted liposomes were compared with that of non-targeted liposomes to draw a comparative study of any enhancement in cellular uptake resulting from liposomal targeting.

2.2.6 ICP-MS uptake studies

Principle

Inductively Coupled Plasma-Mass Spectrometry is perhaps the fastest growing analytical technique for trace elements determination. It is capable of carrying out rapid multi-element determinations at the ultra-trace levels (Thomas, 2013). ICP-MS has a clear advantage over ICP-OES with its superior detection limits and isotopic capabilities. An ICP-MS combines a high temperature ICP (Inductively Coupled Plasma) source with a mass spectrometer. The ICP source converts the atoms of the elements in the sample to ions. These ions are then separated and detected by the mass spectrometer (Thomas, 2013).

Instrumentation

The main components of ICP-MS are nebuliser, spray chamber, plasma torch and detector (Fig 2.2.8). The sample, usually in the liquid form, is pumped into the nebuliser with a peristaltic pump, where it is converted into a fine aerosol with argon gas. The spray chamber separates the fine droplets of the aerosol containing 1-2% of the sample from the larger droplets. The fine aerosol emerging from the spray chamber is transported into the plasma torch via a sample injector (Thomas, 2013).

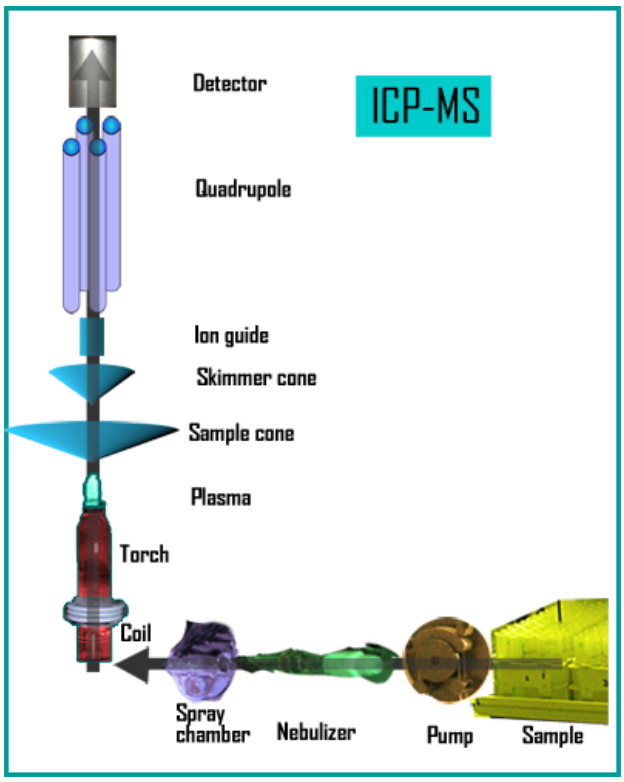

Fig 2.2.8: Schematic representation of ICP-MS instrument (ICP-MS, no date)

The plasma is formed in exactly the same way as ICP-OES, by the interaction of argon gas with an intense magnetic field produced by RF passing through a copper coil through ICP torch. However, this is where the similarity ends. In ICP-OES, whereas the plasma is used to generate photons of light, in ICP-MS, it is used to generate positively charged ions and not photons. In fact, every attempt is made to stop the photons from reaching the detector because they have the potential to increase signal noise. It is the production and the detection of large quantities of these ions that give ICP-MS its characteristic low parts per trillion (ppt) detection capability—about three to four orders of magnitude better than ICP-OES (Thomas, 2013).

Once the ions are produced in the plasma, they are directed into the mass spectrometer via the interface region, which consists of two metallic cones, called the sampler and a skimmer cone, each with a small orifice (0.6–1.2 mm) to allow the ions to pass through to the ion optics. The ion optics serves the purpose of electrostatically focusing the ion beam towards the mass separation device while stopping photons and neutral species

from reaching the detector. The most commonly used mass separation devices are quadrupole, magnetic sector, time of flight, and collision/reaction cell technology, which serve the common purpose of allowing analyte of a particular mass to charge ratio through to the detector while stopping the interfering ions. The final process is to convert the ions into an electrical signal with an ion detector (Thomas, 2013). The basic instrumentation of ICP-MS is depicted in the following Fig 2.2.9.

Fig 2.2.9: A Thermo Scientific X-Series 2 ICP-MS instrument.

Protocol

For the analysis of cellular uptake of liposomal arsenic via ICP-MS, cells from different cell lines were seeded into 75-cm^2 flasks at a density of 1×10^6 cells/flask, with two flasks for each treatment as a doublet. Following a 24-h cell attachment, cells were treated with appropriate liposomal formulation or free arsenic. After incubation for the desired time interval, cells were washed by PBS, trypsinized and counted before they were collected into Falcon tubes for further analysis. Cells were extracted by adding 1 ml of nitric acid while vortexing and heated at 90°C for ten minutes to further complete the digestion. The cellular extract was topped up with deionised water in the ratio similar to ICP-MS matrix and arsenic concentration analysed using ICP-MS. The concentration of arsenic was corrected by cell number and total volume accordingly.

2.2.7 Immunocytochemistry

Principle

Immunocytochemistry (ICC) is a common laboratory technique that is used to visualise the location of specific proteins in cells by exploiting the specific epitope-antibody interactions. Briefly, the cells are attached to a solid support such as a coverslip and then fixed with either 4% paraformaldehyde or ice-cold methanol to preserve tissue morphology and retain the antigenicity of the target epitope. After fixation, the cells have to be blocked with a blocking reagent such as goat serum or bovine serum albumin to prevent non-specific interactions, i.e. binding of the primary antibody to amino acids other than those within the desired epitope of the antigen. These steps are performed prior to incubation of the sample with the primary antibody. Following incubation with the primary antibody, antibody binding is visualized using an appropriate detection system. The method of detection can be direct or indirect, and may generate a fluorescent or chromogenic signal depending on the substrates and conjugated signal tag. Direct detection involves the use of primary antibodies that are directly conjugated to a label. Indirect detection methods utilise a labelled secondary antibody raised against the primary antibody host species (Fig 2.2.10) (Paul, 2003). Indirect methods can also include amplification steps to increase signal intensity. The most common amplification method used in ICC is Avidin-Biotin complex (ABC) method.

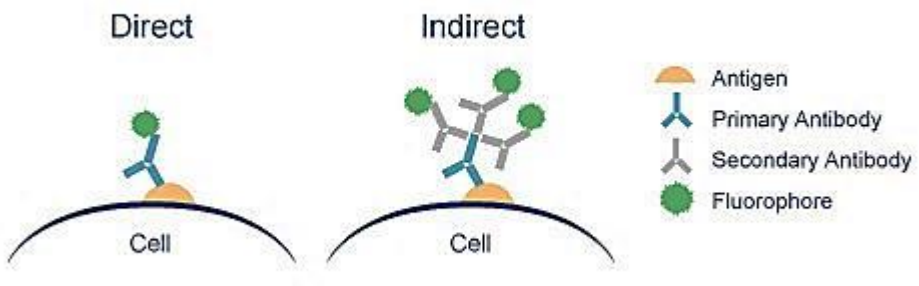

Fig 2.2.10: Indirect and direct detection in ICC (Direct vs indirect immunofluorescence, no date)

ABC method takes advantage of the fact that Avidin, a 68 kDa glycoprotein in egg white, has a strong affinity for Biotin. Biotin is a low molecular weight vitamin that can be conjugated to a variety of biological molecules such as antibodies (Hsu, Raine and Fanger, 1981). Avidin is labelled with peroxidase or fluorescein. If a biotinylated secondary antibody is employed, the signal can be significantly amplified by subsequent incubation with an Avidin-Biotin complex.

For the visualization of epitope-antibody interactions, commonly used labels include fluorophores and enzymes that convert soluble substrates into insoluble, chromogenic end products.

Fluorescent staining

Fluorescence staining is based on the principle that a fluorochrome, conjugated to the primary or secondary antibody, emits light when excited by light of shorter wavelength. Immunofluorescence cytochemical staining is a powerful technique for the simultaneous visualisation of multiple cellular targets. For that purpose, fluorochromes should be chosen that emit light of different wavelength and the primary antibodies should be derived from different species to avoid cross-reactivity. The excitation and emission wavelengths for fluorescent markers used in this study are presented in Table 2.2.1.

Table 2.2.1: The excitation and emission wavelengths of fluorophores used in the study.

Fluorochrome	**Excitation wavelength**	**Emission wavelength**	**Colour**
Cy-5	650nm	667nm	Red
Fluorescein Isothiocyanate (FITC)	490nm	520nm	Green
4',6-diamidino-2-phenylindole (DAPI)	372	456	Blue

The slides are then visualised with confocal microscopy. For amplification of fluorescent signals, Tyramide Signal Amplification (TSA) detection method might also be used that utilises the catalytic activity of horseradish peroxidases (HRP) to activate multiple copies of dye labelled tyramide. (Fig 2.2.11) This signal amplification caused due to multiple tyramide substrate activation per peroxidase label results in ultrasensitive detection of low-abundance targets and the use of smaller amounts of antibodies and hybridization probes.

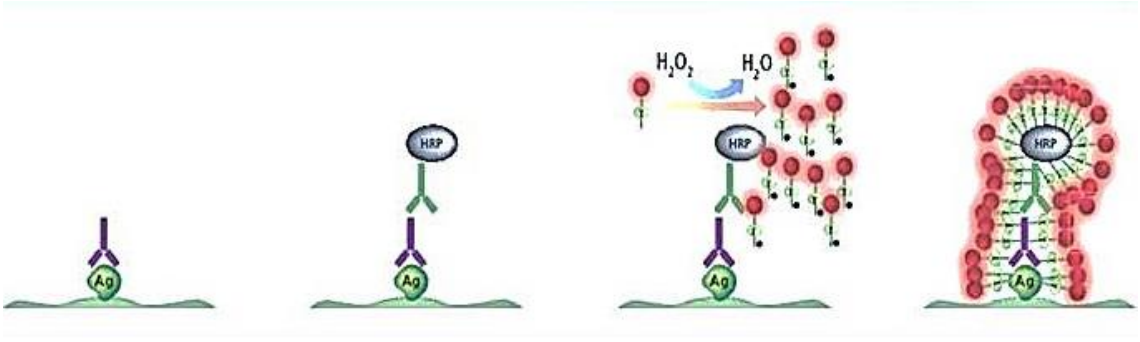

(a) (b) (c) (d)

Fig 2.2.11: TSA signal amplification method (McCloughlin, 2016). (a) Incubation with primary antibody (b) secondary antibody incubation with HRP (c) Incubation with TSA reagent where HRP catalyses formation of TSA free radicals and (d) TSA free radicals form covalent bonds with tyrosine residues proximal to HRP causing signal amplification.

Chromogenic staining

For chromogenic staining, an enzyme is conjugated to either primary or secondary antibody. When a suitable soluble organic substrate is added, the enzyme which is conjugated with the bound antibodies will react with the substrate and generate an insoluble, coloured product. This coloured product is localised to the sites of relevant protein expression. One of the most commonly used enzymes is Horseradish Peroxidase (HRP) which catalyses the oxidation of 3, 3′-diaminobenzidine (DAB) reagent into a dark brown precipitate (Fig 2.2.12). A counterstain is employed along with DAB such

as haematoxylin to stain cellular nucleus. Chromogenic staining is more sensitive than immunofluorescence albeit less convenient due to the necessity of more incubation steps and blocking. Additionally, DAB precipitate is not sensitive to light and can be stored for many years. It also requires only a common light microscope rather than a fluorescent microscope for fluorescent staining (Immunohistochemical Staining Methods, 2013).

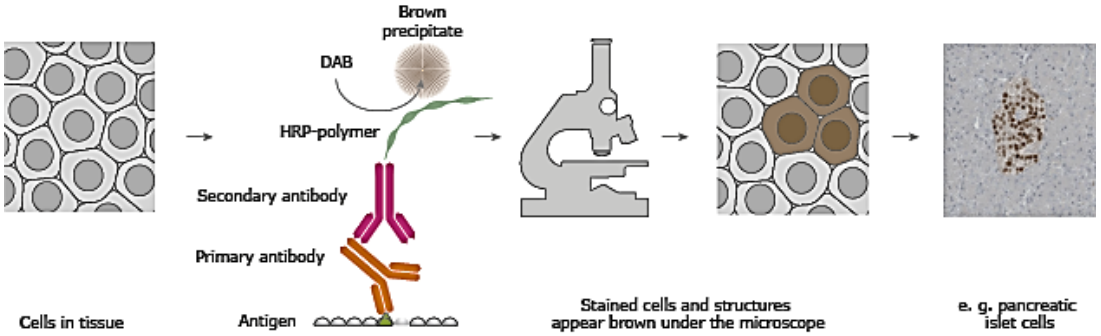

Fig 2.2.12: Principle of chromogenic staining with DAB substrate (Immunohistochemistry, no date).

Protocol

Fluorescent staining

The cells were counted and seeded at a density of 5×10^4/ml on sterile cover slips placed in six-well plates. The cells were grown for overnight attachment followed by washing and fixation with 4 % paraformaldehyde in PBS for 8 mins. 0.1% Triton in PBS was then applied for 7 mins to permeabilise cellular membranes in instances where detection of intracellular proteins was desired, but this permeabilisation step was skipped if surface antigens had to be probed. Unspecific antigenic binding were blocked with 50% horse serum for 8 min before the primary antibody was applied for 90 min at room temperature, which was followed by 30 and 20 min of secondary and tertiary

antibodies respectively, using an ABC universal kit. Visualisation of the desired antigen was made using a Tyramide Signal Amplification (TSA) Cyanine 5 or Fluorescein System. Cover slips were then washed in PBS and mounted on slides using anti-fade mounting media with DAPI and kept for 15 min in dark before examination. The fluorescence emitted from each slide was observed via a confocal microscope and images were recorded accordingly.

Chromogenic staining

For chromogenic staining, a similar protocol was followed as in fluorescent staining till the tertiary antibody incubation from the ABC universal kit. Following that, DAB reagent was applied for 1-2 minutes and washed with PBS as soon as the dark brown precipitate formation was observed. Slides were then counterstained with haematoxylin for 5 mins, followed by a quick rinse in acid alcohol to differentiate and then left in running tap water for 5 mins. The slides were mounted using immunomount and observed under a light microscope and images were recorded accordingly.

2.2.8 Western blot

Principle

Western blotting, also referred to as immunoblotting, is a widely accepted technique to detect specific proteins in a given sample. It employs sodium dodecyl sulphate-polyacrylamide gel electrophoresis (SDS-PAGE) to separate various proteins in a given sample based on the length of their polypeptide following their denaturation. The separated proteins are transferred onto a matrix (usually nitrocellulose or PVDF) and probed with antibodies specific to the target protein. A secondary antibody raised against the primary antibody host species and conjugated to HRP is used which gives a signal in the form of a "band", capable of being analysed. By analysing location and intensity of the band, expression of the target protein in the given cell samples can be determined (Hall, 2004).

Western blot probing involves three major processes: SDS-PAGE, protein blotting and probing.

SDS-PAGE

SDS-PAGE entails the electrophoresis technique based on the principle that under the influence of an electric field, charged particles move towards the opposite electrodes. This results in separation of proteins as their electrophoretic mobility depends on charge, molecular size and structure. Polyacrylamide gel (PAG) is a three dimensional polymer network prepared by free radical polymerisation of acrylamide and a cross linker bisacrylamide, initiated by ammonium persulfate and under the catalytic effect of tetramethylenediamine (TEMED). PAG is a versatile supporting matrix and has multiple electrophoretically desirable features including its being synthetic, transparent, strong, chemically inert and thermo-stable (Kinoshita, Kinoshita-Kikuta and Koike, 2009). It is also amenable towards being prepared with a wide range of pore sizes (Kinoshita, Kinoshita-Kikuta and Koike, 2009).

In the presence of SDS, which is an anionic detergent, electrophoretic mobility is based on molecular weight instead of charge and size of the protein. This is owing to the fact that SDS denatures the proteins and breaks their secondary and tertiary structures by breaking hydrogen bonds between and within the molecules. Stronger reducing agent such as mercaptoethanol further disrupts the disulphide linkages between cysteine residues. These reducing agents linearize the proteins and impart a negative charge to them. This negative charge imparted to the protein molecule due to the binding of SDS causes proteins to unfold into a rod-like shape, with the length proportional to the molecular weight of the protein. The samples are further heated at 90°C which further promote SDS binding and rod-shape formation of the proteins. Bromophenol blue dye is added to the sample to track the movement of protein solution through the gel during the electrophoretic run. As the voltage is applied, the negatively charged proteins-SDS molecules migrate towards the positive electrode in the lower chamber, with proteins of small molecular weight migrating faster than the heavier protein molecules (Fig 2.2.13) (Reisinger and Eichacker, 2007).

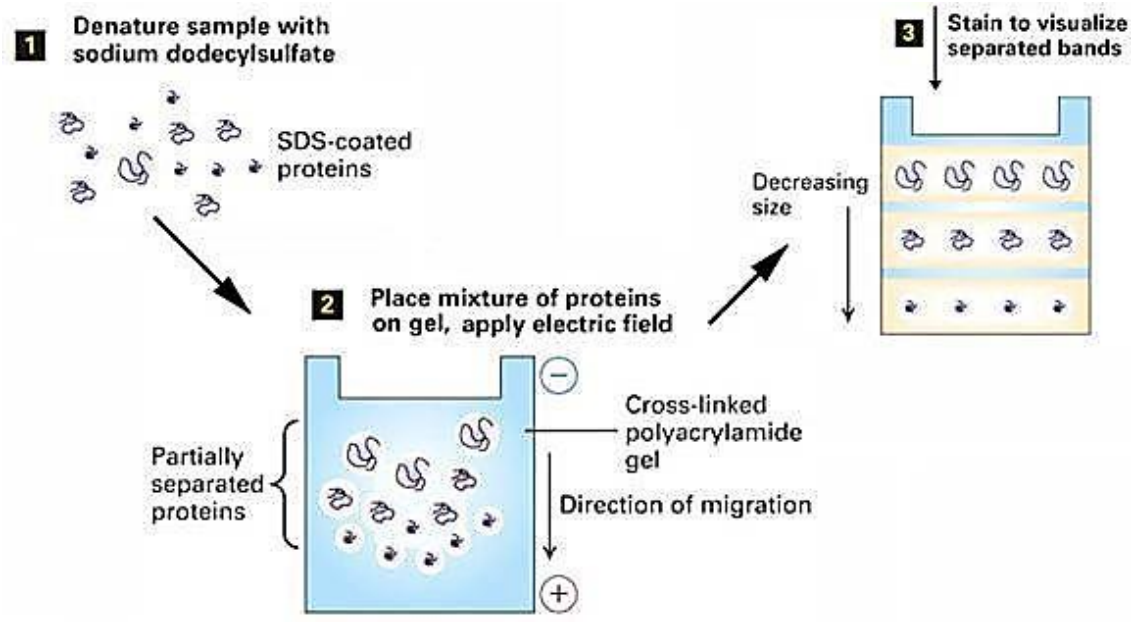

Fig 2.2.13: Illustration of the principles of SDS-PAGE (Molecular Weight Determination of Protein Extracts – Background, no date)

Protein Blotting

Proteins are blotted from the gel onto a membrane, usually made of nitrocellulose (NC) or polyvinylidene difluoride (PVDF) (Fig 2.2.14). NC membranes of 0.45 µm pore size are usually chosen for proteins with molecular weight over 20kDa. Transfer methods are mostly of two types: semi-dry transfer and wet transfer. In the semi-dry transfer, Filter-Gel-Membrane-Filter sandwich is loaded with transfer buffer and the transfer process occurs by current conduction produced by transfer buffer.

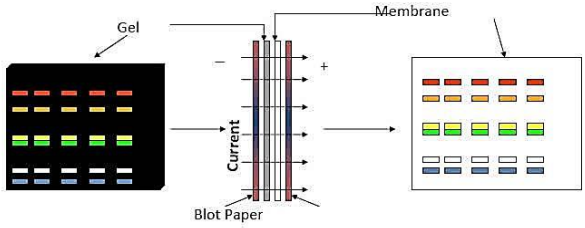

Fig 2.2.14: Transfer of separated proteins from the gel to the membrane (Western Blot Illustrated Assay, no date)

Protein probing

There are four principle steps in the protein probing on nitrocellulose membrane: blocking, primary and secondary antibody incubation, protein detection and analysis. To probe for a specific protein, it is crucial to first block the unreacted sites on the membrane to reduce the amount of non-specific binding during subsequent steps of antibody incubations. Blocking buffers should block all the non-specific sites, must not bind to the epitope of the target protein or cross-react with the antibodies or detection reagents. Typically 5% non-fat dry milk in PBT-T or TBS-T (Tween-20) is the most economic choice. Following the blocking step, the membrane is incubated with a primary antibody specific to the target protein. Membrane is washed to remove the unbound primary antibodies and further incubated with a secondary antibody conjugated to an enzyme, usually HRP. Following the washing steps to again remove unbound secondary antibodies, a substrate specific to the enzyme conjugated to secondary antibody is applied to the membrane. The enzyme converts the substrate to a

coloured product which shows as a visible protein band on the membrane (Fig 2.2.15) (Kurien and Scofield, 2006).

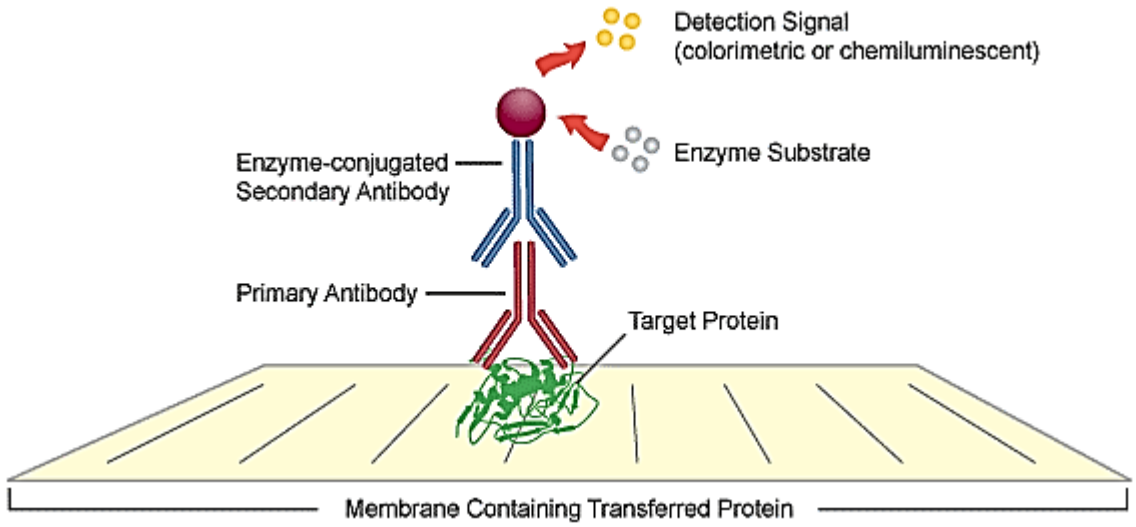

Fig 2.2.15: The probing of membrane for the protein of interest via primary and secondary antibody incubation and detection (Bhandari, 2017).

Protocol

Protein extraction

Cells were seeded and grown overnight in 25cm^2 flasks and incubated with desired treatments for pre-determined length of time. Following the treatment step, cells were washed twice with ice cold PBS and lysed with RIPA buffer and protease inhibitor cocktail at a concentration of 1 ml: 10µl per 1-10×10^6 cells for 30 min at 4°C. Cell lysate was collected with a cell scraper and cleared of cell debris by centrifugation at 10000g for 10 min at 4°C. The cell lysates were either stored at -80°C or quantified for protein amount as the next step in Western blotting.

Protein quantification

Protein concentration was determined by Bradford Assay. Briefly, protein standards were prepared with 2mg/ml BSA stock solution at a range of 0.1-1.4 mg/ml and 5µl of the standards were added to the wells of 96 well plate. 5µl of lysates of cell samples were also added as the unknown samples along with dionised water as control buffer. 250µl of Bradford reagent was added to all the wells, mixed on a shaker for 30 sec and incubated further for 2 min. The absorbance was read at 595nm on FluoStar Omega BMG Plate Reader and the concentration of unknown samples was calculated with the curve obtained after plotting the net absorbance vs protein concentration of the standards.

Protein probing via Western Blotting technique

After calculating the concentrations, samples containing 30µg of protein for each lysate was mixed with reducing loading buffer, separated on an SDS-12% polyacrylamide gel and transferred to nitrocellulose membrane. Total protein quantification for normalisation was done using REVERT total protein staining technique by incubating the membrane with the stain for 5 min, imaging it at 700nm channel on Licor Odyssey Imaging system. Nitrocellulose membranes were then blocked with 5% non-fat dry milk in PBS containing 0.3% Tween 20 for 1 h. It was incubated overnight with primary antibody and anti-β-actin as a loading control (in instances where REVERT total protein stain quantification was not performed) at 4°C. After intensive washings with PBS containing 0.1% Tween, membrane was incubated with HRP conjugated secondary antibody for 1 h at room temperature. After repeated washings, detection was performed with ECL.

2.2.9 Statistical analysis

Statistical analysis described in experimental sections was done with Minitab17. Statistical significance was determined by 2-sample t-test. $P < 0.05$ was considered as statistically significant difference. For flow cytometry, statistical analysis was carried out automatically through BD Calibur software provided. Mean and coefficient of variation (CV) were calculated accordingly. For results from Western blotting studies, the signals were normalised using Image J software and mean and SD calculated. For immunostaining results, an average number from positively stained cells in a total of six fields of each sample were calculated and average percentages were recorded.

Chapter 3

RESULTS

3.1 OPTIMISING LIPOSOMES FOR EFFECTIVE DELIVERY OF ARSENIC TRIOXIDE TO HPV POSITIVE CERVICAL CANCER CELLS: SIZE AND CHARGE STUDY

3.1.1 **Introduction**

3.1.1.1 Background

Cervical cancer is linked to high-risk HPV infections, especially the subtypes HPV-16 and HPV-18 (Appleby et al., 2007; Doorbar et al., 2012; Lorusso et al., 2014). Since, the combination treatment of surgery and/or chemoradiotherapy has severe side effects, alternative treatment options are sought that provide better efficacy and specificity with fewer side effects on the surrounding healthy tissues and cells (Ordikhani et al., 2016; Schiffman et al., 2011). Ideally, an anti-HPV agent that can be taken up more specifically by HPV-infected cells is needed because of the crucial role of high-risk HPV infections in the pathogenesis of cervical cancer. In addition, if a drug carrier can deliver the drug to the cancer cells and release it slowly, a consistent flow of medication, which may enhance the therapeutic effect of the delivered drug, could be

maintained. Moreover, the toxic effects on non-HPV-infected surrounding cells and tissues would be reduced.

Our research team along with others have shown that ATO, as a therapeutic drug, has an inhibitory effect on HPV infected cervical cancer cells HeLa and it downregulates HPV's cancer causing genes (Um et al., 2002; Wen et al., 2012). However, conventional chemotherapeutics, including ATO, face severe limitations in clinical utility to treat solid tumours, either due to their inability to reach target tissue in therapeutic drug concentrations or causing systemic toxicities to surrounding healthy organs and tissues (Chang and Yeh, 2012). Nanotechnology-based drug delivery systems can specifically target cancer cells, avoid their healthy neighbours and also prevent its rapid clearance from the body, thereby resulting in an increase of the drug's therapeutic index (Ordikhani et al., 2016; Shi et al., 2010).

Among the many nanocarriers that have been discovered to date, the oldest and most commonly employed nanoparticles are liposomes (Allen and Cullis, 2013; Farokhzad and Langer, 2009; Sercombe et al., 2015). Liposomes are nano-scaled, spherical compartments which surround an aqueous core capable of encapsulating water soluble drug within a phospholipid bilayer. Aided by PEG layer to evade immune response, these long circulating liposomes show improved pharmacokinetics and bio-distribution in clinical trials minimising toxicity to surrounding organs by accumulating within the target tissue (Chang and Yeh, 2012).

One of the initial attempts to form ATO encapsulated liposomes was by hydrating lipids in a concentrated solution of ATO followed by freeze drying (Kallinteri *et al*., 2004). Zhao *et al*. (2008) prepared liposomes encapsulating ATO and intravenously injected them to investigate their therapeutic effect on C6 gliomas established in rat brains. Liposomal preparation led to a five-fold increase in arsenic concentration in rat brains as compared to ATO solutions, along with fewer side effects. It was observed to induce apoptosis and inhibit tumour angiogenesis by interfering in the expression of VEGF. However, the liposomes formulated suffered acute limitations of stability and were stable only for a maximum of three days, which severely hampered their further therapeutic use.

This lack of stability was to be expected as in physiological solutions, ATO is present as neutral arsenous acid, which rapidly diffuses across the lipid membranes (Kallinteri *et al*., 2004). The formulated liposomes hence were highly unstable with a stability life span of around 3 days. The issue of such "leaky liposomes" was solved when Chen *et al.* (2006) utilised the "remote loading phenomenon" to stably encapsulate ATO in liposomes. Arsenic complexes with transition metal ions such as Ni^{II}, Co^{II} and Pt^{II} and form a precipitate. Utilising this property, liposomes formed were first loaded with acetate solution of a transition metal ion, Ni found to be the most efficient, and then ATO was added to the liposomes formulated (Chen *et al*., 2006). Efflux of protonated acetic acid drove ATO to get loaded within the liposomes where it was stably encapsulated with the transition metal ion in the form of a solid, crystalline precipitate (Fig 3.1.1) (Swindell *et al*., 2013).

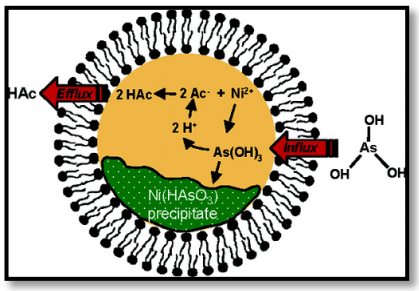

Fig 3.1.1: Schematics of arsenic loading mechanism within a liposome. The external, neutral As $(OH)_3$ diffuses across the membrane and forms insoluble nickel arsenite complex within the liposomes. The protons released associate with basic acetate ions. The weak acetic acid diffuses out of the liposomes in exchange for more As $(OH)_3$ leading to arsenic loading (Chen et al., 2006).

Although drug encapsulating liposomes are an exciting and promising prospect, optimisation is required in order to use them as a desirable drug delivery vehicle. There are many physicochemical characteristics that need to be considered, including size, surface charge, zeta potential, shape, membrane lipid packing, steric stabilization, and PEG fluidity. These features influence the pharmacokinetic properties of liposomes by controlling their clearance process, surface toxicity, MPS recognition, and EPR effect (Chang and Yeh, 2012; Zamboni et al., 2012). Among these factors, size and surface

charge are the two key characteristics of nanoparticles that affect their EPR, immune clearance, and cellular adhesion and uptake (Yu Nie et al., 2012).

While a few studies have investigated the effects of both the surface charge and size of liposomes on cellular uptake, the results have been inconsistent (Dan, 2002; Gabizon et al., 1999; Kijanka et al., 2015; Miller et al., 1998; Yu Nie et al., 2012). Regarding surface charge, Yu Nie et al. (2012) reported that positively-charged cationic liposomes were more readily taken up by cells, both *in vitro* and *in vivo*, because of the interaction with the negatively-charged cell membrane. In contrast, Miller et al. (1998) found that a negative surface charge on liposomes increased endocytosis by some cell types. An earlier study reported that liposome–cellular interaction depends not only on the liposomal charge, but also on the lipid composition and, more importantly, the cell type (Dan, 2002). Therefore, it is crucial to optimise the liposomal construct in order to identify the best charge for the target cancer cell line under investigation.

An optimum size for nanoparticles is also important, as the kidneys rapidly clear any nanoparticle with a size below 10 nm, while those above 150 nm in size would face the risk of recognition and clearance by the body's immune system (Kijanka et al., 2015). However, larger nanoparticles have been reported to benefit from having higher encapsulation efficiencies, which increases drug delivery to the target tissue (Gabizon et al., 1999). Based on the inconsistency of previous findings, this study attempted to identify the most suitable liposomal formulation, with respect to size and charge, for delivering ATO into cervical cancer cells, and thereby enhance the therapeutic potential of the delivered drug.

3.1.1.2 Aims:

The aim of this chapter was to optimise the ATO encapsulating liposomes in terms of best size and charge to increase their efficacy as nano-carriers of ATO to HPV positive cervical cancer cells.

3.1.1.3 Objectives:

i. To synthesise and characterise ATO encapsulating liposomes of different sizes (100nm, 200nm and 400nm) and charges (neutral, positive and negative);
ii. To select the most optimal formulation based on its physicochemical and biological properties (loading efficiency, stability and inherent cytotoxicity);
iii. To investigate the *in vitro* anti-tumoral efficacy and uptake of the most optimal formulation on both HPV positive and negative cell lines, HeLa and HT-3, along with any difference in its anti-cancer response towards them; and
iv. To investigate its toxicity towards normal cells. For that purpose, two normal cell lines, HK and CRL1790 were taken as controls.

3.1.2 **Materials and Methods**

3.1.2.1 Liposome Preparation and Characterisation

Liposomes of different sizes and charges were synthesised as detailed in Chapter 2. Their loading efficiency (As/P ratio) was determined by ICP-OES and mean liposomal size along with zeta potential was calculated via dynamic light scattering on a Zetasizer-Nano ZS. Liposomal stability over a period of a month was assessed by analysing their loading efficiency every week while liposomes were stored at 4°C in buffers of pH 7.4. Drug release as a function of pH was assessed by checking their As/ P ratio when liposomes were dialysed in buffers of pH 4, pH 7 and pH 10 for a period of 1, 2, 4, 6 and 24 h.

3.1.2.2 Cell lines

Two cervical cancer cell lines, HeLa and HT-3 along with two control cell lines, human epidermal keratinocytes HK and human colon epithelial cells CRL-1790 were employed for this study. The following experiments were set up for further investigations following liposomal ATO exposure for different time intervals: cellular toxicity via MTT Assay, flow cytometry analysis for cell apoptosis and quantification of cellular arsenic uptake.

3.1.2.3 Cellular toxicity via MTT Assay

Cytotoxicity of various liposomal formulations of ATO was determined by an MTT Assay as described in Chapter 2. Briefly, the experiment was set up in a 96 well plate, where the toxicity of control empty liposomes was investigated by taking an initial starting amount containing 0.5mM of phospholipid concentration and diluting it in 1:10 ratio to further 6 wells. The ATO encapsulating liposomes contained 30µM of ATO concentration in the initial sample, which was further diluted in the 1:6 ratio down to 6 wells. The wells were seeded with HeLa, HT-3, CRL 1790 and HK at a density of 0.6 million cells per ml and incubated at 37°C in the humidified incubation chamber for 24

h, 48 h and 72 h. After the intended incubation, MTT Assay was performed as per the described protocol and absorbance of the final coloured solution read and quantified via BMG LabTech FLUOstar Omega Plate Reader at a wavelength of 570 nm.

3.1.2.4 Analysis of Cell Apoptosis by Flow Cytometry

Cells from the four different cell lines were seeded at 5×10^5/ml in six-well culture plates and grown overnight for cell attachment. 100nm, neutral liposomes were employed for this experiment. After 24 h of treatment (media only, liposomal ATO at a dilution having 5µM ATO encapsulated, empty liposomes at the same dilution as liposomal ATO, 5µM free ATO), the cells were analysed for apoptosis induction via flow cytometry according to the protocol described for Annexin V FITC apoptosis detection kit (Abcam, UK) used for this study (more details in Chapter 2).

3.1.2.5 Quantitative Analysis of Cellular Uptake of Arsenic by ICP-MS

Cellular uptake was analysed for different treatments at a time period of 6, 24 and 48 h by ICP-MS as described in Chapter 2. For each analysis, cells from the four different cell lines were seeded into sixteen 75-cm^2 flasks at a density of 1×10^6 cells/flask, with two flasks for each treatment as a doublet. Following a 24-h cell attachment, cells were treated as described below: control (cells in untreated media), ATO lipo (5µM ATO encapsulating liposomes), empty lipo (control liposomes at the same dilution as ATO lipo), and ATO (5µM free ATO) and their arsenic concentration determined after the desired time interval.

3.1.2.6 Statistical Analysis

Statistical analysis described in experimental sections was done using Minitab17. Statistical significance was determined by 2-sample t-test. $P < 0.05$ was considered significant. For flow cytometry, statistical analysis was carried out automatically through BD Calibur software provided.

3.1.3 **Results**

3.1.3.1 Liposome Preparation and Characterization

The mean sizes and zeta potential of control liposomes were determined by dynamic light scattering on a Zetasizer-Nano ZS (Malvern Instruments) as represented in Fig 3.1.2. The DLS measurements of the hydrodynamic sizes of the 100nm, 200nm and 400nm liposomes were 138.5 ± 1.22nm, 187 ± 2.96nm and 243 ± 2.68nm respectively (Fig 3.1.2a). All of the charged liposomes were extruded through a 100 nm filter. Positively-charged and neutral PC liposomes had a similar hydrodynamic size of 138.5 ± 1.22 nm and 143.9 ± 3.19 nm, respectively. However, the incorporation of a negatively-charged lipid DSPG slightly increased the particle size to 165.2 ± 3.26 nm (Fig 3.1.2b). No significant differences were observed between these three sizes. The polydispersity index of the investigated vesicles had values from 0.12 to 0.175 indicating homogenous population of liposomes. Regarding the zeta potential, the group of liposomes that exhibited a small negative surface charge, (-) 24.4 ± 0.46 mV were considered neutral. Cationic liposomes possessed a positive charge, (+) 23.2 ± 0.44 mV, and negative liposomes possessed a higher negative charge, (-) 36.4 ± 0.75 mV.

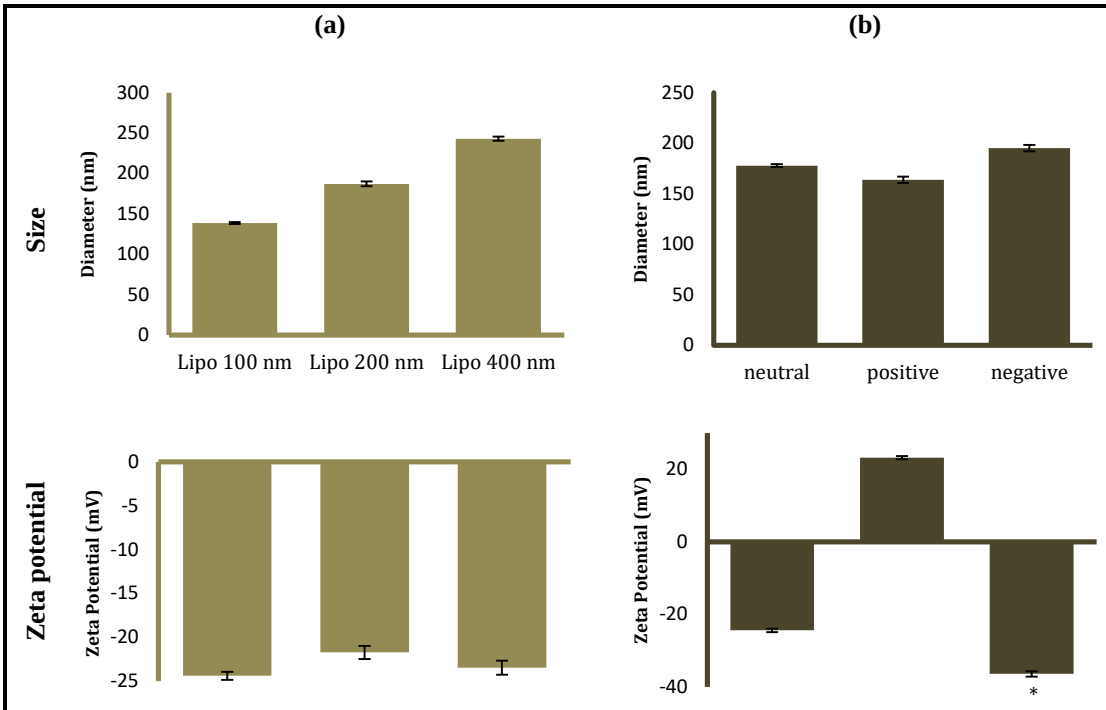

Fig 3.1.2: Diameter and zeta potential of liposomes of (a) different sizes and (b) different charges as measured from Zetasizer with a polydispersity index of around 0.1. All of the different-sized liposomes (100 nm, 200 nm, and 400 nm) have a neutral charge, whereas all of the different-charged liposomes (neutral, positive, and negative) are 100 nm in size. Data are means ± standard deviations of three replicate measurements of at least three independent experiments. * $p \leq 0.05$.

The liposomes were efficiently loaded with arsenic co-encapsulated with transition metal ion Ni. The phospholipids, encapsulated arsenic and nickel in the liposomes were quantified by ICP-OES. The loading efficiencies (encapsulated arsenic/phospholipids) of liposomes of different sizes and charges are depicted in Fig 3.1.3. The loading efficiency was the highest for 100nm neutral liposomes at 24.2 % As/ P ± 0.848. The liposome suspension was stored at 4°C for a month and its stability was deduced by analysing its loading efficiency every week (Fig 3.1.4). Less than 10% arsenic leaked from the liposomes in a time period of 1 month. All the liposomal formulations displayed similar storage stability.

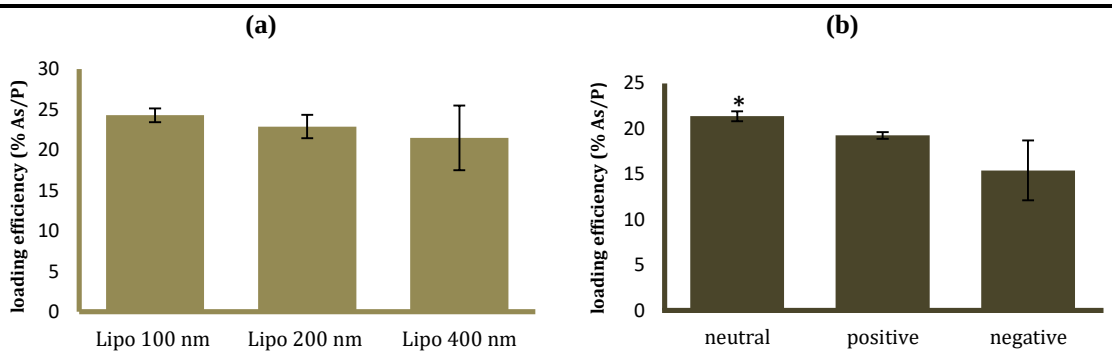

Fig 3.1.3: Loading efficiency of synthesised liposomes of (a) different sizes and (b) different charges. Data are means ± standard deviations of three replicate measurements of at least three independent experiments. An unpaired t test ($p > 0.05$) was used to test for any significant difference in the loading efficiency of liposomes of three sizes (ranging from 100 to 400 nm), and three charges (neutral, negative, and positive). No significant difference was observed between the liposomes of different sizes, although neutral liposomes displayed a significantly higher loading efficiency than the others (* $p < 0.05$).

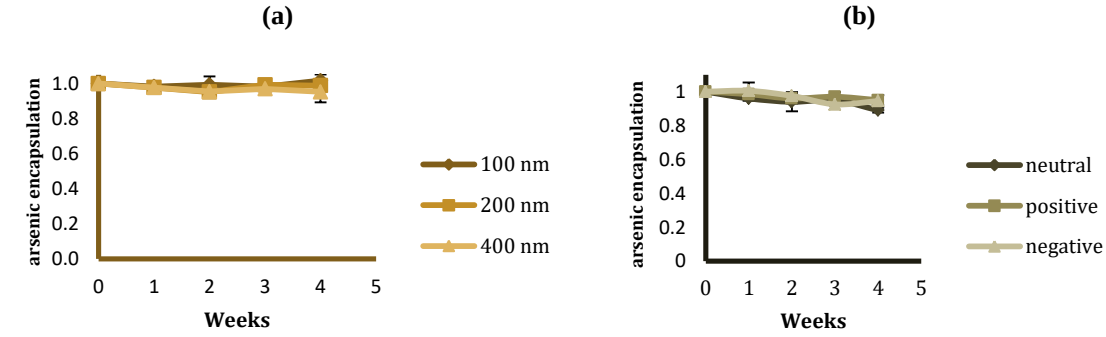

Fig 3.1.4: ATO encapsulated over a period of 4 weeks of storage at 4°C. Data shown is means ± standard deviation from 3 independent experiments.

In order to assess the effect of pH on the liposomal formulation (and hence determine the drug leakage pattern that is initiated when encountering different pH), liposomes were dialysed in buffers of pH 4, pH 7 and pH 10. The amounts of the drug that were retained in the liposomes were examined after periods of 1h, 2 h, 4h, 6h and 24 h (Fig

3.1.5). At pH 4, approximately 40% of the drug was lost within the first four hours. Among the different sizes, the smallest (100nm) liposomes were found to be the most stable at all pH values. With respect to charge, the negatively-charged liposomes displayed a significant loss of stability among the charged vesicles when they were exposed to a higher pH in comparison with those with a neutral or positive charge.

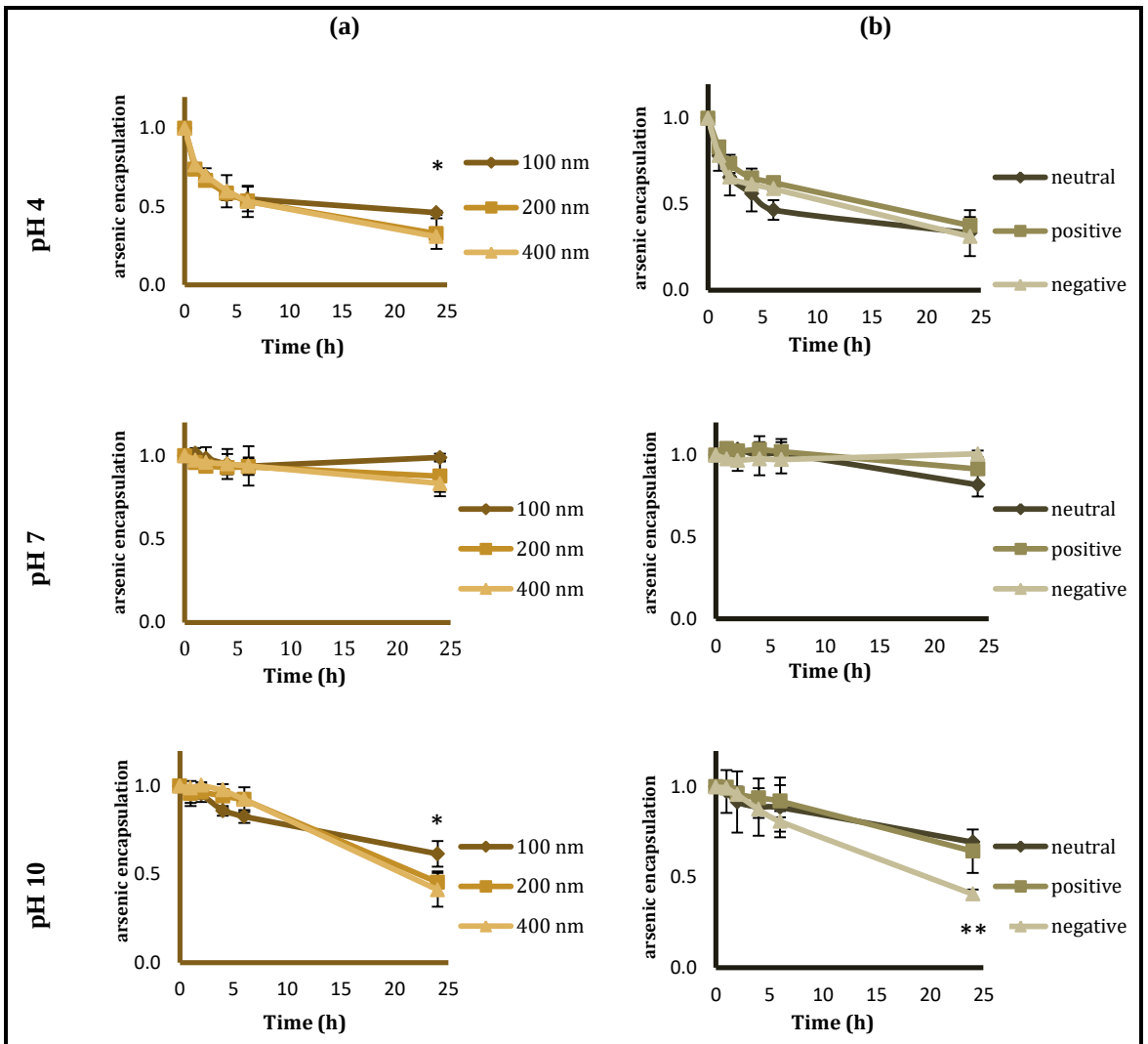

Fig 3.1.5: Stability studies of different liposomal formulations under various pH conditions. ATO was encapsulated in liposomes of (**a**) different sizes and (**b**) different charges after dialysing in buffers at pH 4, pH 7, and pH 10. Data are shown as mean ± SD of three independent experiments. * $p < 0.05$, ** $p < 0.01$.

3.1.3.2 Analysing cytotoxicity of control empty liposomes with differing sizes and charges

The success of nanoparticles as drug carrier relies on their inherent non-toxic properties. Control empty liposomes of various formulations were synthesised and their cytotoxicity analysed via MTT assay on HeLa cell line at 24, 48 and 72 h as depicted in Fig 3.1.6. The phospholipid concentrations of the liposomes were diluted at the same dilution factor that was used for liposomal ATO (encapsulating 5 μM ATO). No significant difference in the cytotoxicity from different-sized liposomes was observed at the relevant concentrations of liposomes. However, when the surface charges were taken into consideration, the empty positively-charged liposomes displayed significant toxicity over an incubation period of 48 h. The 100nm, neutral empty liposomes were not toxic for any cell lines employed at the dilutions for treating the cells till 72 h (Fig 3.1).

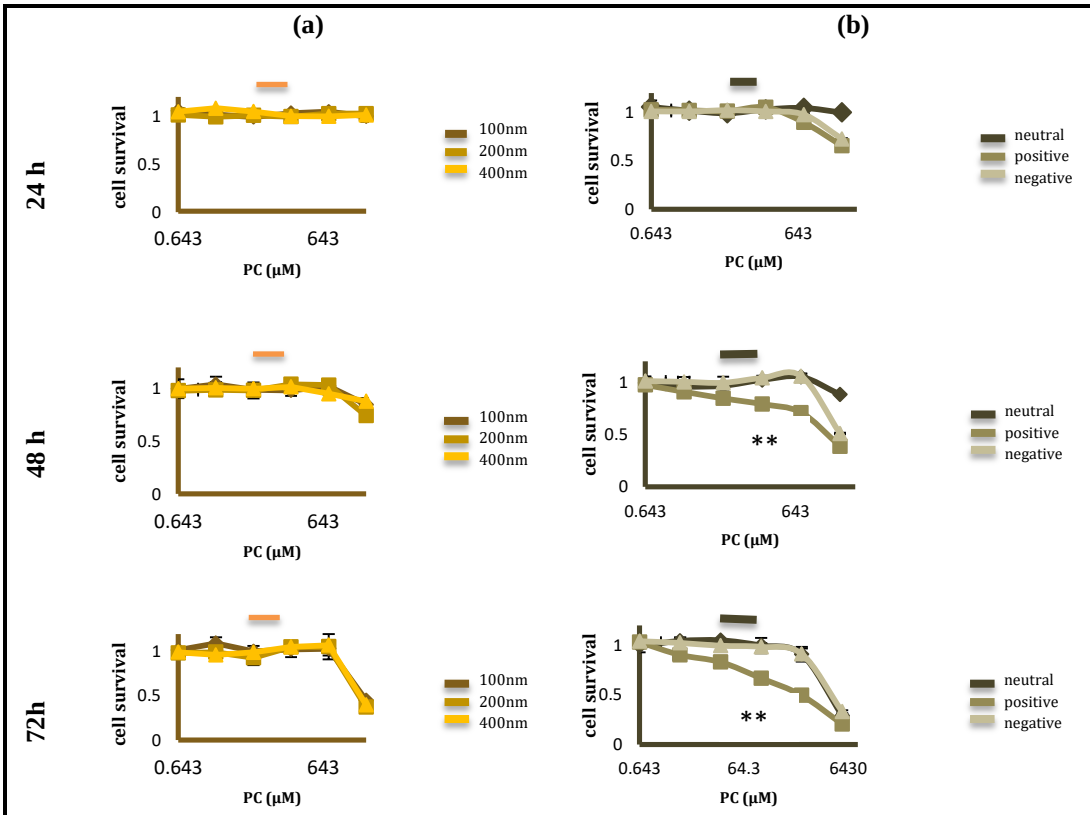

represents the concentrations of phospholipid at dilutions used for treatment of liposomal ATO.

Fig 3.1.6: The MTT assay used to test the cytotoxicity of various control liposomal formulations on cervical cancer cells. The cellular toxicity that is induced by control (empty) liposomes of different (**a**) sizes and (**b**) charges is represented following an incubation period of 24, 48 and 72 h with HeLa cells. The positively-charged liposomes displayed noticeable toxicity at 48 h exposure and at the same dilution factor that was used for diluting liposomal encapsulated ATO. Neutral liposomes were found to show the least toxicity. Data are presented as mean± SD of three replicate experiments; ** $p < 0.01$.

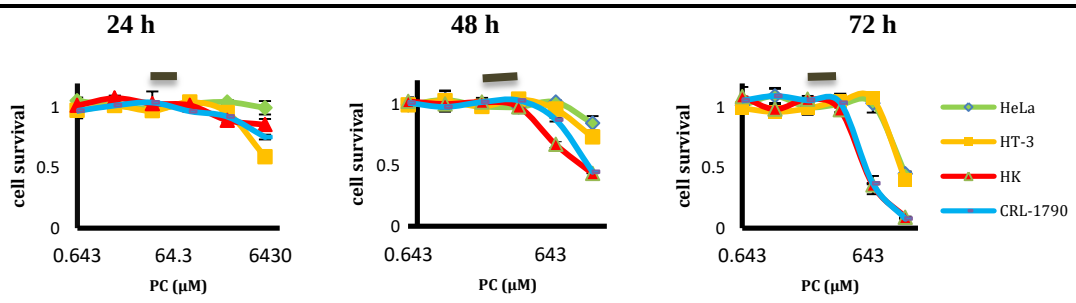

represents the concentrations of phospholipid at dilutions used for treatment of liposomal ATO.

Fig: 3.1.7: The phospholipid concentrations at dilutions used for the treatment of 100nm, neutral liposomes is non-toxic to all the cell lines tested till 72 h, demonstrating their suitability as the drug carrier.

3.1.3.3 Cytotoxicity and Apoptosis induction of ATO-Encapsulated Liposomes in HPV-Positive and HPV-Negative Cervical Cancer Cell Lines

After establishing that neutral liposomes of 100 nm in size were the most stable formulation, possessed the highest encapsulation efficiency, and displayed the least intrinsic toxicity, this form of liposome was chosen as the drug carrier for the remainder of the experiments. The response of cervical cancer cell lines of differing HPV statuses (HPV-positive HeLa and HPV-negative HT-3) to the treatment with ATO, delivered either in the free form or encapsulated in the chosen liposomes, was investigated with regards to cytotoxicity (MTT assay), cellular uptake (ICP-MS), and induction of apoptotic response (flow cytometry).

The dose response curve obtained from MTT assay for free drug and liposomal drug reveals that liposomal encapsulation mitigates toxicity which is in accordance with findings from other cell lines (Chen *et al*., 2006; 2009; Ahn *et al*., 2010) (Fig 3.1.8). This trend became more noticeable as the drug exposure time increased. The differences in the cytotoxicity are cell line dependent.

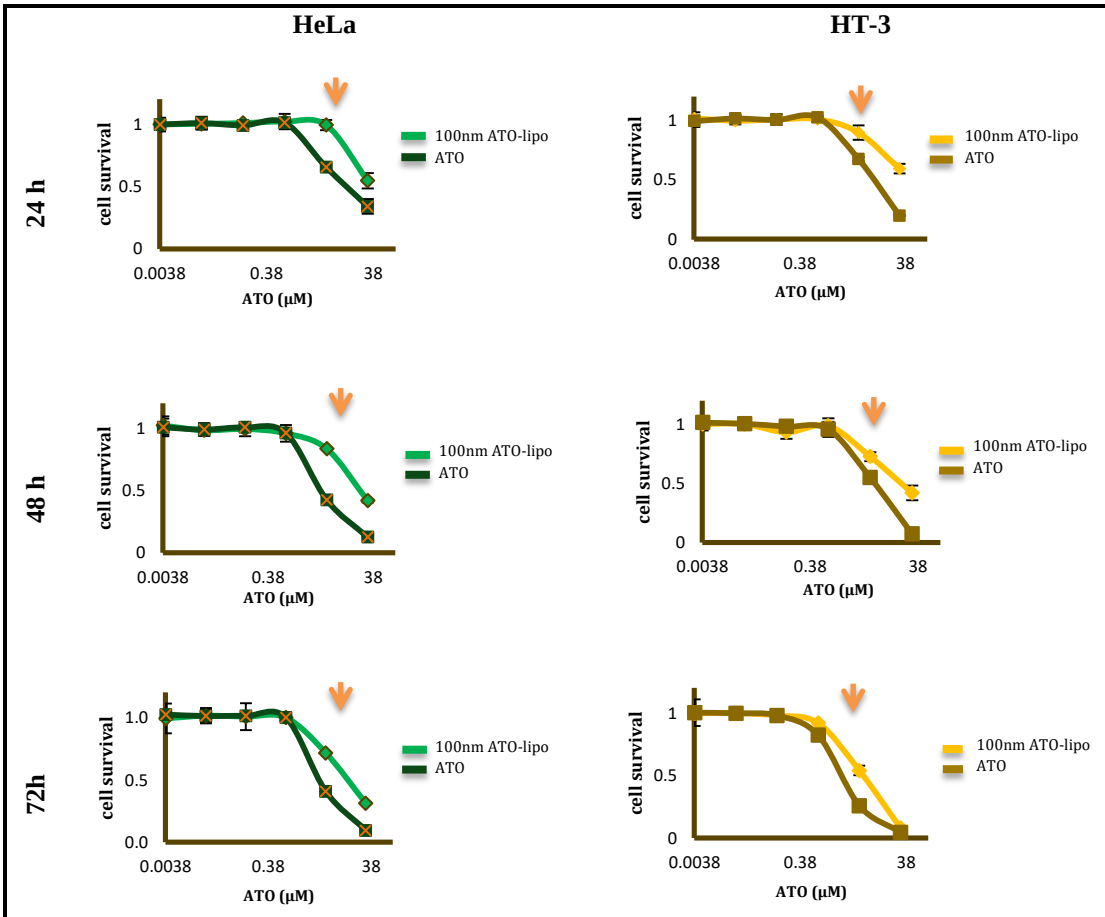

points to 5μM ATO concentrations which is typically used for treatment.

Fig 3.1.8: Liposomal encapsulation attenuates drug toxicity to the cells *in vitro*. HPV positive and negative cervical cancer cells were treated with free ATO and liposomal ATO for a duration of 24 h, 48 h and 72 h. Cell viability was assessed by MTT Assay. Points refer to the means and bars refer to ±SD, where n=3.

We next analysed the cytotoxic mechanism of free ATO and liposomal ATO *in vitro* by using quantitative flow cytometric analysis of apoptosis after a 24 h and 48 h treatment. The cells were labelled by FITC conjugated Annexin-V and PI for the detection of early apoptotic and late apoptotic cells. The fluorescence was detected on FL1 and FL3 channels, respectively, by flow cytometer. The percentage of cell population distributed in different quadrants represents live cells (lower left quadrant, Annexin− PI−), early apoptotic cells (lower right quadrant, Annexin+ PI−), late apoptotic cells (upper right quadrant, Annexin- PI+) and necrotic cells (Annexin+ PI+). The fold increase of apoptotic population according to the control (cells treated with media only) from

different treatments (free ATO and liposomal ATO) is summarized in Fig 3.1.9. More than 90 % of the cells were alive when treated with cell media or control liposomes. For HeLa and HT-3 cells, more apoptotic cells were observed when treated with free ATO, which is consistent with MTT assay findings that liposomal ATO is less potent in inducing cell death.

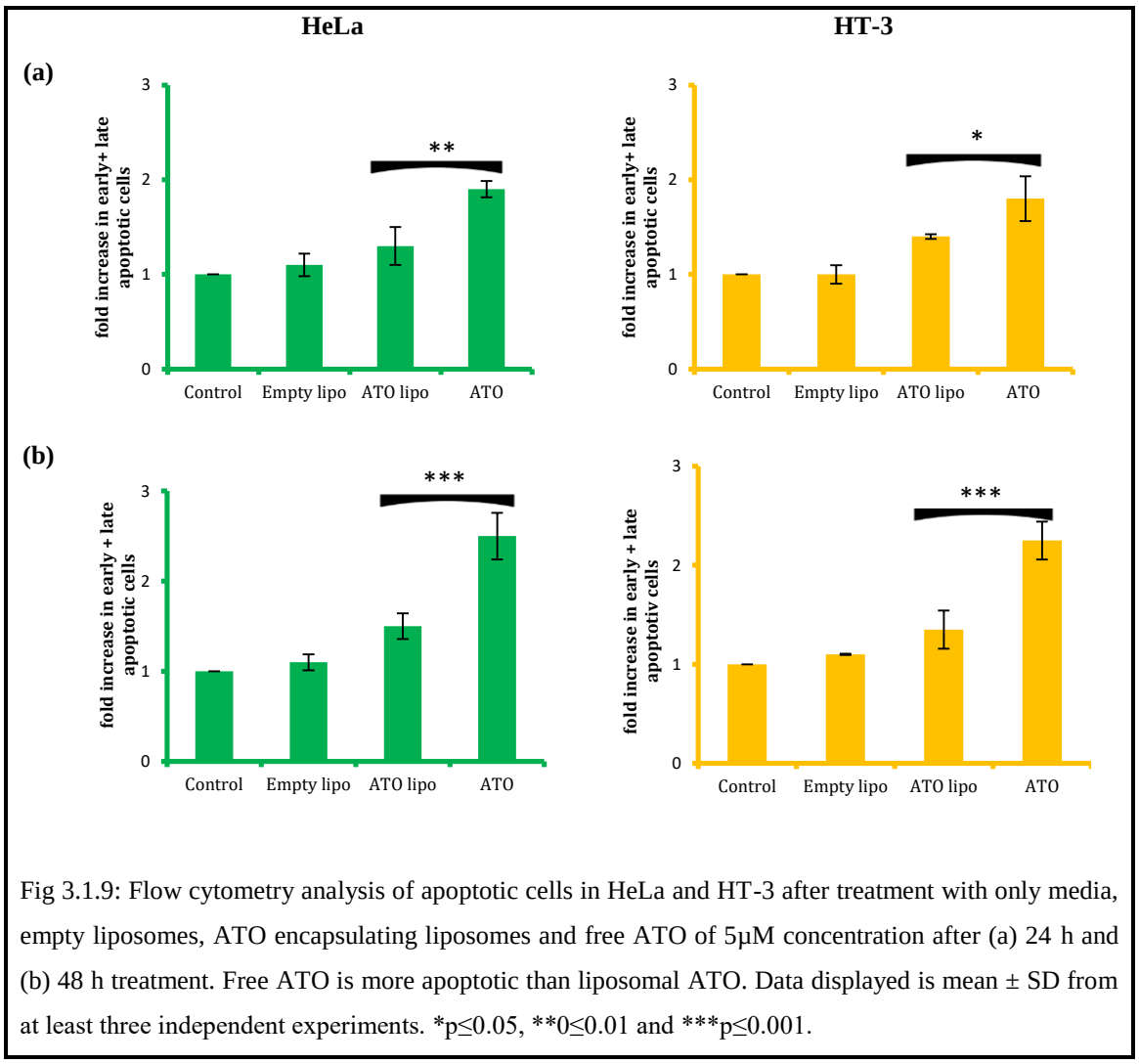

Fig 3.1.9: Flow cytometry analysis of apoptotic cells in HeLa and HT-3 after treatment with only media, empty liposomes, ATO encapsulating liposomes and free ATO of 5µM concentration after (a) 24 h and (b) 48 h treatment. Free ATO is more apoptotic than liposomal ATO. Data displayed is mean ± SD from at least three independent experiments. *p≤0.05, **0≤0.01 and ***p≤0.001.

3.1.3.4 Time course study of cellular uptake of liposomal arsenic

For the cellular uptake studies, the cervical cancer cell lines, HeLa and HT-3, were incubated with media only, empty liposomes, liposomal and free drug with 5µM ATO concentration for a time period of 6 h, 24 h and 48 h. The cellular concentration of arsenic was determined by ICP-MS (Fig 3.1.10). Results showed that no arsenic was detected in all the cell lines when treated with cell media or control liposomes. The uptake of free ATO was higher than liposomal ATO, around 2.5 times higher for HeLa and 6.3 times higher for HT-3 cell line after 6 h incubation. With HT-3, the ratio steadily declined with time from 6.3 to 4.9 and finally to 1.9 after 48 h treatment. It stayed almost similar though for HeLa at 6 h and 24 h treatment, however slightly increased to 4 after 48 h treatment. In both the cell lines, there was a steady increase in arsenic concentration with time, except for free ATO treatment on HT-3, where arsenic concentration for the free drug was observed to go down by a factor of 0.76 from 24 h to 48 h treatment. It was apparent that the uptake for both the treatments is most rapid in the first 24 h and then diminishes with time for the two cell lines tested.

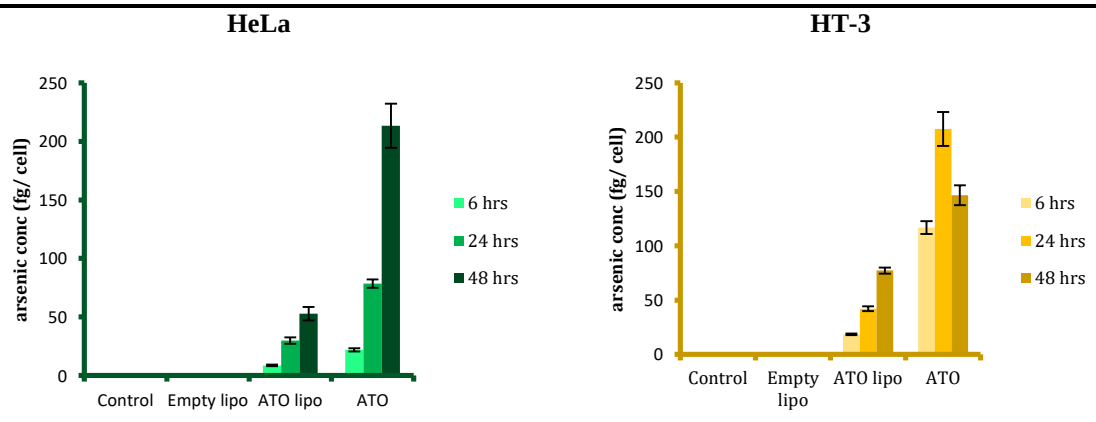

Fig 3.1.10: Arsenic concentration per cell in HeLa and HT-3 as determined by ICP-MS after 6 h, 24 h and 48 h treatment with (a) only media, (b) empty liposomes (c) ATO encapsulating liposomes and (d) free ATO of 5µM concentration. Free ATO is taken up more than liposomal ATO. Data displayed is mean ± SD from five independent experiments.

3.1.3.5 Comparisons of the cytotoxicity and uptake of ATO encapsulating liposomes between HPV positive and negative cell lines

A comparative study was drawn relating the responses of HPV positive HeLa and HPV negative HT-3 cell lines towards liposomal and free ATO in terms of cellular toxicity, apoptotic response and cellular uptake of liposomes and free arsenic (Fig 3.1.11 and 12). The MTT results demonstrated that the cell survival rates after treatment in both cervical cancer cell lines were similar for up to 72 h (Fig 3.1.11a). Moreover, using flow cytometry to measure apoptosis (Figure 3.1.11b), no statistically significant difference was found between the apoptotic populations in HT-3 and HeLa cell lines after incubation with either free or encapsulated ATO for up to 48 h treatment. However, a clear trend of increased cell death induced by directly exposing both of the cell lines to free ATO was observed. The IC50 results that were obtained from the cytotoxicity assays are presented in Figure 3.1.11c. The results display similar values for both of the treatments on HeLa and HT-3 cells after 48 h of incubation.

(a)

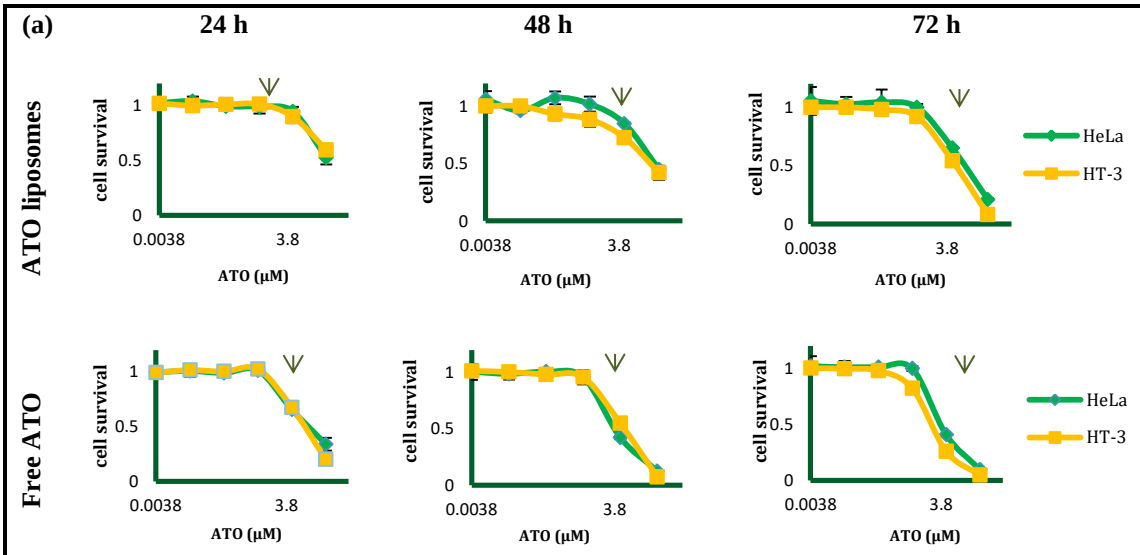

(b)

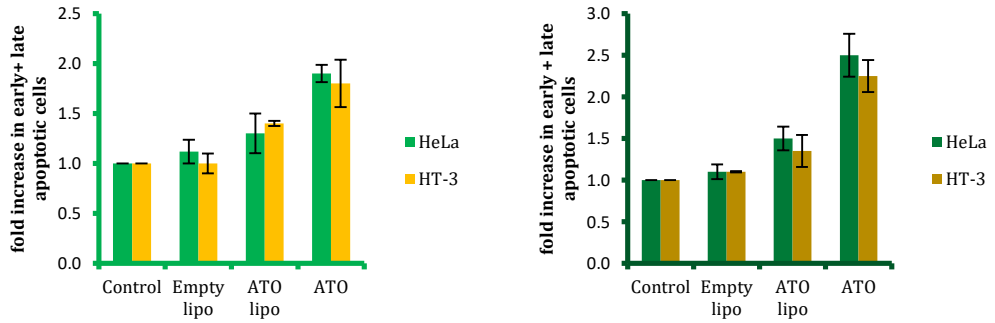

(c)

Cell line	ATO lipo IC50 (µM) (mean±SD)			ATO IC50 (µM) (mean±SD)		
	24h	48h	72h	24h	48h	72h
HeLa	29.7±2.6	24.8±0.5	17.1±0.3	21.0±0.5	14.7±0.0	14.2±0.2
HT-3	35.8±1.1	24.3±0.1	14.6±0.9	17.4±1.2	14.4±1.4	12.2±0.6

⩛ points to 5µM ATO concentrations which is used for treatment.

Fig 3.1.11: The MTT assay and flow cytometry analysis to compare cellular toxicity and apoptosis induction of varying treatments on HeLa and HT-3 cells. (**a**) Cell viability of HeLa and HT-3 cell lines following incubation with liposomal encapsulated ATO (ATO lipo) and free ATO for 24, 48 and 72 h; (**b**) Flow cytometry analysis of apoptotic populations that were treated with complete media as control, empty liposomes, liposomal 5 µM ATO, or 5 µM free ATO on HeLa and HT-3 cell lines following treatment for 24 and 48 h; (**c**) Calculated IC50 values for ATO lipo and free ATO treated HeLa and HT-3 cells after 24, 48, and 72 h. Data are presented as mean ±SD of three replicate experiments.

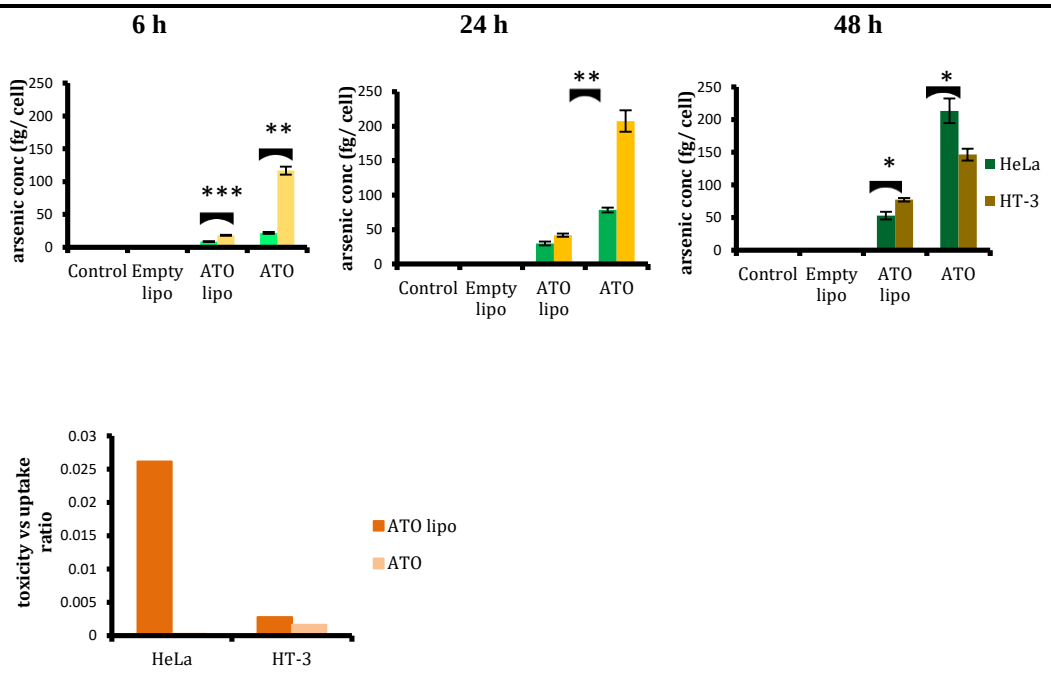

Fig 3.1.12 A comparative study of the arsenic uptake and toxic response of different drug formulations on HeLa and HT-3 cells. (**a**) Comparison of the arsenic uptake by HeLa and HT-3 after 6, 24, and 48 h of treatment, as determined by ICP-MS. Free ATO was taken up more than ATO lipo in both cell lines. However, the uptake was higher in HT-3 for all treatments, except for the free ATO uptake after 48 h. (**b**) Ratios of toxicity vs. uptake of liposomal and free ATO for the two cervical cancer cell lines after 24 h treatment. Data are displayed as mean ± SD from at least three independent experiments;
* $p < 0.05$, ** $p < 0.01$, and *** $p < 0.001$.

Despite a similar response to treatment with free and encapsulated ATO from both of the cell lines with respect to toxicity and induction of apoptosis, the uptake of both free and liposomal arsenic by the cell lines varied at different time points (as can be observed in Figure 3.1.12a). The uptake by HT-3 cells was found to be higher than the uptake by HeLa cells at 6 and 24 h. This trend reversed for the free drug uptake at 48 h treatment, when HeLa cells were observed to have taken up significantly more ATO. In Figure 3.1.12b, toxicity–uptake ratios for HeLa and HT-3 are shown to indicate the level of toxicity that was induced in the cell lines per unit of arsenic taken up by the cells. Liposomal ATO was observed to be more effective than the free drug in inducing toxicity per unit of arsenic uptake in both cell lines. However, liposomal ATO treatment was more toxic to HeLa cells than to HT-3 cells.

3.1.3.6 Selectivity of Liposomal Encapsulated ATO in Killing Cervical Cancer Cells

One of the most crucial aspects of an effective drug formulation is its demonstrable selectivity in its anti-cancer response by sparing normal healthy cells. Hence, after establishing the efficacy of liposomal ATO in inducing cell death per unit of arsenic uptake in HPV-positive HeLa cells, we further investigated the effect of liposomal ATO on non-cancerous cells by choosing two cell lines as controls, namely human keratinocytes (HK) and human colon cells (CRL-1790) (Figure 3.1.13a,b). Among the three cell lines investigated, the uptake of liposomal arsenic was highest in HK cells, with a lower uptake by HeLa and CRL-1790 cells. In contrast, the highest uptake of free ATO was by HeLa cells (Figure 3.1.13a). However, when cytotoxicity was investigated, cell survival was insignificantly affected in CRL-1790 and HK cell lines (Figure 3.1.13b). The ratio of cell death to the amount of arsenic taken up by the cells after incubation with liposomal encapsulated ATO and free ATO for 24 h is presented in Figure 3.1.13c. Liposomal ATO resulted in a higher cell death rate per unit uptake of arsenic than free ATO for HeLa cells, while a minimal toxic effect was observed in the control cells. The IC50 values for the liposomal ATO treatment were calculated, and were higher for the control cell lines than for HeLa cell lines (Figure 3.1.13d).

(a)

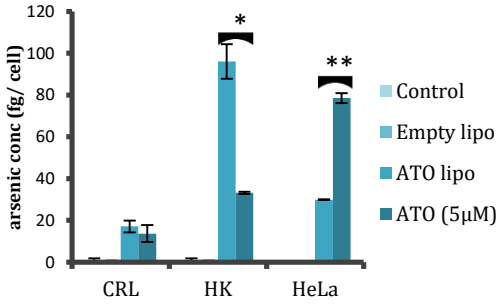

(b)

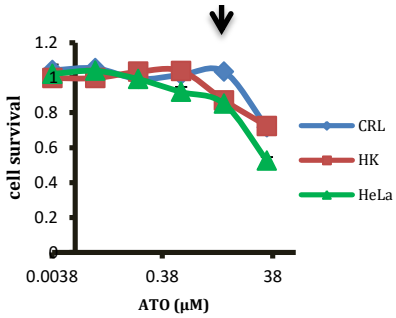

(c)

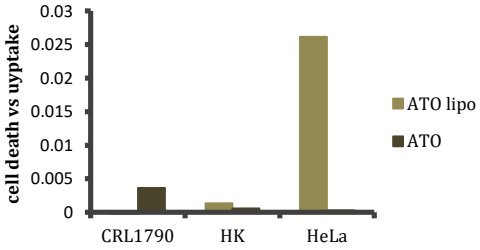

(d)

Cell line	IC50 for ATO-lipo treatment
CRL	48.7±1.2
HK	49.8±2.9
HeLa	29.7±2.6

Fig 3.1.13: Arsenic uptake and toxic response in the control cells and HeLa cells. (**a**) A comparative study of arsenic concentration per cell in CRL-1790, HK and HeLa—as determined via ICP-MS after 24 h of treatment with media, control liposomes, ATO lipo, and free ATO; (**b**) Cell survival following the exposure of cervical cancer and control cell lines to ATO lipo for 24 h—assessed using the MTT assay; (**c**) Cell death–uptake ratio of ATO lipo and free ATO in HeLa cells compared to control cell lines, after treatment for 24 h. ATO lipo is effective in generating toxicity in HeLa cells, while having a non-toxic effect on the normal cells; (**d**) The IC50 values for three cell lines following 24 h of ATO liposomal treatment. Data are displayed as mean ± SD from three replicates; * $p < 0.05$, ** $p < 0.01$.

3.1.4 **Discussion**

Since the recognition of the potential of ATO as a broad spectrum anti-cancer drug, it is being increasingly explored for the treatment of various cancer types (Swindell et al., 2013). However, the systemic toxicities associated with this drug while treating solid cancers impedes its therapeutic use in clinical applications. We have previously shown that a low concentration of ATO (≤2μM) is capable of selectively inducing cellular apoptosis and increasing p53 expression in HPV-positive cervical cancer cells *in vitro* (Wen et al., 2012). However, increasing the ATO dosage to 5μM resulted in most of the cells being killed because of drug-induced toxicity, irrespective of their HPV status. In order to reduce ATO's toxicity and raise its therapeutic index, liposomal encapsulated ATO at 5μM concentration was used to treat cervical cancer cells (Wang et al., 2016). The results from our previous study indicated that, although liposomal ATO was less readily taken up by cells than free ATO (Chen et al., 2009), the delivered ATO was able to reduce the oncogene E6 expression while exhibiting reduced toxicity (Wang et al., 2016). Since the size and surface charge of liposomes play important roles in drug stability and sustained release, an optimised liposome formulation with appropriate physical features would be essential for further improving the drug loading efficiency and boosting the killing effects for cancer cells. Therefore, the aim of this work was to optimise the liposomal design, with respect to size and charge, for use as drug delivery vehicles to specifically target HPV-positive cervical cancer cells *in vitro*. Liposomes of different sizes (100 nm, 200 nm, and 400 nm) and different charges (neutral, positive, and negative) were synthesised, with ATO co-encapsulated with a transition metal ion (Ni^{2+}) in a stable, precipitate form.

For the preparation of liposomes, soy PC was chosen as along with conferring high stability to the vesicles, it has a lower phase transition temperature eliminating the requirement of high temperatures during liposome synthesis/ drug incubation and specialised heating blocks as is the case with DSPG (Wang et al., 2016). Cholesterol plays a vital role in the stability of the liposomes by imparting rigidity to the lipid layer with some studies indicating an inverse relationship between the leakage of drug from liposomes in the bloodstream and its cholesterol content (de Meyer and Smit, 2009). However, by imparting rigidity, it also affects the loading efficiency of the drug within

the liposomes (Magarkar et al., 2014). Hence, to strike a balance between good stability and maximum encapsulation efficiency, a molar ratio of 45% of cholesterol for neutral liposomes and 33% cholesterol for charged liposomes was selected. DSPG and DDAB were chosen to impart negative and positive charge to the liposomes respectively (Gabizon et al., 1982; Filion and Phillips, 1997).

The size measurement analysis indicated a disparity between the actual and expected sizes of the formed liposomes. The 200 nm liposomes were closest to the expected size, with the 100 nm liposomes being slightly larger and the 400 nm liposomes being smaller. This could be caused by the choice of filter extruders (discontinuous syringe filtration vs. continuous high-pressure devices), the inaccuracy of the actual pore diameter of the commercial filter, or the particle size analysis technique that was employed (Berger et al., 2001). However, as these liposomes still displayed an expected incremental size range, it was decided to proceed with the planned analysis.

Circulating liposomes with stability in the retention of drugs is a desirable feature in order to ensure that a sufficient amount of the drug reaches the target tissue. Our stability tests showed that all the liposomes, irrespective of sizes and charges, displayed high stability with a loss of less than 10% of arsenic over four weeks storage at 4°C. The pH stability studies were carried out under three pH conditions (pH 4, pH 7 and pH 10). The liposomes displayed highest stability at pH 7 which is the physiological pH. At the acidic pH 4, to be encountered in the acidic tumour milieu or endocytic pathways of cancer cells, liposomes underwent a rapid release of arsenic with a loss of more than 50% of the drug within the first four hours, after which the release tapered off. In alkaline conditions, the arsenic release was gradual with time reaching up to 50% in 24 hours. Among the studied sizes, 100 nm liposomes were the most stable at all three pH values. Negative liposomes displayed instability at higher pH, most likely owing to the changes in lipid orientation in the alkaline conditions leading to liposome disintegration (Dimitriu, 2001).

The results from the drug loading efficiency studies among different formulations indicated that 100 nm neutral liposomes had the highest drug encapsulation. Since the success of nanoparticles as drug carriers relies on them being inherently non-toxic, we further tested whether these liposomes displayed any intrinsic toxicity towards the cells.

This was tested by incubating their empty counterparts with HeLa cells for 24, 48 and 72 h. The dilutions of liposomes that were tested for toxicity studies were the same as the dilutions that were used for preparing liposomal encapsulated ATO samples (liposomes encapsulating 5μM ATO). Size did not have any significant effect on toxicity in the range that was tested (Figure 3.1.6a). However, among the charged liposomes, positively-charged liposomes began to display toxicity to HeLa cells after 48 h of incubation, killing almost 20% of cells at the dilutions that were employed for the treatment (Figure 3.1.6b). One possible reason suggested for the high toxicity of cationic lipids is their translocation to the cell membrane, which eventually results in its destabilisation (Soenen, Brisson and De Cuyper, 2009). This finding excludes positively-charged liposomes from being employed as drug carriers for ATO delivery to cervical cancer cells, even though a higher uptake by cells was previously observed with this type of liposome (Yu Nie et al., 2012). Moreover, negatively-charged liposomes were demonstrated to be unstable at a higher pH. Considering the above reasons, 100 nm, neutral liposomes were chosen as the carrier for ATO delivery and were used for further *in vitro* analysis.

The cells were incubated with free and liposomal ATO of 5μM concentration for a period of 24 h, 48 h and 72 h and their cytotoxicity assessed by MTT assay. Liposomal encapsulation alleviated ATO toxicity *in vitro* for both the cell lines. The higher toxicity of free ATO than its liposomal counterpart was confirmed by the investigation of rate of apoptosis by flow cytometry, which clearly showed that free ATO generated higher apoptosis than liposomal ATO for both cell lines. The toxicity from both the treatments increased with drug exposure time in both of the cervical cancer cell lines that were tested (Fig 3.1.8).

Cellular uptake studies showed that arsenic was transported more readily within the cells when the free form was applied with concentrations of 78.5±3.5 and 207.4±15.5 fg/cell in HeLa and HT-3 respectively after 24 h treatment. The cellular uptake of liposomal ATO was 2.6 times lower for HeLa and 4.9 times lower for HT-3. In HeLa cells, there was a steady increase in intracellular arsenic concentration with both the treatments as incubation period was increased from 6 to 48 hours. This trend was also observed with liposomal ATO in HT-3, however not with the free form of arsenic. After 24 h, the intracellular arsenic concentration decreased in HT-3 cell line, which might

refer to a possibility of activation of cellular efflux mechanisms in HT-3 cells. This trend was not observed in HeLa cells, with ATO concentrations continuing to increase at 48 h. It could be postulated that this was related to the presence of HPV within the cell. The mechanism behind this warrants further investigation.

An interesting observation was that for both the cell lines, free ATO was taken up more rapidly within the first 24 hours than liposomal ATO. However, the rate of increase in intracellular arsenic was higher for liposomal ATO from 24 h to 48 hours. This confirms the hypothesis that liposomes act as a depot for the drugs and allow a slow release of ATO in an extended time frame, resulting in a prolonged anti-tumour activity even after the treatment has been stopped 16. This is contrary to the free drug which is taken up rapidly and non-specifically, killing the cells in the process and with a potential to cause "rebound" tumour growth associated with maximal tolerated dose (MTD) based chemotherapy (Ahn et al., 2010). Delivering ATO by liposomes may prevent this rebound tumour growth by gradually and steadily loading the tumour with the drug as opposed to peak-trough kinetics associated with chemotherapeutic drugs (Ahn et al., 2010).

A comparative study on the toxicity, apoptosis inducing responses and arsenic cellular uptake was performed in HPV positive and negative cell lines and it was revealed that the toxicity profile for both liposomal and free drug was quite similar for HPV negative HT-3 and positive HeLa cell lines at 24 and 48 h. These results were confirmed by the flow cytometric analysis of apoptosis where statistically similar apoptosis was induced in both the cell lines after 24 and 48 hours treatment of liposomal and free ATO.

The comparable toxicity of free and liposomal ATO towards both cell lines might initially be thought of as a result of similar arsenic uptake by these cells. However, the uptake studies gave completely contradictory findings with HT-3 taking up considerably more arsenic from both the treatments. It was observed that HT-3 takes up around 1.4 times more arsenic from liposomal ATO treatment and around 2.6 times more from free ATO treatment in the first 24 hours. This point towards a higher susceptibility of HeLa cell line towards the treatments as despite a lower uptake of arsenic, they display an appreciable toxicity profile. To further reinforce the argument, toxicity vs uptake ratio was plotted for both HeLa and HT-3 cell lines for liposomal and

free ATO treatment. It was found that liposomal ATO induced 71 times more toxicity per unit arsenic in HeLa than HT-3. In contrast, free ATO was more efficient in inducing toxic response per unit arsenic in HT-3 cells, which demonstrates the selective nature of liposomal encapsulated ATO for HPV-positive HeLa cells. This finding further supports the suitability of the optimised formulation of liposomes as the desired nanocarrier for introducing arsenic to HPV-positive cell lines.

One of the main aims of employing nanotechnology in pharmaceutics is to deliver the drug specifically to the cancer cells while sparing the normal cells. There has been a lack of literature reporting on studies involving non-cancerous cell lines while investigating liposomal ATO efficacy *in vitro*. Hence, after establishing the effectiveness of the liposomal construct for HPV-positive cervical cancer cells, we decided to investigate the toxicity and uptake response profile of non-cancerous control cells to liposomal treatment. Two control cell lines were chosen for this study, namely human keratinocytes (HK) and human colon (CRL-1790) cells. The uptake of liposomal arsenic by HK cells was found to be higher than in the other cell lines (Figure 3.1.13a). The second control cell line, CRL-1790, displayed lower intracellular arsenic concentrations than HeLa cells after incubation with liposomal ATO (Figure 3.1.13a). However, after 24 h of treatment with liposomal encapsulated ATO, results showed that the non-cancerous cell lines were the least affected by the treatment, with cell survival rates close to 95% at the same length of incubation and the same dose of the treatment (Figure 3.1.13b). This is independent of the amount of ATO uptake by the cells. This finding suggests that liposomal-delivered ATO could be a promising candidate for targeting cervical cancer cells, because it demonstrated less toxicity to the non-cancerous cells, even at a much higher concentration. It may be the case that when liposomal-encapsulated ATO reaches the cells, it results in bio-physical changes in the cell membrane that may in turn affect the cellular transport systems. Different types of cells may react to these changes in different ways. However, HeLa cells appear to be more vulnerable to this drug treatment, which could be relevant to HPV.

The cell death–uptake ratio indicates the toxicity induced per unit of liposomal arsenic uptake, and is an effective means of comparing the efficacy of a treatment on different cell populations. For an ideal treatment, the cell death–uptake ratio would be low for normal cells and high for the target cancer cell population. Our results indicated that this

ratio was indeed lowest for the control cell populations and highest for HeLa cells, indicating that liposomal-encapsulated ATO is a promising treatment for HPV-positive cervical cancers. When IC50 (the half maximal inhibitory concentration) was calculated for the cell lines, it was found to be the highest for the two normal cell lines; corroborating the above result that larger dose of the treatment is required for generating the similar cell death in normal cells as cancer cells. These results emphasise the advantage of employing liposomal systems to deliver ATO to cervical cancer cells.

3.1.5 **Conclusion**

Treatment of cancer patients with chemotherapeutics has always been associated with debilitating side effects, systemic toxicities and unfavourable bio-distribution. Advent of nanotechnology based drug carriers with better pharmacokinetics, distribution, ability to escape immune clearance while being non-toxic to healthy tissues have provided us with a solution to most of the cancer related problems. Approval of Doxil by FDA in 1995 has even further strengthened the confidence in these nanotechnology based therapeutics. However, the road to the translation of nanomedicine into clinical practice requires thorough understanding of pharmacokinetics, toxicity and efficacy of the drug formulation. The nanocarrier has to be carefully optimised and its efficacy against the target cancer cells tested. Herein, we prepared six liposomal formulations with three sizes (100nm, 200nm and 400nm) and charges (neutral, positive and negative) and tested them for their loading efficiencies, stability, anti-cancer toxicity, cellular uptake and apoptotic response by the cancer cells. Of all the formulations, 100nm, neutral liposomes were chosen as the most optimal owing to best loading efficiency, high stability and least intrinsic toxicity. The liposomal encapsulation attenuated the toxicity of the drug, allowed for its sustained release while sparing the normal cells. The next step was to further improve the therapeutic potential of these optimised liposomes by conjugating them with cancer cell specific ligand. This can be achieved by screening the target HeLa cells for most overexpressed surface marker and choosing a ligand to conjugate to the optimised formulation of liposome henceforth. The screening of surface markers is detailed in the following section.

3.2 SCREENING OF SURFACE MARKERS

3.2.1 **Introduction**

3.2.1.1 Background

Anti-cancer drugs usually cause systemic toxicities as their principle mechanism of action is to target cells with high proliferation rates (Sapra and Allen, 2003). This marginal selectivity towards malignant cells results in high toxicities to the rapidly dividing normal cells including hair follicles, haematopoietic cells, mucosal lining of the gastrointestinal tract and germ cells leading to deleterious side effects including nausea and vomiting, stomatitis and mucositis among others (Sapra and Allen, 2003). These side effects limit the effective dose that can be administered to a patient which might lead to relapse of the cancer or even development of tumour resistance. This low selectivity of anti-cancer drugs for tumour cells is due to the fact that cancer cells share some common features with the host cells from which they originate, hence finding specific features from cancer cells in order to uniquely target those cells become challenging (Sapra and Allen, 2003).

Intensive research has been ongoing to overcome these challenges and drug delivery via liposomes has been one such major advance in this direction. In addition to reducing systemic toxicities, liposomes also alter pharmacokinetics and bio-distribution of anti-cancer drugs by allowing their “passive” accumulation within solid tumours (Jain, 1987). Passive targeting has been reported to increase the drug concentrations within the tumour manifolds than that of the free form where liposomes release the drugs in a sustained manner either within the tumour interstitium or following uptake by the tumour cells (Jain, 1987).

In order to further increase the specificity in the drug delivery by liposomes to the target cells, efforts have been focussed on the development of ligand conjugated liposomes (Allen et al., 1995). These liposomes have targeting moieties conjugated to their surface

which selectively delivers the drug payload to the desired site of action (Allen et al., 1994; Kirpotin et al., 1997; Carter, 2001). The conjugated moieties facilitating this form of active targeting are basically any molecule which can selectively recognise and bind to antigens or receptors overexpressed or selectively expressed by cancer cells (Fig 3.2.1) (Allen et al., 1995; Allen, Hansen and de Menezes 1995). These molecules can be antibody, antibody fragments, natural or synthetic ligands. Hence, a crucial aspect for utilising active targeting is to first find that receptor which is either exclusive to the cancer in question or is overexpressed as compared to the surrounding healthy tissue. Since very few antigens either exist or are known that are exclusive to a particular cancer, it is more common to rely on the receptors overexpressed on tumour cells relative to normal cells (Sapra and Allen, 2003).

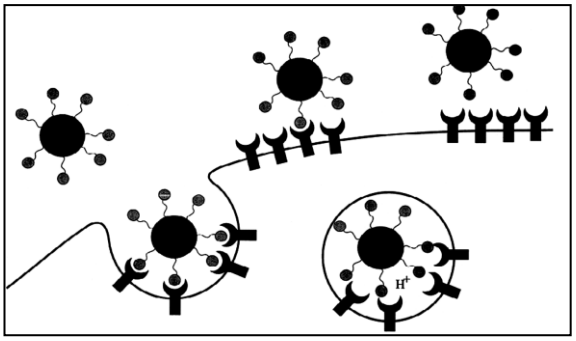

Fig 3.2.1: Receptor mediated endocytosis pathway of ligand conjugated nanoparticles (Sudimack and Lee, 2000)

To successfully utilise active targeting, there are a few considerations to bear in mind: firstly, the receptor density should be high on the target cells; secondly, the receptor should not be shed during the treatment and lastly, the receptor expression should not be too heterogeneous (Dubowchik and Walker, 1999; Kindt et al., 2007; Regimbald et al., 1996). The heterogeneity of receptor expression in tumour cells arises due to their genetic instability and the ability of antigens expressed on their surface to present different glycosylation patterns for conjugation (Kindt et al., 2007). Under such circumstances, two situations can arise: the cells which lack the receptor might escape

cytotoxic effects of targeted liposomes leading to disease relapse, or the receptor negative cells might still be killed from the drug released in the vicinity by the liposomes, known as "bystander effect" (Kindt et al., 2007). Hence, a thorough investigation is required to screen for surface markers on target tumour cells to select the one which is most expressed with minimal heterogeneity. The most well established surface receptors which are routinely employed for targeting by liposomes are folate receptors, transferrin receptors and epithelial receptors including epidermal growth factor receptor (EGFR) (Byrne, Betancourt and Brannon-Peppas, 2008).

Folate receptors

Folate receptor (FR), also known as high affinity membrane folate binding protein, is a 38-40 kDa glycosyl phosphatidylinositol anchored glycoprotein which is significantly upregulated in cancer cells as opposed to normal cells (Lee and Low, 1995; Pan et al., 2002; Sudimack and Lee, 2000; Zhao and Lee, 2004; Low and Antony, 2004). In humans, two isotypes have been identified for FR, α and β (Sudimack and Lee, 2000). Among the two isotypes, FR α is the one that binds to folic acid and its various derivatives have been reported to be highly overexpressed in ovarian, colorectal, endometrial, breast, renal, head and neck, lung and brain cancer (Sapra and Allen, 2003; Sudimack and Lee, 2000). FR β is routinely overexpressed in cancers of non-epithelial origin including sarcomas and acute myeloid leukaemia, however they were reported to be absent in the cell lines established from them (Ross et al., 1999). Targeting FRα with folic acid conjugated liposomes presents itself with several advantages: a, since folic acid is required for the synthesis of purines and pyrimidines along with several other important cellular processes, the drug cargo attached to it is internalised and released in the cytoplasm; b, unlike normal cells which only transport reduced folate across their membranes but not any conjugate forms, cancer cells transport folate conjugates as well through folate receptors as an alternate route and lastly, c, folate receptors, while being overexpressed in most cancers, are generally absent in normal tissues with the exception of placenta, choroid plexus and weak expression in kidney, thyroid and lungs (Low and Antony, 2004; Sudimack and Lee, 2000). Even when expressed in normal tissue, FR demonstrates a highly polarised distribution on normal epithelia (Lu and Low, 2012). For instance, in proximal tubules, FR are only present on the urine facing surface of the tubule cells or in the blood brain barrier, they are only concentrated on the brain side

(Lu and Low, 2012). This polarised distribution of folate receptors is lost once the tissue becomes malignant and spreads throughout the entire tumour surface (Patrick et al., 1997). Hence, targeting via folate receptors should not damage healthy tissues with FR expression (Lu and Low, 2012). Moreover, folic acid (Fig 3.2.2) is an ideal targeting ligand because it is small in size (the smaller drug ligands conjugate have a better pharmacokinetics and reduced possibilities of immunogenicity), it is inexpensive, non-immunogenic and non-toxic, stable in both storage and circulation and amenable for conjugation with high receptor binding affinity (Low and Antony, 2004; Sudimack and Lee, 2000).

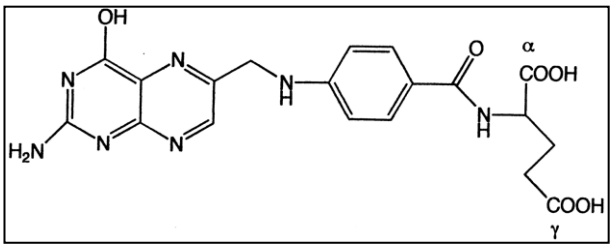

Fig 3.2.2: The structure of folic acid with α and γ carboxyl groups depicted; conjugation of folic acid with the foreign molecule through its γ carboxyl group retains its high binding affinity with FR (Sudimack and Lee, 2000).

Transferrin receptors

Transferrin receptor (referred to as TfR1) is a type II receptor which resides on the cell surface and is a main port of entry for iron bound with transferrin (Tf), which is a serum non-heme glycoprotein, into the proliferating cells (Fig 3.2.3) (Singh, 1999). After binding with its receptor, Tf is internalised where iron dissociates in the acidic environment of endosomes and TfR1 is recycled back to the cell surface (Singh, 1999). Since, the proliferating cells including cancer cells have an increased requirement of iron, transferrin receptors are reported to be overexpressed in them, their expression correlating with cancer stage or tumour progression (Gatter et al, 1983; Daniels et al.,

2012). Tf conjugated nanotherapeutics have already entered human clinical trials with cisplatin, adriamycin and diphtheria toxin (Faulk et al., 1990; Head, Wang and Elliott, 1997; Rainov and Soling, 2005). An important consideration while using Tf ligand for targeting is to improve its iron-binding affinity as that, in turn, affect its binding to the transferrin receptors (Bellocq et al., 2003). Also, high levels of Tf circulating in the blood might reduce the cytotoxicity of transferrin conjugates considerably (Daniels et al., 2012). As Tf conjugates can interact both with TfR1 and TfR2 (a second member or TfR family which is mainly localised in hepatocytes), this can lead to liver toxicity (Daniels et al., 2012).

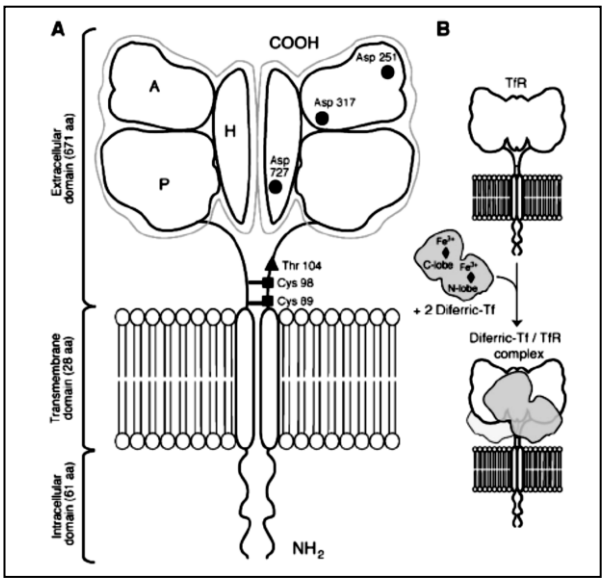

Fig 3.2.3: Schematic representation of TfR: (a) The receptor is a heterodimer with two monomers joined together by disulphide bridges at cysteine 89 and 98. The extracellular domain consists of tree sub-domains: apical A, helical H and protease like domain (P) and (b) binding of the iron conjugated transferrin with its receptor (Daniels et al., 2012; 2006).

Epidermal growth factor receptor

These tyrosine kinases receptors, upon binding to the growth factor ligand, mediate cell signalling pathways required for growth and proliferation (Laskin and Sandler, 2004). EGFR binds to six known ligands including EGF, transforming growth factor-α (TGF-α), betacellulin, amphiregulin, epiregulin and heparin binding EGF (HB-EGF) (Laskin and Sandler, 2004). Among these, EGF and TGF-α are the most commonly used ligands and upon binding to the receptor, the complex gets internalised within the cell (Byrne et al., 2008). EGFR is over expressed in almost one third of cancers including colorectal, lung, brain and breast cancers (Byrne, Betancourt and Brannon-Peppas, 2008).

The present study was the next step in our original attempt to synthesise robust, targeted liposomal constructs of ATO for HPV positive cervical cancer cells. Previously, we optimised the liposomal formulation to be used for cervical cancers and demonstrated that 100 nm, neutral liposomes encapsulating ATO were the most optimal design. Results from further testing their biological properties showed that these liposomes attenuated drug toxicity and increased the anti-cancer activity of ATO towards HPV positive cell lines while sparing normal cells *in vitro*. ATO encapsulated in liposomes was selective in its action by being more effective against HPV positive cells than HPV negative cells. Therefore, attempts were made to further enhance the specificity of these liposomes towards HPV positive cervical cancer cells by finding the most suitable ligand for conjugation to specifically target these cells. To achieve this goal, cell lines were screened for the three abovementioned cell surface receptors.

3.2.1.2 Aims:

The aim of this section was to find the most appropriate ligand which could be conjugated to the optimised ATO encapsulated liposomes to actively target HPV positive cervical cancer cells *in vitro.*

3.2.1.3 Objectives:

(i) To screen the two cervical cancer cells, HeLa and HT-3, for the surface markers (folate receptor, transferrin receptor and EGFR);

(ii) To identify the surface marker which is most differentially expressed in the two cells lines; i.e. highly expressed in HeLa cells while being negligibly expressed in HT-3, in order to find the best targeting ligand for liposomes targeting specifically the HPV positive cervical cancer cells.

3.2.2 **Materials and Methods**

3.2.2.1 Cell culture

Two cervical cancer cell lines, HeLa and HT-3, and two control cell lines for folate receptor expression, human lung carcinoma A549 and HeLa derivative human nasopharyngeal epidermal carcinoma cells KB were employed in this study. For folate receptor experiments, HeLa and KB cells were cultured in RPMI1640 media with no folic acid, HT-3 in McCoy's (modified) 5A media and A549 in Ham's F12 Nutrient Mixture, while for the other receptors' experiments, HeLa was cultured in normal RPMI media. All media used contained 10 % foetal calf serum, 100 U/ml of penicillin and 100 mg/ml streptomycin and cells were grown in 75-cm^2 flasks. The following experiments were then set up for further studies including Western blot and immunocytochemical staining using both chromogenic and fluorescent labelling.

3.2.2.2 Western blot analysis

Expression of folate, transferrin and EGF receptors on HPV positive and negative cervical cancer cell lines were determined by Western blotting as detailed in Chapter 2. For folate receptor expression, two cell lines, a positive and negative control, KB and A549 respectively, were also included. The primary antibodies used were rabbit anti-FOLR1 polyclonal antibody, rabbit anti-transferrin and anti-EGFR antibody (1:1000 dilution). Protein quantification was done using REVERT total protein stain technique on Licor Odyssey imaging system, except in one experiment for folate receptor analysis where the housekeeping gene β-actin was used for normalisation. In that case, mouse anti-β-actin antibody was used in 1:3000 dilution.

3.2.2.3 Chromogenic labelling immunocytochemical staining analysis

Chromogenic labelling for folate, transferrin and EGF receptors following immunocytochemical staining for the above mentioned four cell lines were carried out as per the protocol described in Chapter 2. The primary antibodies used were the same

as those used in Western blotting experiments. The dilutions used however were 1 in 50 for FOLR 1 and 1 in 100 for anti-transferrin and anti-EGFR antibody in PBS.

3.2.2.4 Confocal imaging of folate receptor expression

The cells were stained with fluorescent labelling for folate receptor and imaged via a confocal microscope according to the protocol described in Chapter 2.

3.2.2.5 Statistical analysis

Statistical analysis described in experimental sections was carried out with Minitab17 using 2-sample t-test. $P \leq 0.05$ was considered as statistically significant difference. For results from Western blotting studies, the signals were normalised using Image J software and mean and SD were calculated. For immunostaining results, an average number from positively stained cells in a total of six fields of each stained slide were calculated and average percentages were recorded.

3.2.3 **Results**

3.2.3.1 Folate receptor is the most differentially expressed receptor in HPV positive HeLa and HPV negative HT-3 cell lines.

Western blot analysis

The expression of folate receptor α, transferrin receptor and EGFR were examined in HPV positive and HPV negative cervical cancer cell lines, HeLa and HT-3 respectively, via Western blotting. For folate receptor, results showed a distinct band at around 37 kDa for HeLa cell line while a very faint band was observed for HT-3 cell line. The signal intensity for the bands obtained was normalised employing REVERT total protein stain (Fig 3.2.4). The relative folate expression of HT-3 was henceforth found to be negligible compared to HeLa.

While probing for transferrin receptor expression, a band at around 98 kDa was observed for both the cell lines, with expression on HeLa around 1.5 times more than HT-3. Similarly for EGF receptor, both the cell lines displayed a band at around 134 kDa, although HeLa expressed 1.3 times more EGF receptors than HT-3 (Fig 3.2.4). For all the receptors therefore, the expression on HeLa was higher than HT-3, however, folate receptor singularly displayed the maximum difference by being appreciably expressed on HeLa (around 14 times more) than HT-3. Hence, these results offer a possibility of selecting folic acid as the ligand of choice for conjugating to the liposomes to make them further selective to HPV positive HeLa cell line.

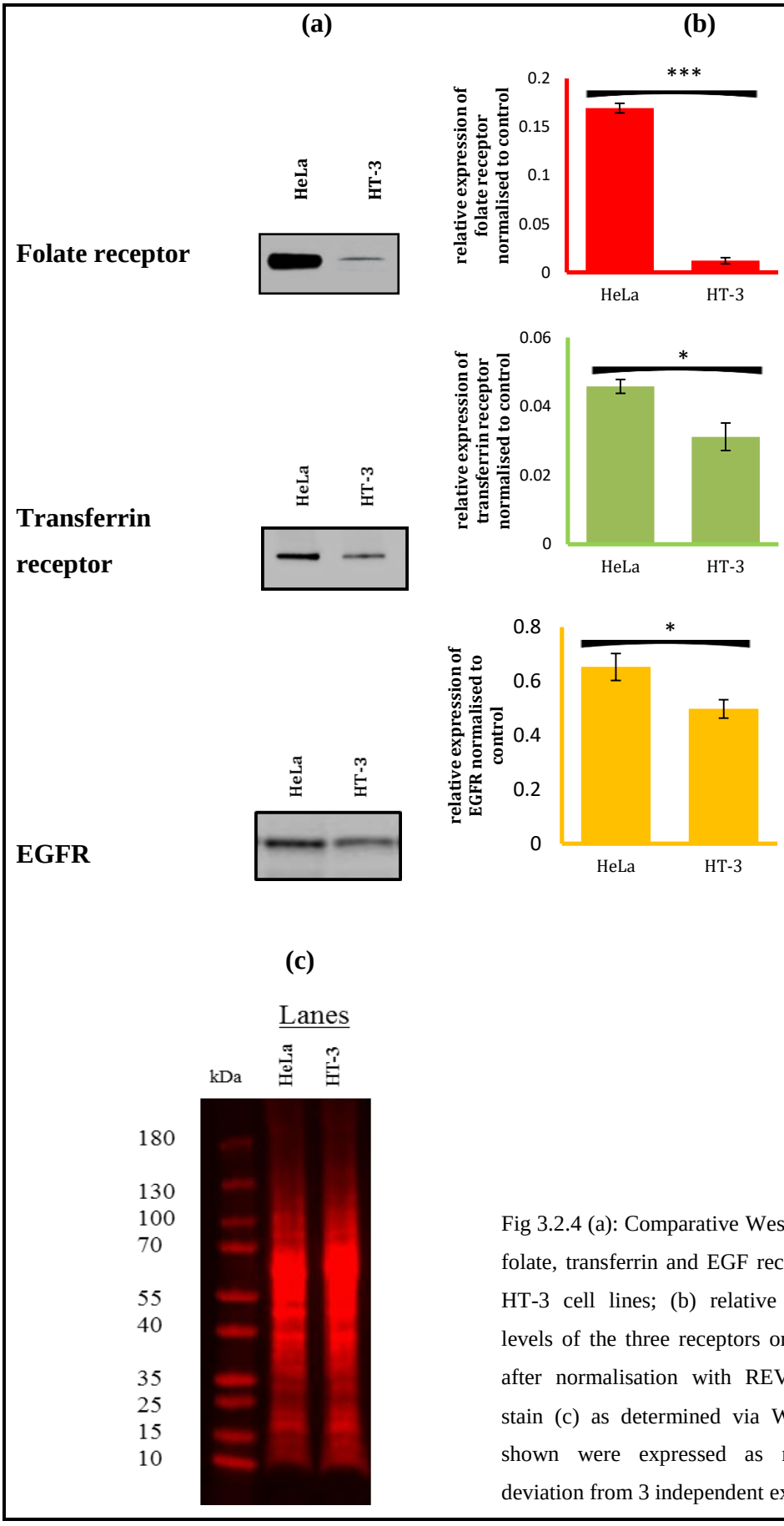

Fig 3.2.4 (a): Comparative Western blot analysis of folate, transferrin and EGF receptors in HeLa and HT-3 cell lines; (b) relative protein expression levels of the three receptors on the two cell lines after normalisation with REVERT total protein stain (c) as determined via Western blot. Data shown were expressed as means ± standard deviation from 3 independent experiments.

Chromogenic staining

The results obtained from Western blot were further validated by chromogenic stanining of the three receptors on HeLa and HT-3 cell lines (Fig 3.2.5). Chromogenic staining with DAB substrate was performed to evaluate the receptor expression levels on the cells. Consistent with the previous results, folate receptor expression displayed the maximum difference in the two cell lines by being expressed much more in HeLa cells than in HT-3 cells. The staining for EGFR and transferrin receptors on both the cell lines were observed to be of similar magnitude, with expressions on HeLa slightly more than HT-3, corroborating the Western blotting results.

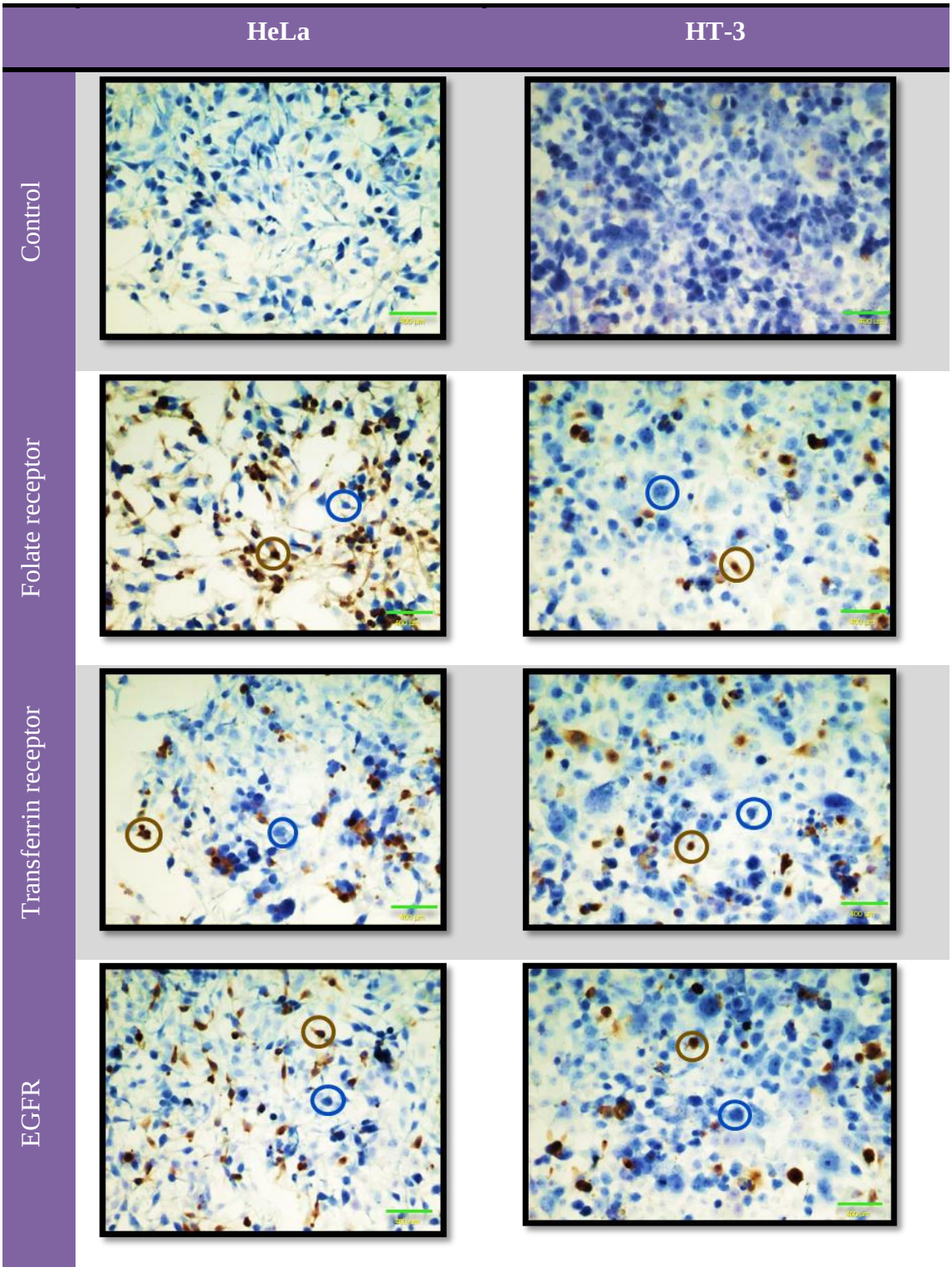

Fig 3.2.5: Immunocytochemical staining of folate, transferrin and EGF receptor expression in HeLa and HT-3 cells. DAB chromogen stained the receptor and cells were counterstained with hematoxylin to reveal the nuclear/ DNA location. The cells stained brown represents the presence of the receptor while the cells stained blue are devoid of the receptor. Cells encircled brown and blue in each image are representative of presence and absence of the expressed surface receptor respectively.

3.2.3.2 Folate receptor expression analysis with the controls

Western blot analysis

After establishing that the folate receptor is the most differentially expressed out of the three receptors investigated in the two cervical cancer cell lines; a positive control KB cells and a negative control A549 cells for folate receptor expression, were included to further validate our experiments and consolidate our previous results. Western blotting analysis of folate receptor expression showed a prominent band for the positive control and no band for negative control (Fig 3.2.6). A distinct band was observed for HeLa cell line, while a faint band was observed for HT-3. The relative level of folate expression of HeLa was half of KB expression, while the expression of HT-3 was much less than KB and HeLa cells. β-actin was employed as a loading control and its signal strength was consistent for all the lanes, therefore, equal amount of protein was loaded for each sample.

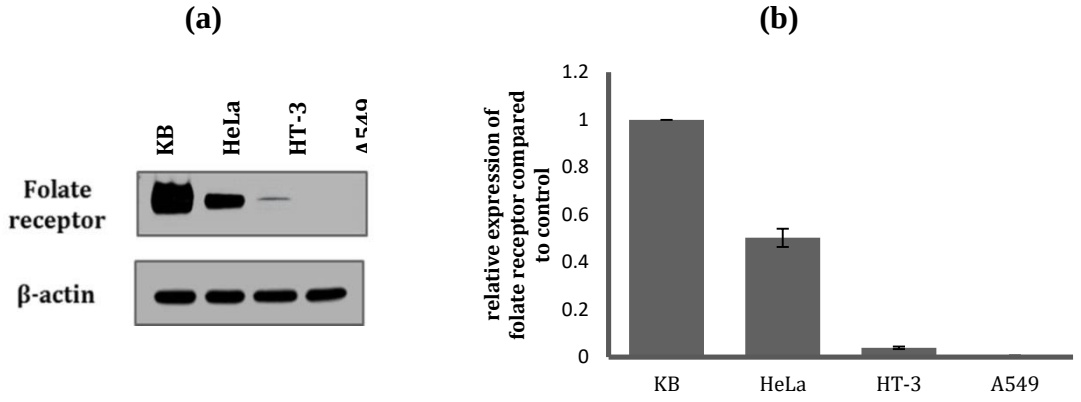

Fig 3.2.6 (a): Western blot analysis of folate receptor expression on KB, HeLa, HT-3 and A549 cell lines. (b) Relative protein expression levels of folate receptor from the four cell lines after normalisation with β-actin protein levels as determined via Western blot. Data shown were means ± standard deviation from 3 independent experiments.

Chromogenic staining

The four cell lines were further stained for folate receptor with DAB substrate and counter-stained with haematoxylin to reveal nuclear location. Similar to the results from Western blot, KB displayed clear surface staining with almost 90% of the cells positively stained. Around half of the HeLa cells were also stained positive while A549, the negative control, did not stain for the folate receptor. Around 10% of HT-3 cells stained positive for folate receptor (Fig. 3.2.7).

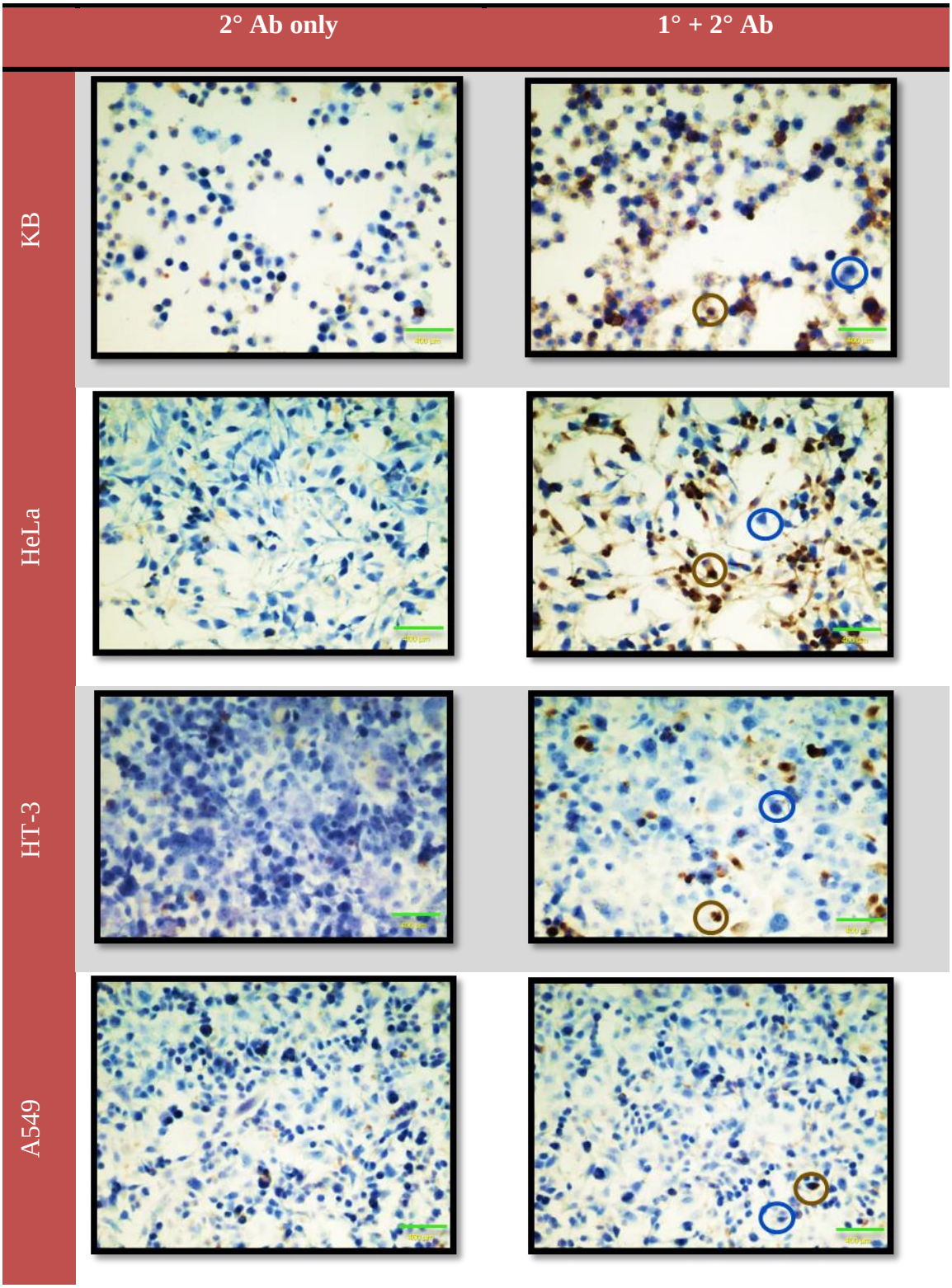

Fig 3.2.7: Immunocytochemical staining of folate receptor expression of KB, HeLa, HT-3 and A549 cell lines. DAB chromogen stained the folate receptor and cells were counterstained with hematoxylin to reveal the nuclear/ DNA location. Cells encircled brown are representative of positive receptor staining while cells encircled blue represents negative receptor expression.

Fluorescent staining

Fluoresent labelling followed by visualisation via confocal microscopy was also performed to further confirm the results obtained earlier (Fig 3.2.8). KB and HeLa showed clear surface staining for most of the cells with higher percetage of stained cells in KB than HeLa which confirmed the Western blot result. HT-3 did not show significant staining for folate receptor and A549 stained negative which are also consistent with the previous results.

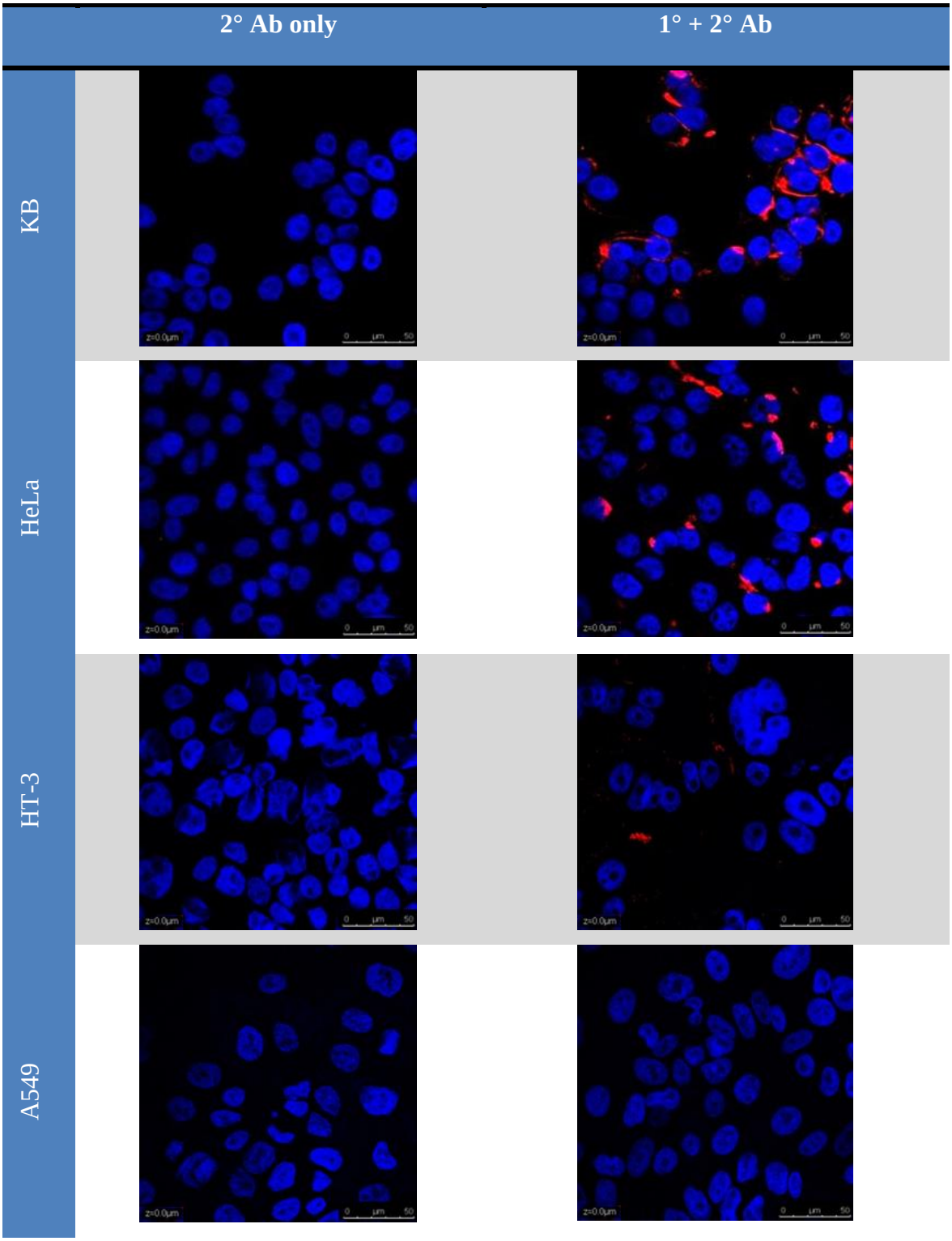

Fig 3.2.8: Confocal microscopic examination of folate receptor expression in KB, HeLa, HT-3 and A549 cell lines. Red fluorescence showed the expression of folate receptor. Cells were counterstained with DAPI (in blue) to reveal the nuclear/ DNA location.

3.2.4 Discussion

In the search for the best ligand to target HPV positive cervical cancer cell lines, we screened both HPV positive and negative cell lines, HeLa and HT-3, for the three most important, widely employed surface markers: folate receptor, transferrin receptor and EGFR. The first surface marker to be screened was folate receptor. Folic acid is a very small molecule which can be easily conjugated to a liposomal surface having H_2N-PEG-DSPE moieties via carbodiimide coupling in high densities (Gabizon et al., 1999). Its small size ensures the liposomal conjugate does not have complications extravasating from the leaky vasculature of tumour and accumulating via EPR effect and also not be recognised by MPS which targets larger particles for immune clearance (Sudimack and Lee, 2000). The second surface marker transferrin receptor, on the other hand, requires optimisation to increase its iron binding affinity as that directly reflects on its receptor binding potential (Byrne, Betancourt and Brannon-Peppas, 2008). Moreover, transferrin circulating in blood compromises the cytotoxic ability of the liposomal conjugates (Byrne, Betancourt and Brannon-Peppas, 2008). As for EGFR, some of the antibodies and small molecules targeting EGFR are already in clinical development; however they have been reported to generate immunologic response that may hinder repeated treatment, unlike folic acid which is non-toxic and non-immunogenic (Low and Antony, 2004; Dancey and Schoenfeldt, 2001).

With the primary objective of identifying a surface marker which is ideally over-expressed by HeLa cells albeit not by HT-3 to provide targeting specific to HPV positive cervical cancer cells, we employed two techniques, Western blotting and chromogenic staining using DAB substrate, for the preliminary investigation of the expression of the three surface markers mentioned above on these two cell lines. While investigating the folate receptor expression, Western blot results gave highly encouraging results where the expression of the receptor on HeLa cells was appreciably high while it was negligible in HT-3. For the other two surface markers, both cell lines expressed them and HeLa was found to express both of them more than HT-3 (1.5 times more for transferrin and 1.3 times more for EGFR). However, the difference in their expression between the two cell lines was not as distinct as the folate receptor expression (HeLa expressed the marker around 14 times more than HT-3). To

corroborate the above findings, chromogenic staining of the receptors was employed on both cell lines for all the three receptors. Western blotting results were validated when around 70% of the HeLa cells stained positively for folate receptor in comparison of less than 10% of positive staining for HT-3 cells. Around 20-30% HeLa cells stained positive for both the other receptors and similar staining was observed for HT-3 cell lines albeit slightly lesser than HeLa cells. Based on the results, folic acid was chosen as the ligand to be used for liposomal conjugation targeting specifically the HPV positive cervical cancer cells.

Further validation for using folate acid as the ligand of choice was also carried out by including two control cells lines, KB as positive control (FR+) and A549 as negative control (FR-) (Chen et al., 2009; Nukolova et al., 2011). Western blot results indicated that folate receptor expression was very high for KB cells and negligible for the negative control, A549, validating the accuracy of the experiments. HeLa also displayed a strong expression, with relative intensity after normalisation to loading control β-actin as around 50% to that of KB. Their expression on HT-3 cell surface, on the other hand, was negligible. To further validate the findings, both fluorescent staining and chromogenic staining were performed on HeLa and HT-3 cells along with the control cell lines. Chromogenic staining with DAB substrate showed a clear surface staining for folate receptor for KB cells and HeLa cells and negligible staining for FR- A549 cells. KB had a higher expression than HeLa, confirming the previous results. This staining pattern was replicated with confocal microscopy images of folate receptor: 90% of KB cells showed intense surface staining, around 60% staining for HeLa cells and 10% for HT-3 cells.

3.2.5 Conclusion

Harnessing the power of nanotechnology in the field of drug delivery has given us opportunities to design passive or active targeted drug delivery system. Non-targeted drug carrier systems can extravasate in the tumour tissue via EPR effect and result in differential accumulation in tumour tissue versus healthy tissue. Moreover, if appropriate ligands are attached to the surface of these nano-carriers, that may act as "homing devices" and significantly enhance the selective delivery of drug to the target tissue. Herein, we investigated three most well established cell surface receptors, folate, transferrin and EGF receptors, against HPV positive and HPV negative cell lines to search for the most appropriate ligand for conjugating to ATO encapsulated liposomes towards a final goal of specifically targeting HPV positive cervical cancer cells. From the results obtained and the inherent advantages of employing folic acid as a targeting ligand, folic acid was selected as the suitable ligand for our future experiments. Our next step was to conjugate folic acid to ATO liposomes and assess their efficiency in the cellular uptake or inducing anti-cancer response in the FR positive HPV positive cervical cancer cells. We have already seen from our previous research that HeLa is inherently more susceptible to the liposomal treatment than HT-3. Additionally, as HeLa express more folate receptors than HT-3 cells, active targeting might further enhance the specificity of the liposomal construct, tailoring it for an effective anti-cancer response towards HPV positive cervical cancer cell lines.

3.3 TARGETING HPV POSITIVE CERVICAL CANCER CELLS WITH ARSENIC TRIOXIDE ENCAPSULATING FOLATE CONJUGATED LIPOSOMES

3.3.1 **Introduction**

3.3.1.1 Background

Since 40 years, application of nanotherapeutics has provided a distinct possibility of delivering therapeutic agents in a far more efficient manner than that could be achieved through conventional drug delivery (Strebhardt and Ullrich, 2008). Nanoparticles have the potential to encapsulate poorly soluble drugs, protect the therapeutic compounds from degradation and modify their blood circulation and tissue distribution profiles (Bertrand et al., 2014).

The tumour distribution profile of nanoparticles is primarily governed by three interrelated processes: their extravasation from the fenestrated blood vessels into the tumour interstitium; their further penetration into the tumour extravascular tissue and finally, their interaction with the intracellular targets within the tumour milieu (Bertrand et al., 2014). The first two factors, describing the passive targeting phenomenon, result in the transport of nanocarriers from leaky tumour fenestrations into the tumour interstitium where they are retained due to poor lymphatic drainage, characteristic of the tumour tissue (Danhier, Feron and Preat, 2010). It is dependent on the forces of diffusion and convection which are reliant simultaneously on both the tumour microenvironment and characteristics of diffusing nanoparticle such as size, surface properties, shape and concentration within tumour blood vessels (Bertrand et al., 2014).

The third parameter involving the interaction of nanoparticle with the intracellular target is more complex and can be greatly benefitted from the active targeting strategies of the drug encapsulating nanoparticles. Active targeting, also referred to as ligand-mediated targeting, employs the specific affinity of ligands decorated on the surface of the nanoparticles towards specific receptors or surface molecules overexpressed in target cells, tissues or organs (Cheng et al., 2012; Kamaly et al., 2012; Koshkaryev et al., 2013; Peer et al., 2007; Shi et al., 2011). Aided by the EPR effect, which allows the nanoparticle carrying the drug payload to remain in the vicinity of the target cells, active targeting facilitates its cellular internalisation via the specific ligand-receptor interaction (Byrne, Betancourt and Brannon-Peppas, 2008). This is important as although the EPR effect does improve the target tissue distribution profile of the circulating nanoparticles, it alone does not guarantee that the drug would reach its pharmacological target (Bertrand et al., 2014). In the absence of any specific affinity between the nanoparticles and the target cancer cells, the chemotherapeutic payload would either have to reach its target on its own or endanger itself diffusing back to the vasculature (Dreher et al., 2006). Therefore, effects of the drug treatment will be greatly benefited from active targeting strategies by increasing the intra-tumoral uptake of the encapsulated drug by enhancing its internalisation by the target cell after extravasation and helping it reach its pharmacological target (Kirpotin et al., 2006; Bartlett et al., 2007; Li et al., 2008). Briefly, active targeting is advantageous as it increases the tumour residence time for nanoparticles, enhances their affinity for the target cells and helps them to reach their intracellular destination though receptor mediated endocytosis (Fig 3.3.1) (Bertrand et al., 2014). Therefore active targeting is increasingly being recognised as an effective strategy to enhance the therapeutic indices of anti-cancer drugs.

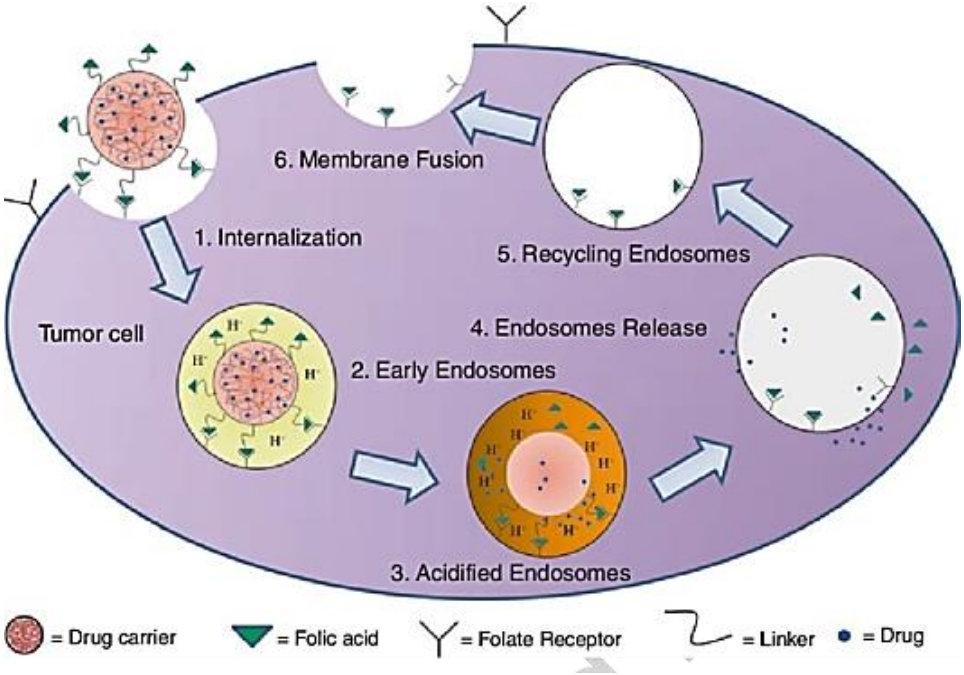

Fig 3.3.1: Receptor mediated endocytosis for folate conjugated nanocarrier in cells expressing FR (Pawar, Domb and Kumar, 2014).

The efficiency of any actively targeting system *in vitro*, and most importantly *in vivo*, can be assessed by two important parameters: targeting specificity and delivery capacity of the drug delivery vehicle (Bertrand et al., 2014). The specificity is mainly determined from the choice of the ligand and how it interacts with the off-target molecules and cells (Bertrand et al., 2014). The delivering capacity depends on the structure and composition of the nanoparticle itself like its physicochemical properties such as the size and charge of the nanoparticle, the ligand density among others (Gu et al., 2008; Jiang et al., 2008; Valencia et al., 2011; Wu and Chu, 2013). Some of the other important factors that affect the efficacy of active targeting include the administration route or the non-specific binding of proteins during its passage though the bloodstream. Since these targeted delivery systems rely heavily on their being in the circulation for an extended period of time, followed by their extravasation into the tumour interstitial space, where they can interact with their antigenic substrate, it is imperative to surface functionalise these nanoparticles with the hydrophilic polymer PEG. PEG layer serves to delay the opsonisation of the nanoparticles and therefore evade the uptake and clearance by MPS (Sapra and Allen, 2003).

First described in 1980, this strategy of actively targeting cancer cells by conjugating nanoparticles with ligands rapidly became one of the most successful ways of improving the efficacy of nanotherapeutics, at least in animal models (Huang, Huang and Kennel, 1980). The ligands were selected based on the high specificity and affinity for the surface markers overexpressed on the target cells and the ability to trigger receptor mediated endocytosis following binding. Following our previous findings, we selected folic acid as the ligand of choice as FR was the most differentially expressed receptors out of the three tested tumour markers screened from HPV positive and HPV negative cell lines.

Folic acid is a low molecular weight vitamin required by eukaryotic cells for *de novo* nucleotide synthesis (Stephenson, Low and Lee, 2004). Since the eukaryotes lack the necessary enzymes required for biosynthetic pathways for folic acid, their survival depends on mechanisms to capture folates to sustain life, which involves the presence of membrane spanning glycoproteins serving as transporting receptors for folates into the cells (Stephenson, Low and Lee, 2004). The FRs are overexpressed on a variety of cancer cells, probably owing to a greater requirement for uncontrolled growth, characteristic of cancer cells (Stephenson, Low and Lee, 2004).

Folates have a very high specificity and affinity (K_D=~10-9M) for its receptors (Bertrand et al., 2014). Tethering folic acid to the surface of nanoparticles is also beneficial in that, unlike high molecular weight ligands like antibodies, aptamers or proteins, it does not increase the hydrodynamic size of the nanoparticle appreciably and hence, does not interfere with the tumour accumulation due to any size restrictions (Danhier, Feron and Preat, 2010). Moreover, some studies showed that FR targeted liposomal delivery had the potential to reverse multidrug resistance or bypass it (Gabizon et al., 2004; Torchillin, 2010).

Folate targeting nanoparticles have shown promising results as therapeutic and diagnostic agents, when evaluated in preclinical settings (Lee and Low, 1995; Ni, Stephenson and Lee, 2002; Pan et al., 2002; Sudimack and Lee, 2000; Werner et al., 2011; Zhao and Lee, 2004). It has been employed as a targeting moiety for many nanotherapeutic platforms like quantum dots, gold nanoparticles, dendrimers, iron oxide and liposomes (Bazak et al., 2015). Folate conjugated liposomes have been tested with a wide range of drug payload including cytotoxics, genes or anti-sense oligonucleotides

(Goren et al., 2000; Lee and Low, 1994; Pan, Qualls and Thompson, 2001; Reddy et al., 2002; Wang and Lee, 2002; Wang et al., 1995; Zhou et al., 2002). Six of the drugs directly conjugated to folate have entered into human clinical trials (Low and Kularatne, 2009). In all the cases, it was observed that folate conjugates not captured by folate receptor in FR negative tissues were rapidly excreted from the body, limiting the off-target toxicity (Low and Kularatne, 2009; Mathias et al., 1998; Siegel et al., 2003; Wang et al., 1997). Additionally, it has been reported that presence of physiological levels of folate in the bloodstream has minimal effect on the FR specific tumour uptake of the folate conjugates owing to the higher affinity of the liposomes conjugated to multiple ligands for the cell surface receptors (Licciardi et al., 2006).

For the purpose of designing an actively targeting system, there are quite a few parameters that need careful consideration and optimisation. One of them is how the ligand is attached to the liposome. If the ligand is conjugated directly to the phospholipid headgroup, as was done initially, the steric barrier imposed by the PEG layer interfered with the coupling efficiencies and binding capacity of the ligand conjugated nanoparticles (Klibanov et al., 1991). To circumvent this issue, ligands were coupled to PEG terminus which prevented their masking by the PEG layer and easier accessibility to their targeted antigens (Laemon and Low, 2001).

The importance of PEG spacer in FR targeting was succinctly established by Lee and Low for KB cells using both targeted and non-targeted liposomes (Lee and Low, 1994). Liposomes with folate tethered to a long PEG spacer (250 Å) displayed a higher uptake than either non-targeted or targeted liposome with short spacer length (Lee and Low, 1994). In another study by Gabizon et al., placing the ligand on a longer PEG spacer length of 3350 Da, as opposed to 2000 Da PEG layer used for steric stabilisation, increased the uptake of conjugated liposomes substantially (Gabizon et al., 1999). However, it has also been speculated that if ligand is conjugated to a longer PEG spacer than the other PEG chains involved in the PEG brush, the extra length of the long spacer might undergo mushroom-like folding, leading to limited exposure of ligand. Therefore, it might even be better to have the same length spacer as the surrounding PEG brush (Wang and Thanou, 2010). This ambiguity in literature therefore requires a thorough investigation on the appropriate spacer PEG length to be used for folate conjugation, targeting the specific tumour under investigation.

It is also imperative to optimise the ligand density on the surface of the liposomes. While a higher ligand density might be desirable to increase the binding avidity between the liposomes and the target antigen, it might also give rise to potential immunogenic concerns (Sapra and Allen, 2003). A higher coverage of PEGylated liposomes with ligands might shield the steric stabilisation effect of PEG layer and consequently result in a higher recognition by plasma proteins leading to opsonisation (Wang and Thanou, 2010). Apart from these biological effects, there is not much data on physical implications of high ligand density, demonstrating a need to optimise this factor to maximise targeting abilities of the nanocarriers (Wang and Thanou, 2010).

As a complimentary strategy to EPR, ligand functionalised nanoparticles offer the potential to further augment the efficacy of nanotherapeutics in treating diseases. Although, there have been multiple studies reporting the enhanced uptake by FR positive cells following folate conjugation to liposomes carrying the therapeutic payload (Canal et al., 2010; Zhang et al., 2010; Zhang et al., 2010; Zhao and Lee, 2004), there has been few efforts, if any, to definitively determine the optimal spacer length for folic acid conjugation on liposomal physicochemical characteristics, inhibitory potency and *in vitro* performance on cervical cancer cells with differing HPV status.

3.3.1.2 Aims:

The aims of this chapter are to design folate targeted ATO encapsulating liposomes and assess the effect of ligand spacer length on cellular uptake and inhibitory potency against HPV positive cervical cancer cells *in vitro*.

3.3.1.3 Objectives:

(i) To synthesise folate conjugated, ATO encapsulating liposomes with ligand spacer length similar to the surrounding PEG brush and assess any enhancement in the cellular uptake due to ligand conjugation, compared to unconjugated liposomes in KB, HeLa, HT-3 and A549 cell lines with differing FR expression.

(ii) To examine any further improvement in cellular uptake on increasing PEG spacer length for folate conjugation and selecting the optimal PEG spacer length for ligand targeting (Fig 3.3.2).

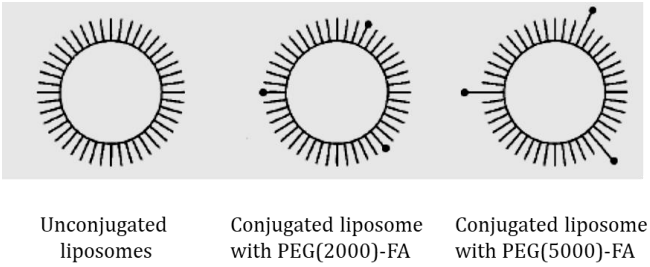

Fig 3.3.2: The three liposomal formulations prepared for the study: **L1**, unconjugated liposomes, **L2**, conjugated liposomes with FA-PEG spacer length of 2000Da and **L3**, conjugated liposomes with FA-PEG spacer length of 5000Da.

(iii) To investigate and assess the differences in cellular uptake and *in vitro* cytotoxicity between the free drug (ATO), non-targeted and the optimised targeted liposomal formulation.

3.3.2 **Materials and Methods**

3.3.2.1 Liposome preparation and characterisation

Unconjugated and folate conjugated labelled liposomes with different spacer length were synthesised as detailed in Chapter 2. Their loading efficiency (As/P ratio) was determined by ICP-OES and mean liposomal size was calculated via dynamic light scattering on a Zetasizer-Nano ZS. Liposomal stability over a period of a month was assessed by analysing their loading efficiency every week while liposomes were stored at 4°C in buffers of pH 7.4.

3.3.2.2 Cell culture

HPV positive and negative cervical cancer cell lines, HeLa and HT-3, were employed in this study. KB and A549 cells were taken as FR positive and negative controls respectively. KB and HeLa cells were grown in folate-free RPMI-1640 media (for a minimum of 2 months before each experiment), HT-3 cells in McCoy's 5A (modified) media and A549 cells in Ham's F12 Nutrient Mixture with 10% FBS and 1% penicillin-streptomycin. The following experiments were set up to investigate cellular uptake following liposomal ATO exposure for different time intervals: confocal microscopic visualisation, flow cytometry, plate reader analysis and ICP-MS studies. Cellular toxicity was investigated via MTT Assay.

3.3.2.3 Qualitative cellular uptake analysis by confocal microscopic visualisation of liposomal arsenic

Cells were plated, 24 to 48 h before each experiment, on sterile 22-mm coverslips inside six-well plates at a density of 5×10^4/ml. Following attachment, the cells were exposed to DiIC18(3)-DS labelled liposomes (L1, L2 and L3) for various time intervals at 37°C in the incubator. The employed liposomal dilutions had an arsenic concentration of 18µmol/L. After the intended time period, the spent media was removed and cells were

washed three times with PBS and fixed with PBS-buffered 4% paraformaldehyde at 25°C for 8 minutes. The coverslips were again washed with PBS and mounted on a slide using DAPI, staining nuclei in blue containing anti-fade ProLong Gold reagent (Life Technologies Ltd, Paisley, UK). The fluorescence emitted from each slide was observed via a confocal microscope (Leica Microsystems, Wetzlar, Germany).

3.3.2.4 Flow cytometric analysis of liposomal arsenic uptake

Cells were seeded at 5×10^5/ml in six-well culture plates and grown overnight before exposing to the above mentioned DiIC18(3)-DS labelled liposomal formulations at a dilution having arsenic concentration of 18µmol/L for various time intervals at 37°C. After the intended time interval, the cells were trypsinized, washed twice by PBS and then collected into FACS tubes with 500µl PBS. All samples were analysed using FACSCalibur (BD, Oxford, UK). For DiIC18(3)-DS, the maximum excitation was obtained with He-Ne laser at 555nm and fluorescence emission intensities were observed at >570nm using FL-2 filter. For each sample, a minimum of 10,000 cells were collected. Data were analysed using CellQuest Pro software from BD Biosciences. The ratio of cells staining positive with labelled conjugated liposomes to cells staining positive for labelled unconjugated liposomes was calculated to give an estimate on the differences in uptake of liposomes of different formulations. All measurements were performed in duplicates from at least three different experiments.

3.3.2.5 Plate reader analysis of liposomal uptake by cells

Cells were seeded at 1×10^5/ml in 96 well plates and allowed to attach overnight. Cells were further exposed to labelled liposomes at arsenic concentration of 18µmol/L for various time intervals at 37°C. Following the treatment, the cells were washed twice with PBS and the fluorescence measured via BMG LabTech FLUOstar Omega Plate Reader. As with the flow cytometric analysis, the ratio of cells staining positive with labelled conjugated liposomes to cells staining positive for labelled unconjugated liposomes was calculated and analysed.

3.3.2.6 Quantitative analysis of liposomal drug uptake via ICP-MS

Cellular uptake was analysed for different treatments at a time period of 6 h, 24 h and 48 h by ICP-MS as described in Chapter 2. Following a 24-h cell attachment, cells were treated with liposomal formulations as mentioned above and free drug with an arsenic concentration of 10µmol/L. Their arsenic concentration was determined and quantified after the desired time interval.

3.3.2.7 *In vitro* cellular cytotoxicity assay

Cytotoxicity of various liposomal formulations of ATO was determined by an MTT Assay as described in Chapter 2. Briefly, the experiment was set up in a 96 well plate, where the toxicity of control empty liposomes was investigated by taking an initial starting amount containing 0.5mM of phospholipid concentration and diluting it in 1:10 ratio to further 6 wells. The ATO encapsulating liposomes contained 30µM of ATO concentration in the initial sample which was further diluted in 1:6 at a final working arsenic concentration of 5µM for treating the cells. The wells were seeded with HeLa, HT-3, KB and A549 at a density of 0.6 million cells per ml and incubated at 37°C in the humidified incubation chamber for 24 h, 48 h and 72 h. After the intended incubation, MTT Assay was performed as per the described protocol and absorbance of the final coloured solution read and quantified via BMG LabTech FLUOstar Omega Plate Reader at a wavelength of 570 nm.

3.3.2.8 Statistical analysis

Statistical analysis described in experimental sections was done using Minitab17. Statistical significance was determined by 2-sample t-test. $P< 0.05$ was considered significant. For flow cytometry, statistical analysis was carried out automatically though BD Calibur software provided. For confocal microscopy results, an average number from positively stained cells in a total of six fields of each sample were calculated and average percentages were recorded.

3.3.3 **Results**

3.3.3.1 Liposome preparation and characterisation

Three labelled unconjugated and conjugated liposomal formulations (L1, L2 and L3) were synthesised and their concentrations of P, As and Ni were determined by ICP-OES. All the liposomal formulations were found to be efficiently loaded with arsenic, with loading efficiency (As/P) depicted in Fig 3.3.3 (a). The loading efficiency was similar for all formulations, irrespective of the presence or absence of folic acid conjugation. The stability of liposome suspension was analysed by storing it at 4°C for a month and calculating its loading efficiency every week (Fig 3.3.3 (b)). Less than 5% arsenic leaked from the liposomes in a time period of 1 month. All the liposomal formulations displayed similar storage stability. The mean sizes of control liposomes were determined by dynamic light scattering on a Zetasizer-Nano ZS as represented in Fig 3.3.3 (c). The DLS size measurement of L1, L2 and L3 were 138.5±1.2nm, 134.4±1.7nm and 142.6±3.1nm, demonstrating that ligand conjugation had no considerable effect on the liposomal size. The polydispersity index for the investigated vesicles ranged from 0.1 to 0.15, indicating a homogenous population.

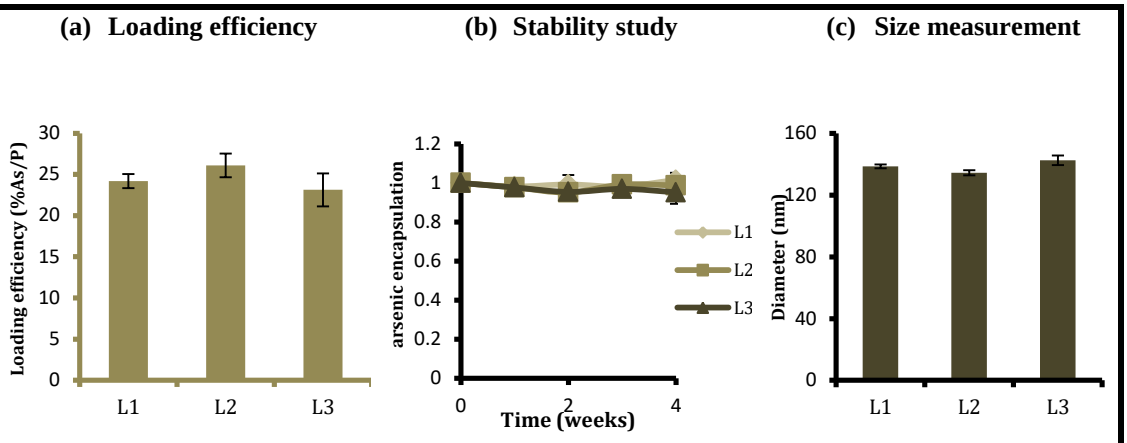

Fig 3.3.3: Characterisation of sythesised liposomes: (a) loading efficiency (%As/P), (b) ATO encapsulated over four weeks of storage at 4°C, and (c) Diameter of liposomes as measured from Zetasizer with a polydispersity index of around 0.1. Conjugation or length of conjugating PEG spacer does not have any considerable effects on either loading efficiency, stability over time in storage or size of the liposomes. Data are means ± standard deviations of three replicate measurements of at least three independent experiments.

3.3.3.2 Folate conjugation enhances liposomal uptake in FR positive cells

Confocal microscopy analysis

Any enhancement in liposomal uptake due to folate conjugation in FR positive cell lines was examined by confocal laser scanning microscopy (CLSM). It allowed the evaluation of intracellular fate of liposomes as a function of time from various cell lines. From previous findings on the surface receptor expression on the two cervical cancer cell lines investigated, HeLa cells were found to positively stain for FR while HT-3 stained minimally for the receptor. A positive control and a negative control cell line for FR expression, KB and A549 respectively, were also included to validate the robustness of the experiments, with their receptor expression in the order of KB> HeLa>HT-3>A549. With the initial goal of observing any improvement in liposomal uptake due to ligand conjugation, liposomes were first conjugated with folic acid using a PEG spacer having the same length as the surrounding PEG brush. Confocal microscopic visualisation of cellular association of DiIC18(3)-DS labelled liposomes is depicted in Fig 3.3.4.

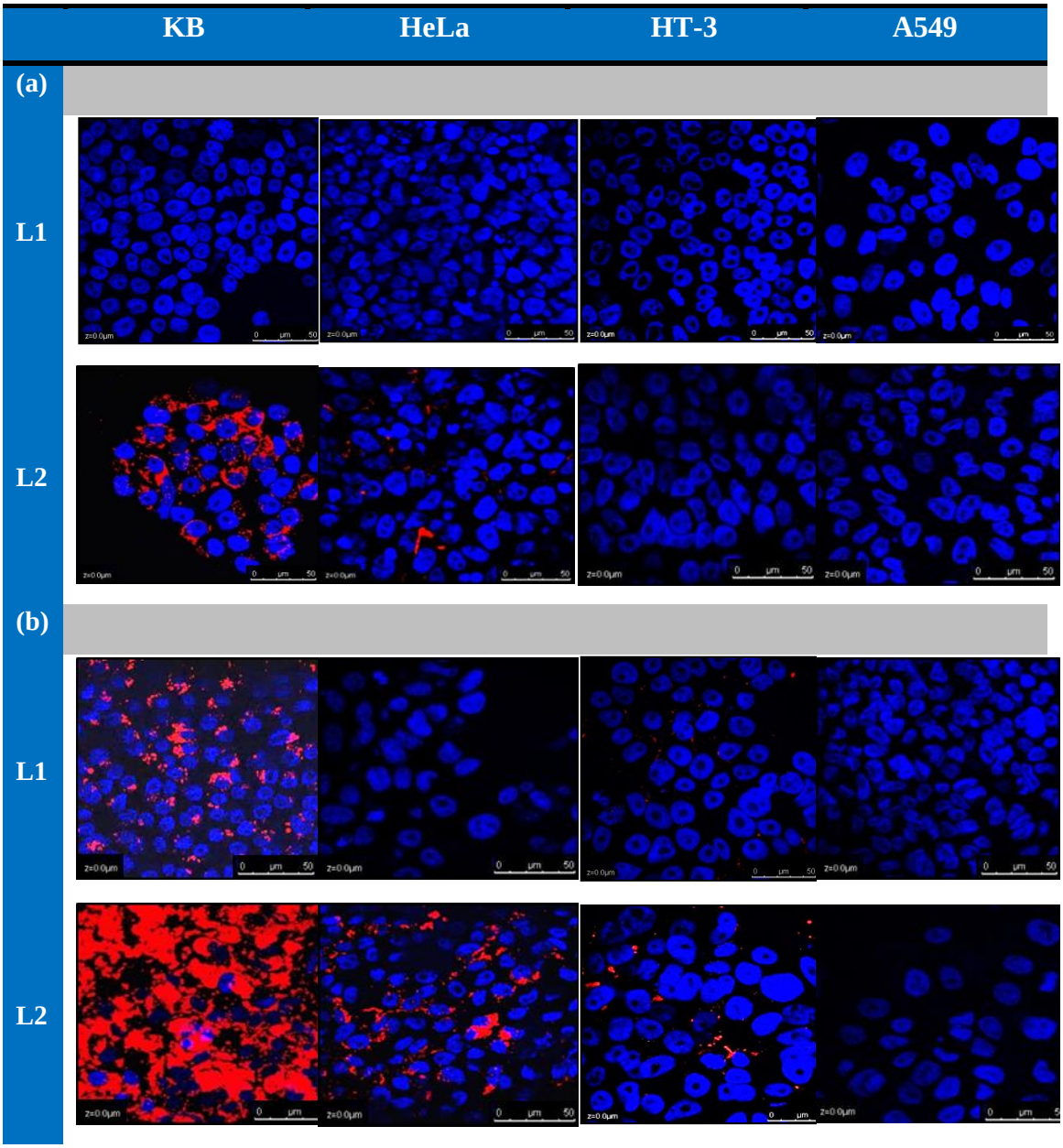

Fig 3.3.4: Confocal micrographs showing cellular uptake of DiIC18(3)-DS-labelled L1 and L2 liposomes (red in colour) after the treatment of (a) 2 h and (b) 24 h. Cells were counterstained with DAPI (blue colour) to reveal the nuclear/ DNA location. Folate targeted liposomes are selectively and efficiently taken up by FR positive cells KB and HeLa (according to the FR expression in the order of KB>HeLa). At 2 h treatment, the cell membrane association of liposomes is evident whereas at 24 h, the internalisation and accumulation of liposomes in the cytosol is observed.

By keeping all the parameters for confocal microscopic visualisation the same (PMT and % laser), it was possible to draw a comparative study of cellular uptake of

liposomes, with or without ligand conjugation. Following 2 h exposure in folate free media, KB displayed a significant cellular binding with the conjugated liposomes followed by HeLa, as evidenced from the red fluorescence seen around the cell surface from the DiIC18(3)-DS label of the liposomes. This obvious cellular association was however, not visible in either HT-3 or A549 cells. Such cellular uptake was not present with the non-conjugated liposomes. Subsequent 24 h exposure of the liposomes to the cell lines indicated a widespread internalisation and accumulation of conjugated liposomes in the cytosol of KB cell line, which was demonstrated by red fluorescence around the nuclei. Similar trend was also observed in HeLa cells with increased amounts of red fluorescence seen intracellularly at 24 h, which was followed by HT-3. As for A549, no cellular uptake of the conjugated liposomes was observed, which demonstrates the selective nature of the conjugated ligand. After 24 h exposure, the unconjugated liposomes exhibited some cellular internalisation in KB cells and diminutive fluorescence in HT-3 cells but none for HeLa and A549.

Flow cytometric analysis

The results obtained from confocal microscopy analysis were further validated by flow cytometry (Fig 3.3.5). The cells from the four cell lines were exposed to fluorescently labelled liposomes for a period of 2 h, 6 h and 24 h. A ratio of cells staining positive for conjugated liposomal uptake to non-conjugated liposomal uptake was calculated for each cell line to estimate the efficacy of folic acid conjugation in enhancing the liposomal cellular internalisation. At 2 h, flow cytometry results showed that the cellular uptake of targeted liposomes in KB cell line was about 50 times that of non-targeted liposomes (Fig 3.3.5 (a)). For HeLa and HT-3 cell line, the targeted liposomes were taken up around 2.1 and 1.6 times more than the non-targeted liposomes respectively. Whereas there was no significant difference in the liposomal uptake due to folate conjugation in A549 cell line.

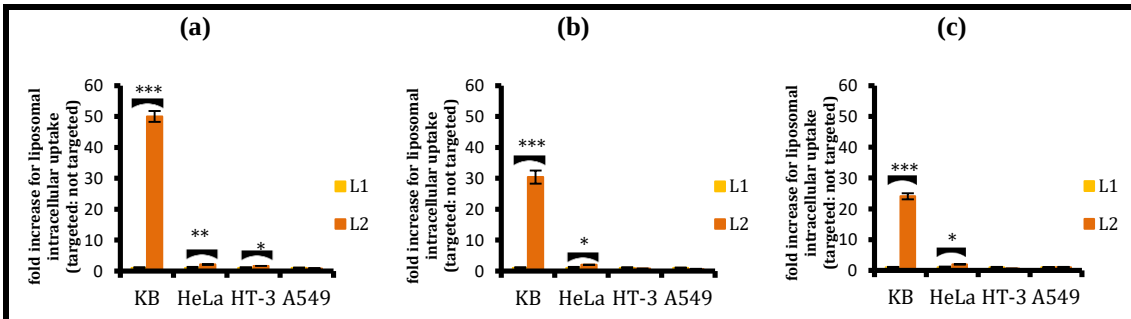

Fig 3.3.5: Comparison of the cellular uptake of L1 and L2 by flow cytometry at the end of (a) 2 h, (b) 6 h, and (c) 24 h treatment. Data are means ± standard deviations of duplicate measurements of at least three independent experiments. Unpaired t test was used to test if there is any significant difference in the uptake between L1 and L2 liposomes in the four cell lines. The uptake of cells due to folate conjugation is found to be significantly high for KB cells and HeLa cells, although it decreases with time. L2 is taken up more than L1 in the first two hours in HT-3 cells as well. *p≤0.05, **p≤0.01, and ***p≤0.001.

On increasing the liposomal incubation time from 2 h to 6 h, the trend of liposomal uptake remained the same for all studied cell line. For instance, KB displayed a significant higher liposomal intracellular uptake (30.4 times higher) with ligand conjugation than HeLa cells (only 2 times higher). HT-3 however, like A549, displayed no significant difference at this time interval. On further increasing the exposure time to 24 h, the targeted liposomes were taken up 24 times and 2 times more than non-targeted liposomes in KB and HeLa respectively, whereas HT-3 and A549 displayed no significant difference.

The results obtained from flow cytometry studies demonstrated a steady decrease in the difference between the uptakes of conjugated and non-conjugated liposomes for KB cell line, going from 50 times higher at 2h to 30.4 and eventually 24.1 times at 24 h. For HeLa, the difference (two times higher for targeted liposomes) remains almost constant with the time interval till 24 h. HT-3 displayed a 1.6 times higher uptake of targeted liposomes at 2 h; however this difference reduced with the increase in exposure time, with both of them displaying similar uptake at 6 h and 24 h. A549 cell line has no effect of ligand conjugation in its uptake of liposomes at any time interval investigated.

Plate reader analysis

An additional uptake assay was performed in 96 well plates by reading the fluorescence of cells incubated with fluorescent targeted and non-targeted liposomes via a microplate reader. A comparison was drawn of the differential cellular uptake by analysing the ratio of fluorescence of cells incubated with targeted liposomes to non-targeted liposomes followed by blank correction (Fig 3.3.6). As expected, the FR positive KB cells display the maximum difference among all the cell lines between fluorescence in cells incubated with targeted liposomes to non-targeted liposomes at all the three time intervals investigated; the difference being 5.15 ± 0.18 fold at 2 h, 3.22 ± 0.13 fold at 6 h and 1.9 ± 0.12 at 24 h. In HeLa, the fluorescence of the cells incubated with liposomes, albeit appreciable, is lower than KB and so is the associated ratio of targeted to non-targeted liposomes, with it being 2.81 ± 0.18 , 2.58 ± 0.06 and 1.82 ± 0.04 times at 2 h, 6 h and 24 h respectively. HT-3 cells display a higher cellular uptake of targeted liposomes in the first 6 h but the difference is nullified as the incubation time proceeds. At 24 h, there is no significant difference between cellular uptakes of targeted and non-targeted liposomes for HT-3 cell line, as measured from the fluorescence generated by the cells. FR negative control cell line, A549, exhibits no significant difference in the uptakes of liposomes from the ligand conjugation.

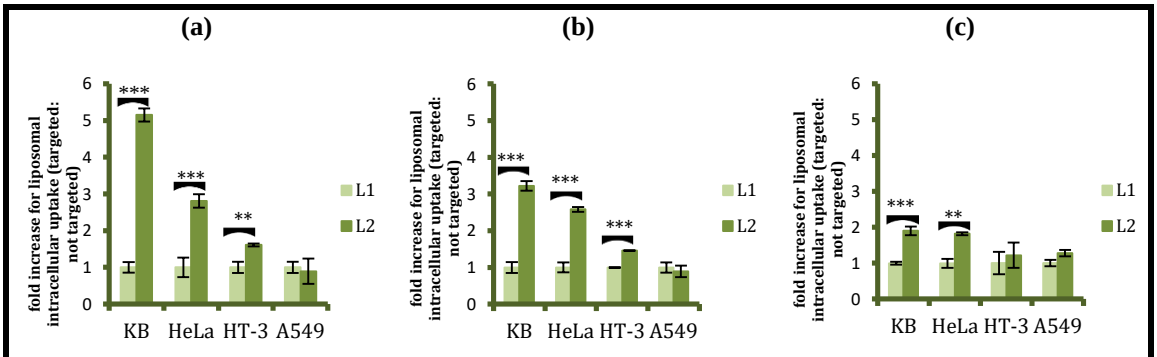

Fig 3.3.6: Comparison of liposomal uptake by the four cell lines with plate reader analysis at the end of (a) 2 h, (b) 6 h, and (c) 24 h treatment. KB and HeLa cells display a significant enhancement in liposomal uptake after folate conjugation, corresponding with their high FR expression on their cells' surfaces. HT-3 also display a small but significant enhancement in L2 uptake till 6 h, after which the enhancement is nullified. Data are means ± standard deviations of duplicate measurements of at least three independent experiments. **p≤0.01, ***p≤0.001.

Similar to the flow cytometry results, the difference between the liposomal uptakes was observed with ligand conjugation for different cell lines and the differences were reduced when the treatment time increased to 24 h. This reduction, while being true for all the cell lines investigated, is more evident from 6 to 24 h than from 2 to 6 h. Also, it is more obvious for KB cells than HeLa cells.

Quantitative liposomal arsenic cellular uptake via ICP-MS

Cellular liposomal arsenic was quantified with ICP-MS after performing calibrations using arsenic ionic standards and Ga ion as internal standard. For every experiment performed, we obtained a linear correlation for arsenic with squared correlation coefficients R^2>0.997. With this calibration, cellular arsenic was quantified by measuring the total amount of As following digestion of the cells from the four cell lines treated with media only, ATO encapsulating conjugated and unconjugated liposomes for 6h, 24 h and 48 h. A comparative study of the liposomal treatment was then drawn for cellular arsenic, as depicted in Fig 3.3.7.

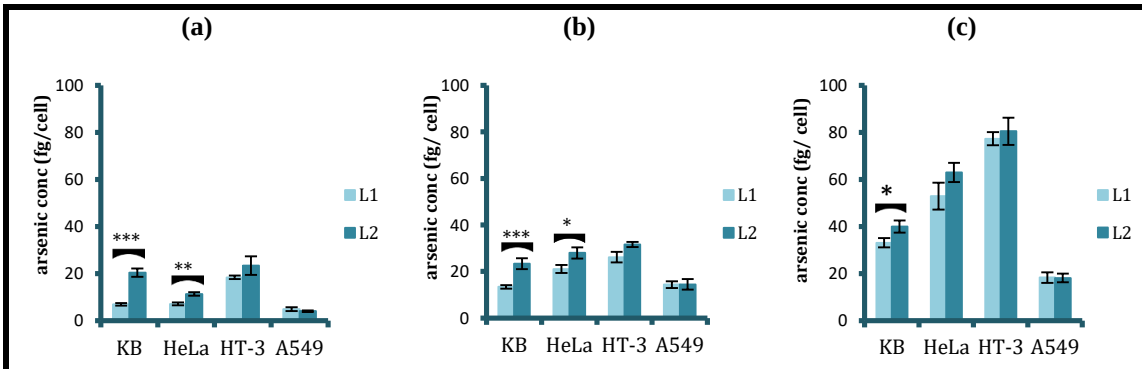

Fig 3.3.7: Arsenic concentration per cell as determined by ICP-MS in the four cell lines after (a) 6 h, (b) 24 h, and (c) 48 h treatment with L1and L2 liposomes. There is a significant difference in their uptake in FR positive KB and HeLa cells, with L2 being taken up more than L1. The arsenic concentration increases with time for all the cell lines. Data shown is the mean ± SD of three independent experiments. *p≤0.05, **p≤0.01, and ***p≤0.001.

The results showed that as the time of incubation increased, the cellular arsenic increased for all the treatments for the four cell lines investigated. KB displayed the highest difference in the cellular uptake of liposomal arsenic after ligand conjugation by taking up around 3 times more at 6 h and 1.7 and 1.2 times more at 24 h and 48 h respectively. HeLa, at 6 h, takes up 1.6 times more targeted liposomes than non-targeted ones, with this difference tapering off to 1.2 times at 48 h. Corroborating the previous findings, the cellular uptake studies by ICP-MS are consistent with the flow cytometry studies and plate reader analysis in that the difference between the uptakes of targeted and non-targeted liposomes decreases with time. Since, KB cells have the highest folate expression on their cell surface; this decline is more pronounced than HeLa cells. HT-3, with minimal expression of cell surface FRs, displays slight difference in the first few hours but with time, this difference is nullified and targeted and non-targeted liposomes are taken up by the cells equally. A549 cells, being FR negative, display no difference in the cellular uptakes from ligand conjugation as expected. Regarding the total arsenic content in the cells from the treatment, ICP-MS studies show that HT-3 cell line takes up more liposomal arsenic in general than all the four cell lines regardless of the ligand conjugation, while A549 takes up the least.

3.3.3.3 Increasing folic acid conjugating PEG spacer length enhances the targeting by liposomes

It has previously been reported in the literature that spacer length of the conjugated ligand impacts the efficacy of the cellular uptake of the nano-vehicle (Peng et al., 2013). To assess this aspect, a third formulation of liposomes was prepared where folic acid was conjugated to a PEG spacer having longer length (5000Da) than the surrounding PEG brush (2000Da). The above mentioned techniques including confocal microscopy, flow cytometry, plate reader analysis and ICP-MS arsenic quantification were once again employed to assess any enhancement in cellular targeting by liposomes from increasing the spacer length of PEG conjugating folic acid.

Confocal microscopy analysis

Keeping the parameters for confocal microscopic visualisation the same, a comparative study was drawn for the cellular uptakes of the three liposomal (L1, L2 and L3) formulations. The control cell lines, FR+ KB and FR- A549, were included along with the cervical cancer cell lines, HPV+ HeLa and HPV- HT-3. The cells were treated for 2 h, 4 h, 6 h and 24 h, fixed in 4% paraformaldehyde and stained with DAPI for nuclear imaging.

Liposomes without surface functionalisation showed neither membrane accumulation nor cellular internalisation in any of the cell lines till 24 h as evidenced by the lack of liposomal fluorescence (Fig 3.3.8). In contrast, ligand conjugation, specifically with 5000Da PEG spacer length, mediated an efficient fluorescence uptake in FR positive cell lines. After 2 h incubation, L3 was found to exhibit high cellular binding, for around 90% of KB cells, 25% of HeLa and 5% for HT-3, as shown by the red fluorescence around the cell surface. L2 liposomes exhibited minor cellular uptake by KB cells. A549 had no effect of ligand conjugation on its liposomal uptake.

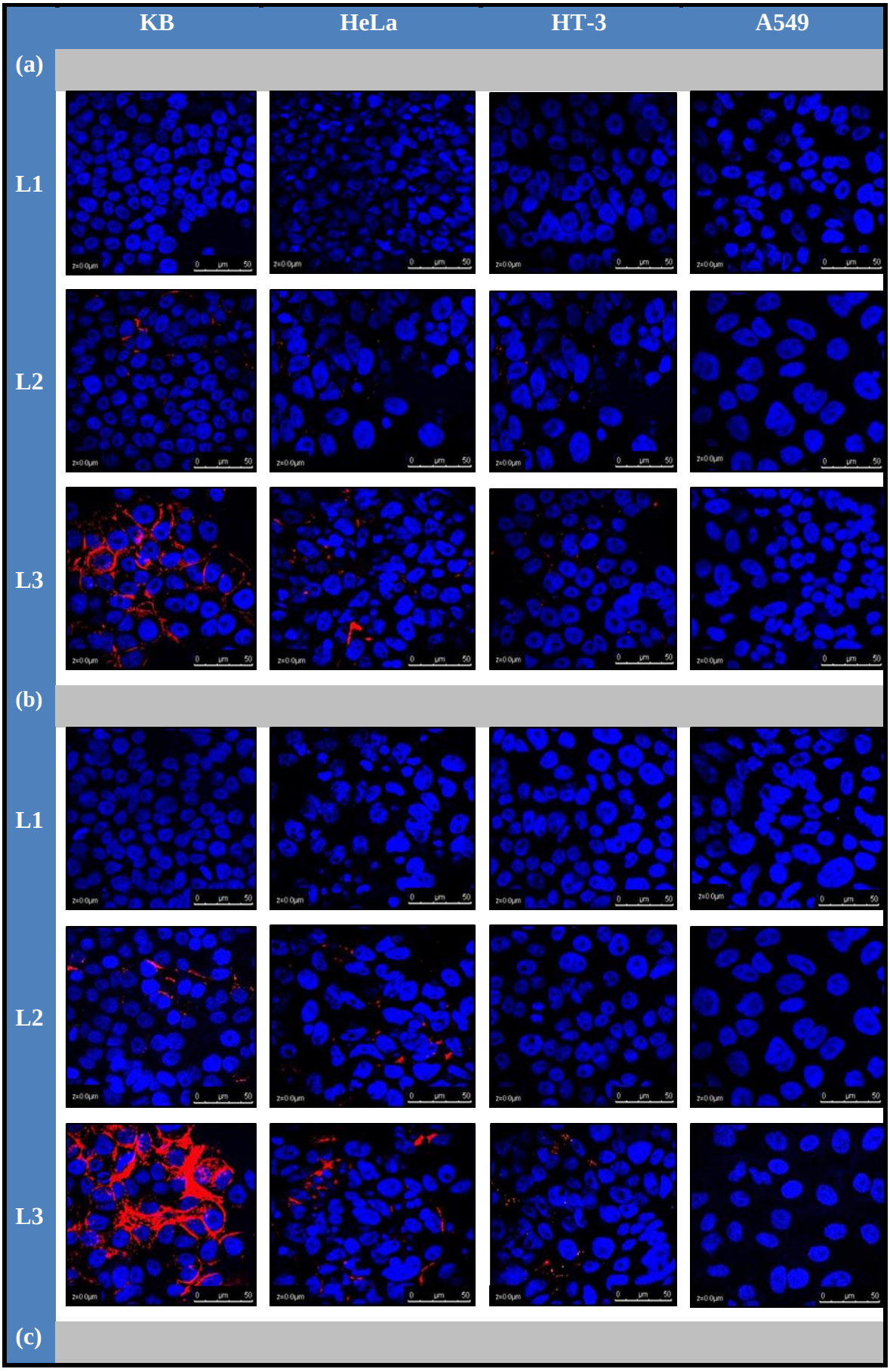
KB
HeLa
HT-3
A549
(a)
L1
L2
L3
(b)
L1
L2
L3
(c)

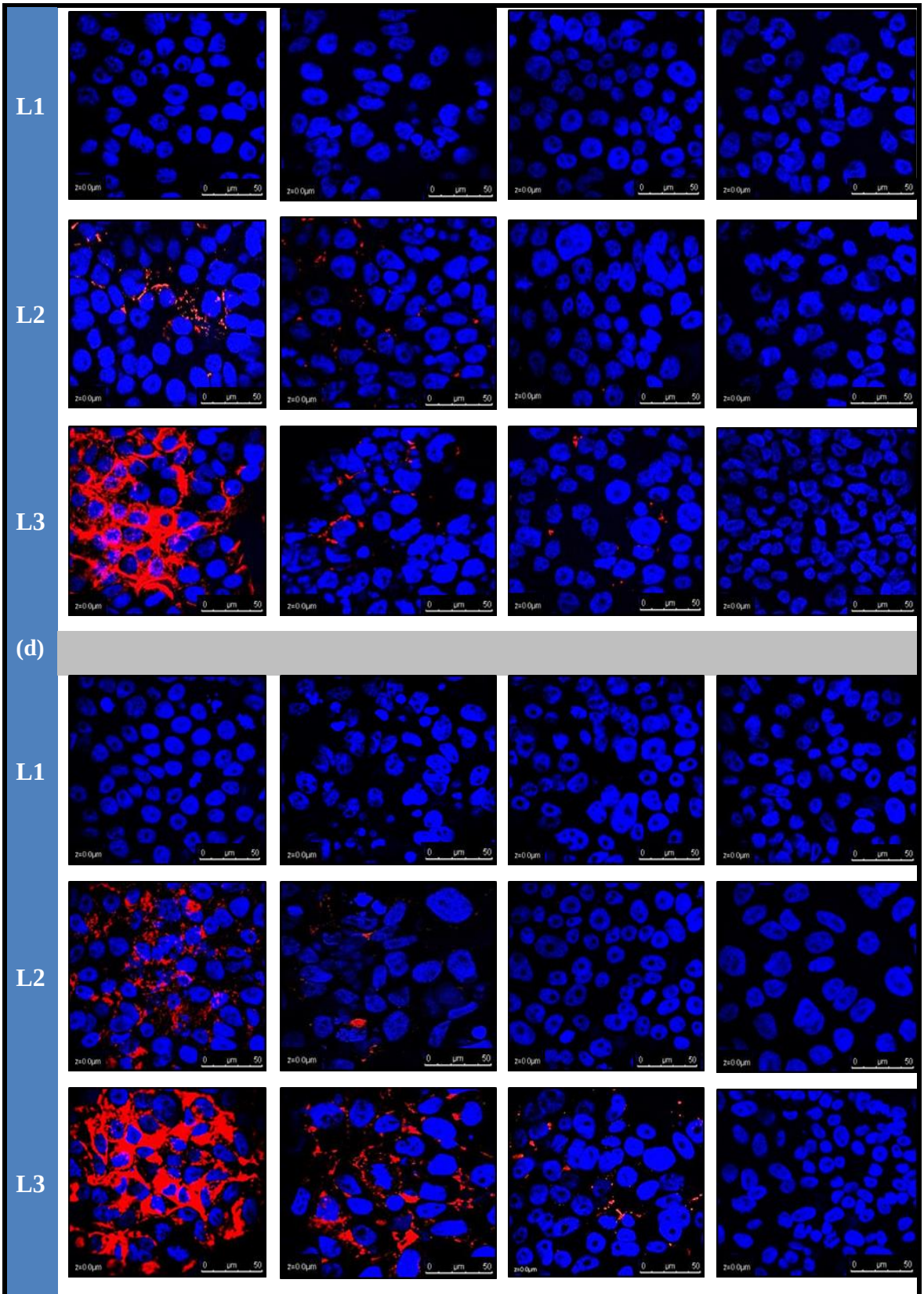

Fig 3.3.8: Confocal micrographs showing cellular uptake of DiIC18(3)-DS-labelled L1, L2 and L3 after treatment of (a) 2 h, (b) 4 h, (c) 6 h and (d) 24 h. Cells were counterstained with DAPI to reveal the nuclear/ DNA location. Among targeted liposomes, L3 were much more efficient than L2 in being taken

up by cells according to their FR expression, therefore the uptake in KB was highest followed by HeLa. HT-3 also took up more L3 than L2 while A549 cells had no effect on their uptake from liposomal conjugation.

With time, KB cells demonstrated increasing large scale cellular internalisation and accumulation of L3 in their cytosol, as seen by the red fluorescence surrounding the DAPI-stained nuclei. L2 was also seen to enter most of the KB cells by 24 h, but to a much lesser extent than L3, displaying the latter's higher efficiency in being taken up by the FR positive cells. For HeLa and HT-3 as well, L3 was more efficient in being taken up by the cells than L2, with L3 entering almost all the HeLa cells by the end of 24 h. The cellular uptake of conjugated liposomes (L2 or L3) in HeLa was always higher than HT-3.

Flow cytometric analysis

The cellular uptake of the three liposomal formulations were quantitatively analysed by flow cytometry, validating the previous confocal microscopy results (Fig 3.3.9). The four cell lines were treated with the three different formulations for a time period of 2 h, 6 h and 24 h. To compare the differences in cellular uptake of the different liposomal formulations, a ratio was obtained for the cells staining positive to conjugated liposomes (L2 or L3) to the cells staining positive to the unconjugated liposomes (L1) (Fig 3.3.10). The results indicated that folate conjugation to the liposomes resulted in a dramatic increase in the cellular uptake by KB cell line. This was true, irrespective of the length of the treatment or the ligand conjugating PEG spacer length, although, the uptake did increase by increasing the PEG spacer length by around 1.2 times at the end of 24 h. For HeLa, L3 uptake was around twice the L2 uptake for the time intervals investigated. HT-3 also showed a higher uptake of L3 than L2 (around 1.3 times) by the end of 24 h. A549, as expected, displayed similar cellular uptake of liposomes, regardless of the ligand conjugation.

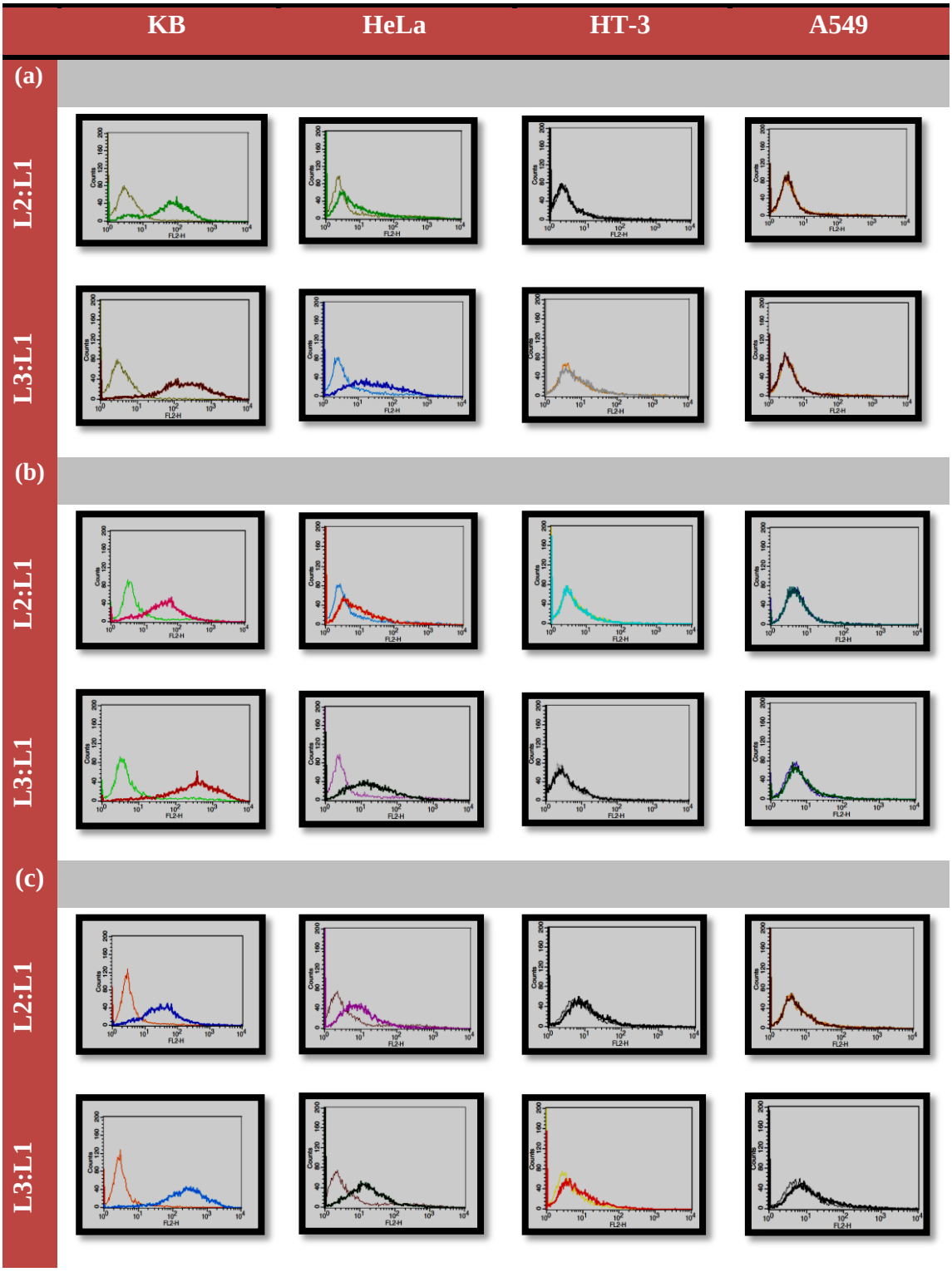

Fig 3.3.9: Flow cytometry analysis of cellular uptake of DiI-labelled conjugated liposomes (L2 or L3) as compared to unconjugated liposomes L1 after treatment of (a) 2 h, (b) 6 h and (d) 24 h. Among targeted liposomes, L3 liposomes are much more efficient than L2 in being taken up by FR+ cells. The enhancement in the uptake is according to FR expression, therefore the uptake in KB is highest followed by HeLa. HT-3 and A549 cells display no enhancemet in uptake from liposomal conjugation. The difference between the uptakes in KB and HeLa also decreases with time.

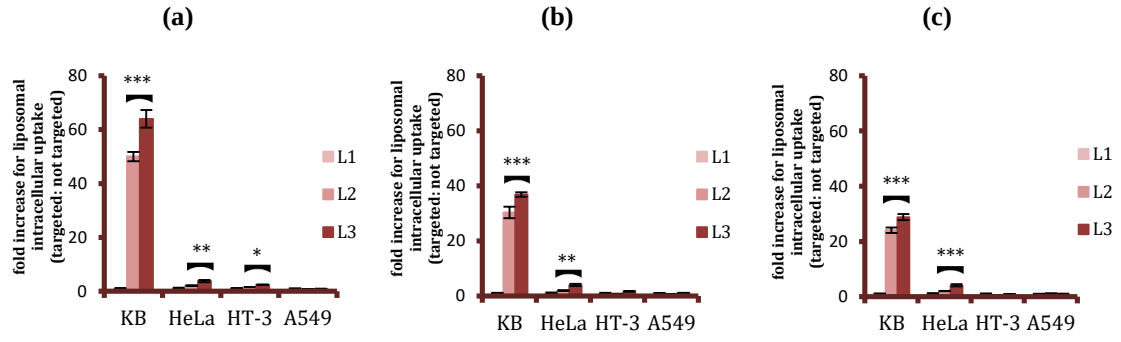

Fig 3.3.10: Comparison of the cellular uptake of non-targeted (L1) and targeted liposomes (L2 and L3) by flow cytometry at the end of (a) 2 h, (b) 6 h, and (c) 24 h treatment. Unpaired t test is used to assess any significant difference in the uptakes between the conjugated liposomes, L2 and L3. L3 uptake is significantly higher in both KB and HeLa cells. The difference between targeted and non-targeted liposomes decrease with time. HT-3 also displays a significantly higher uptake of L3 in the first 2 hours of treatment. Data are means ± standard deviations of three replicate measurements of at least three independent experiments. *p≤0.05, **p≤0.01, and ***p≤0.001.

As with the trend seen in L2 uptake before (Fig 3.3.5), the difference between the conjugated (in this case L3) and non-conjugated liposomes (L1) steadily decreased with the time interval. This decrease resulted in HT-3 taking up all the liposomal formulations equally by 24 h despite showing some higher uptake of L3 in the initial few h. In KB, this effect was much more profound, more for L3 than L2. In contrast, HeLa displayed a steady difference between conjugated (L2 and L3) and non-conjugated liposomes (L1) in the time period tested (24 h).

Plate Reader Analysis

The additional uptake assay to gauge any enhancement in cellular uptake after ligand conjugation to the liposomes was by reading the fluorescence of the cells via microplate reader and comparing L2/L3 treated to L1 treated cells. Results corroborated the findings from confocal and flow cytometry studies as depicted in Fig 3.3.11. Conjugated liposomes (both L2 and L3) were taken up in much higher proportions than non-conjugated L1 in KB and HeLa cells, whereas A549 and HT-3 displayed no difference in uptake from ligand conjugation. This decrease in the difference between

L3 and L1 uptake was very obvious in KB but not so in HeLa, as seen from the previous experimental techniques.

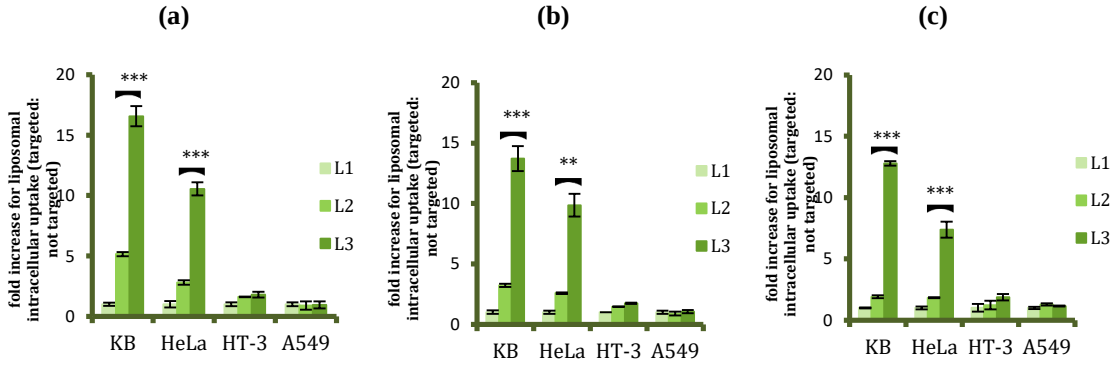

Fig 3.3.11: Comparison of cellular uptake of the three liposomal formulations L1, L2 and L3 by the four cell lines with plate reader analysis at the end of (a) 2 h, (b) 6 h, and (c) 24 h treatment. L3 uptake is significantly higher than L2 in KB and HeLa. The difference between targeted and non-targeted liposomes decrease with time. Data are means ± standard deviations of three replicate measurements of at least three independent experiments. **p≤0.01, and ***p≤0.001.

L3 liposomal formulation had a significantly higher uptake than L2 for FR positive cells. They were taken up around 6.7 times more by KB cells and 4 times more by HeLa cells at the end of 24 h. HT-3 and A549 cells remained unaffected in their liposomal uptake from ligand conjugation. In fact, conjugated liposomes were taken up slightly less than the non-conjugated liposomes in A549 cells by a factor of 0.9.

ICP-MS quantitative arsenic cellular uptake

Quantifying arsenic by ICP-MS in cells treated with L1, L2 and L3 revealed that conjugating liposomes with folic acid tethered to a longer PEG spacer length resulted in a significant increase in the liposomal uptake by FR positive cells (Fig 3.3.12). The four cell lines were treated for 6 h, 24 h and 48 h. At the end of 6 h, L3 liposomes were taken up 2.1, 2.5, 1.3 and 0.8 times more for KB, HeLa, HT-3 and A549 respectively. As is obvious, A549 cells were not affected in their liposomal uptake by an increase in ligand

conjugating spacer length. This observation was also valid for the 24 h and 48 h treatment. HT-3, despite showing a slight increase in L3 uptake compared to L2 uptake during the first six hours, reached a similar level with further prolonged treatments. KB cells took up 2 times more arsenic with L3 treatment at the end of 48 h treatment while HeLa cells, despite starting out with 2.5 times more L3 uptake than L2 at 6 h, eventually tapers off to a factor of 1.2 at the end of 48 h liposomal incubation.

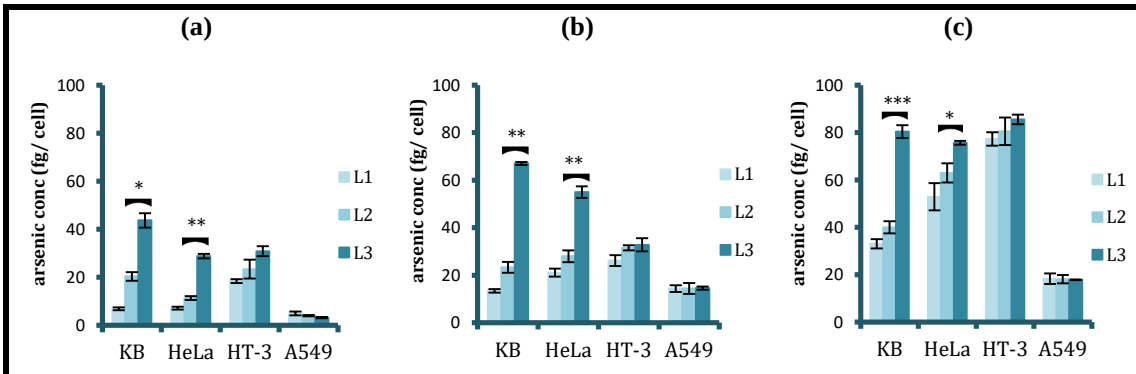

Fig 3.3.12: Arsenic concentration per cell as determined by ICP-MS in the four cell lines after (a) 6 h, (b) 24 h, and (c) 48 h treatment with the unconjugated (L1) and conjugated (L2 and L3) liposomes. L3 is taken up more than L2 in FR positive KB and HeLa cells. HT-3 has a higher uptake of liposomes in general, regardless of ligand conjugation. The arsenic concentration increases with time for all the cell lines. Data shown is the mean ± SD of three independent experiments. *p≤0.05, **p≤0.01, and ***p≤0.001.

As noted previously, HT-3 inherently takes up more liposomal arsenic than the remaining cell lines, which is not dependent on the folate conjugation or its conjugating spacer length. With a 6 h treatment, KB, HeLa and A549 cells have approximately the same cellular arsenic when treated with unconjugated liposomes. However, when the liposomes are conjugated, specifically with 5000Da PEG spacer length, KB cells were shown to take up around 6 times more arsenic and HeLa cells took up around 4 times more arsenic than with L1. A549 did not show a significant increase in liposomal arsenic uptake following the increase in treatment times, displaying a level of

unresponsiveness towards the treatment. At 48 h, although there is no statistically significant difference in the arsenic cellular concentration from L1 and L2 treatment, L3 treated KB and HeLa cell lines demonstrated a significantly higher cellular arsenic concentration which indicates that L3 is superior to L2 in increasing arsenic cellular uptake in FR positive cells.

3.3.3.4 Analysing cytotoxicity of control empty liposomes with differing spacer lengths of conjugated ligand

The results above clearly indicated the advantages of using a long PEG spacer to tether folic acid to the liposomes for enhancing their uptake in FR positive cells. However, in order to employ them successfully as arsenic nanocarriers to manage cervical cancer, it becomes imperative to investigate any inherent cytotoxicity that they might possess due to the presence of long PEG spacers. Since our focus is on cervical cancers and presence or absence of HPV gene sequences, further experiments were carried out on HeLa, HT-3 and KB cells only. KB cell line was included as despite being derived from epidermal mouth carcinoma, it had been contaminated with HeLa cells at some point. Therefore, it is positive for HPV-18 DNA sequences. Empty, unloaded liposomes of various formulations were synthesised and their cytotoxicity analysed on these cell lines via MTT assay at 48 h as depicted in Fig 3.3.13. The dilutions employed for the empty liposomal treatment had their phospholipid concentrations corresponding to ATO liposomes with 5µM encapsulated ATO concentration. At the dilutions used for treatment and the time period involved, none of the liposomes were toxic for any cell line. With these results in consideration, L3 liposomes, out of the three, proved to be the best liposomal formulation to achieve targeting in FR positive cell lines.

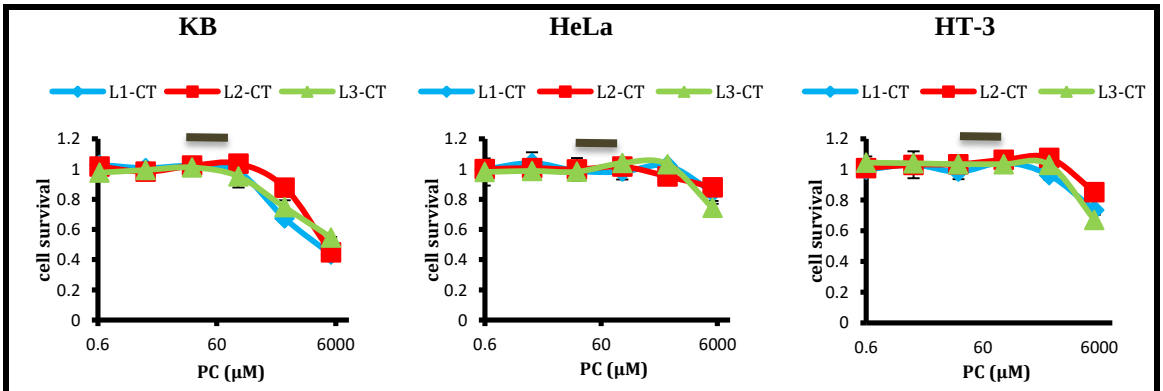

represents the concentrations of phospholipid at dilutions used for treatment of liposomal ATO.

Fig 3.3.13: Toxicity studies by MTT Assay of the control empty liposomes (L1, L2 and L3) on KB, HeLa and HT-3 cell lines after 48 h treatment. Increasing the spacer length for ligand conjugation does not result in increase of cytotoxicity as the phospholipid concentrations at dilutions used for the treatment of liposomes (L1, L2 or L3) are non-toxic to all the cell lines tested at 48 h, demonstrating the suitability of L3 as the drug carrier. Points refer to the means and bars refer to ±SD, where n=3.

3.3.3.5 Quantitative analysis of cellular uptake of arsenic

After establishing that L3 liposomes were more efficient than L2 in being taken up by the FR positive cells while not possessing any inherent toxicity of their own, further experiments were carried out with “L3” as the targeted liposomes, “L1” as their unconjugated counterparts, “ATO” as the drug in free form and media only as “con”. The cells were treated for 6 h, 24 h and 48 h, digested and their arsenic intake was quantified by ICP-MS (Fig 3.3.14).

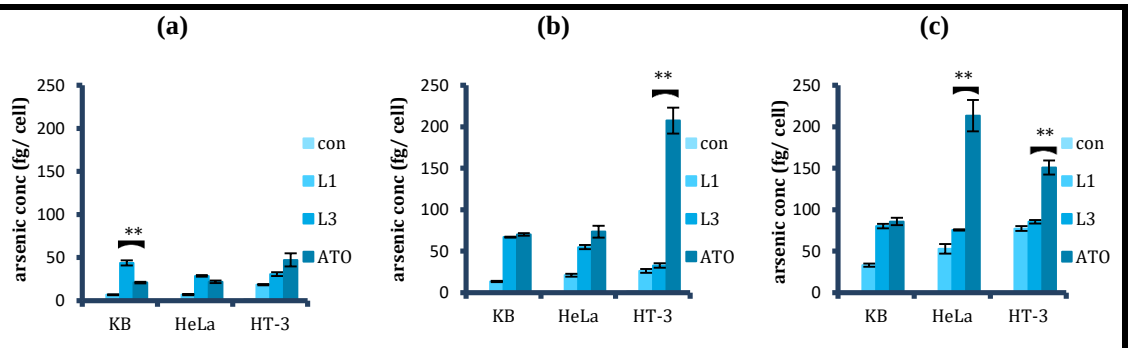

Fig 3.3.14: Arsenic concentrations per cell in KB, HeLa and HT-3 as determined by ICP-MS after (a) 6 h, (b) 24 h and (c) 48 h treatment with only media, unconjugated ATO liposomes L1, FA conjugated ATO liposomes L3 and free ATO of 5μM concentration. Data displayed is mean ± SD from five independent experiments. Unpaired t test is used to calculate any significant difference in the arsenic intake from L3 and ATO treatments, **p≤0.01. L3 is taken up more than free ATO in KB at 6 h, after which their uptakes are equalised when the time of treatment is increased to 24 h and 48 h. The cellular arsenic intake from free ATO gets higher than L3 in HeLa at 48 h, whereas for HT-3 it gets higher from 24 h.

Results showed that after 6 h of treatment, targeted liposomes L3 were taken up more than free ATO in both KB and HeLa, with cellular arsenic concentration in the order of con<L1<ATO<L3. Arsenic concentration due to L3 uptake was 2.1 and 1.3 times than from ATO in KB and HeLa cells respectively. Prolonging the incubation period to 24 h and further to 48h resulted in equalising of cellular arsenic concentration from both the L3 and ATO treatments in KB cells. In contrast, with the prolonged incubation time,

free ATO was taken up more than L3 in HeLa cells, 1.3 and 2.8 times more at 24 h and 48 h respectively. In HT-3 cells, free ATO was always taken up more than the liposomal counterparts, both conjugated and non-conjugated, in the time periods tested. The results showed a consistent increase in the cellular arsenic concentration as the incubation time period increased for all the cell lines and the treatments, except the control. There was one anomaly seen in HT-3 cellular arsenic concentration however. From 24 h to 48 h, the arsenic concentration per HT-3 cell, instead of increasing, saw a significant decrease from 207.4fg to 150.8fg.

3.3.3.6 Toxicity studies of liposomal arsenic using optimised formulation

With differing cellular uptake of liposomal and free ATO, the cervical cancer cell lines, HPV positive HeLa and HPV negative HT-3, along with KB, were next evaluated for cytotoxicity induction from these treatments. The dose response curve obtained from MTT assay for free drug and liposomal drug revealed that liposomal encapsulation mitigated toxicity except in the case of KB, where the targeted liposomes L3 induced more toxicity than free ATO in the first 48 h (Fig 3.3.15). At 72 h, L3 and ATO had almost the same dose response curve. For HeLa and HT-3 cells, however, free drug always induced more toxicity than L3. At the dilutions used for treatment, i.e. at 5 µM ATO concentration, free drug caused toxicity to around 23% more cells than L3 in HeLa, whereas for HT-3, this difference was around 28% at the end of 48 h treatments.

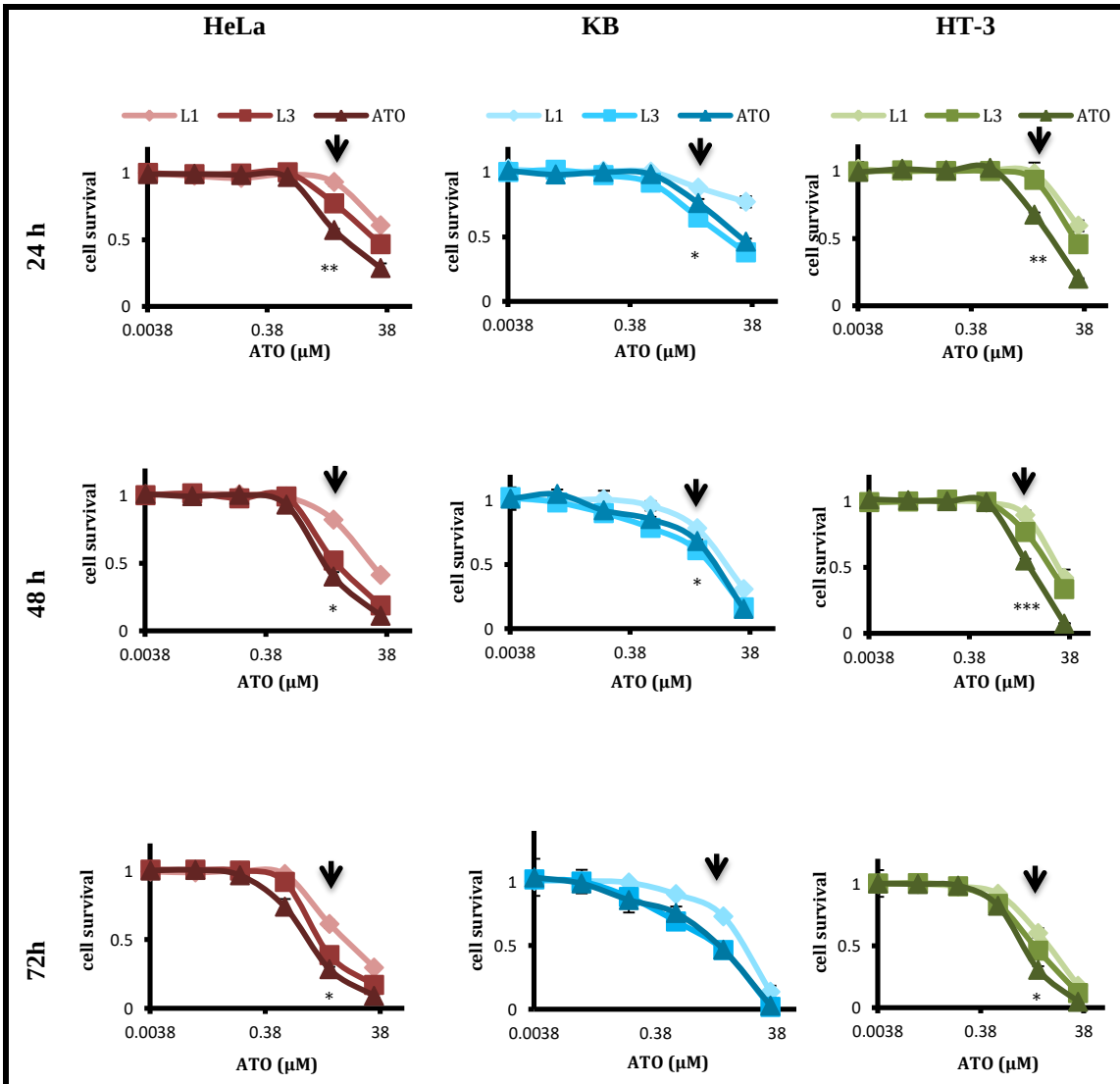

points to 5µM ATO concentrations which is typically used for treatment.

Fig 3.3.15: MTT test analysis to compare cellular toxicity of non-targeted and targeted liposomal formulations of ATO along with the free drug on HeLa, KB and HT-3 cells at 24 h, 48 h and 72 h. Points refer to the means and bars refer to ±SD, where n=3. Unpaired t test ($p > 0.05$) was used to test if there is any significant difference in the cytotoxicity between L3 and ATO at 5µM ATO concentration. Liposomal encapsulation attenuates drug toxicity to the cells *in vitro*, except for KB cell line where L3 liposomes were more toxic than free ATO till 48 h, after which their cytotoxicity equalised. For HeLa and HT-3, free ATO induced more toxicity than either liposomal constructs at all time intervals investigated.

* $p \leq 0.05$, ** $p \leq 0.01$ and *** $p \leq 0.001$.

In Figure 3.3.16, cell death–uptake ratios for KB, HeLa and HT-3 cells were shown to indicate the level of cell death that was induced in the cell lines per unit of arsenic taken up by the cells. Targeted liposomal ATO was more effective than the free drug in inducing cell death per unit of arsenic uptake in both receptor positive KB and HeLa cell lines, whereas free ATO was more effective in inducing response in HT-3 cells. Additionally, between KB and HeLa cells, the liposomal ATO treatment was more effective for HeLa cells than KB cells per unit arsenic.

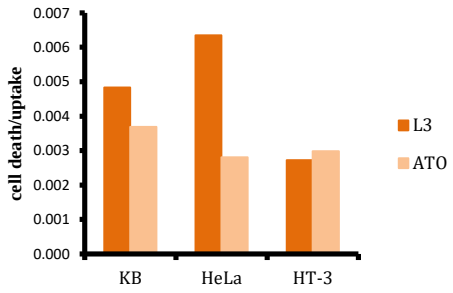

Fig 3.3.16: Ratios of cell death vs. uptake of targeted liposomal and free ATO for KB, HeLa and HT-3 cells after 48 h treatment. Targeted liposomes induced highest cell death per unit arsenic uptake in HeLa cells. Targeted liposomes were more effective in inducing response than free ATO in FR+ KB and HeLa cells.

3.3.4 **Discussion**

We described in this chapter the synthesis of folate targeted ATO encapsulating liposomes and the effect of increasing the ligand spacer length on cellular uptake and inhibitory potency against FR positive cancer cells *in vitro*, with particular emphasis on HPV and FR positive cervical cancer cells. To prepare targeted liposomes against HPV positive HeLa cervical cancer cells, folic acid was the ligand of choice as its receptor was the most differentially expressed out of the three receptors investigated on cervical cancers with differing HPV status. In addition, folic acid is also inexpensive and stable with low molecular weight having simple conjugation chemistry with relative low immunogenicity (Byrne, Betancourt and Brannon-Peppas, 2008; Talekar et al., 2011; Yu et al., 2010). It has a very high affinity for the FR presented on tumour's cell surface and is rapidly endocytosed (Talekar et al., 2011). Since folic acid is a vitamin required by the eukaryotic cells for the biosynthesis of nucleotide bases, any cargo attached to it remains within endosomes and then released into cytoplasm rather than being shuttled to the lysosome for destruction (Talekar et al., 2011; Byrne, Betancourt and Brannon-Peppas, 2008). Folate targeting of liposomal drug carriers have been reported to increase the therapeutic efficacy in a number of cases but it requires careful optimisation for effective therapeutic applications for selected tumours (Gabizon et al., 2004; Stephenson, Low and Lee, 2004; Reddy, Allagadda and Leamon, 2005).

The foremost necessity of synthesising an actively targeted nanoparticle was to design it so that it possessed extended circulation times, as mostly, an increased nanoparticles' affinity for the target antigens could not compensate for the natural clearance processes (Bertrand et al., 2014). Actively targeted nanoparticles without sufficient steric stabilisation from a PEG layer tend to lose their receptor binding ability due to non-specific interactions with colloidal proteins (Salvati et al., 2013). Additionally, since the physical stability of the targeted liposomes without the PEG layer was also not very well explored, in the initial experiments, only the ligand conjugating PEG spacer was included in the liposomal mix to prepare a targeted ATO delivery system, without the addition of the brush forming PEG layer. It resulted in unstable liposomal formulations which aggregated during the drug loading itself, regardless of the length of the ligand PEG spacer. Adding $mPEG_{2000}$-DSPE to the liposome mix stabilised the targeted

formulations and prevented them from aggregating. This might be due to the reason that surface grafted PEG chains, even at low concentrations, could provide sufficient steric barrier to prevent fusion of liposomal membranes (Holland et al., 1996).

There was another parameter that required careful optimisation: the ligand density on the surface of the nanoparticle. Thermodynamically, the binding of a ligand to a receptor facilitates the binding of its neighbouring ligands; these multiple interactions lead to clustering of the receptors, wrapping of the membrane and eventual internalisation of the bound nanoparticle (Mammen, Choi and Whitesides, 1998). These multivalent interactions lead to an enhanced avidity of the nanoparticle towards the target cell and prevents its detachment from the cell surface. However, *in vitro*, a higher ligand density does not necessarily translate to an enhanced cellular uptake (Weissleder et al., 2005). In some cases, it was shown that increasing the ligand density above a certain threshold resulted in saturation of the cooperative effects of the ligands, leading to unfavourable effects on cellular binding (Elias et al., 2013). Moreover, the presence of a dense ligand covering on the nanoparticles was also known to make them more prone to being recognised by the cells of MPS which consequently, led to a loss of their "stealth" surface characteristics (Kamaly et al., 2012). Hence, in order to bypass any such negative effects and to ensure high nanoparticle avidity to the surface receptors, it becomes necessary to optimise ligand density on the nanoparticles for every particular cancer type.

There have been reports of ligand molar ratio to range from 0.03 to 0.5% in literature for folate targeting liposomes (Reddy et al., 2002; Saul et al., 2003; Gabizon et al., 1999; Pan, Wang and Lee, 2002; Pan et al., 2002). In our experiments, it was observed that using 0.3mol% DSPE-PEG_{2000}-FA and 1.7 mol% of $mPEG_{2000}$-DSPE in the liposomal mixture formed stable L2 liposomes. However, the same (0.3 mol %) or higher amount of DSPE-PEG_{5000}-FA could not be used to prepare stable L3 liposomes and it invariably led to the aggregation of liposomes as soon as they were synthesised, despite the presence of a stabilising PEG_{2000} brush layer. After adjusting molar ratios of components, employing 0.1 mol % of DSPE-PEG_{5000}-FA and 1.9 mol% of $mPEG_{2000}$-DSPE gave stable L3 liposomal formulations. The same ratio was henceforth used for preparing L2 liposomes as well for comparison purpose. Cholesterol and soy PC were used in the same proportions as was detailed in the Chapter 3 (i) towards the formation of optimised neutral 100nm liposomes. The instability of L3 liposomes with higher

ligand density might be explained from studies where high folate density on the surface of nanoparticles were known to produce dimers, trimers and quartet self-assembled folate structures, causing aggregation of nanoparticles; with the longer ligand conjugating PEG spacer expediting the process (Ohguchi et al., 2008).

At the molar ratio employed for synthesis of targeted liposomes, ligand conjugation had no effect on either the size of the nanoparticles, nor did it impair their loading efficiency and stability (Fig 3.3.3). All the formulations (L1, L2 and L3) had similar sizes, i.e. around 140nm and achieved high loading efficiency with arsenic to phospholipid of 0.25 molar ratio. Our stability tests showed that all the liposomes, irrespective of ligand conjugation, were homogenous and stable with a loss of less than 10% of arsenic over four weeks storage at 4°C.

Owing to a possibility that PEG brush might mask the targeting abilities of the ligand if it is conjugated to a PEG spacer of equal length, our first investigation was to assess whether folate targeting alone, without conjugating to a longer PEG spacer, could cause any enhancement in cellular uptake. For that purpose, we synthesised L2 liposomes having the ligand conjugating PEG spacer and surrounding PEG brush layer of equal length, i.e. 2000Da. We evaluated the differences in cellular uptake from four different techniques: confocal microscopy, flow cytometry, fluorescence reading via plate reader and cellular arsenic quantification via ICP-MS.

Confocal microscopy studies indicated high liposomal binding of L2, though not of L1, to the surface of FR positive KB cells at 2 h (Fig 3.3.4). This surface receptor association of L2, was also present for HeLa cell line, albeit to a much lesser degree, but not for any other cell line. Increasing the incubation time to 24 h saw a widespread internalisation of targeted liposomes in KB cells, followed by HeLa and then HT-3 cells. A549 cells did not show any liposomal uptake after conjugation. These results were in accordance to the hypothesis that folate targeted arsenic loaded liposomes would be efficiently and selectively taken up by FR positive cells and that since from the previous chapter it was incurred that the FR expression followed the trend in cell lines as KB>HeLa>> HT-3>A549, the cellular uptake of targeted liposomes would also follow the same behaviour. From the confocal images of KB and HeLa cells in particular, the cell surface association of targeted liposomes at 2 h and then subsequent internalisation and accumulation within the cytoplasm at 24 h was very obvious,

indicating to the process of endocytosis. Non-targeted liposomes L1 too were taken up by KB cells at the end of 24 h, although to a much lesser extent than targeted liposomes, showing a certain level of vulnerability of KB cell line towards the treatment.

These results were corroborated by flow cytometric analysis of cellular uptake of fluorescent liposomes (Fig 3.3.5). Results showed that even in the first two hours, KB cells took up almost 50 times more L2 than L1. This drastic enhancement in liposomal uptake was however not reflected in other cell lines; however, HeLa did take up twice as much as L2 than L1. HT-3 cells also took up more L2 than L1, albeit to a lesser extent that HeLa. A549 cells, as expected, showed no difference in liposomal uptake based on conjugation.

The difference between the cellular uptake of conjugated and non-conjugated liposomes decreased with prolonging the exposure time, which might be due to two contributing factors: an increase in non-specific uptake of unconjugated liposomes and a subsequent decrease in the uptake of conjugated liposomes due to a possible saturation of the targeted receptors on the cell surface. For KB, this effect was very much pronounced; the difference between L2 and L1 went from 50 fold at 2 h to around 24 times in 24 h. HeLa, being less FR+ did not exhibit this drastic decrease in this difference, with L2 still being taken up twice more than L1 at the end of 24 h. In HT-3 cells, the uptake of both targeted and non-targeted liposomes equalised within the first 6 h.

From the plate reader results as well, KB cells displayed the maximum difference in cellular fluorescence arising between L2 and L1 uptake, followed by HeLa and HT-3 (Fig 3.3.6). Additionally, as with the flow cytometry analysis, we saw a consistent decrease in the uptake difference between L2 and L1 with increasing incubation times. The reason for it, as hypothesised above, was further corroborated after quantifying cellular arsenic via ICP-MS (Fig 3.3.7). Results showed that after an initial high surge of liposomal L2 arsenic intake by FR+ cells, the rate at which L2 was taken up almost invariably slowed down in comparison with L1. This led to a bridging of the gap between L2 and L1 uptakes in cells. However, as seen from ICP-MS studies, the difference between L2 and L1 intake was considerable, almost three-fold for KB cells and 1.6 and 1.3 times for HeLa and HT-3 respectively. This, further confirmed by the above findings, established beyond doubt that folic acid conjugation to liposomes, even to a PEG spacer of similar length as the surrounding PEG brush, was able to effectively

target the FR positive cells with efficiency and selectivity. However, to be positive that the surrounding PEG layer was not masking the conjugation abilities of the ligand, even to a small extent, we decided to next conjugate folic acid to a PEG spacer of longer length and observe any further enhancement in uptake within FR+ cell lines. Since, the previous studies had employed FA-PEG3350 (Chen et al., 2009); we decided to use even longer PEG spacer length of 5000Da for making targeted liposomes and investigate any increase in cellular uptake along with any inherent toxicity that might arise from employing longer PEG spacers for ligand conjugation.

Folic acid was subsequently conjugated to a PEG spacer having longer length (5000Da) than the surrounding PEG brush (2000Da). The above mentioned techniques including confocal microscopy, flow cytometry, plate reader analysis and ICP-MS arsenic quantification were once again employed to assess any enhancement in cellular targeting. Keeping all the settings and parameters same for comparative analysis, confocal microscopic images very distinctly showed the superiority of using a longer PEG spacer for ligand conjugation (Fig 3.3.8). At the end of the initial 2 h incubation, L3 liposomes clearly displayed strong cell surface attachment in around 80% of FR+ KB cells, in contrast to 10% of KB cells with L2 liposomes. Additionally, around 20% of HeLa cells showed membrane attachment with L3, but none with either L2 or L1. A little attachment (around 5%) was also seen with L3 in HT-3 cells. A549 showed no cellular association with L3, exhibiting the selectivity of the conjugated ligand. As the incubation period was increased to 4 h, 6 h and eventually 24 h, KB cells saw a widespread internalisation and accumulation of L3 in their cytosol. L3 was also taken up in almost all the HeLa cells and around 20% of HT-3 cells. In contrast, L2, albeit more effective that L1, was visibly less effective than L3 in being taken up by FR+ cells.

Results from flow cytometry also established that L3 had a superior uptake in FR+ cells (Fig 3.3.10). It was taken up almost twice as much as L2 in the first 24 hours in HeLa; whereas in HT-3, its uptake was only 1.3 times more than L2. Fluorescence reading from the plate reader showed that at the end of 24 h, KB cells incubated with L3 had 6.7 times more fluorescence that L2 (Fig 3.3.11). Additionally, this value was 4, 1.5 and 0.9 times for HeLa, HT-3 and A549 respectively, clearly displaying the superior targeting abilities of L3 liposomes than L2. ICP-MS studies also validated the findings and the results showed that the cellular arsenic content from L3 uptake was almost 3 times

higher than L2 uptake in KB cells and two times higher in HeLa cells at the end of 24 h (Fig 3.3.12). This enhanced uptake was however not very significant in the case of HT-3 cells, clearly owing to the weak FR expression by its cells. FR- A549 cells displayed a similar uptake for all the liposomes, irrespective of conjugation or non-conjugation.

From the above results, it was established beyond doubt that L3 instigated the highest uptake in FR+ cells while being very selective in its targeting abilities and therefore should be the logical choice for delivery vehicle of arsenic in FR rich HeLa and KB cells with HPV infection. However, for it to function as a successful delivery vehicle, it needed to test negative for any inherent cytotoxicity. Since we intended to elaborate our work on investigating the therapeutic potential of arsenic in HPV infected cervical cancers and the time period chosen for the our previous studies had been 48 h, all the liposomal formulations henceforth were tested for any intrinsic cytotoxicity to the cells by incubating the empty liposomes with HeLa and HT-3 cells, along with KB cells (owing to them being positive for HPV infection), for 48 h. The dilutions of liposomes tested for toxicity studies included the ones that corresponded with the liposomal concentration with encapsulated 5µM ATO that were typically used for treatment. All the liposomes, including L3, were non-toxic at the dilutions to be used for treatment. This finding was in agreement with the study by Peng et al. (2013) where they observed that the conjugated docetaxel delivery systems targeting prostrate specific membrane antigen with longer spacer length had no significant toxicity *in vitro* and *in vivo*, i.e. in major organs of the treated mice bearing C4-2 tumour xenograft.

Consequently, the inherent non-cytotoxicity of L3 liposomes along with their superior targeting abilities led us to select them among the other formulations as the optimised design for the targeted ATO nano-carrier. Further *in vitro* analyses was henceforth carried out with L3 as the conjugated liposomes, L1 as their unconjugated counterparts and free ATO on HPV positive KB and HeLa and HPV negative HT-3 cells.

Cellular uptake studies showed that usually arsenic was transported more readily within the cells when the free form was applied. However, owing to the very high FR expression of KB cells which render them most amenable towards folate targeting and consequent liposomal uptake, L3 liposomes transported twice more arsenic in the first six hours of treatment. This trend was also seen with HeLa, though to a lesser extent (1.3 times more than free ATO), again due to a high FR expression. As the treatment

time increases however, we reported an equalising of the cellular arsenic concentration from L3 and ATO treatment in KB cells while an increasing arsenic concentration with free ATO treatment in HeLa cells. In HT-3 cells however, free form of the drug was always taken up more than the liposomal forms, with not much difference between L1 and L3 uptake.

The cells were further incubated with free and liposomal ATO of 5μM concentration for a period of 24 h, 48 h and 72 h and their cytotoxicity assessed by MTT assay. As expected, KB cells displayed the maximum vulnerability towards L3 treatment, where L3 liposomes able to induce 1.5 times more cell death than the free drug itself at 24 h. L3 liposomes killed almost 35% of KB cells, as opposed to free ATO and L1 which killed 24% and 12% cells respectively. In contrast, free ATO generated higher cell death than either liposomal formulations for both HeLa and HT-3 cells. The difference between L3 and free ATO toxicity reduced for all the cell lines as the time of treatment increased. This might probably have arisen from the increasing non-specific cellular association of liposomes along with passive arsenic release contributing to the lessening of the differences between the cytotoxicities.

The cell death–uptake ratio indicated the cell death induced per unit of arsenic uptake, and is an effective means of comparing the efficacy of a treatment on different cell populations. Our results indicated that for targeted liposomal treatment, this ratio was higher for HPV positive HeLa and KB cells than HPV negative HT-3 cells. Moreover, targeted liposomes were more efficient in inducing cell death than free ATO in FR positive cells per unit arsenic taken up, in contrast to HT-3 cells. Interestingly, targeted liposomal ATO was found to be most effective in inducing its response towards HeLa cells, which again point to a certain susceptibility of the cell line towards liposomal treatment, an aspect that warrants further research.

3.3.5 **Conclusion**

The success of a targeted drug delivery system, tailored to the specific cancer under investigation, depends on the thorough optimisation of the nano-carrier's various parameters. From the previous chapters, we observed that for treating HPV positive cervical cancers, neutral 100nm liposomes were the most optimal formulation amongst different sizes and charges and folic acid was the best targeting ligand. Henceforth in this chapter, we synthesised folic acid conjugated, 100 nm neutral ATO encapsulating liposomes and examined the impact of varying spacer length on their targeting abilities for treating HPV positive cervical cancer. Folate targeting, particularly when the ligand was attached to a longer PEG spacer, led to an appreciable enhancement in cellular uptake by FR positive cancer cells. This formulation, along with being efficient and highly specific, had no inherent toxicity of its own at the dilutions used for the treatment, making it very suitable for it to be used as the delivery vehicle of ATO to HPV positive cervical cancer cells. Our next step would be to investigate the molecular mechanism behind the action of free and liposomal ATO with particular emphasis on the HPV's E6 and E7 oncoproteins, apoptotic protein activated caspase-3 and tumour suppressors' p53 and pRb.

3.4 INVESTIGATING MECHANISM OF ACTION OF THE LIPOSOMAL AND FREE ARSENIC TRIOXIDE ON HPV ASSOCIATED CANCERS *IN VITRO*

3.4.1 **Introduction**

3.4.1.1 Background

The HPV infection is reported to occur at some point in 75% of sexually active women, making it the most sexually transmitted infection in the world (Yim and Park, 2005). Through several epidemiological studies supported by molecular technology, HPV has been identified as the causal agent in cervical cancer development (Bosch et al., 2002). Despite the widespread infection, only 10% of infected women develop precancerous lesions of which 8% develop early cancer limited to the epithelial layer of the uterine cervix (Yim and Park, 2005). However, if left untreated, these precancerous lesions may develop into invasive cancer at a later stage (Yim and Park, 2005).

The HPV family includes over 100 HPV types, of which 15 types are classified as high risk HPVs involved in over 95% of cervical cancer cases (Bosch et al., 2001). Of these, HPV-16 and HPV-18 are the two primary high risk types which are responsible for 50% and 10% of invasive cancer respectively (Munoz et al., 1992). Studies have indicated that persistent presence of high risk HPV infection is critical for development, maintenance and progression to CIN (Remmink et al., 1995). HPV infection are also indicated to play a crucial role in the pathogenesis of other carcinomas such as upper respiratory digestive tract cancers, urogenital tumours and cancers of different human organ types (NeufCoeur et al., 2009; Shukla et al., 2009; Sutcliffe et al., 2010).

The mechanism by which HPV induces cancer in humans has been investigated intensively and these investigations have highlighted the crucial roles of oncoproteins of HPV E6 and E7 in inducing cancer (Tommasino, 2013; Lazo, 1999; McGlennen, 2000). HPVs have double stranded, circular DNA genome, 8 kb in size, which encodes for 8 proteins of which E6 and E7 oncoproteins are necessary for malignant transformation (Walboomers et al., 1999). Besides the transforming properties, E6 and E7 have additional functions including regulation of chromosomal stability and cell cycle, transmembrane signalling, immortalisation of primary cell lines and transformation of established cell lines (Yim and Park, 2005). Post HPV infection, de-regulation of viral E6 and E7 oncogenes expression drive cellular proliferation and stimulate host cells to re-enter the cell cycle (Doorbar, 2007). The carcinogenic potential of E6 and E7 viral proteins lies in their selectively degrading p53 and retinoblastoma RB gene products respectively, resulting in the inactivation of two crucial negative regulatory cellular proteins and the consequent cellular immortalisation and transformation (Fig 3.4.1) (Bosch et al., 2002; Mansur and Androphy, 1993).

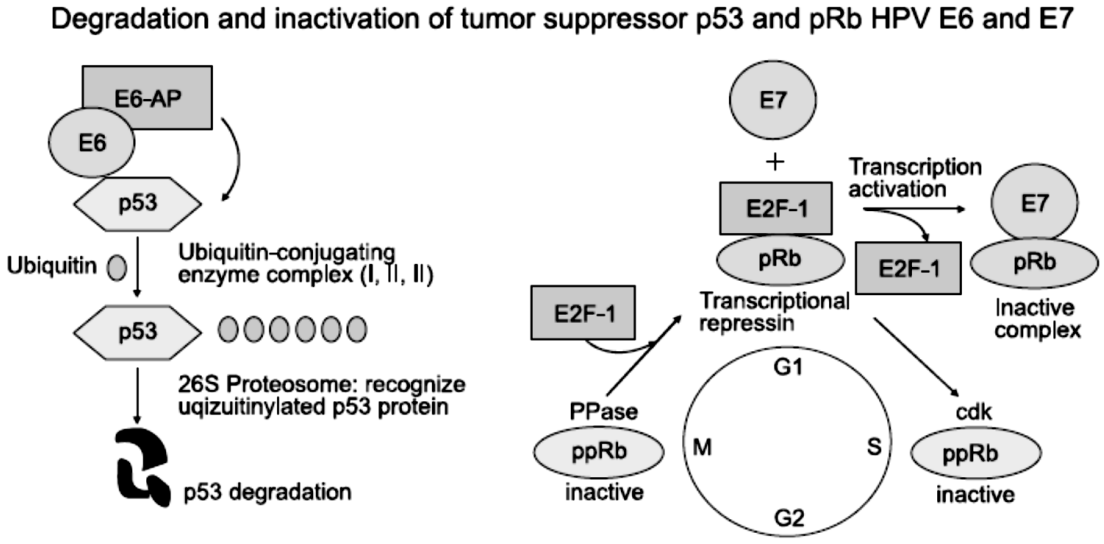

Fig 3.4.1: The role of HPV's E6 and E7 oncoproteins in the inactivation of tumour suppressors' p53 and pRb (Yim and Park, 2005).

E6 is an anti-apoptotic protein and its carcinogenesis lies with its ability to associate with p53, which promotes its ubiquitination and proteasome dependent degradation (Doorbar, 2007). E6 protein stimulates degradation of tumour suppressor p53 by forming a trimeric complex, consisting of E6, p53 and the cellular ubiquitination enzyme E6-AP (Yim and Park, 2005). This E6 stimulated degradation of p53 disrupts the control over cell cycle progression and apoptosis, compromising the effectiveness of cellular DNA damage response and causing accumulation of secondary mutations, collectively resulting in the growth of tumour cells (Doorbar, 2007; Um et al., 2002). Besides the abovementioned p53 degradation, E6 protein has oncogenic potential independent of p53 as well (Yim and Park, 2005).

E7 associates with hypophosphorylated form of the cell cycle regulator pRb and consequently disrupts its binding with the E2F family of transcription factors (Doorbar, 2007). These transcription factors are responsible for repressing the expressions of replication enzyme genes, forming a direct correlation with the tumour suppressor function of Rb (Lipinski and Jacks, 1999). The E2F on being released from the pRb-E2F complex activates cellular genes promoting host cell and viral DNA replication (Doorbar, 2007). E7 and E6 have been known to work cooperatively as well as independently of each other in inhibiting apoptosis and mediating cell proliferation (Doorbar, 2007; Nguyen et al., 2003; Thomas et al., 2002).

Therefore, since the oncogenic potential of HPV lies in the expression of E6 and E7 genes and their product, they represent the logical targets for developing molecular therapies for cervical cancer and that the inhibitors should target the functions of both the oncoproteins (Horner et al., 2004; Lin et al., 2009; Soliman et al., 2004). Hence, a drug downregulating E6 and E7 oncogenes expression and disrupting the linkage of E6-p53 and E7-pRb to liberate p53 and pRb in HPV infected cells may have the potential to restore the altered biological functions of the cells and allow them to carry on with the normal process of apoptosis. ATO has been reported to downregulate E6/ E7 oncogenes expression and reduces survival of HPV-18 infected HeLa cells (Um et al., 2002; Wang et al., 2016).

ATO is being therapeutically used since 200BC, initially in traditional Chinese medicine (Ho et al., 2005). As an anti-cancer agent, it proved highly successful on

patients with APL, a subtype of acute myeloid leukaemia. The success following its clinical trials on APL patients as a single agent or in combination with conventional chemotherapy led to its approval by FDA as its frontline therapy (Antman, 2001). The same kind of clinical success was subsequently translated for other haematological malignancies (Swindell et al., 2013). Since then, ATO has been extensively studied as an anti-cancer drug with an effort to further extend its application to treat solid tumours. Studies indicate that ATO demonstrates significant anti-cancer activity on a variety of solid cancer lines and tumour models including lung, endometrium, skin, liver, colorectal, pancreas, breast, kidney, ovarian and cervical cancers, albeit without appreciable clinical success in human patients (Bornstein et al., 2005; Dilda and Hogg, 2007; Kito et al., 2003; Lam et al., 2014; Maeda et al., 2001; Murgo, 2001; Park et al., 2003; Wang et al., 2014; Zekri et al., 2013). Employing ATO to treat solid tumours has drawbacks as higher doses are required for their treatment in comparison to haematological malignancies (Liu et al., 2006). This is to overcome rapid clearance of arsenic and its products from the blood by reticuloendothelial system and allow further penetration into the solid tumour mass (Liu et al., 2006). The higher dosages though, have been reported to cause systemic toxicities such as long term memory damage, liver failure, cardiac failure and peripheral neuropathy, limiting its clinical utility (Evens, Tallman and Gartenhaus, 2004).

Moreover, even though the mechanism of action of ATO for blood cancers has been carefully elucidated and reviewed, it is not fully understood for solid tumours (Evens, Tallman and Gartenhaus, 2004). Some of the mechanisms reported for its anti-cancer activity are induction of apoptosis (Emadi & Gore, 2010), mitochondrial toxicity (Larochette et al., 1999), generation and accumulation of ROS (Platanias, 2009), along with interference in telomerase activity (Zhou et al. 2007), tubulin polymerisation, DNA repair or cell cycle progression (Kroemer & de Thé, 1999). It has also been reported to inhibit proliferation of carcinogenic cells and angiogenesis by either down-regulating VEGF or inducing apoptosis in endothelial cells (Miller et al., 2002). However, the exact mechanisms for treating specific tumours remain ambiguous.

Our research team, with focus on HPV infected cervical cancers, had previously employed ATO as the treatment drug and shown it to be effective against the cancer cells (Wen et al., 2012). However, its efficacy was evident only when it was used at a low concentration (up to 2 μM), as concentrations higher than 2μM were toxic to

majority of the cells (Wen et al., 2012). Further study carried out by the same research group showed that ATO encapsulated in liposomes improved arsenic's therapeutic index and observed that the liposomal formulation was effective in inducing apoptosis and reducing HPV E6 oncogene expression in HeLa (Wang et al., 2016). However, the impact on HPV E7 oncogene expression and the relationship between E6-p53 and E7-pRb post treatment was not completely explored. Moreover, it was also not shown how ATO, if encapsulated in liposomes with ligands specifically targeting HPV positive cancer cells, would regulate the expressions of E6 and E7 oncogenes and whether there would be any differences in their mode of action from free ATO and unconjugated liposomal ATO. Therefore, in this study we first optimised the ATO carrying liposomal design (Akhtar et al., 2018) and conjugated them with ligands specifically tailored for HPV positive cervical cancer treatment. Using the optimized liposomes (100 nm neutral) and folic acid being the ligand of choice, an *in vitro* study was further carried out to investigate the mode of action of free ATO, liposomal-encapsulated ATO and folate conjugated liposomal ATO on HPV infected and non-infected cancer cells though evaluation of apoptosis induction and expression levels of apoptotic protein active caspase-3, HPV-E6 and E7 oncoproteins along with p53 and pRb tumour suppressor proteins.

3.4.1.2 Aims:

The aims of this chapter are to investigate and compare the mode of action of ATO when it is delivered free or encapsulated in unconjugated and folate conjugated liposomes on HPV positive and negative cancer cells *in vitro* and to assess the best delivery method for HPV associated cervical cancer cells.

3.4.1.3 Objectives:

(i) To investigate whether active targeting approach using FA-conjugated liposomes (ATO-FA-L2) is better at inducing apoptosis in HPV positive cancers than non-targeted liposomes (ATO-L1).

(ii) To compare the efficacy between ATO delivered free or through targeted liposomal approach for cervical cancer cell treatment.

(iii) To assess the mechanisms of action of ATO delivered via the three disparate techniques by examining the downregulation of oncogenes E6 and E7 and upregulation of tumour suppressor proteins p53/ pRb and apoptotic protein activated caspase-3.

(iv) To investigate which ATO delivery method is the most selective and effective for treating HPV positive cervical cancer cells.

3.4.2 **Materials and methods**

3.4.2.1 Materials

The list of materials employed for the study, including Annexin V-FITC/PI apoptosis detection kit, antibodies for protein detection, reagents for Western blotting, confocal and flow cytometry analysis, have been enlisted in Chapter 2. The FA-targeted and non-targeted liposomes were prepared and characterised as detailed in Chapter 3 (iii).

3.4.2.2 Cell culture

Two cervical cancer cell lines, HeLa and HT-3, and HPV positive HeLa derivative human nasopharyngeal epidermal carcinoma cells KB were employed in this study. HeLa and KB cells were cultured in RPMI1640 media with no folic acid and HT-3 cells in McCoy's 5A (Modified) media containing 10 % foetal calf serum, 100 U/ml of penicillin and 100 mg/ml streptomycin in 75-cm^2 flasks. The following experiments were then set up for further studies including Western blot, fluorescent staining and flow cytometry analysis.

3.4.2.3 Analysis of Cell Apoptosis by Flow Cytometry

Cells from the three different cell lines were seeded at 5×10^5/ml in six-well culture plates and grown overnight for cell attachment. After 48 h of treatment (media only, 5µM ATO encapsulating ATO-L1 and ATO-FA-L2 liposomes and 5µM free ATO), the cells were analysed for apoptosis induction via flow cytometry according to the protocol described for Annexin V–FITC/PI apoptosis detection kit (Abcam, UK) used for this study (more details in Chapter 2).

3.4.2.4 Western blot analysis

Expression of active caspase-3, p53, pRb, E6 and E7 proteins in the cell lines were determined by Western blotting as detailed in Chapter 2. The treatment was arranged as follows: media only, 5µM ATO encapsulated liposomes ATO-L1 and ATO-FA-L2 and 5µM free ATO for a period of 48 h. The primary antibodies used were rabbit monoclonal anti-active caspase-3, mouse monoclonal anti-p53 and mouse monoclonal anti-Rb antibodies in 1:500 dilutions, mouse monoclonal anti-HPV 18 E7 in 1:1000 dilutions and mouse monoclonal anti-HPV 18 E6 in 1:100 dilutions. The secondary antibodies employed were goat anti-mouse and goat anti-rabbit IgG-HRP antibodies in 1 in 3000 dilutions. Protein quantification was done using REVERT total protein stain technique on Licor Odyssey imaging system.

3.4.2.5 Fluorescent staining analysis

Single fluorescent staining for active caspase-3, p53, pRb, E6 and E7 proteins and double fluorescent staining for E6 and p53; and E7 and pRb proteins in the cell lines under investigation were carried out as per the protocol described in Chapter 2. The cells were treated with media only, 5µM ATO encapsulated ATO-L1 and ATO-FA-L2 liposomes and 5µM free ATO for 48 h. The primary antibodies used were the same as those used in Western blotting experiments. The dilutions used however for single staining for all the antibodies were 1:100 in PBS. The signal was amplified using ABC kit and detected via TSA Fluorescein system or TSA Cys-5 system. In case of double staining of E6/p53 and E7/pRb, the first primary antibody used was mouse monoclonal anti-HPV 18 E6 (1:50) and mouse monoclonal anti-HPV 18 E7 (1:100) respectively which was detected with TSA-Cys-5 system. The second primary antibody was rabbit polyclonal anti-p53 antibody (1:100) and rabbit polyclonal to pRb (1:100) respectively detected by secondary antibody goat anti-rabbit IgG conjugated with FITC (1:100). The nuclei were counterstained and the slides mounted using Vectashield hard set mounting media with DAPI. A confocal microscope (Leica Microsystems, Wetzlar, Germany) was used to capture the images of single and double fluorescent staining using the antibodies as described above.

3.4.2.6 Flow cytometry analysis of intracellular antigen staining

The cells were stained for active caspase-3, p53 and pRb proteins with primary antibodies rabbit monoclonal to Rb (1:100 dilution), rabbit monoclonal to active caspase-3 (1:200 dilution) and mouse monoclonal to p53 (1:100 dilution). The secondary antibodies employed were goat anti-rabbit IgG-FITC and goat anti-mouse IgG-FITC (1:500 dilution) and flow cytometry analysis of the protein expression was carried out as per the protocol described in Chapter 2.

3.4.2.7 Statistical analysis

Statistical analysis described in experimental sections was done with Minitab17. Statistical significance was determined by 2-sample t-test. $P< 0.05$ was considered significant. For results from Western blotting studies, the signals were normalised using Image J software and mean and SD were calculated. For immunostaining results, an average number from positively stained cells in a total of six fields of each sample were calculated and average percentages were recorded. For flow cytometry, statistical analysis was carried out automatically though BD Calibur software provided.

3.4.3 **Results**

3.4.3.1 ATO encapsulated in targeted liposomes induce higher apoptosis for HPV positive cancer cells than non-targeted liposomes

HPV positive HeLa and KB cells were exposed to the following treatments as follows: control (cells in RPMI media only) and 5μM ATO encapsulating ATO-L1 and ATO-FA-L2 liposomes for 48 h. They were further labelled with FITC-conjugated Annexin-V and PI for the detection of early and late apoptotic populations respectively. The fluorescence was detected by flow cytometer on its FL1 and FL3 channels respectively. The percentages of cell populations distributed in the different quadrants depicting live (lower left), early (lower right) and late apoptotic/necrotic cells (upper region) were calculated and the fold increase of apoptotic population (early + late) from various treatments (ATO-L1 and ATO-FA-L2) according to the control is summarised in Fig 3.4.2.

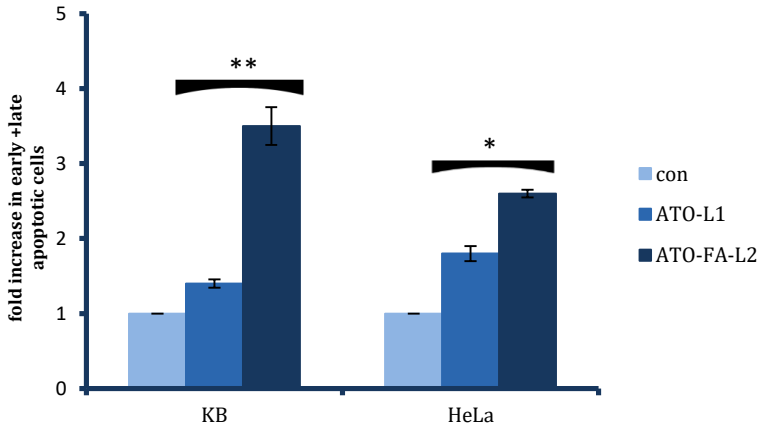

Fig 3.4.2: Flow cytometry analysis of apoptotic cells in KB and HeLa after treatment with only media, 5μM ATO encapsulating ATO-L1 and ATO-FA-L2 after 48 h treatment. An unpaired t test was used to test for any significant difference in the apoptotic population in cells after treatment with ATO-L1 and ATO-FA-L2. Targeted liposomal ATO induced more apoptosis than non-targeted liposomal ATO. *$p \leq 0.05$; **$p \leq 0.01$. Data displayed is mean ± SD from at least three independent experiments.

Results showed that ATO-FA-L2 induced higher apoptosis in both KB and HeLa cells than non-targeted liposomes. This difference was more pronounced for KB cells with ATO-FA-L2 treatment producing 2.5 times more apoptotic cells than the ATO-L1 treatment; whereas it was 1.4 times higher with ATO-FA-L2 than ATO-L1 in HeLa cells. The unconjugated liposomal treatment, however, induced higher apoptosis in HeLa cells with 1.8 times more apoptotic cells than the control as compared to the 1.4 times more apoptotic cells in KB.

To further characterise the apoptosis observed in the targeted and non-targeted liposomal ATO treated cells, the expression of activated caspase-3 was investigated via Western blotting, confocal microscopy and flow cytometry analysis. Western blotting results clearly showed a distinct band of active caspase-3 at around 17kDa for the treated cells for both KB and HeLa cell lines. The band was very prominent for ATO-FA-L2 treatment, fainter for ATO-L1 treatment while being negligible for the control. The signal intensity for the bands obtained was normalised employing REVERT total protein stain (Fig 3.4.3). As expected, the activation of caspase-3 was most pronounced in ATO-FA-L2 treated KB cell line. Active caspase-3 expression was observed to be 1.6 and 1.9 times higher for ATO-FA-L2 treatment than ATO-L1 for KB and HeLa cells respectively.

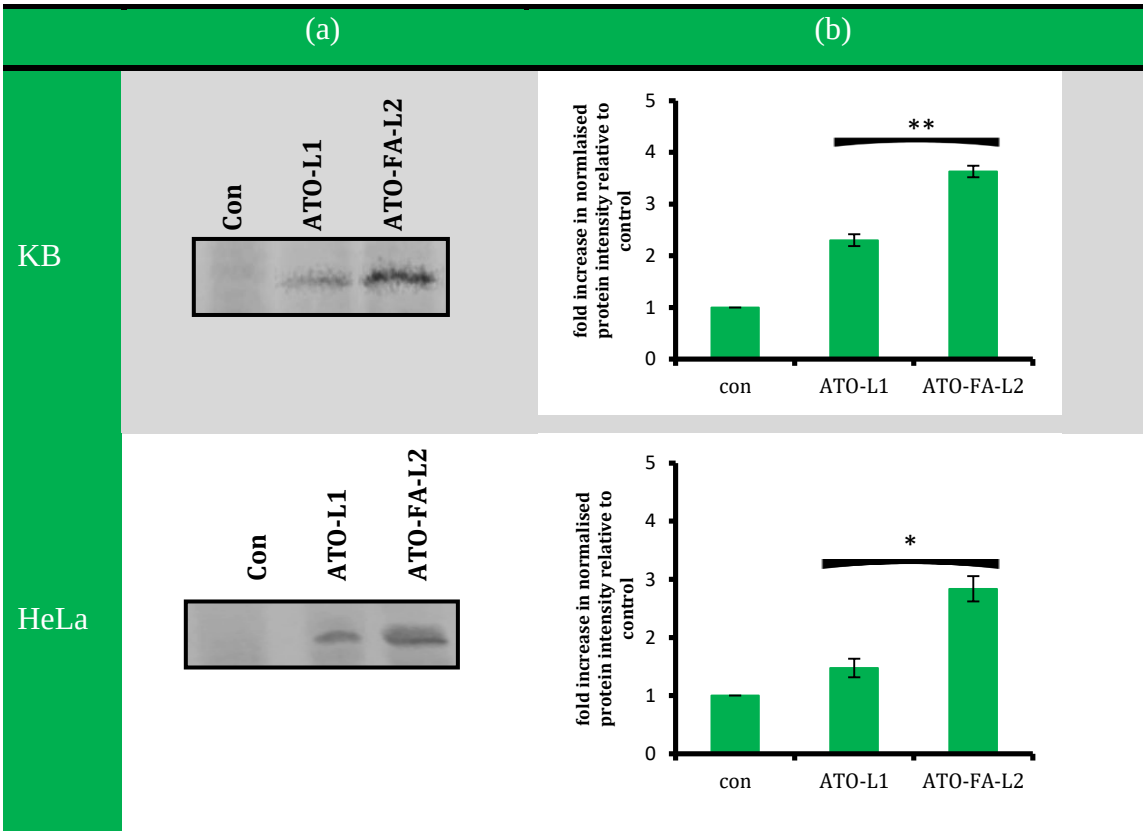

Fig 3.4.3 (a): Comparative Western blot analysis of active caspase-3 expression in KB and HeLa cell lines after ATO-L1 and ATO-FA-L2 treatment for 48 h; (b) relative protein expression levels on the two cell lines after normalisation with REVERT total protein stain as determined via Western blot. Data shown is means ± standard deviation from 3 independent experiments. Active caspase-3 is expressed more after ATO-FA-L2 treatment than ATO-L1. * $p \leq 0.05$; ** $p \leq 0.01$

The results obtained from Western blot were further corroborated by fluorescent staining of active caspase-3 in KB and HeLa cells after 48 h treatment (Fig 3.4.4). As with the Western blot, the expression of active caspase-3 was more prominent with ATO-FA-L2 treatment than ATO-L1 in both cell lines, while being almost negligible for control. The analysis of its expression via flow cytometry also validated the previous findings in that the targeted liposomal treatment was more efficient in activating the apoptosis related protein caspase-3 than the non-targeted liposomal ATO (Fig 3.4.5).

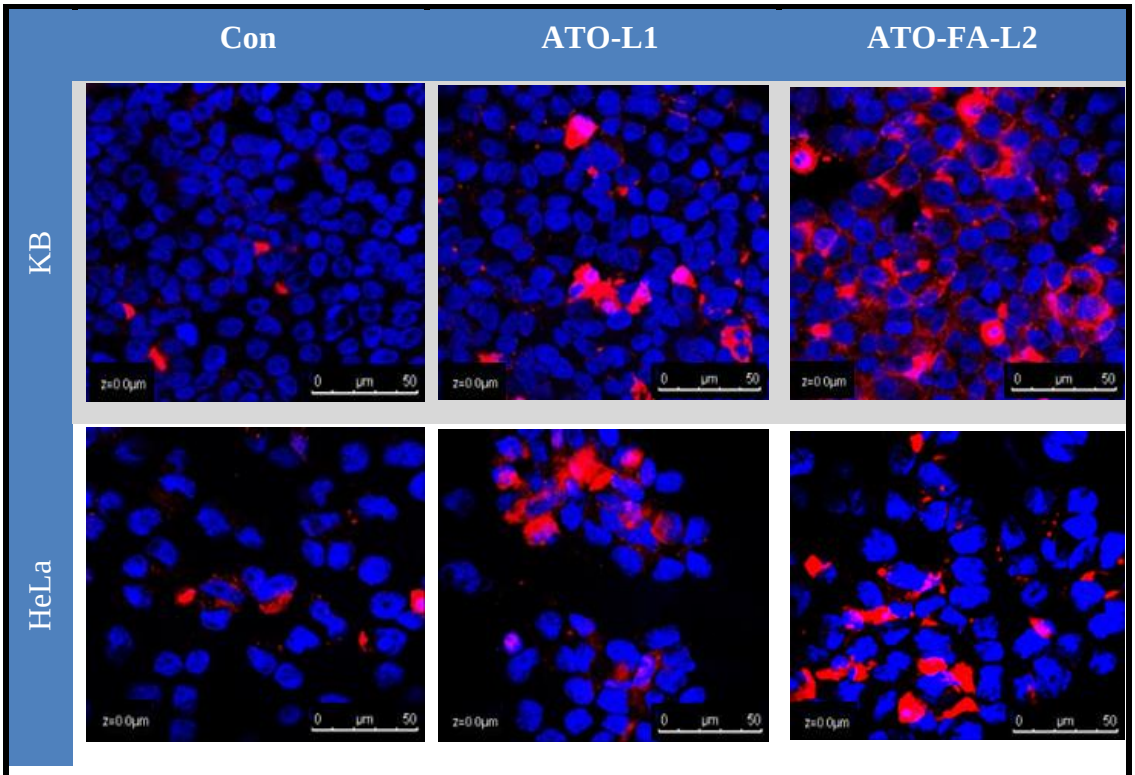

Fig 3.4.4: Confocal microscopic examination of active caspase-3 expression in KB and HeLa cells following ATO-L1 and ATO-FA-L2 treatment. Cells were counterstained with DAPI to reveal the nuclear/ DNA location. ATO-FA-L2 liposomes activated more caspase-3 than ATO-L1 liposomes in both the cells.

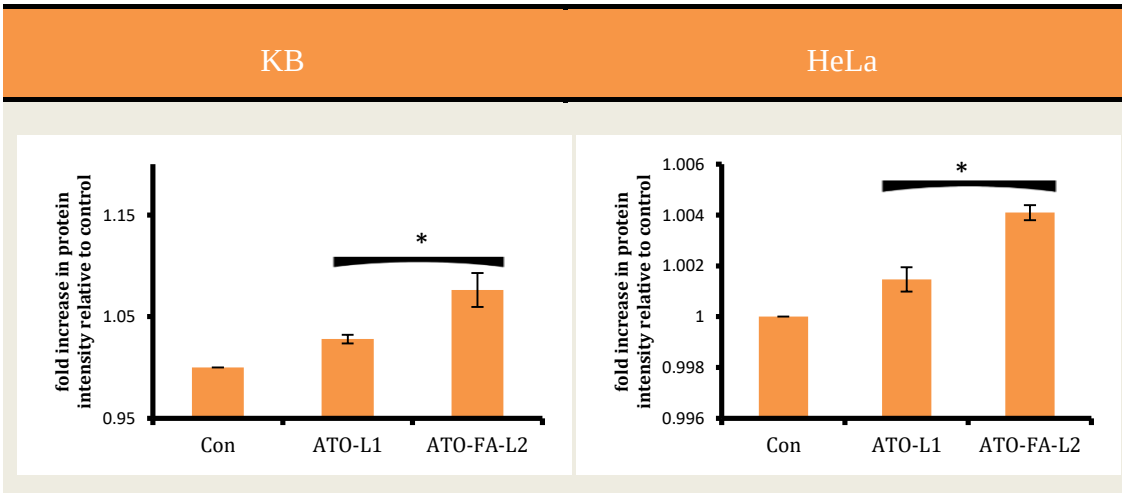

Fig 3.4.5: Flow cytometry analysis of active caspase-3 expression in KB and HeLa cells post ATO-L1 and ATO-FA-L2 treatment. Data shown is means ± standard deviation from 3 independent experiments. * $p \leq 0.05$.

3.4.3.2 Targeted liposomes are more efficient in downregulating oncogenes expression and upregulating tumour suppressors than non-targeted liposomes in HPV positive cells

Expression levels of E6 and E7 oncoproteins and their relationship with pRb and p53 tumour suppressors were investigated though Western blotting and single and double immunostaining of E6 and E7 oncoproteins and p53 and pRb tumour suppressors.

Western blotting results clearly showed that targeted liposomal ATO was significantly more efficient in downregulating both E6 and E7 oncoproteins in KB and HeLa cell lines than non-targeted liposomal ATO (Fig 3.4.6). Moreover, it was also observed that compared to ATO-L1, the downregulation of their expression was higher with ATO-FA-L2 treatment for HeLa cells than KB cells for both E6 and E7 proteins. The tumour suppressors' p53 and pRb also displayed a marked increase in their expression with ATO-FA-L2 treatment for both the cell lines. However, in this instance, the fold increase of tumour suppressors with ATO-FA-L2 treatment, compared to ATO-L1 treated cells, was higher for KB cells than HeLa cells.

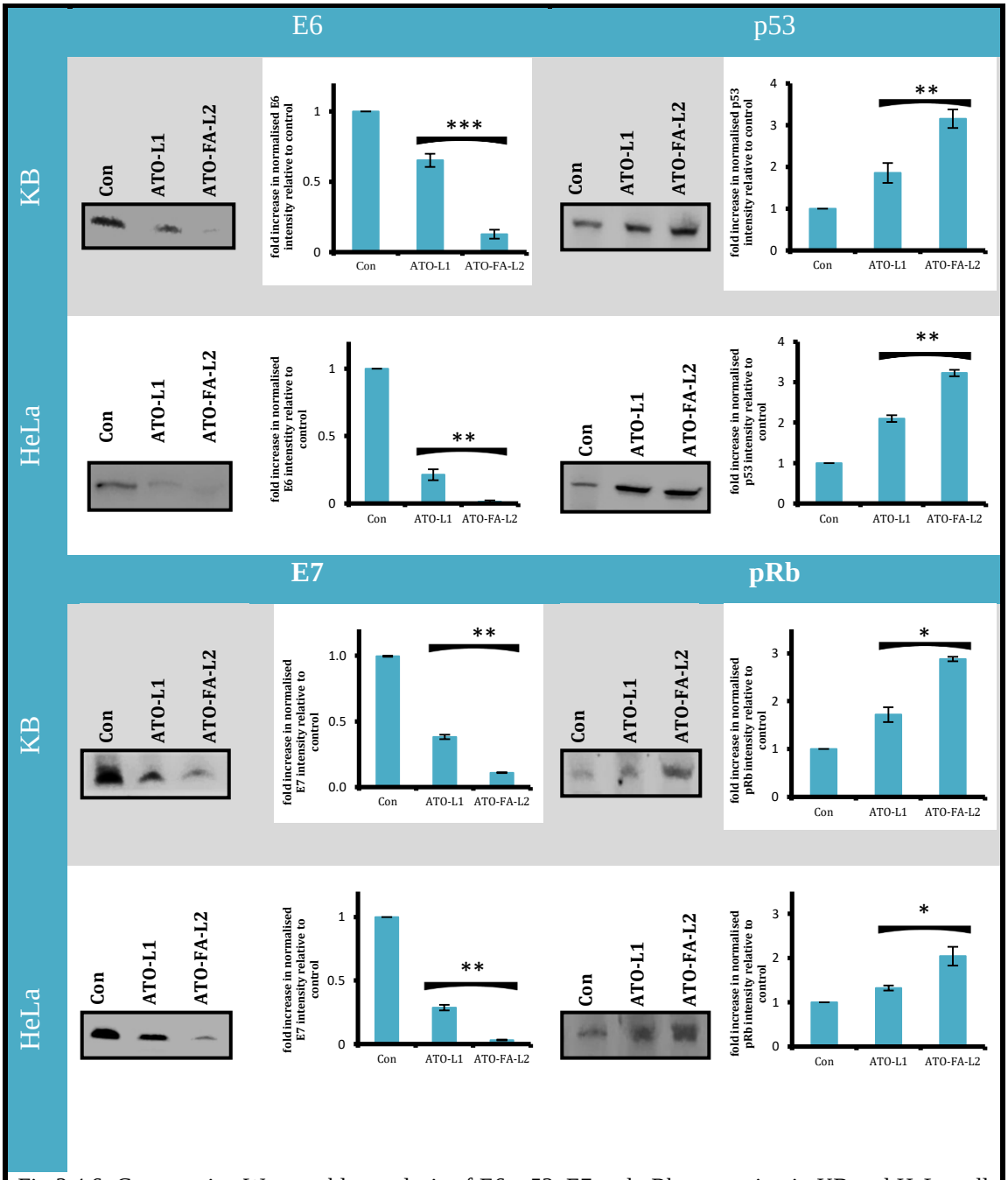

Fig 3.4.6: Comparative Western blot analysis of E6, p53, E7 and pRb expression in KB and HeLa cell lines and relative protein expression levels on the cell lines after normalisation with REVERT total protein stain as determined via Western blot. Data shown were expressed as means ± standard deviation from 3 independent experiments. Targeted liposomes ATO-FA-L2 were more efficient in inducing response than ATO-L1 in both cell lines for all the proteins investigated. *p≤0.05; **p≤0.01 and ***p≤ 0.001.

KB and HeLa cells were stained for E6, E7, p53 and pRb proteins after a 48 h exposure to 5μM ATO encapsulating non-conjugated and FA-conjugated liposomes. The cell lines were examined under confocal microscopy (Fig 3.4.7). The results corroborated the above Western blot findings as the expression levels of E6 and E7 oncoproteins diminished significantly more after ATO-FA-L2 treatment than ATO-L1 for both the cell lines. The tumour suppressors' p53 and pRb expression levels were elevated instead, more significantly by ATO-FA-L2 than ATO-L1, for both KB and HeLa cells. The oncoproteins were expressed in the cytoplasm around the DAPI stained nuclei whereas both the tumour suppressors were localised within the nucleus.

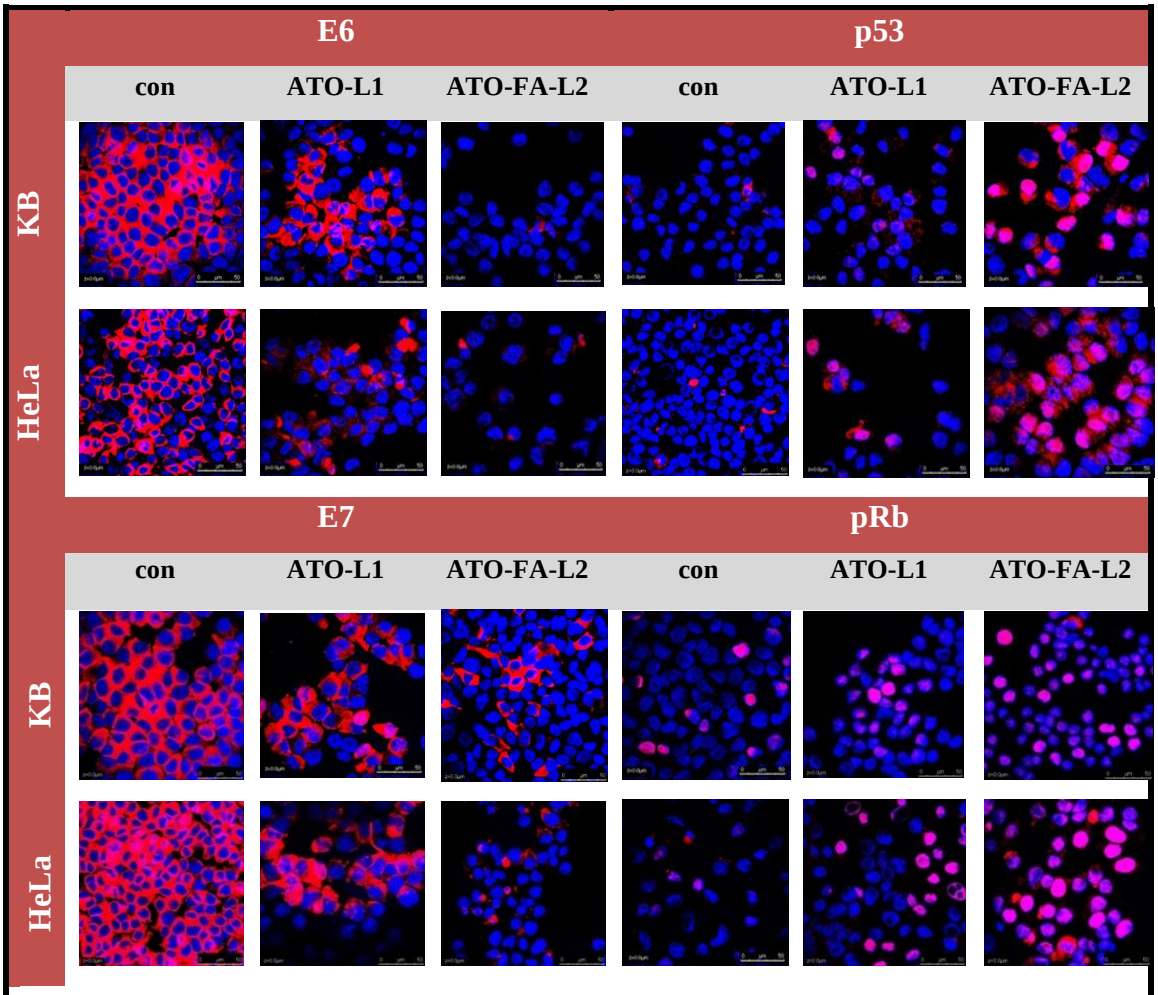

Fig 3.4.7: Confocal microscopic examination of E6-p53 and E7-pRb in KB and HeLa cells following ATO-L1 and ATO-FA-L2 treatment via single immunostaining. Cells were counterstained with DAPI to reveal the nuclear/ DNA location. ATO-FA-L2 liposomes downregulated oncoproteins and upregulated tumour suppressors more than ATO-L1 liposomes in both the cells.

Since the main oncogenecity of E6 lies in stimulating the degradation of p53 and E7 with interfering in the function of pRb, their relationship was investigated in KB and HeLa cells after 48 h-liposomal ATO exposure though double immunostaining of HPV 18 E6-p53 and HPV 18 E7-pRb (Fig 3.4.8). Along with validating the above findings of higher efficiency of ATO-FA-L2 in downregulating oncogenes while upregulating tumour suppressors, confocal staining results showed a slight difference in the expression of the p53 between the two cell lines. In ATO-FA-L2 treated KB cells, whereas p53 staining is found to be sharp and seen in fewer cells, it is diffused but present in more cells in HeLa. This is also seen with pRb staining, where HeLa cells display diffused staining in more cells as compared to KB cells, where the expression is more prominent but in fewer cells.

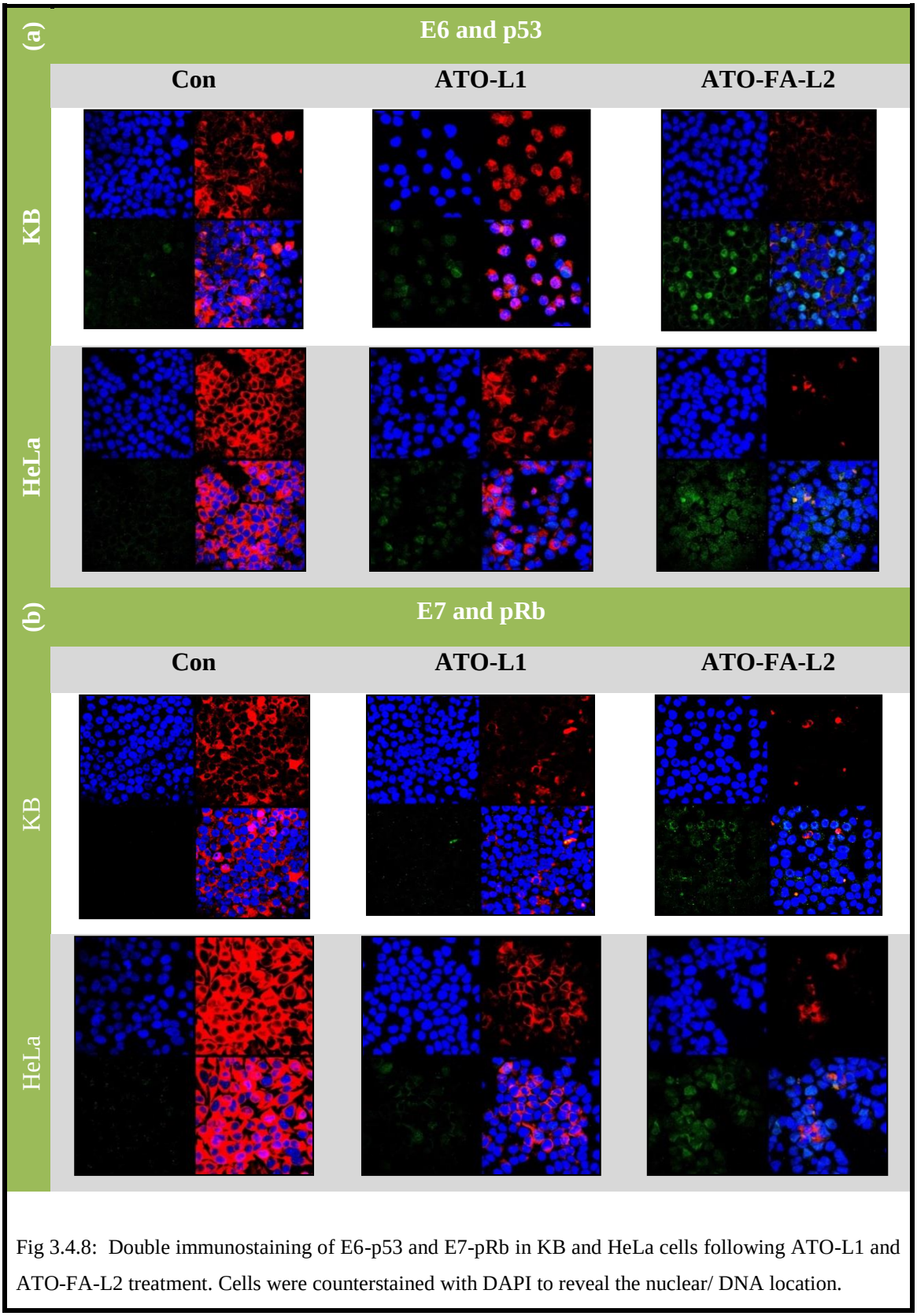

Fig 3.4.8: Double immunostaining of E6-p53 and E7-pRb in KB and HeLa cells following ATO-L1 and ATO-FA-L2 treatment. Cells were counterstained with DAPI to reveal the nuclear/ DNA location.

3.4.3.3 FA-conjugated liposomes are selective in their action by targeting HPV positive HeLa cells more than HPV negative HT-3 cells.

After establishing that FA-conjugated liposomes are more efficient in inducing apoptosis, reducing oncogene levels and increasing tumour suppressors in HeLa cells and with a final goal of selectively targeting HPV positive cervical cancers, their selectivity was further investigated by comparing their action on HPV negative cervical cancer cells. Towards this aim, HPV negative cervical cancer HT-3 cell line was introduced and was subjected to unconjugated and FA-conjugated liposomal ATO treatment for 48 h. It was further examined for the abovementioned mechanisms by conducting the following experiments including apoptosis induction, expression of apoptotic protein active caspase-3 and tumour suppressors' p53 and pRb.

Results from flow cytometry apoptosis assay clearly indicated that ATO-FA-L2 liposomes were more efficient in inducing apoptosis in HeLa cells than HT-3 cells (Fig 3.4.9). Compared to the control, ATO-FA-L2 induced 2.6 times more apoptotic cells in HeLa whereas only 1.4 times more apoptotic cells in HT-3. The expression of active caspase-3 in HT-3 was investigated via Western blotting, immunostaining and flow cytometry and compared with HeLa. Western blotting results clearly showed that compared to the control cells, active caspase-3 was expressed much more strongly in HeLa than HT-3 following ATO-FA-L2 treatment (Fig 3.4.10). This was also evident from both the flow cytometry analysis of the apoptotic protein (Fig 3.4.11) and confocal analysis where active caspase-3 stained more strongly for HeLa cells than HT-3 cells (Fig 3.4.12).

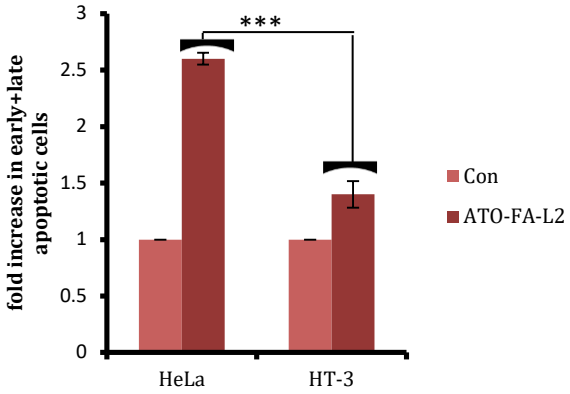

Fig 3.4.9: Flow cytometry analysis of apoptotic cells in HeLa and HT-3 after comparing treatments with only media and 5μM ATO encapsulating FA-conjugated liposomes (ATO-FA-L2) post 48 h treatment. Targeted liposomal ATO-FA-L2 induced higher apoptosis in HeLa than HT-3; *** $p \leq 0.001$. Data displayed were displayed as mean ± SD from at least three independent experiments.

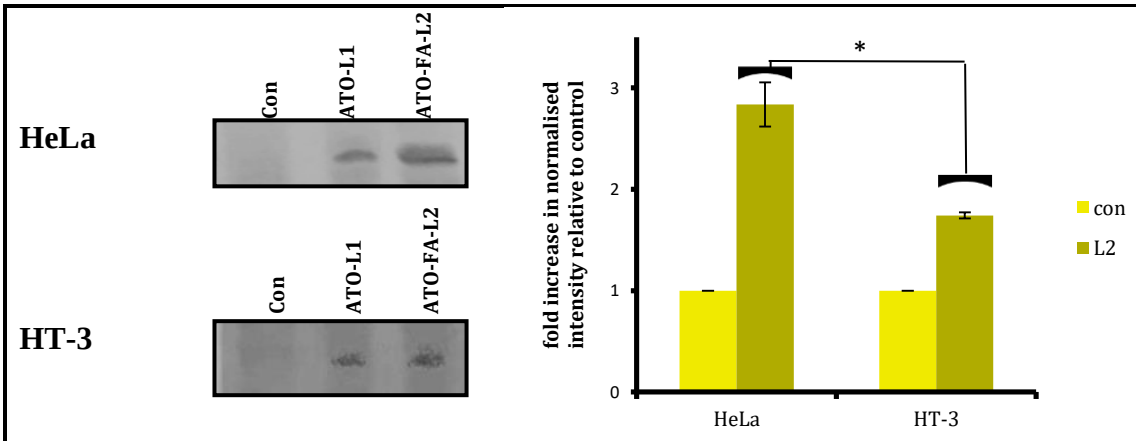

Fig 3.4.10 (a): Western blots of active caspase-3 expression in HeLa and HT-3 cells after ATO-L1 and ATO-FA-L2 treatments for 48 h; (b) relative protein expression levels on the two cell lines after normalisation with REVERT total protein stain as determined via Western blot; only control and ATO-FA-L2 protein levels are shown for comparison purposes. Data shown is means ± standard deviation from 3 independent experiments. * $p \leq 0.05$. Active caspase-3 was expressed more in HeLa after ATO-FA-L2 treatment than HT-3.

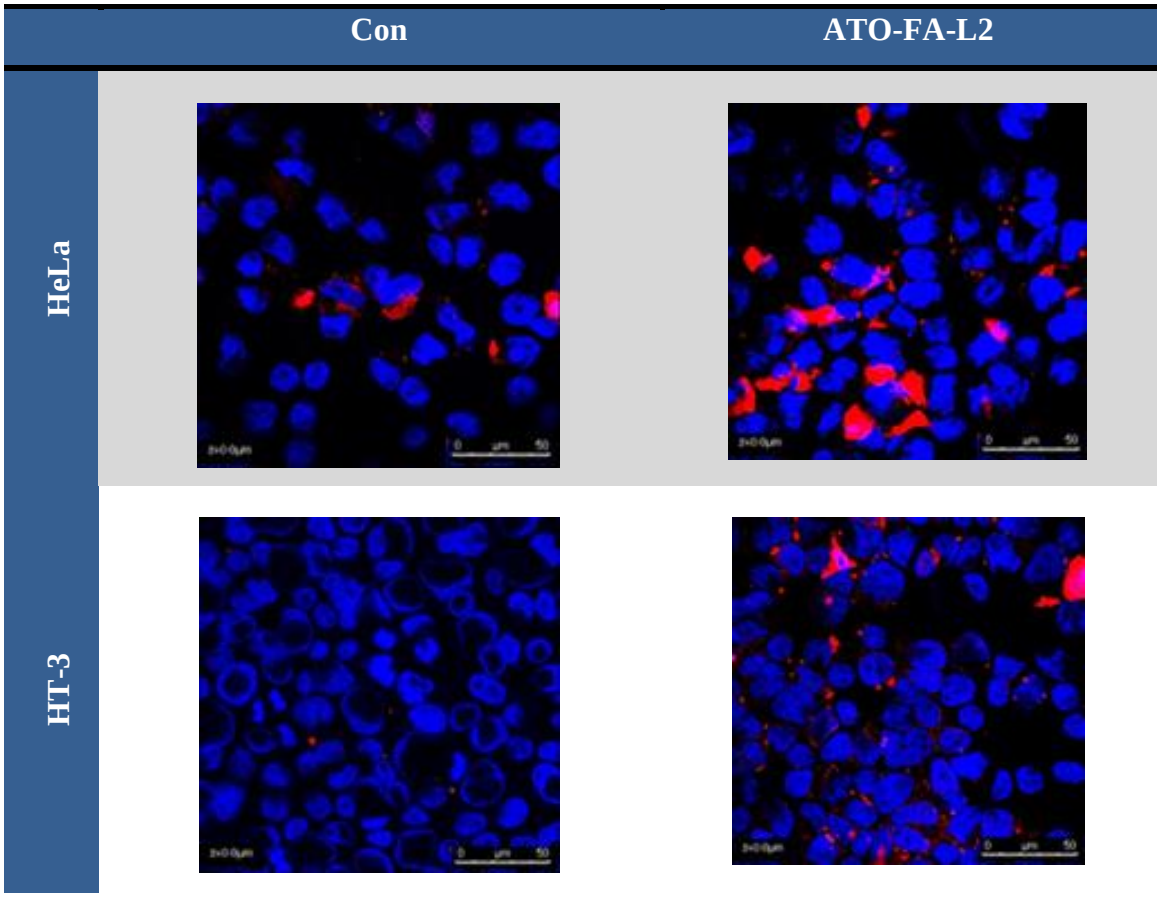

Fig 3.4.11: Confocal microscopic examination of active caspase-3 expression in HeLa and HT-3 cells following ATO-FA-L2 treatment. Cells were counterstained with DAPI to reveal the nuclear/ DNA location.

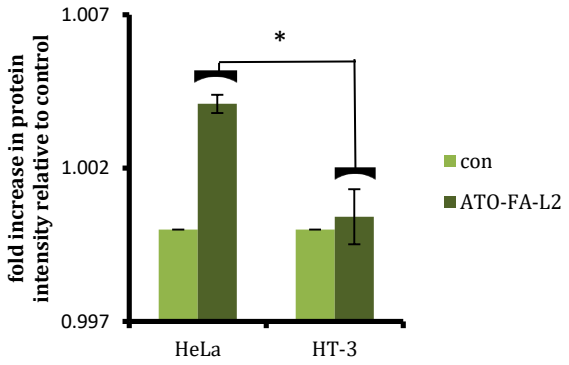

Fig 3.4.12: Flow cytometry analysis of active caspase-3 expression in KB and HeLa cells post control and ATO-FA-L2 treatment. Data shown is means ± standard deviation from 3 independent experiments. *p≤0.05.

Further exploring the cause of lower apoptosis induced in HT-3 cells, the tumour suppressors' expression was investigated. Western blot results showed that for both the tumour suppressors, there was a significant difference in their expression between HeLa and HT-3 cells when treated with ATO-FA-L2 liposomes, with HeLa expressing almost 2.3 times more p53 and 1.3 times more pRb than HT-3 from their respective controls (Fig 3.4.13). The confocal images also show a consistent higher expression of both the tumour suppressors in HeLa cells as compared to HT-3 cells from ATO-FA-L2 treatment (Fig 3.4.14).

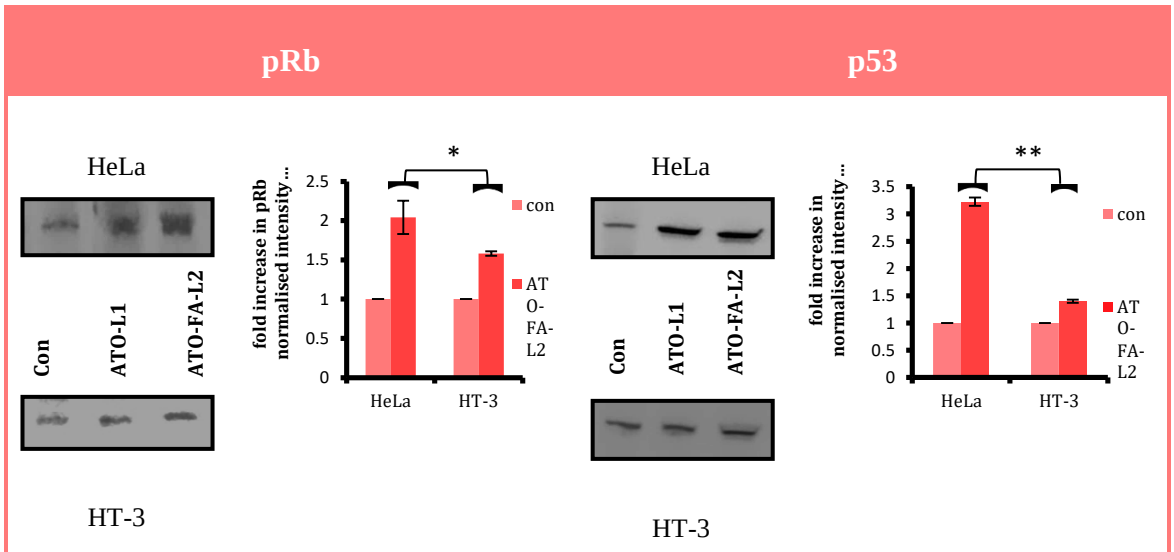

Fig 3.4.13: Western blots of pRb and p53 expression in HeLa and HT-3 cells after ATO-L1 and ATO-FA-L2 treatments for 48 h; (b) relative protein expression levels on the two cell lines after normalisation with REVERT total protein stain as determined via Western blot; only control and ATO-FA-L2 protein levels are shown for comparison purposes. Data shown is means ± standard deviation from 3 independent experiments. * $p \leq 0.05$, ** $p \leq 0.01$. p53 and pRb proteins were expressed more in HeLa cells after ATO-FA-L2 treatment than HT-3 cells.

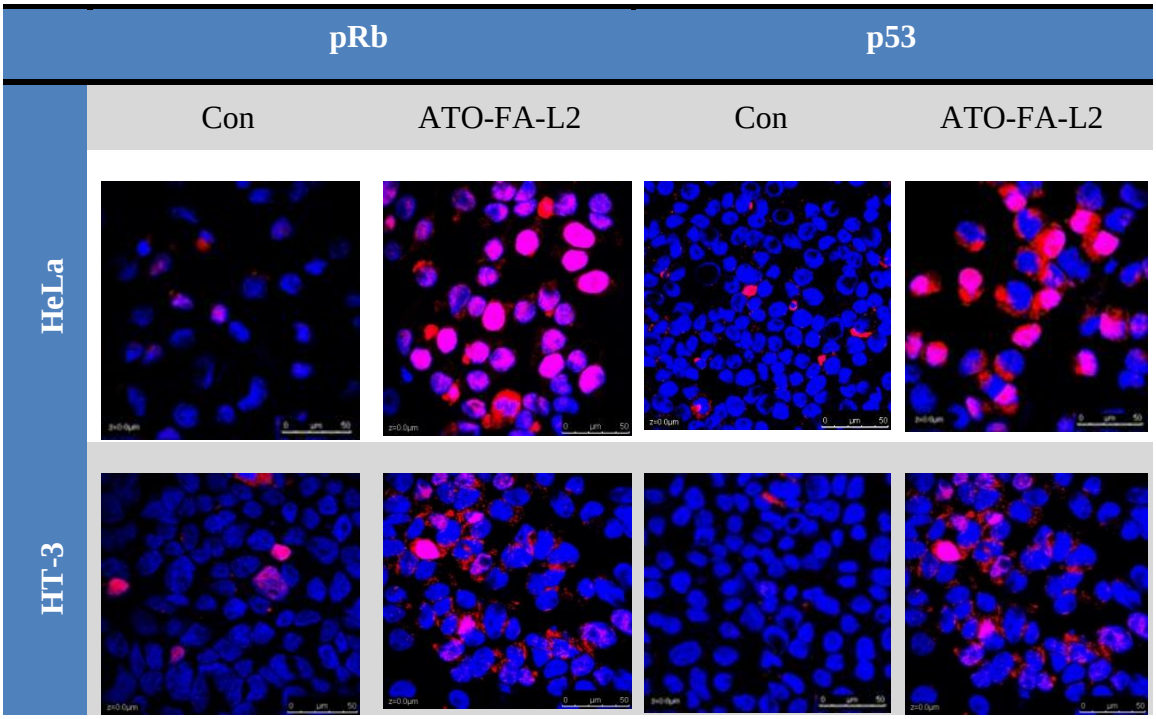

Fig 3.4.14: Confocal microscopic examination of p53 and pRb expression in HeLa and HT-3 cells following ATO-FA-L2 treatment. Cells were counterstained with DAPI to reveal the nuclear/ DNA location.

3.4.3.4 Comparative study for oncogenes and tumour suppressors' expression from free and FA-liposomal ATO treatment in HPV positive cells.

HPV positive KB and HeLa cells were treated with free ATO to compare the drug's mode of action when it is delivered in its free form as opposed to when it is delivered liposomally (ATO-FA-L2). A comparative study was thereby drawn and the results from Western blotting showed that free drug was more effective than ATO-FA-L2 in reducing the expression of E6 in both cell lines and E7 in KB cells (Fig 3.4.15). The E7 expression, however, was comparable from both treatments in HeLa cells. Moreover, the tumour suppressors displayed comparable expressions with either treatment in both cells

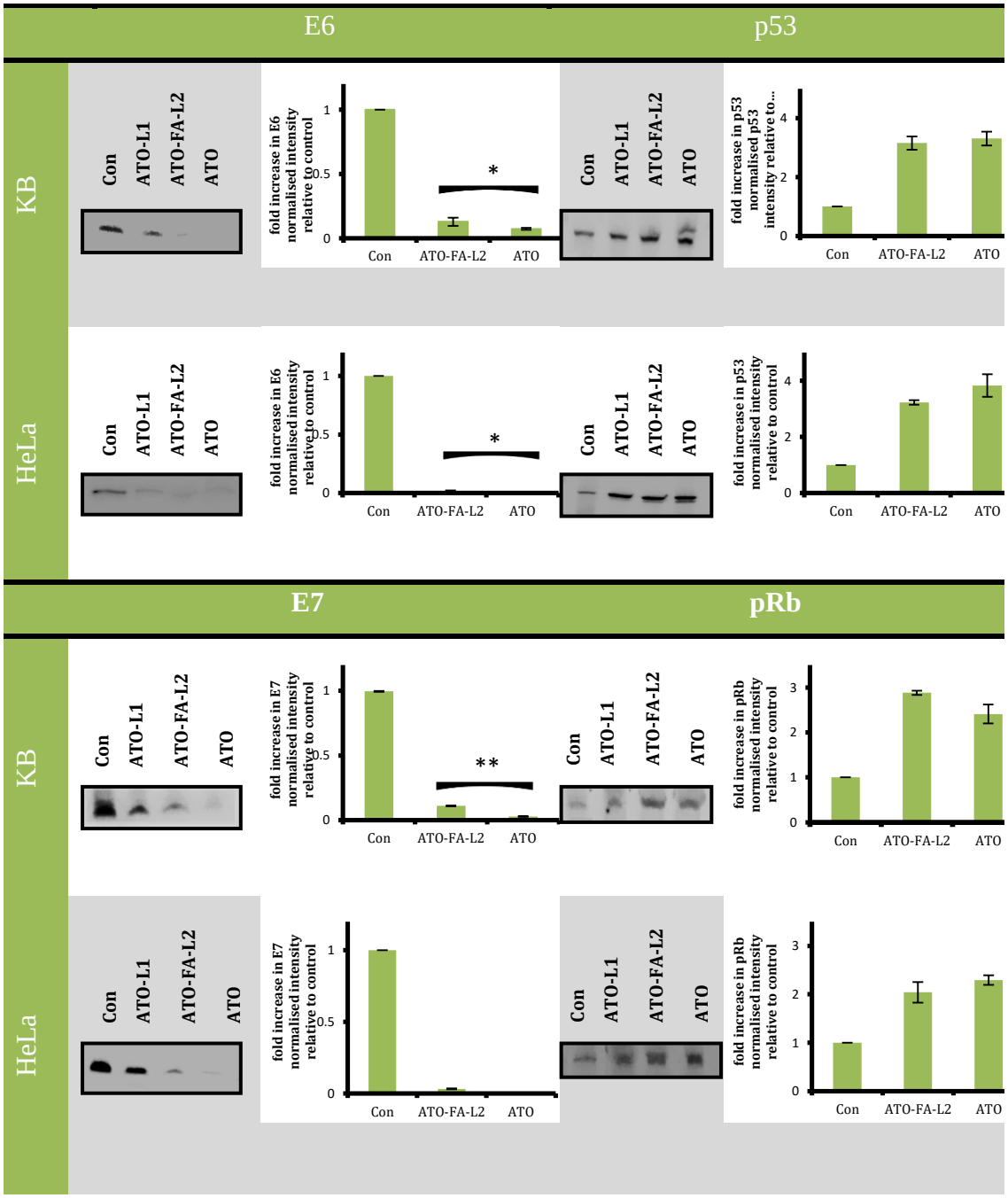

Fig 3.4.15: Comparative western blot analysis of E6, p53, E7 and pRb expression in KB and HeLa cell lines and relative protein expression levels on the cell lines after normalisation with REVERT total protein stain as determined via Western blot after 48 h treatment. Only protein expression levels from control, ATO-FA-L2 and ATO treatment are analysed for comparison purposes here. Data shown is means ± standard deviation from 3 independent experiments. * $p \leq 0.05$, ** $p \leq 0.01$

When the cells were immunostained to be viewed under confocal microscope, images unexpectedly, did not show any significant difference in the expression of E6 for KB

and HeLa cells treated with ATO-FA-L2 or ATO (Fig 3.4.16). With E7 protein however, the results were the same as Western blotting, with an elevated expression for KB cells with ATO-FA-L2 treatment while no significant difference in HeLa cells with either treatments. The expression of tumour suppressors' p53 and pRB was comparable with both the treatments for KB and HeLa cells.

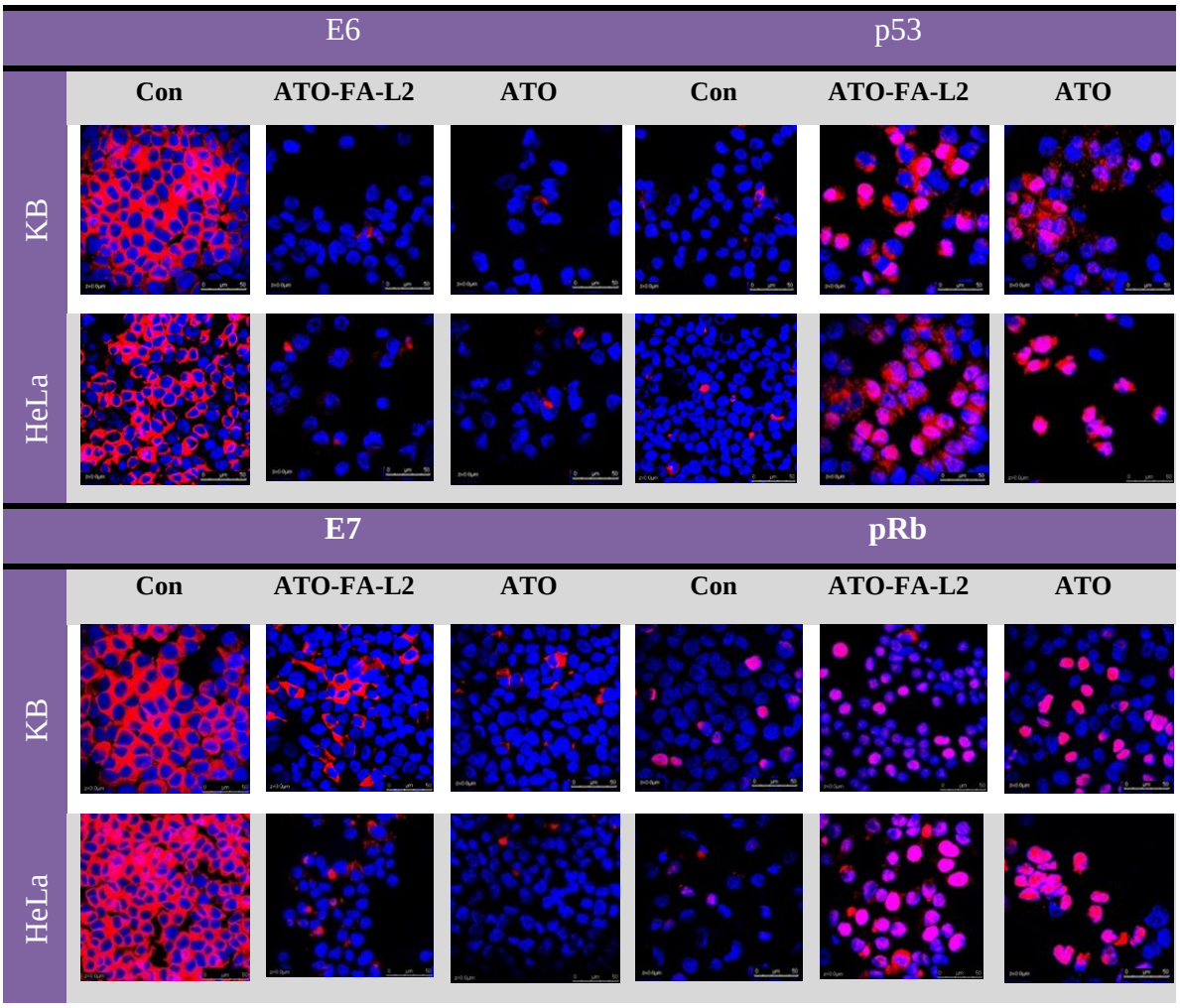

Fig 3.4.16: Confocal microscopic examination of E6-p53 and E7-pRb in KB and HeLa cells following ATO-FA-L2 and ATO treatment via single immunostaining. Cells were counterstained with DAPI to reveal the nuclear/ DNA location. Staining was comparable for ATO-FA-L2 and ATO treatments for all proteins except in the case of E7, where KB stained more with ATO than ATO-FA-L2.

The expression of tumour suppressors were further analysed with flow cytometry and corroborating the above findings, no significant difference in both p53 and pRb expression was observed with either treatment (Fig 3.4.17).

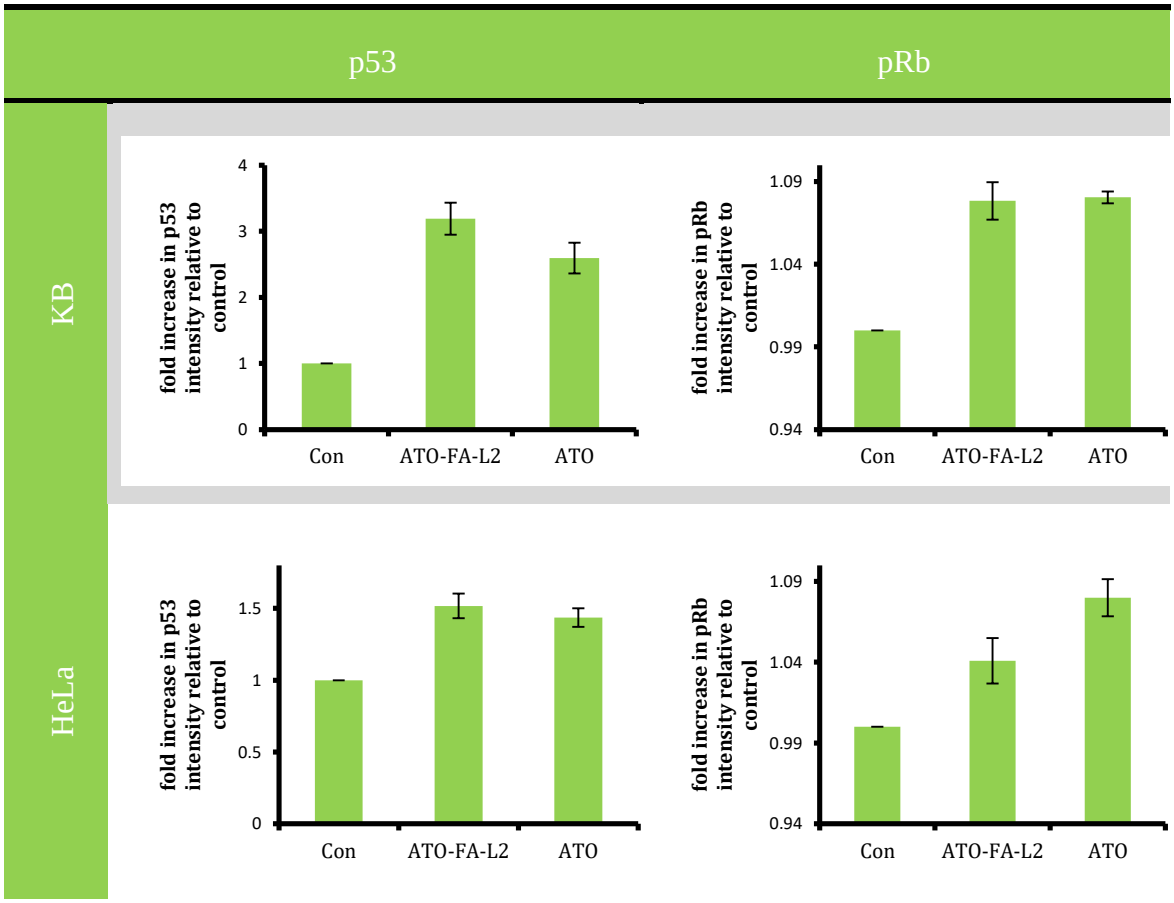

Fig 3.4.17: Flow cytometry analysis of p53 and pRb expression in KB and HeLa cells post ATO-FA-L2 and ATO treatment. Data shown is means ± standard deviation from 3 independent experiments.

3.4.3.5 Targeted liposomal ATO are more selective in inducing HPV infected cancer cell apoptosis and down-regulating HPV oncogenes

FA-liposomal ATO had demonstrated high selectivity in targeting HPV positive cancers. However, as free ATO marginally showed higher efficiency in downregulating oncogenes more despite being comparably effective for tumour suppressors' expression, free ATO was also tested whether it was as selective towards HPV positive cancers as the targeted liposomal ATO was. HPV negative HT-3 cells, henceforth, were incubated with free ATO for 48 h and investigated for apoptosis induction and tumour suppressors' upregulation.

Apoptosis assay via flow cytometry revealed that free ATO was not selective in its action by inducing high apoptosis in both HeLa and HT-3 cells unlike ATO-FA-L2 which induced higher apoptosis only in HeLa and not in HT-3 (Fig 3.4.18). ATO treatment resulted in a significantly higher apoptotic population from ATO treatment in HT-3 than ATO-FA-L2 liposomal treatment. The apoptosis induced in HeLa from free ATO and ATO-FA-L2 treatment was observed to be comparable.

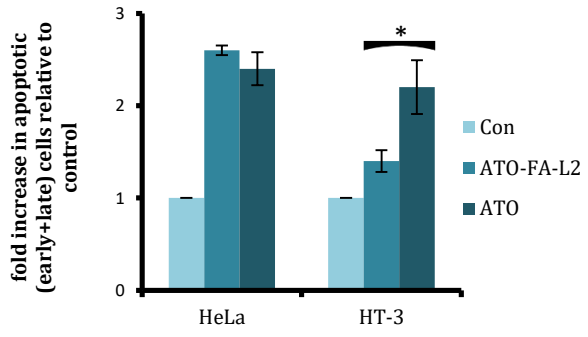

Fig 3.4.18: Flow cytometry analysis of apoptotic cells in HeLa and HT-3 after treatment with only media, 5µM ATO encapsulating FA-conjugated liposomes (ATO-FA-L2) and 5µM free ATO after 48 h treatment. Free ATO induced high apoptosis in both cell lines; * $p \leq 0.05$. Data displayed is mean ± SD from at least three independent experiments.

Investigations into the apoptotic protein active caspase-3 expression also revealed the same findings in Western blot that whereas ATO-FA-L2 resulted in a higher expression of the protein in only HeLa cells, ATO treatment elevated the protein's expression in both HeLa and HT-3 (Fig 3.4.19); probing its expression though immunostaining and flow cytometry also validated the above findings (Fig 3.4.20; Fig 3.4.21). Whereas staining for activated caspase-3 was similar for ATO-FA-L2 and ATO in HeLa cells, HT-3 displayed an elevated expression of the protein from ATO treatment only. Flow cytometry investigation also yielded the same result with a significant difference in the protein expression in HT-3 cells between ATO-FA-L2 and ATO treatment while being negligible for HeLa cells.

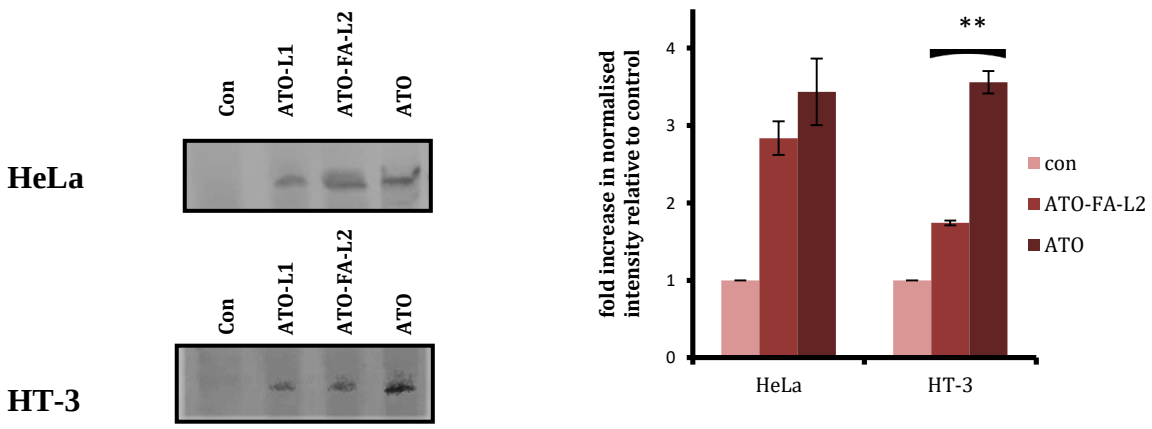

Fig 3.4.19: Western blots of active caspase-3 expression in HeLa and HT-3 cells after ATO-L1, ATO-FA-L2 and ATO treatments for 48 h; (b) relative protein expression levels on the two cell lines after normalisation with REVERT total protein stain as determined via Western blot; the analysis of normalised intensity is shown only for control , ATO-FA-L2 and ATO protein levels for comparison purposes. Data shown is means ± standard deviation from 3 independent experiments. **p≤0.01.

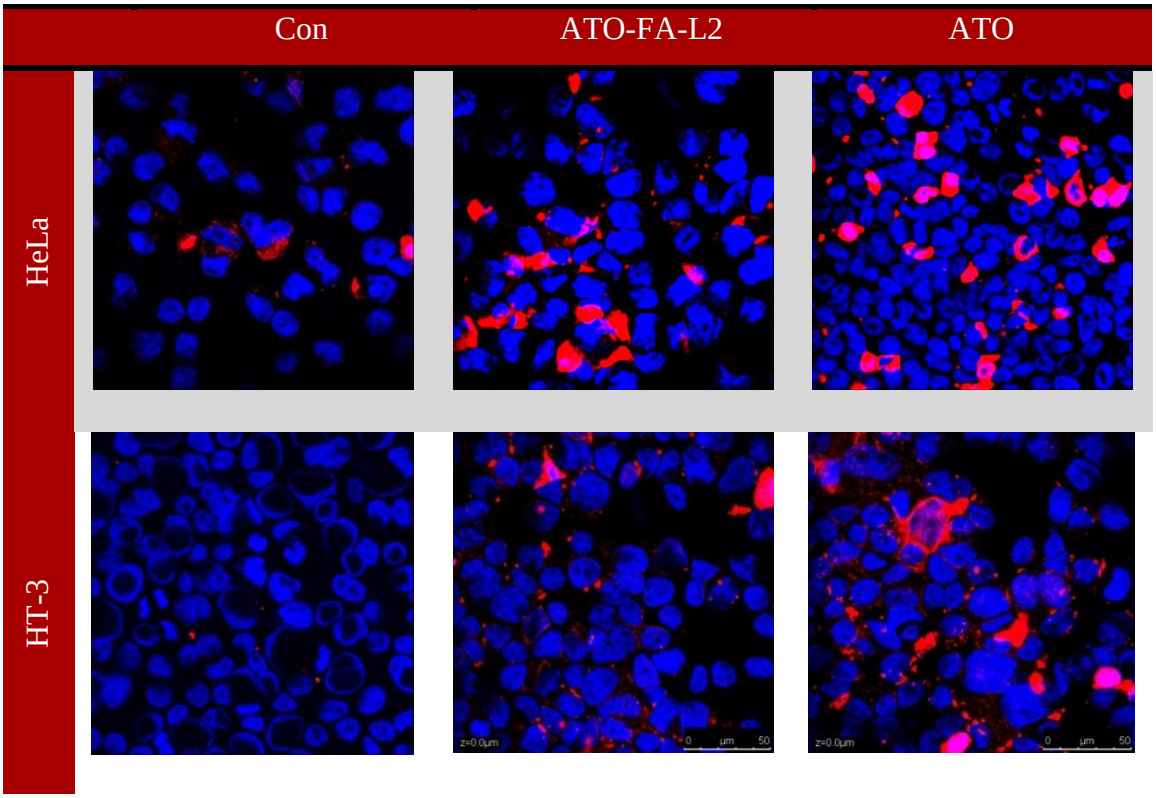

Fig 3.4.20: Confocal microscopic examination of active caspase-3 expression in HeLa and HT-3 cells following ATO-FA-L2 and ATO treatment. Cells were counterstained with DAPI to reveal the nuclear/ DNA location.

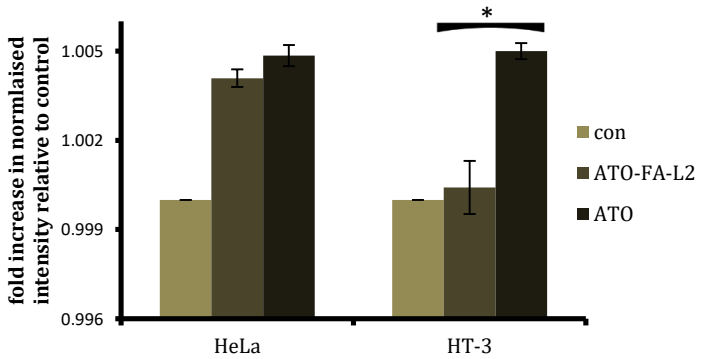

Fig 3.4.21: Flow cytometry analysis of active caspase-3 expression in HeLa and HT-3 cells post ATO-FA-L2 and ATO treatment. Data shown is means ± standard deviation from 3 independent experiments. *p≤0.05.

To further characterise the apoptosis induced in the cells, ATO-FA-L2 and ATO treated HeLa and HT-3 cells were further investigated for any upregulation of tumour suppressors resulting from the treatment. As expected, ATO treatment resulted in upregulation of both pRb and p53 in KB and HeLa cells. However, ATO-FA-L2 was effective in upregulating these proteins only in HeLa and not for HT-3 cells. Western blot results showed a significant difference in p53 and pRb protein levels in HT-3 while none for HeLa cell line from both the treatments (Fig 3.4.22). The results were further confirmed with similar staining of the proteins in HeLa for ATO-FA-L2 and ATO, while a significantly elevated staining for ATO treated HT-3 cells than ATO-FA-L2 treated HT-3 cells (Fig 3.4.23).

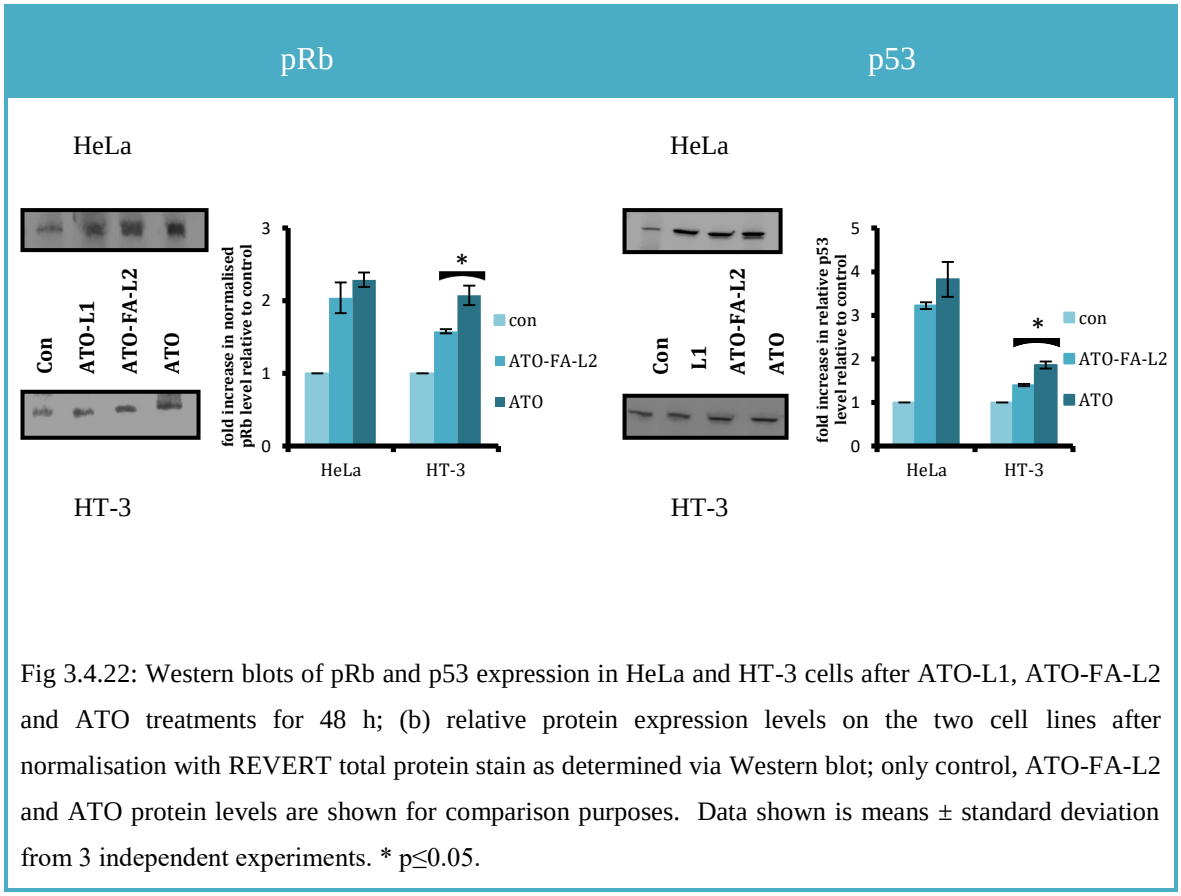

Fig 3.4.22: Western blots of pRb and p53 expression in HeLa and HT-3 cells after ATO-L1, ATO-FA-L2 and ATO treatments for 48 h; (b) relative protein expression levels on the two cell lines after normalisation with REVERT total protein stain as determined via Western blot; only control, ATO-FA-L2 and ATO protein levels are shown for comparison purposes. Data shown is means ± standard deviation from 3 independent experiments. * $p \leq 0.05$.

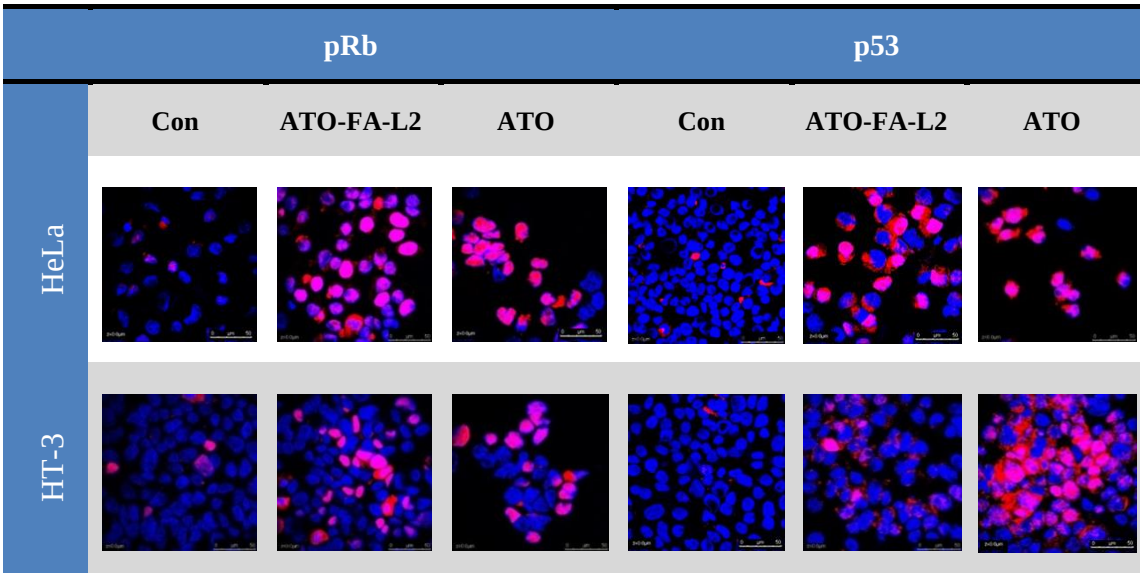

Fig 3.4.23: Confocal microscopic examination of p53 and pRb expression in HeLa and HT-3 cells following ATO-FA-L2 and ATO treatment. Cells were counterstained with DAPI to reveal the nuclear/ DNA location.

3.4.4 **Discussion**

This study shows that encapsulating anti-cancer drug ATO in folate tethered liposomes enhances the drug's specificity in selectively targeting HPV positive cancers. In addition to improving the therapeutic index of the drug, liposomal encapsulation makes it more efficient than its free form in selectively inducing apoptosis, downregulating HPV oncogenes and increasing the tumour suppressors' expression in HPV cancer cells. This presents a potential approach of significantly increasing the potency and specificity of ATO towards management of cervical cancers of HPV origin.

HPV, typically the high risk types, have been confirmed as the causal agents of cervical cancer (NeufCoeur et al., 2009; Shukla et al., 2009; Sutcliffe et al., 2010). HPV's E6 and E7 oncoproteins are the key potentiators of the oncogenic process and crucial in bringing about the host cell immortalisation and transformation (Mansur and Androphy, 1993; Um et al., 2002). E6 operates by mediating the tumour suppressor protein p53 degradation, whereas E7 binds to and inactivates another crucial regulatory molecule pRb (Barbosa and Schlegel, 1989).

The p53 tumour suppressor gene product is a nuclear-DNA binding phosphoprotein which plays an important role in DNA damage recognition, DNA repair, triggering cellular apoptosis after identifying genetic injury and cell cycle regulation (Bellamy, 1997). Since it limits the oncogenic potential of viral oncogenes, viruses such as HPV have evolved counterstrategies to evade induction of apoptosis by stimulating ubiquitination and proteasome dependent degradation of p53 (Um et al., 2002). Similarly, pRb exhibits significant tumour suppressive properties by regulating cell cycle progression (Berman et al., 2008). Its overexpression results in G1 cell cycle arrest whereas its acute extirpation causes quiescent cells to re-enter cell cycle (Sage et al., 2003). In order to perform its inhibitory function, the hypophosphorylated form of pRb binds to and inhibits the E2F family of transcription factors (Trimarchi and Lees, 2002). HPV's E7 disrupts this pRb-E2F bond and the E2Fs released induce the transcription of cellular genes essential for S-phase entry and cell division (Doorbar, 2007).

Owing to the crucial role of p53 and pRb in cell cycle regulation and apoptotic responses, any factors which inhibit p53 and pRb may cause apoptosis inhibition, unchecked cell proliferation and loss of epithelial cell adhesion, leading to development of cancer (Dyson, 1998; Howie, Katzenellenbogen and Galloway, 2009; Nevins, 1998). Therefore, any strategy that can inhibit E6 and E7 protein expression and upregulate tumour suppressors' p53 and pRb levels would be desirable as a therapeutic agent for managing HPV related cancers, including cervical cancers.

ATO has been reported to downregulate E6 and E7 oncogene expression and increase p53 protein (Um et al., 2002; Wen et al., 2012). When encapsulated in liposomes to improve its therapeutic index, ATO was observed to be effective in reducing HPV-E6 protein levels and inducing apoptosis in HPV positive HeLa cells 43, (Wang et al., 2016; Wen et al., 2012). Following the synthesis and optimisation of targeted ATO encapsulating liposomes specifically for HPV cancers, herein we studied the mechanism of action of ATO on HPV positive and negative cells and any differences that might arise when ATO is delivered in its free form, within unconjugated and conjugated liposomes.

Stable nanoparticulate form of folic acid tethered liposomal ATO were synthesised as in the previous results chapter. HPV-positive HeLa cells were employed for investigating the mechanism of action of ATO on HPV infected cervical cancer when being delivered in the abovementioned three disparate forms. Another HPV positive HeLa derivative nasopharyngeal KB cells and HPV negative cervical cancer HT-3 cells were used as control cell lines. FR expression on these cells was also investigated in the previous chapter III (ii) and the receptor was found to be expressed on the cell surface in the order of KB>HeLa>>HT-3 cells.

The first hypothesis to be investigated was that conjugating liposomes with folic acid would increase the liposomal efficiency in targeting HPV positive cells while inducing apoptosis in those cells. This was based on the fact that HPV positive KB and HeLa cells were FR positive while HPV negative HT-3 displayed minimal FR expression. This hypothesis proved to be true when investigation of rates of apoptosis measured via flow cytometry demonstrated an increased efficiency of FA-conjugated liposomes over non-conjugated liposomes in inducing apoptosis in HPV positive cells. For this part of

the analysis, both KB and HeLa cells were treated with non-targeted and targeted liposomal ATO for 48 h. Results showed that among the liposomal delivery methods, ATO delivered via targeted liposomes had a clear advantage of inducing higher apoptosis in the HPV positive cells than non-targeted liposomes (Fig 3.4.2). Predictably, the level of apoptosis induction was dependent on the cellular uptake of arsenic which in turn was dependent on the FR expression on the cell surface. Since KB cells had a higher FR expression than HeLa cells, FA-liposomal ATO generated higher apoptotic population in KB than HeLa cells. Non-targeted liposomes, on the other hand, induced more apoptosis in HeLa as compared to KB cells. This observation was striking as HeLa cells were also found to display this definite susceptibility towards ATO delivered in liposomal form when compared to HPV negative HT-3 cells as shown in the previous chapter III (i).

To further characterise the apoptosis induced in the cells, the expression of active caspase-3 was investigated via Western Blotting, confocal microscopy and flow cytometry analysis. Caspases are a class of cysteine proteases that are crucial mediators of apoptosis by cleaving key cellular proteins resulting in morphological features characterised by nuclear condensation and fragmentation (Miller et al., 2002). Among them, caspase-3 is a frequently activated death protease and its activation is a crucial requirement for many typical hallmarks of apoptosis (Porter and Janicke, 1999).

Western blotting results showed that the targeted liposomal ATO treatment resulted in a significantly higher activation of caspase-3 than the non-targeted liposomal ATO for both the cell lines (Fig 3.4.3). This finding was consistent with the confocal microscopy results which showed a considerably elevated staining of active capase-3 in KB and HeLa cells incubated with ATO-FA-L2 compared to ATO-L1 liposomes (Fig 3.4.4). Results from flow cytometry analysis (Fig 3.4.5) also confirmed the above results which are consistent with the higher apoptosis observed with targeted liposomal treatment for HPV associated cancers.

To examine the potential pathways for apoptosis induction in HPV infected cancer cells following liposomal treatment, the expression of the key potentiators of HPV related cancers, E6 and E7 oncoproteins and the tumour suppressor proteins' p53 and pRb were investigated in KB and HeLa cell lines. Predictably, targeted liposomes were more

efficient than non-targeted liposomes in downregulating oncogenes expression and upregulating the tumour suppressors in both cell lines. The Western blotting results showed that in both KB and HeLa, there was a significant difference between the protein levels resulting from the two treatments, with targeted liposomes more efficient at reducing the oncoproteins levels and increasing tumour suppressors (Fig 3.4.6).

Results also showed that non-targeted liposomes, however, downregulated E6 and E7 proteins more in HeLa, compared to KB cells. This is in accordance with the above results where non-conjugated liposomes induced higher apoptosis in HeLa. Surprisingly, even the downregulation of oncoproteins following ATO-FA-L2 treatment was more in HeLa cells, despite KB cells having higher FR expression and consequently higher cellular uptake of FA-lipo-ATO. This result again points to the possibility of HeLa cells possessing higher sensitivity for liposomal treatment.

Confocal microscopy images corroborated the above findings with targeted liposomes visibly reducing E6 and E7 protein levels in both KB and HeLa while elevating the expression of p53 and pRb more than the non-targeted liposomes (Fig 3.4.7). In addition, from the confocal images it could also be seen that the downregulation of both the oncoproteins and upregulation of tumour suppressors resulting from ATO-FA-L2 treatment was more pronounced in HeLa cells when compared to KB cells, validating the Western blot results.

To further understand the relationship between E6-p53 and E7-pRb, the cells were double immunostained and the images displayed a reciprocal relationship between the oncoprotein and the tumour suppressor it inhibits (Fig 3.4.8). When the liposomal treatment reduced the oncoprotein, a corresponding increase in the tumour suppressor that the oncoprotein associates with and inactivates, is demonstrated. These findings are consistent with the expected consequences of specific inhibition of HPV early gene (E6 and E7) expression: after viral integration, the HPV-E6 protein of high-risk types of HPV binds to and stimulates p53 degradation, whereas E7 protein inactivates pRb. By inhibiting constituently expressed E6 and E7, p53 and pRb accumulates, inducing apoptosis, as seen in flow cytometry analysis and also the presence of highly activated caspase-3.

As with the previous results, ATO-FA-L2 is observed to be more efficient than ATO-L1 in both cell lines. Interestingly, in the double immunostained images, the pattern of the increased staining of both tumour suppressors was different for KB and HeLa. For KB, though fewer cells expressed the suppressor proteins, the staining in each cell was abundantly elevated; unlike in HeLa, where more cells stained for the protein, but the expression level remained lower than KB cells. One hypothesis explaining this observation might be that KB cells, despite having a higher FR expression, might have a more heterogeneous distribution of the receptor among its cell population, whereas HeLa might possess a more homogenous distribution of the receptor. Therefore, targeted liposomes would enter some KB cells in a much higher concentration than the remaining cells, whereas they would enter more uniformly in the HeLa cells. However, this hypothesis requires further investigation which remains outside the scope of this study.

After establishing the superiority of conjugated liposomes over non-conjugated liposomes in targeting HPV positive cells, it was essential to test their selectivity towards these cells as our main aim is to design drug carriers for ATO specifically targeting HPV positive cervical cancers. Towards this goal, HPV negative HT-3 cervical cancer cells were also exposed to targeted liposomes for 48 h and their apoptotic responses along with their expression levels of tumour suppressors were investigated and compared with HPV positive HeLa cervical cancer cells. Investigation into the rates of apoptosis via flow cytometry analysis revealed that targeted liposomes were selective in their action by inducing significantly higher apoptosis in HeLa cells compared to the HT-3 cells (Fig 3.4.9). This was reflected in the much lower expressed levels of activated caspase-3 in HT-3 cells following ATO-FA-L2 treatment than HeLa. Predictably, analysis of the tumour suppressors' expression levels also revealed that ATO-FA-L2 did not show much efficacy in enhancing their accumulation in HT-3 cells, unlike HeLa.

Ligand conjugated liposomal encapsulation of ATO alleviated the drug's off-target toxicity and increased their uptake in the targeted cells, as was observed in the previous chapter. However, to establish any superiority of liposomal ATO over the drug in its free form, it was crucial to investigate and compare their mode of action and finally, their selectivity towards cancers of HPV origin.

As the first step, the mode of action of ATO delivered free and in targeted liposomal form was compared to assess which delivery method is more effective, specifically for HPV positive cells. For that, KB and HeLa cells were exposed to both 5µM free drug and FA-conjugated liposomes encapsulating 5µM ATO for 48 h. Western blotting results showed that free ATO downregulated both the oncoproteins more than ATO-FA-L2 in KB cells (Fig 3.4.15). For HeLa cells however, the results were a bit different where though free ATO downregulated E6 protein more than ATO-FA-L2, there was no significant difference observed for the protein E7 with either treatment. Moreover, despite the apparent higher efficacy of free drug in reducing oncogene expression, the results further disclosed that the amount of tumour suppressor proteins upregulated was comparable for both the treatments in KB and HeLa cells. A possible explanation for the results can be that the oncogene downregulation and tumour suppressors' upregulation is not a strictly reciprocal phenomenon. E6 and E7 proteins, apart from inactivating p53 and pRb, have also been reported to cause immortalisation of cells though other pathways as well (Yim and Park, 2005).

Fluorescent immunostaining corroborated the Western blot findings by displaying a comparable increase in tumour suppressors' staining from either treatment (Fig 3.4.16). Additionally, the downregulation of E7 oncogene from free ATO treatment was more prominent in KB cells while being comparable for HeLa cells. Surprisingly though, confocal images deviated from the above findings by not showing any appreciable difference in the E6 staining in KB and HeLa cells following either treatment. To settle this disparity, Western blot results were given preference over confocal microscopy due to the former being a more robust, quantitative technique. The tumour suppressors' expression was also analysed via flow cytometry and the results validated the above findings (Fig 3.4.17).

Since specificity towards the targeted cells remains one of the most crucial requirements of an effective therapeutic agent, it was essential to assess the specificity of free drug for HPV positive cancer cells in the light of the knowledge that free ATO did prove to be more effective in downregulating oncogenes despite the tumour suppressors' accumulation being similar from both the treatments. Henceforth, HPV negative HT-3 cells were also assessed for apoptosis induction and protein expression analysis to

evaluate which of the treatments (free ATO or targeted liposomal ATO) was more specific in its action towards HPV positive cells.

Results clearly demonstrated that unlike targeted liposomal ATO, free drug was not selective in its action. Apoptosis assay via flow cytometry revealed that free ATO induced similarly high apoptosis in both HeLa and HT-3 cells unlike the targeted liposomal ATO, which specifically induced higher apoptotic population in HeLa cells (Fig 3.4.18). This result was further confirmed when the investigation into the activation of caspase-3 revealed that whereas free ATO did not distinguish between HeLa and HT-3 cells in activating caspase-3, resulting in similar high expression levels; ATO delivered in targeted liposomal form induced its activation significantly more in HeLa cells than HT-3. Moreover, in accordance with the apoptosis findings, the investigation into the tumour suppressors' expression re-instates the non-selective mode of action of free ATO, increasing the tumour suppressors in both HeLa and HT-3; unlike ATO-FA-L2 which is significantly much more effective for HeLa than HT-3.

3.4.5 **Conclusion**

ATO has been established as an effective anti-cancer drug which has the potential to induce apoptosis and inhibit proliferation of various human cancer cell lines. However, its lack of specificity and off-target toxicity has necessitated research into various delivery methods which could efficiently overcome the above mentioned barriers and target specific tumours. Herein, we have shown a promising strategy for targeting HPV infected cancer cells using FA conjugated liposomal ATO. This active targeting approach, in addition to alleviating ATO's toxicity, has higher selectivity for HPV cancers in inducing apoptosis, reducing HPV-E6 and E7 oncogenes and increasing the expression of tumour suppressor proteins' p53 and pRb. Further investigation of molecular mechanisms of ATO delivered liposomally, employing active targeting approach, on other HPV-attributable cancers is warranted.

Chapter 4

FINAL DISCUSSION AND CONCLUSION

4.1 DISCUSSION

Cervical cancer has been and continues to be a major worldwide health concern, mainly in developing countries (Soliman, Slomovitz and Wolf, 2004). In the past few decades, great advancements have been made in understanding the molecular basis of the disease and most importantly, HPV has been consistently identified as the causal agent in its development. The current treatment entailing invasive procedures of surgery and chemoradiotherapy with debilitating side effects has sparked an intensive research into therapies which can specifically target HPV (Downs, 2011). As HPV encodes for 8 genes, out of which E6 and E7 are the primary oncoproteins, any strategy that can control or inhibit these oncoproteins would be desirable for use as a therapeutic tool to manage HPV associated cancers, such as cervical cancer (Wen et al., 2012).

Among the potential anti-cancer drugs, previous work has demonstrated that ATO reduces the oncogene E6 expression and can be used as an effective agent to treat HPV-infected cervical cancer cells (Wen et al., 2012). ATO is a potent clinical agent for the treatment of acute promyelocytic leukemia and has demonstrated significant clinical success for other haematological malignancies (Wang and Chen, 2008; Zhu et al., 2002). Clinical response of solid tumours following ATO treatment has been compromised despite reported anti-cancer effects against a variety of solid tumour cell lines. This is due to a requirement of much higher dosages for the treatment, which are

often accompanied with severe side effects (Dilda and Hogg, 2007; Liu et al., 2006). The requirement for higher dosages might be owing to the low half-life of plasma arsenic, ~12 h after IV administration (Ni et al., 1997). The *in vitro* studies also indicated that ATO was selective in its action only when it was used in low concentrations (~2μM), inducing cellular apoptosis and increasing p53 expression in HPV positive cervical cancer cells (Wen et al., 2012). When the dosage was increased to 5μM however, most of the cells were killed from drug-induced toxicity, irrespective of HPV status (Wen et al., 2012).

Therefore, an effective delivery system was needed which could reduce ATO's off-target toxicity and expand its clinical utility by increasing its accumulation at tumour sites, extending its circulation time in blood and specifically targeting HPV infected cancer cells (Allen and Cullis, 2004). Encapsulating ATO in liposomes was one such strategy which had the potential to improve the drug's therapeutic index by reducing its side effects and increasing drug concentration in tumours through the EPR effect. In addition, if the liposomes were conjugated with targeting ligands, the encapsulated drug could be directed to the target sites with minimal disturbance to the surrounding cells and tissues (Allen and Cullis, 2004).

Therefore, our research team encapsulated ATO in liposomes and investigated their *in vitro* anti-cancer activity for HPV positive cervical cancer cells (Wang et al., 2016). Liposomal ATO was found to have the effect of reducing HPV E6 expression and inducing apoptosis in HeLa cell, while being less toxic to normal cells. These results gave us a good starting point to further design our liposomal construct to be a targeted, robust, pH responsive nano-carrier capable of selectively delivering ATO to HPV infected cervical cancer cells. We also explored the anti-cancer effects of the liposomally delivered ATO and the mode of action of the liposomal ATO in comparison to the free form ATO.

As the first step towards the design of such a drug carrying liposomal construct, we optimised the physical parameters of liposomes, mainly in terms of best size and charge, specifically tailored for our target cells. These factors play a crucial role in drug loading efficiency, liposomal stability and cellular uptake, and as their effect is dependent on cell types, we examined the effect of these factors for cervical cancer cells with varying

HPV status (Akhtar et al., 2018). Consequently, ATO encapsulating liposomes of different sizes (100 nm, 200 nm, and 400 nm) and different charges (neutral, positive, and negative) were synthesised and tested on HPV positive HeLa cells. All the liposomes were stable at 4°C for a month and were pH sensitive, allowing them to unload the drug cargo when pH was lowered to 6 or 5, as found in endosomes or lysosomes (Ira, Renate and Ari, 1986).

Among the differently charged liposomes, neutral liposomes were found to be the best formulation as they had the highest encapsulation efficiency whereas negative liposomes were found to be unstable at higher pH and positive liposomes displayed toxicity of their own when incubated with cells for more than 48 h. When size of liposomes was taken into consideration, 100nm liposomes were found to be the most stable at all the pH range tested and since smaller nanoparticles are more adept at evading MPS (Danhier, Feron and Preat, 2010), we chose 100nm liposomes among the different sizes. Consequently, 100 nm, neutral liposomes were finally chosen as the most optimal carrier for ATO delivery and were used for further *in vitro* studies (Akhtar et al., 2018).

The ATO encapsulating liposomes were investigated for their selectivity towards targeting HPV positive cells by incubating them with HeLa cells and this was compared with HPV negative HT-3 cells. Additionally, as one of the main aims of employing nanotechnology in pharmaceutics is to deliver the drug specifically to the cancer cells while sparing the normal cells, liposomal ATO was also assessed for its toxicity towards cells and intracellular uptake response profile in non-cancerous control cells. Two control cell lines were chosen for this study, namely human keratinocytes (HK) and human colon (CRL-1790) cells.

A ratio of cell death induced to the amount of arsenic taken up by the cells was calculated for all the cell lines as it is an effective means of comparing the efficacy of a treatment on different cell populations- cancerous cells and normal control cells. For an ideal treatment, the cell death–uptake ratio would be low for normal cells and high for the target cancer cell population. Our results indicated that this ratio was indeed lowest for the control cell populations and highest for HeLa cells. Moreover, liposomal ATO was 71 times more toxic to HeLa cells than HT-3 cells per unit of intracellular arsenic.

In contrast, free ATO was more efficient in inducing a toxic response in HT-3 cells per unit arsenic, demonstrating the selective nature of liposomal ATO for HPV positive HeLa cells. This selectivity might be attributed to a possibility that when liposomal-encapsulated ATO reaches the cells, it results in bio-physical changes in the cell membrane, in turn affecting the cellular transport systems. As different types of cells may react to these changes in different ways, HeLa cells appear to be more vulnerable to this drug treatment, which could be relevant to HPV. These results were evidence of the potential of liposomal-encapsulated ATO as a promising strategy for treating HPV-positive cervical cancers (Akhtar et al., 2018).

In the tumour microenvironment, these long-circulating PEGylated nanocarriers can take advantage of the EPR effect in accumulating within the tumour interstitium (Danhier, Feron and Preat, 2010). But unless there is a specific affinity between the nanoparticles and the target cancer cells, the chemotherapeutic payload would either have to reach its target on its own or endanger itself diffusing back to the vasculature (Dreher et al., 2006). This affinity could be achieved by active targeting strategies with ligands decorated on the surface of the nanoparticles capable of binding to the receptors overexpressed in diseased cells (Kamaly et al., 2012).

Hence, after optimising the physical parameters of the liposomes, the next step was to find the most appropriate ligand which could be conjugated to these optimised ATO liposomes, and this entire system could act as “homing device” to actively target HPV positive cervical cancer cells. Towards that aim, both HPV positive HeLa and HPV negative HT-3 cells were screened for the three most widely employed surface markers, i.e. folate receptor, transferrin receptor and epidermal growth factor receptor. The ideal surface marker would be the one that was most differentially expressed between the two cell lines, for instance, overexpressed in HeLa cells while minimally expressed in HT-3 cells.

Out of the three surface markers investigated, folate receptor was the most differentially expressed receptor by being highly expressed in HeLa and negligibly expressed in HT-3 cells. Both the cell lines expressed transferrin receptors and EGFR, but the difference in their expression between the two cell lines was not as distinct as the folate receptor expression. Consequently, folic acid was the ligand of choice for our attempt in

designing targeted ATO liposomes for HPV positive cells. Folic acid, as a ligand, also offered other advantages, such as small size, low immunogenicity and ease of conjugation to the liposomal surface (Low and Antony, 2004; Dancey, 2001). Further validation for using folic acid as the ligand of choice was carried out by including two control cells lines, KB as positive control (FR+) and A549 as negative control (FR-) (Chen et al., 2009; Nukolova et al., 2011). The results indicated that folate receptor expression was very high for KB cells and negligible for the negative control, A549, validating the accuracy of the experiments.

Reiteratively, in order to design folate targeted, ATO encapsulating liposomes specifically tailored for our target cells, there were few parameters that needed careful consideration and optimisation. First, folic acid had to be tethered to the PEG terminus instead of being attached to the phospholipid headgroup, to avoid masking of the ligand's binding affinity to the target antigens by the surrounding PEG brush layer (Klabinov et al., 1991). Second, the presence of an unconjugated PEG brush layer was essential to prevent aggregation of the nanoparticles as was seen in the study. Ligand density on the surface of the liposomes also needed to be optimised as high ligand density could increase cellular internalisation but on the other hand, also make the nanoparticles more prone for aggregation *in vitro* and for recognition by MPS *in vivo* (Kamaly et al., 2012). After several trial and errors, employing 1.9 mol % of brush layer forming PEG and 0.1mol% of ligand conjugating PEG was found to give stable FA-conjugated ATO encapsulating liposomes. Therefore, this formulation of FA-conjugated liposomal ATO was used for the subsequent studies.

Another parameter that needed optimising was the ligand conjugating PEG spacer length. Since some studies indicated that employing ligand conjugating PEG spacers of the same length as the surrounding PEG brush layer might result in the masking of the targeting abilities of the ligand, our first investigation was to assess this aspect (Lee and Low, 1994). For that purpose, we synthesised targeted liposomes having the ligand conjugating PEG spacer and surrounding PEG brush layer of equal length, i.e. 2000Da. We then evaluated the differences in cellular uptake with increasing incubation times from four different techniques: confocal microscopy, flow cytometry, fluorescence reading via plate reader and cellular arsenic quantification via ICP-MS.

The results from the all the techniques were consistent and indicated that FA-conjugated liposomes were efficiently and selectively taken up by the cells according to the status of FR expression on their cell surface. As folate receptor expression follows the order of KB>HeLa>> HT-3>A549 in cell lines, the cellular uptake of targeted liposomes also displayed the same pattern. As the time of incubation increased, the cellular internalisation of targeted liposomes in FR+ KB and HeLa cells also increased. Accordingly, the difference between the cellular uptake of targeted and non-targeted liposomes was maximum in KB and none for FR- A549 cells. It was also observed that this difference between the cellular uptakes of conjugated and non-conjugated liposomes decreased with prolonging the exposure time, which might be due to two contributing factors: an increase in non-specific uptake of unconjugated liposomes and subsequent decrease in the uptake of conjugated liposomes due to a possible saturation of the targeted receptors on the cell surface. Indeed, quantifying cellular arsenic via ICP-MS gave results that after an initial high surge of targeted liposomal arsenic intake by FR+ cells, the rate at which it was taken up almost invariably slowed down in comparison with non-targeted liposomes. This led to a bridging of the gap between their uptakes in cells.

These findings established that folic acid conjugation to liposomes, even to a PEG spacer of similar length as the surrounding PEG brush, was able to effectively target the FR+ cells with improved efficiency and selectivity in comparison to the untargeted liposomal ATO. However, to be positive that the surrounding PEG layer was not masking conjugation abilities of the ligand, even to a small extent, we decided to conjugate folic acid to a PEG spacer of longer length and observe any further enhancement in ATO cellular uptake from FR+ cell lines. Since the previous studies had employed 3350Da for the PEG spacer length (Chen et al., 2009), we decided to use even longer PEG spacer length of 5000Da for making targeted liposomes and investigate a possible increase in cellular uptake along with any inherent toxicity that might arise from employing longer PEG spacers for ligand conjugation.

Targeted liposomes were prepared with folic acid conjugated to PEG spacer of 5000Da length. The results on improving cellular uptake were obvious. Longer PEG spacer for FA conjugation made liposomes much more efficient in being taken up by the FR+ cells than liposomes with FA-PEG spacer of equal length to the surrounding PEG brush. This

enhancement was not evident for HT-3 and A549 cells due to the weak/ absent expression of FR by those cells. The superior performance of targeted ATO liposomes with 5000Da FA-PEG spacer thus made them a logical choice as the delivery vehicle of ATO. Moreover, results also showed that the presence of the longer FA-PEG spacer did not increase the liposomal construct's inherent toxicity for any of the cell lines tested. Consequently, targeted liposomes with FA-PEG5000 PEG spacer was chosen as the optimised design for the targeted ATO nano-carrier as they had low inherent cytotoxicity along with their superior targeting abilities.

In order to assess the performance of targeted liposomal ATO over free form ATO as a treatment for HPV positive cells, once again we calculated the abovementioned ratio of cell death induced to the amount of arsenic taken up by the cells following the 48 h treatment. The results indicated that this cell death-uptake ratio was higher from liposomal ATO treatment for both HPV positive KB and HeLa cells than from free ATO treatment, whilst the ratio was lower for HPV negative HT-3 cells. This indicated that liposomal ATO was more effective in inducing cell death to KB and HeLa cells per unit arsenic taken up while free ATO was more effective for HT-3 cells. Moreover, the ratio was highest for HeLa cells indicating the superior efficacy of the liposomal ATO treatment for this cell line. As a final part of this study, the mode of action of ATO when delivered in its free form or encapsulated in non-conjugated and conjugated liposomes was investigated and compared between each other and the best delivery method was identified to target and treat HPV positive cervical cancer cells *in vitro*.

As mentioned earlier, the key proteins responsible for oncogenecity of HPV are E6 and E7 proteins which operate by inactivating two crucial negative regulatory molecules p53 and pRb respectively (Barbosa and Schlegel, 1989). Therefore, to investigate the mode of action of ATO delivered via the three disparate routes, emphasis was given to study the changes in expression levels of oncoproteins E6 and E7 and tumour suppressor proteins' p53 and pRb following the treatment. Since the oncoproteins inhibit cellular apoptosis, the treated cells were also investigated for apoptosis induction and the expression levels of apoptotic protein, active caspase-3. The techniques employed were Western blotting, flow cytometry and confocal microscopy for protein expression analysis and flow cytometry for apoptosis induction studies.

The results from mechanism studies clearly showed that targeted liposomes were far more superior to non-targeted liposomes in inducing apoptosis response in HPV positive KB and HeLa cells. They resulted in a significantly higher activation of caspase-3, a crucial requirement for many typical hallmarks of apoptosis (Porter and Janicke, 1999). Additionally, they were more efficient in downregulating oncoproteins and upregulating tumour suppressors than non-targeted liposomes in both cells. This could be caused from a significantly higher uptake of conjugated liposomes in FR + HPV infected cells.

An interesting observation was that among the two HPV positive cell lines KB and HeLa, the non-targeted liposomes were significantly more efficient in inducing apoptosis and downregulating E6 and E7 in HeLa cells than KB cells. This result again pointed to a certain susceptibility of HeLa cells towards ATO delivered in liposomal form, which was previously noted while comparing its toxicity vs uptake ratio with HT-3 cells (Akhtar et al., 2018). Moreover, even the downregulation of E6 and E7 oncoproteins following targeted liposomal treatment was surprisingly more in HeLa cells than KB, despite KB having higher FR expression and consequently higher cellular uptake of targeted liposomal ATO. All these results suggest a possibility of HeLa cells possessing higher sensitivity for liposomal encapsulated ATO treatment, an aspect that warrants further investigation.

Immuno-double staining of treated cells for E6-p53 and E7-pRb revealed an expected reciprocal relationship between the oncoprotein and the tumour suppressor it inhibits. When the liposomal treatment reduced the oncoprotein, a corresponding increase in the tumour suppressor that the oncoprotein associates with and inactivates, is demonstrated. These finding were consistent with the expected consequence of inhibition of HPV oncoproteins' E6 and E7, which would lead to accumulation of p53 and pRb, induction of apoptosis and activation of the most common death protease, caspase-3.

After establishing the superiority of targeted liposomes over non-targeted liposomes, the next step was to compare the anti-cancer activity of targeted liposomal ATO with free ATO for HPV positive cells. Results indicated that free ATO was more efficient in downregulating E6 and E7 in KB cells than targeted liposomes. Free ATO also demonstrated higher efficacy than targeted liposomes in downregulating E6 in HeLa

cells, but the expression of E7 was comparable from both the treatments. Surprisingly, for both KB and HeLa, the upregulation of tumour suppressors was comparable from either treatment.

Acknowledging that ATO delivered in its free form appeared to downregulate oncogenes more than the targeted liposomes, even though the tumour suppressors were comparably upregulated from either treatment, it was important to further investigate which of the two delivery methods was more selective for HPV positive cells. This aspect was important as selectivity towards the target cells remain one of the most crucial requirements of an effective therapeutic agent. Towards this goal, HPV negative HT-3 cervical cancer cells were also exposed to targeted liposomes and free ATO for 48 h and the apoptotic responses along with the expression levels of tumour suppressors were investigated and compared with HPV positive HeLa cervical cancer cells.

Results clearly indicated that while targeted liposomal ATO was selective in its action, free ATO was not. Targeted liposomes induced significantly higher apoptosis in HeLa than HT-3. The upregulation of tumour suppressors and activation of caspase-3 were also more pronounced in HeLa than HT-3 following targeted liposomal treatment. In contrast, free ATO induced similarly high apoptosis in both the cells. Moreover, the investigation into the tumour suppressors' expression and activation of caspase-3 reinstated the non-selective nature of free ATO as it induced similar levels in both the cell lines irrespective of HPV status. These findings emphasized the advantages of targeted liposomes over other delivery methods (including free form or in non-conjugated liposomes) as a therapeutic system for HPV positive cancers, including cervical cancer.

4.2 FUTURE WORK

The high biocompatibility and versatile nature of liposomes have made these nanoparticles an excellent choice for transporting drugs specifically to target cancer cells. In the current research, we have shown a promising strategy for targeting ATO to HPV positive cervical cancer cells using folate-tethered drug encapsulating liposomes. These targeted liposomes were more efficient than non-targeted liposomes and more selective than free ATO in their action towards the target HPV positive cervical cancer cells, which establish them as the best delivery method of ATO to our target cells. This was also supported by the calculated cell death to uptake ratio as a comparative measure of the efficacy of a treatment for different cell populations, where FA-conjugated liposomal ATO induced higher toxicity in HPV positive HeLa and KB cells per unit arsenic taken up than free ATO.

Investigations on the mechanism of actions of both liposomal delivered ATO and ATO in free form, however, demonstrated that free ATO downregulated oncogenes more efficiently than the targeted liposomes, even though the upregulation of tumour suppressors and apoptosis induction was comparable from either treatment. This brings us to a conclusion that the higher anti-cancer activity of ATO delivered through targeted liposomes maybe attributed to the activation of different or additional pathways. Some factors which warrant further investigations include mitochondrial toxicity, reactive oxygen species generation and accumulation, inhibition of transcription of hTERT gene (Chen et al., 2015). These investigations could provide an important basis for future attempts to co-encapsulate synergistic agents or alter liposomal composition in further improving the therapeutic potential of ATO. This could be important at understanding how we can design/synthesize better therapeutic vaccines for HPV infections and their associated cancers as most currently available HPV vaccines are for prevention purposes rather than therapeutics (Chabeda et al., 2018).

Results from the current *in vitro* study is promising with targeted liposomal ATO as a potential therapy for cervical cancer, as the first stage in evaluating the therapeutic potential of a drug or drug delivery platform in cancer therapy is to test it on human cancer cell lines. *In vitro* studies, as demonstrated above, can be very useful in assessing

features such as nanoparticle uptake, subcellular localization, intracellular drug delivery and cytotoxic killing among others. In this study, human cancer cell lines such as HPV positive HeLa and HPV negative HT-3 served as the fundamental model in a monolayer culture *in vitro*. To substantiate this study further, it will be essential to include other cervical cancer cell lines, including HPV-16 SiHa and CaSki, HPV-18 ME-180 and HPV negative C33-A cells (Ordikhani et al., 2016).

Acknowledging the fact that as tumour models, these two dimensional (2D) cell cultures have limited efficacy, the three dimensional (3D) *in vitro* models could be employed as they have been reported to indicate higher malignancy, invasiveness and drug resistance, characteristic of the *in vivo* tumour environment than cell cultures (Ordikhani et al., 2016). *In vivo* testing on xenograft models in athymic nude or severe combined immunodeficient mice and orthotopically implanted tumours with relevant microenvironments may further be employed to investigate crucial information about absorption, metabolism, distribution, toxicity, efficacy and excretion of nanoparticles in rodent models as appropriate (Zamboni et al., 2012). Once the formulation proves efficacious for experimental models, it then has to go through clinical trials to eventually acquire FDA approval (Zamboni et al., 2012).

4.3 CONCLUSION

In conclusion, we have shown a promising strategy for targeting ATO to HPV positive cervical cancer cells using folate-tethered liposomes *in vitro*. In the initial step, liposomes were loaded with ATO and optimised in terms of best size and charge for the target cells. 100nm, neutral liposomes were observed to be the best formulation as they showed highest ATO encapsulation, maximum stability and least intrinsic toxicity. In the following *in vitro* studies, they displayed higher anti-cancer activity towards HeLa cells than either non-HPV cervical cancer cells or non-cancerous normal cells. The therapeutic efficacy of liposomes towards HPV positive cells was further enhanced by conjugating folic acid to the liposomes as the cells were found to overexpress folate receptor on their cellular surface. The resulting folate liposomal drug showed higher anti-cancer activity against HPV positive cancer cells and was more selective than free ATO by inducing higher apoptosis, downregulating oncogenes and upregulating tumour suppressors in HPV positive HeLa cells than other cell lines. Future preclinical studies will elucidate the role of EPR passive targeting and folate-directed active targeting *in vivo*. Our results provide a rationale for ATO therapy in further animal studies through the folate-targeted liposomal delivery system. This targeting system can be extended to treatments of other HPV associated cancers, including urogenital cancer, upper respiratory tract cancers and other epithelial cancers associating with HPV infections in order to further improve the therapeutic profile of the drug.

Bibliography

Apoptosis. Flow cytometry. Available at: http://www.flow-cytometry.us/index.php?page=apoptosis (Accessed: 16 August 2018.

Direct vs indirect immunofluorescence: Abcam. Available at: https://www.abcam.com/secondary-antibodies/direct-vs-indirect-immunofluorescence (Accessed: 17 August 2018).

Flow cytometery. Mybiosource.com. Available at: https://www.mybiosource.com/learn/testing-procedures/flow-cytometery/ (Accessed: 16 August 2018.

ICP-MS: Radboud University. Available at: https://www.ru.nl/science/gi/facilities-activities/elemental-analysis/icp-ms/ (Accessed: 17 May 2018).

Immunohistochemical Staining Methods. 2013: Dako Denmark A/S, An Agilent Technologies Company. Available at: https://www.agilent.com/cs/library/technicaloverviews/public/08002_ihc_staining_methods.pdf (Accessed: 17 August 2018).

Immunohistochemistry: The Human Protein Atlas. Available at: https://www.proteinatlas.org/learn/method/immunohistochemistry#refs (Accessed: 17 August 2018).

Molecular Weight Determination of Protein Extracts - Background. Available at: https://www.chem.fsu.edu/chemlab/bch4053l/Protein%20Characterization/MW%20Determination/background.html (Accessed: 17 August 2018).

Western Blot Illustrated Assay: Novus Biologicals. Available at: https://www.novusbio.com/support/support-by-application/Western-blot/illustrated-assay.html (Accessed: 17 August 2018).

Principle of ICP Optical Emission Spectrometry (ICP-OES) (2018): Hitachi High-Technologies GLOBAL. Available at: https://www.hitachi-hightech.com/global/products/science/tech/ana/icp/descriptions/icp-oes.html.

Adan, A., Alizada, G., Kiraz, Y., Baran, Y. and Nalbant, A. (2017) 'Flow cytometry: basic principles and applications', *Critical reviews in biotechnology,* 37(2), pp. 163-176.

Aggarwal, P. (2014) 'Cervical cancer: can it be prevented?' *World journal of clinical oncology,* 5(4), pp. 775.

Ahn, R. W., Chen, F., Chen, H., Stern, S. T., Clogston, J. D., Patri, A. K., Raja, M. R., Swindell, E. P., Parimi, V. and Cryns, V. L. (2010) 'A novel nanoparticulate formulation of arsenic trioxide with enhanced therapeutic efficacy in a murine model of breast cancer', *Clinical cancer research*, pp. 1078-0432. CCR-10-0068.

Akhtar, A., Wang, S. X., Ghali, L., Bell, C. and Wen, X. (2017) 'Recent advances in arsenic trioxide encapsulated nanoparticles as drug delivery agents to solid cancers', *Journal of biomedical research*, 31(3), pp. 177.

Akhtar, A., Wang, S. X., Ghali, L., Bell, C. and Wen, X. (2018) 'Effective Delivery of Arsenic Trioxide to HPV-Positive Cervical Cancer Cells Using Optimised Liposomes: A Size and Charge Study', *International journal of molecular sciences,* 19(4), pp. 1081.

Allen, T. M., Agrawal, A. K., Ahmad, I., Hansen, C. B. and Zalipsky, S. (1994) 'Antibody-mediated targeting of long-circulating (StealthR) liposomes', *Journal of Liposome Research*, 4(1), pp. 1-25.

Allen, T. M., Brandeis, E., Hansen, C. B., Kao, G. Y. and Zalipsky, S. (1995) 'A new strategy for attachment of antibodies to sterically stabilized liposomes resulting in efficient targeting to cancer cells', *Biochimica et Biophysica Acta (BBA)-Biomembranes*, 1237(2), pp. 99-108.

Allen, T. M. and Chonn, A. (1987) 'Large unilamellar liposomes with low uptake into the reticuloendothelial system', *FEBS letters*, 223(1), pp. 42-46.

Allen, T. M. and Cullis, P. R. (2004) 'Drug delivery systems: entering the mainstream', *Science*, 303(5665), pp. 1818-1822.

Allen, T. M. and Cullis, P. R. (2013) 'Liposomal drug delivery systems: from concept to clinical applications', *Advanced drug delivery reviews*, 65(1), pp. 36-48.

Allen, T. M., Hansen, C. B. and de Menezes, D. E. L. (1995) 'Pharmacokinetics of long-circulating liposomes', *Advanced Drug Delivery Reviews*, 16(2-3), pp. 267-284.

Ãlvarez-Barrientos, A., Arroyo, J., Canton, R., Nombela, C. and Sanchez-Perez, M. (2000) 'Applications of Flow Cytometry to Clinical Microbiology', *Clinical Microbiology Reviews*, 13(2), pp. 167-195.

Androphy, E. J., Hubbert, N. L., Schiller, J. T. and Lowy, D. R. (1987) 'Identification of the HPV-16 E6 protein from transformed mouse cells and human cervical carcinoma cell lines', *The EMBO journal*, 6(4), pp. 989-992.

Antinore, M. J., Birrer, M. J., Patel, D., Nader, L. and McCance, D. J. (1996) 'The human papillomavirus type 16 E7 gene product interacts with and trans-activates the AP1 family of transcription factors', *The EMBO journal*, 15(8), pp. 1950-1960.

Antman, K. H. (2001) 'Introduction: the history of arsenic trioxide in cancer therapy', *The oncologist*, 6(Supplement 2), pp. 1-2.

Appleby, P., Beral, V., Berrington de Gonzalez, A., Colin, D., Franceschi, S., Goodhill, A., Green, J., Peto, J., Plummer, M. and Sweetland, S. (2007) 'International Collaboration of Epidemiological Studies of Cervical, Cancer. Cervical cancer and hormonal contraceptives: Collaborative reanalysis of individual data for 16,573 women with cervical cancer and 35,509 women without cervical cancer from 24 epidemiological studies', *Lancet*, 370(9599), pp. 1609-1621.

Arbyn, M., Castellsague, X., de Sanjose, S., Bruni, L., Saraiya, M., Bray, F. and Ferlay, J. (2011) 'Worldwide burden of cervical cancer in 2008', *Annals of oncology*, 22(12), pp. 2675-2686.

Arends, M. J., Morris, R. G. and Wyllie, A. H. (1990) 'Apoptosis. The role of the endonuclease', *The American Journal of Pathology*, 136(3), pp. 593-608.

Aronson, S. M. (1994) 'Arsenic and old myths', *Rhode Island medicine*, 77(7), pp. 233-234.

Bangham, A. D., Standish, M. M. and Watkins, J. C. (1965) 'Diffusion of univalent ions across the lamellae of swollen phospholipids', *Journal of molecular biology*, 13(1), pp. 238-IN27.

Barbosa, M. S. and Schlegel, R. (1989) 'The E6 and E7 genes of HPV-18 are sufficient for inducing two-stage in vitro transformation of human keratinocytes', *Oncogene*, 4(12), pp. 1529-1532.

Barnett, A. A., Haller, J. C., Cairnduff, F., Lane, G., Brown, S. B. and Roberts, D. J. H. (2003) 'A randomised, double-blind, placebo-controlled trial of photodynamic therapy using 5-aminolaevulinic acid for the treatment of cervical intraepithelial neoplasia', *International journal of cancer*, 103(6), pp. 829-832.

Bartlett, D. W., Su, H., Hildebrandt, I. J., Weber, W. A. and Davis, M. E. (2007) 'Impact of tumor-specific targeting on the biodistribution and efficacy of siRNA nanoparticles measured by

multimodality in vivo imaging', *Proceedings of the National Academy of Sciences*, 104(39), pp. 15549-15554.

Bazak, R., Houri, M., El Achy, S., Kamel, S. and Refaat, T. (2015) 'Cancer active targeting by nanoparticles: a comprehensive review of literature', *Journal of cancer research and clinical oncology*, 141(5), pp. 769-784.

Bellamy, C. O. C. (1997) 'p53 and apoptosis', *British medical bulletin*, 53(3), pp. 522-538.

Bellocq, N. C., Pun, S. H., Jensen, G. S. and Davis, M. E. (2003) 'Transferrin-containing, cyclodextrin polymer-based particles for tumor-targeted gene delivery', *Bioconjugate chemistry*, 14(6), pp. 1122-1132.

Berger, N., Sachse, A., Bender, J., Schubert, R. and Brandl, M. (2001) 'Filter extrusion of liposomes using different devices: comparison of liposome size, encapsulation efficiency, and process characteristics', *International journal of pharmaceutics*, 223(1-2), pp. 55-68.

Berman, S. D., Yuan, T. L., Miller, E. S., Lee, E. Y., Caron, A. and Lees, J. A. (2008) 'The retinoblastoma protein tumor suppressor is important for appropriate osteoblast differentiation and bone development', *Molecular Cancer Research*, 6(9), pp. 1440-1451.

Bertrand, N., Wu, J., Xu, X., Kamaly, N. and Farokhzad, O. C. (2014) 'Cancer nanotechnology: the impact of passive and active targeting in the era of modern cancer biology', *Advanced drug delivery reviews*, 66, pp. 2-25.

Bhandari, B. (2017) *Western Blot Technique: Principle, Procedures and Uses*: Microbe Online. Available at: https://microbeonline.com/Western-blot-technique-principle-procedures-advantages-and-disadvantages/ (Accessed: 17 August 2018).

Bhattacharjee, S. (2016) 'DLS and zeta potential- What they are and what they are not?' *Journal of Controlled Release*, 235, pp. 337-351.

Bornstein, J., Sagi, S., Haj, A., Harroch, J. and Fares, F. (2005) 'Arsenic Trioxide inhibits the growth of human ovarian carcinoma cell line', *Gynecologic oncology*, 99(3), pp. 726-729.

Bosch, F. X., Lorincz, A., MuÃ±oz, N., Meijer, C. and Shah, K. V. (2002) 'The causal relation between human papillomavirus and cervical cancer', *Journal of clinical pathology*, 55(4), pp. 244-265.

Bosch, F. X., Rohan, T., Schneider, A., Frazer, I., Pfister, H., Castellsague, X., de Sanjose, S., Moreno, V., Puig-Tintore, L. M., Smith, P. G., Munoz, N. and zur Hausen, H. (2001) 'Papillomavirus research update: highlights of the Barcelona HPV 2000 international papillomavirus conference', *Journal of Clinical Pathology*, 54(3), pp. 163-175.

Bose, A. (2016) 'Physicochemical characterization of nanoparticles'. Available at: http://www.pharmainfo.net/book/emerging-trends-nanotechnology-pharmacy/3physicochemical-characterization-nanoparticles (Accessed 2018 16th August).

Bulbake, U., Doppalapudi, S., Kommineni, N. and Khan, W. (2017) 'Liposomal formulations in clinical use: an updated review', *Pharmaceutics*, 9(2), pp. 12.

Byrne, J. D., Betancourt, T. and Brannon-Peppas, L. (2008) 'Active targeting schemes for nanoparticle systems in cancer therapeutics', *Advanced drug delivery reviews*, 60(15), pp. 1615-1626.

Cadron, I., Van Gorp, T., Amant, F., Leunen, K., Neven, P. and Vergote, I. (2007) 'Chemotherapy for recurrent cervical cancer', *Gynecologic oncology*, 107(1), pp. S113-S118.

Canal, F., Vicent, M. J., Pasut, G. and Schiavon, O. (2010) 'Relevance of folic acid/polymer ratio in targeted PEG-“epirubicin conjugates', *Journal of Controlled Release*, 146(3), pp. 388-399.

Carter, P. (2001) 'Improving the efficacy of antibody-based cancer therapies', *Nature Reviews Cancer*, 1(2), pp. 118.

Casagrande, N., De Paoli, M., Celegato, M., Borghese, C., Mongiat, M., Colombatti, A. and Aldinucci, D. (2013) 'Preclinical evaluation of a new liposomal formulation of cisplatin, lipoplatin, to treat cisplatin-resistant cervical cancer', *Gynecologic oncology*, 131(3), pp. 744-752.

Chabeda, A., Yanez, R. J. R., Lamprecht, R., Meyers, A. E., Rybicki, E. P. and Hitzeroth, I. I. (2018) 'Therapeutic vaccines for high-risk HPV-associated diseases', *Papillomavirus Research*, 5, pp. 46-58.

Chang, H.-I. and Yeh, M.-K. (2012) 'Clinical development of liposome-based drugs: formulation, characterization, and therapeutic efficacy', *International journal of nanomedicine*, 7, pp. 49.

Charles, B. and Fredeen, K. J. (1997) 'Concepts, instrumentation and techniques in inductively coupled plasma optical emission spectrometry', *Perkin Elmer Corporation*.

Chen, B., Liu, Q., Popowich, A., Shen, S., Yan, X., Zhang, Q., Li, X.-F., Weinfeld, M., Cullen, W. R. and Le, X. C. (2015) 'Therapeutic and analytical applications of arsenic binding to proteins', *Metallomics*, 7(1), pp. 39-55.

Chen, G.-Q., Shi, X.-G., Tang, W., Xiong, S.-M., Zhu, J., Cai, X., Han, Z.-G., Ni, J.-H., Shi, G.-Y. and Jia, P.-M. (1997) 'Use of arsenic trioxide (As2O3) in the treatment of acute promyelocytic leukemia (APL): I. As2O3 exerts dose-dependent dual effects on APL cells', *Blood*, 89(9), pp. 3345-3353.

Chen, H., MacDonald, R. C., Li, S., Krett, N. L., Rosen, S. T. and O'Halloran, T. V. (2006) 'Lipid encapsulation of arsenic trioxide attenuates cytotoxicity and allows for controlled anticancer drug release', *Journal of the American Chemical Society*, 128(41), pp. 13348-13349.

Chen, H., Pazicni, S., Krett, N. L., Ahn, R. W., Pennerâ€ • Hahn, J. E., Rosen, S. T. and O'Halloran, T. V. (2009) 'Coencapsulation of Arsenic- • and Platinum- • based Drugs for Targeted Cancer Treatment', *Angewandte Chemie International Edition*, 48(49), pp. 9295-9299.

Cheng, Z., Al Zaki, A., Hui, J. Z., Muzykantov, V. R. and Tsourkas, A. (2012) 'Multifunctional nanoparticles: cost versus benefit of adding targeting and imaging capabilities', *Science*, 338(6109), pp. 903-910.

Chou, W.-C., Hawkins, A. L., Barrett, J. F., Griffin, C. A. and Dang, C. V. (2001) 'Arsenic inhibition of telomerase transcription leads to genetic instability', *The Journal of clinical investigation*, 108(10), pp. 1541-1547.

Chu, B. (2008) 'Dynamic light scattering', *Soft matter characterization*: Springer, pp. 335-372.

Coleman, D. L., Gregonis, D. E. and Andrade, J. D. (1982) 'Blood-materials interactions: the minimum interfacial free energy and the optimum polar/apolar ratio hypotheses', *Journal of biomedical materials research*, 16(4), pp. 381-398.

Contributors, W. (2018) *Zeta potential*: Wikipedia, The Free Encyclopedia. Available at: https://en.wikipedia.org/w/index.php?title=Zeta_potential&oldid=841536979.

Cram, L. S. (2003) *Flow cytometry, an overview. Advanced Flow Cytometry: Applications in Biological Research*: Springer, Dordrecht.

Cullen, A. P., Reid, R., Campion, M. and Lorincz, A. T. (1991) 'Analysis of the physical state of different human papillomavirus DNAs in intraepithelial and invasive cervical neoplasm', *Journal of virology*, 65(2), pp. 606-612.

Dan, N. (2002) 'Effect of liposome charge and PEG polymer layer thickness on cell- liposome electrostatic interactions', *Biochimica et Biophysica Acta (BBA)-Biomembranes*, 1564(2), pp. 343-348.

Dancey, J. E. and Schoenfeldt, M. (2001) 'Clinical trials referral resource. Epidermal growth factor receptor inhibitors in clinical trials', *Oncology (Williston Park, NY)*, 15(6), pp. 748.

Danhier, F., Feron, O. and Preat, V. (2010) 'To exploit the tumor microenvironment: passive and active tumor targeting of nanocarriers for anti-cancer drug delivery', *Journal of controlled release*, 148(2), pp. 135-146.

Daniels, T. R., Bernabeu, E., Rodriguez, J., Patel, S., Kozman, M., Chiappetta, D. A., Holler, E., Ljubimova, J. Y., Helguera, G. and Penichet, M. L. (2012) 'The transferrin receptor and the targeted delivery of therapeutic agents against cancer', *Biochimica et Biophysica Acta (BBA)-General Subjects*, 1820(3), pp. 291-317.

Daniels, T. R., Delgado, T., Rodriguez, J. A., Helguera, G. and Penichet, M. L. (2006) 'The transferrin receptor part I: Biology and targeting with cytotoxic antibodies for the treatment of cancer', *Clinical immunology*, 121(2), pp. 144-158.

de Meyer, F. d. r. and Smit, B. (2009) 'Effect of cholesterol on the structure of a phospholipid bilayer', *Proceedings of the National Academy of Sciences*, 106(10), pp. 3654-3658.

Dilda, P. J. and Hogg, P. J. (2007) 'Arsenical-based cancer drugs', *Cancer treatment reviews*, 33(6), pp. 542-564.

Doorbar, J. (2005) 'The papillomavirus life cycle', *Journal of clinical virology*, 32, pp. 7-15.

Doorbar, J. (2007) 'Papillomavirus life cycle organization and biomarker selection', *Disease markers*, 23(4), pp. 297-313.

Doorbar, J., Quint, W., Banks, L., Bravo, I. G., Stoler, M., Broker, T. R. and Stanley, M. A. (2012) 'The biology and life-cycle of human papillomaviruses', *Vaccine*, 30, pp. F55-F70.

Downs Jr, L. S., Chura, J. C., Argenta, P. A., Judson, P. L., Ghebre, R., Geller, M. A. and Carson, L. F. (2011) 'Ifosfamide, paclitaxel, and carboplatin, a novel triplet regimen for advanced, recurrent, or persistent carcinoma of the cervix: a phase II trial', *Gynecologic oncology*, 120(2), pp. 265-269.

Downs, L. (2011) 'Advances in cervical cancer treatment', *Gynecologic oncology*, 121(3), pp. 431-433.

Dreher, M. R., Liu, W., Michelich, C. R., Dewhirst, M. W., Yuan, F. and Chilkoti, A. (2006) 'Tumor vascular permeability, accumulation, and penetration of macromolecular drug carriers', *Journal of the National Cancer Institute*, 98(5), pp. 335-344.

Dubowchik, G. M. and Walker, M. A. (1999) 'Receptor-mediated and enzyme-dependent targeting of cytotoxic anticancer drugs', *Pharmacology & therapeutics*, 83(2), pp. 67-123.

Ducat, E., Evrard, B., Peulen, O. and Piel, G. (2011) 'Cellular uptake of liposomes monitored by confocal microscopy and flow cytometry', *Journal of drug delivery science and technology*, 21(6), pp. 469-477.

Dumitriu, S. (2001) *Polymeric biomaterials, revised and expanded*. Crc Press.

Duncan, K. J., Eckert, K. A. and Clawson, G. A. (2009) 'Mechanisms of growth inhibition in human papillomavirus positive and negative cervical cancer cells by the chloromethyl ketone protease inhibitor, succinyl-alanine-alanine-proline-phenylalanine chloromethyl ketone', *Journal of Pharmacology and Experimental Therapeutics*, 330(1), pp. 359-366.

Dyson, N. (1998) 'The regulation of E2F by pRB-family proteins', *Genes & development*, 12(15), pp. 2245-2262.

Elias, D. R., Poloukhtine, A., Popik, V. and Tsourkas, A. (2013) 'Effect of ligand density, receptor density, and nanoparticle size on cell targeting', *Nanomedicine: nanotechnology, biology and medicine*, 9(2), pp. 194-201.

Emadi, A. and Gore, S. D. (2010) 'Arsenic trioxide - an old drug rediscovered', *Blood reviews*, 24(4-5), pp. 191-199.

Evens, A. M., Tallman, M. S. and Gartenhaus, R. B. (2004) 'The potential of arsenic trioxide in the treatment of malignant disease: past, present, and future', *Leukemia research*, 28(9), pp. 891-900.

Farokhzad, O. C. and Langer, R. (2009) 'Impact of nanotechnology on drug delivery', *ACS nano*, 3(1), pp. 16-20.

Faulk, W. P., Taylor, C. G., Yeh, C. J. and McIntyre, J. A. (1990) 'Preliminary clinical study of transferrin-adriamycin conjugate for drug delivery to acute leukemia patients', *Molecular biotherapy*, 2(1), pp. 57-60.

Federman, N. and Denny, C. T. (2010) 'Targeting liposomes toward novel pediatric anticancer therapeutics', *Pediatric research*, 67(5), pp. 514-519.

Ferlay, J., Soerjomataram, I., Dikshit, R., Eser, S., Mathers, C., Rebelo, M., Parkin, D. M., Forman, D. and Bray, F. (2015) 'Cancer incidence and mortality worldwide: sources, methods and major patterns in GLOBOCAN 2012', *International journal of cancer*, 136(5), pp. E359-E386.

Filion, M. C. and Phillips, N. C. (1997) 'Anti- • inflammatory activity of cationic lipids', *British journal of pharmacology*, 122(3), pp. 551-557.

Funk, J. O., Waga, S., Harry, J. B., Espling, E., Stillman, B. and Galloway, D. A. (1997) 'Inhibition of CDK activity and PCNA-dependent DNA replication by p21 is blocked by interaction with the HPV-16 E7 oncoprotein', *Genes & development*, 11(16), pp. 2090-2100.

Gabizon, A., Dagan, A., Goren, D., Barenholz, Y. and Fuks, Z. (1982) 'Liposomes as in vivo carriers of adriamycin: reduced cardiac uptake and preserved antitumor activity in mice', *Cancer Research*, 42(11), pp. 4734-4739.

Gabizon, A., Horowitz, A. T., Goren, D., Tzemach, D., Mandelbaum-Shavit, F., Qazen, M. M. and Zalipsky, S. (1999) 'Targeting folate receptor with folate linked to extremities of poly (ethylene glycol)-grafted liposomes: in vitro studies', *Bioconjugate chemistry*, 10(2), pp. 289-298.

Gabizon, A., Shmeeda, H., Horowitz, A. T. and Zalipsky, S. (2004) 'Tumor cell targeting of liposome-entrapped drugs with phospholipid-anchored folic acid-“PEG conjugates', *Advanced drug delivery reviews*, 56(8), pp. 1177-1192.

Gatter, K. C., Brown, G., Trowbridge, I. S., Woolston, R. E. and Mason, D. Y. (1983) 'Transferrin receptors in human tissues: their distribution and possible clinical relevance', *Journal of clinical pathology*, 36(5), pp. 539-545.

Goldburg, W. I. (1999) 'Dynamic light scattering', *American Journal of Physics*, 67(12), pp. 1152-1160.

Goren, D., Horowitz, A. T., Tzemach, D., Tarshish, M., Zalipsky, S. and Gabizon, A. (2000) 'Nuclear delivery of doxorubicin via folate-targeted liposomes with bypass of multidrug-resistance efflux pump', *Clinical Cancer Research*, 6(5), pp. 1949-1957.

Gref, R., Domb, A., Quellec, P., Blunk, T., MÃ¼ller, R. H., Verbavatz, J. M. and Langer, R. (1995) 'The controlled intravenous delivery of drugs using PEG-coated sterically stabilized nanospheres', *Advanced drug delivery reviews*, 16(2-3), pp. 215-233.

Gregoriadis, G. and Ryman, B. E. (1971) 'Liposomes as carriers of enzymes or drugs: a new approach to the treatment of storage diseases', *Biochemical Journal,* 124(5), pp. 58P.

Gu, F., Zhang, L., Teply, B. A., Mann, N., Wang, A., Radovic-Moreno, A. F., Langer, R. and Farokhzad, O. C. (2008) 'Precise engineering of targeted nanoparticles by using self-assembled biointegrated block copolymers', *Proceedings of the National Academy of Sciences,* 105(7), pp. 2586-2591.

Gullotti, E. and Yeo, Y. (2009) 'Extracellularly activated nanocarriers: a new paradigm of tumor targeted drug delivery', *Molecular pharmaceutics,* 6(4), pp. 1041-1051.

Gustafsson, L., Ponten, J., Zack, M. and Adami, H. O. (1997) 'International incidence rates of invasive cervical cancer after introduction of cytological screening', *Cancer causes & control,* 8(5), pp. 755-763.

Haley, B. and Frenkel, E. 'Nanoparticles for drug delivery in cancer treatment'. *Urologic Oncology: Seminars and original investigations*: Elsevier, 57-64.

Hall, R. A. (2004) *Studying protein-protein interactions via blot overlay or Far Western blot. Protein-Protein Interactions*: Humana Press.

Haller, J. S. (1981) *American medicine in transition, 1840-1910.* University of Illinois Press.

Harro, C. D., Pang, Y.-Y. S., Roden, R. B. S., Hildesheim, A., Wang, Z., Reynolds, M. J., Mast, T. C., Robinson, R., Murphy, B. R. and Karron, R. A. (2001) 'Safety and immunogenicity trial in adult volunteers of a human papillomavirus 16 L1 virus-like particle vaccine', *Journal of the National Cancer Institute,* 93(4), pp. 284-292.

Haung, M. and Hieftje, G. (1989) 'Simultaneous measurement of spatially resolved electron temperatures, electron number densities and gas temperatures by laser light scattering from the ICP', *Spectrochimica Acta Part B: Atomic Spectroscopy,* 44(8), pp. 739-749.

Head, J. F., Wang, F. and Elliott, R. L. (1997) 'Antineoplastic drugs that interfere with iron metabolism in cancer cells', *Advances in enzyme regulation,* 37, pp. 147-169.

Heath, T. D., Montgomery, J. A., Piper, J. R. and Papahadjopoulos, D. (1983) 'Antibody-targeted liposomes: increase in specific toxicity of methotrexate-gamma-aspartate', *Proceedings of the National Academy of Sciences,* 80(5), pp. 1377-1381.

Ho, P. C. (2005) '33As metallotherapeutic arsenic compounds', *Metallotherapeutic Drugs and Metalâ€• Based Diagnostic Agents: The Use of Metals in Medicine*, pp. 297-311.

Holland, J. W., Hui, C., Cullis, P. R. and Madden, T. D. (1996) ' Poly (ethylene glycol)− lipid conjugates regulate the calcium-induced fusion of liposomes composed of phosphatidylethanolamine and phosphatidylserine', *Biochemistry,* 35(8), pp. 2618-2624.

Horner, S. M., DeFilippis, R. A., Manuelidis, L. and DiMaio, D. (2004) 'Repression of the human papillomavirus E6 gene initiates p53-dependent, telomerase-independent senescence and apoptosis in HeLa cervical carcinoma cells', *Journal of virology,* 78(8), pp. 4063-4073.

Howie, H. L., Katzenellenbogen, R. A. and Galloway, D. A. (2009) 'Papillomavirus E6 proteins', *Virology,* 384(2), pp. 324-334.

Hsu, S. M., Raine, L. and Fanger, H. (1981) 'Use of avidin-biotin-peroxidase complex (ABC) in immunoperoxidase techniques: a comparison between ABC and unlabeled antibody (PAP) procedures', *Journal of Histochemistry & Cytochemistry,* 29(4), pp. 577-580.

Huang, A., Huang, L. and Kennel, S. J. (1980) 'Monoclonal antibody covalently coupled with fatty acid. A reagent for in vitro liposome targeting', *Journal of Biological Chemistry,* 255(17), pp. 8015-8018.

Inglis, S., Shaw, A. and Koenig, S. (2006) 'HPV vaccines: commercial research & development', *Vaccine,* 24, pp. S99-S105.

International Collaboration of Epidemiological Studies of Cervical, C. (2006) 'Carcinoma of the cervix and tobacco smoking: collaborative reanalysis of individual data on 13,541 women with carcinoma of the cervix and 23,017 women without carcinoma of the cervix from 23 epidemiological studies', *International journal of cancer,* 118(6), pp. 1481-1495.

International Collaboration of Epidemiological Studies of Cervical, C. (2006) 'Cervical carcinoma and reproductive factors: collaborative reanalysis of individual data on 16,563 women with cervical carcinoma and 33,542 women without cervical carcinoma from 25 epidemiological studies', *International journal of cancer,* 119(5), pp. 1108-1124.

Ira, M., Renate, F. and Ari, H. (1986) 'Acidification of the Endocytic and Exocytic Pathways', *Annual Review of Biochemistry,* 55(1), pp. 663-700.

Jackson, R. and Grainge, J. W. (1975) 'Arsenic and cancer', *Canadian Medical Association Journal,* 113(5), pp. 396.

Jain, R. K. (1987) 'Transport of molecules across tumor vasculature', *Cancer and Metastasis Reviews,* 6(4), pp. 559-593.

Jain, R. K. (1987) 'Transport of molecules in the tumor interstitium: a review', *Cancer research,* 47(12), pp. 3039-3051.

Jiang, W., Kim, B. Y. S., Rutka, J. T. and Chan, W. C. W. (2008) 'Nanoparticle-mediated cellular response is size-dependent', *Nature nanotechnology,* 3(3), pp. 145.

Jones, B. (2009) 'Toxicity after cervical cancer treatment using radiotherapy and chemotherapy', *Clinical Oncology,* 21(1), pp. 56-63.

Kallinteri, P., Fatouros, D., Klepetsanis, P. and Antimisiaris, S. G. (2004) 'Arsenic trioxide liposomes: encapsulation efficiency and in vitro stability', *Journal of liposome research,* 14(1-2), pp. 27-38.

Kamaly, N., Xiao, Z., Valencia, P. M., Radovic-Moreno, A. F. and Farokhzad, O. C. (2012) 'Targeted polymeric therapeutic nanoparticles: design, development and clinical translation', *Chemical Society Reviews,* 41(7), pp. 2971-3010.

Kang, Y.-H., Yi, M.-J., Kim, M.-J., Park, M.-T., Bae, S., Kang, C.-M., Cho, C.-K., Park, I.-C., Park, M.-J. and Rhee, C. H. (2004) 'Caspase-independent cell death by arsenic trioxide in human cervical cancer cells: reactive oxygen species-mediated poly (ADP-ribose) polymerase-1 activation signals apoptosis-inducing factor release from mitochondria', *Cancer research,* 64(24), pp. 8960-8967.

Kang, Y.-J., O'Connell, D. L., Tan, J., Lew, J.-B., Demers, A., Lotocki, R., Kliewer, E. V., Hacker, N. F., Jackson, M. and Delaney, G. P. (2015) 'Optimal uptake rates for initial treatments for cervical cancer in concordance with guidelines in Australia and Canada: Results from two large cancer facilities', *Cancer epidemiology,* 39(4), pp. 600-611.

Katanyoo, K., Tangjitgamol, S., Chongthanakorn, M., Tantivatana, T., Manusirivithaya, S., Rongsriyam, K. and Cholpaisal, A. (2011) 'Treatment outcomes of concurrent weekly carboplatin with radiation therapy in locally advanced cervical cancer patients', *Gynecologic oncology,* 123(3), pp. 571-576.

Kijanka, M., Dorresteijn, B., Oliveira, S. and van Bergen en Henegouwen, P. M. P. (2015) 'Nanobody-based cancer therapy of solid tumors', *Nanomedicine,* 10(1), pp. 161-174.

Kim, H.-A., Seo, J.-K., Kim, T. and Lee, B.-T. (2014) 'Nanometrology and its perspectives in environmental research', *Environmental health and toxicology,* 29.

Kindt, T. J., Goldsby, R. A., Osborne, B. A. and Kuby, J. (2007) *Kuby immunology.* Macmillan.

Kinoshita, E., Kinoshita-Kikuta, E. and Koike, T. (2009) 'Separation and detection of large phosphoproteins using Phos-tag SDS-PAGE', *Nature protocols,* 4(10), pp. 1513.

Kirpotin, D. B., Drummond, D. C., Shao, Y., Shalaby, M. R., Hong, K., Nielsen, U. B., Marks, J. D., Benz, C. C. and Park, J. W. (2006) 'Antibody targeting of long-circulating lipidic nanoparticles does not increase tumor localization but does increase internalization in animal models', *Cancer research,* 66(13), pp. 6732-6740.

Kirpotin, D. B., Park, J. W., Hong, K., Shao, Y., Shalaby, R., Colbern, G., Benz, C. C. and Papahadjopoulos, D. (1997) 'Targeting of liposomes to solid tumors: the case of sterically stabilized anti-HER2 immunoliposomes', *Journal of Liposome Research,* 7(4), pp. 391-417.

Kito, M., Matsumoto, K., Wada, N., Sera, K., Futatsugawa, S., Naoe, T., Nozawa, Y. and Akao, Y. (2003) 'Antitumor effect of arsenic trioxide in murine xenograft model', *Cancer science,* 94(11), pp. 1010-1014.

Klibanov, A. L., Maruyama, K., Beckerleg, A. M., Torchilin, V. P. and Huang, L. (1991) 'Activity of amphipathic poly (ethylene glycol) 5000 to prolong the circulation time of liposomes depends on the liposome size and is unfavorable for immunoliposome binding to target', *Biochimica et Biophysica Acta (BBA)-Biomembranes,* 1062(2), pp. 142-148.

Koshkaryev, A., Sawant, R., Deshpande, M. and Torchilin, V. (2013) 'Immunoconjugates and long circulating systems: origins, current state of the art and future directions', *Advanced drug delivery reviews,* 65(1), pp. 24-35.

Kroemer, G. and de The, H. (1999) 'Arsenic trioxide, a novel mitochondriotoxic anticancer agent?' *Journal of the National Cancer Institute,* 91(9), pp. 743-745.

Kurien, B. T. and Scofield, R. H. (2006) 'Western blotting', *Methods,* 38(4), pp. 283-293.

Kwong, Y. L. and Todd, D. (1997) 'Delicious poison: arsenic trioxide for the treatment of leukemia', *Blood,* 89(9), pp. 3487-3487.

Lam, S.-K., Mak, J. C.-W., Zheng, C.-Y., Li, Y.-Y., Kwong, Y.-L. and Ho, J. C.-M. (2014) 'Downregulation of thymidylate synthase with arsenic trioxide in lung adenocarcinoma', *International journal of oncology,* 44(6), pp. 2093-2102.

Larochette, N., Decaudin, D., Jacotot, E., Brenner, C., Marzo, I., Susin, S. A., Zamzami, N., Xie, Z., Reed, J. and Kroemer, G. (1999) 'Arsenite induces apoptosis via a direct effect on the mitochondrial permeability transition pore', *Experimental cell research,* 249(2), pp. 413-421.

Lasic, D. D. (1996) 'Doxorubicin in sterically stabilized liposomes', *Nature,* 380(6574), pp. 561.

Laskin, J. J. and Sandler, A. B. (2004) 'Epidermal growth factor receptor: a promising target in solid tumours', *Cancer treatment reviews,* 30(1), pp. 1-17.

Lazo, P. A. (1999) 'The molecular genetics of cervical carcinoma', *British journal of cancer,* 80(12), pp. 2008.

Leamon, C. P. and Low, P. S. (2001) 'Folate-mediated targeting: from diagnostics to drug and gene delivery', *Drug discovery today,* 6(1), pp. 44-51.

Lee, R. J. and Low, P. S. (1994) 'Delivery of liposomes into cultured KB cells via folate receptor-mediated endocytosis', *Journal of Biological Chemistry,* 269(5), pp. 3198-3204.

Lee, R. J. and Low, P. S. (1995) 'Folate-mediated tumor cell targeting of liposome-entrapped doxorubicin in vitro', *Biochimica et Biophysica Acta (BBA)-Biomembranes,* 1233(2), pp. 134-144.

Leisching, G. R., Loos, B., Botha, M. H. and Engelbrecht, A. M. (2015) 'The role of mTOR during cisplatin treatment in an in vitro and ex vivo model of cervical cancer', *Toxicology*, 335, pp. 72-78.

Li, S.-D., Chen, Y.-C., Hackett, M. J. and Huang, L. (2008) 'Tumor-targeted delivery of siRNA by self-assembled nanoparticles', *Molecular Therapy*, 16(1), pp. 163-169.

Licciardi, M., Giammona, G., Du, J., Armes, S. P., Tang, Y. and Lewis, A. L. (2006) 'New folate-functionalized biocompatible block copolymer micelles as potential anti-cancer drug delivery systems', *Polymer*, 47(9), pp. 2946-2955.

Lin, Z., Bazzaro, M., Wang, M.-C., Chan, K. C., Peng, S. and Roden, R. B. S. (2009) 'Combination of proteasome and HDAC inhibitors for uterine cervical cancer treatment', *Clinical Cancer Research*, 15(2), pp. 570-577.

Lipinski, M. M. and Jacks, T. (1999) 'The retinoblastoma gene family in differentiation and development', *Oncogene*, 18(55), pp. 7873.

Liu, B., Pan, S., Dong, X., Qiao, H., Jiang, H., Krissansen, G. W. and Sun, X. (2006) 'Opposing effects of arsenic trioxide on hepatocellular carcinomas in mice', *Cancer science*, 97(7), pp. 675-681.

Lorusso, D., Petrelli, F., Coinu, A., Raspagliesi, F. and Barni, S. (2014) 'A systematic review comparing cisplatin and carboplatin plus paclitaxel-based chemotherapy for recurrent or metastatic cervical cancer', *Gynecologic oncology*, 133(1), pp. 117-123.

Low, P. S. and Antony, A. C. (2004) 'Folate receptor-targeted drugs for cancer and inflammatory diseases', *Advanced drug delivery reviews*, 56(8), pp. 1055-1058.

Low, P. S. and Kularatne, S. A. (2009) 'Folate-targeted therapeutic and imaging agents for cancer', *Current opinion in chemical biology*, 13(3), pp. 256-262.

Lu, M., Wang, H., Wang, Z., Li, X.-F. and Le, X. C. (2008) 'Identification of reactive cysteines in a protein using arsenic labeling and collision-induced dissociation tandem mass spectrometry', *Journal of proteome research*, 7(8), pp. 3080-3090.

Lu, Y. and Low, P. S. (2012) 'Folate-mediated delivery of macromolecular anticancer therapeutic agents', *Advanced drug delivery reviews*, 64, pp. 342-352.

Maeda, H., Bharate, G. Y. and Daruwalla, J. (2009) 'Polymeric drugs for efficient tumor-targeted drug delivery based on EPR-effect', *European journal of pharmaceutics and biopharmaceutics*, 71(3), pp. 409-419.

Maeda, H., Hori, S., Nishitoh, H., Ichijo, H., Ogawa, O., Kakehi, Y. and Kakizuka, A. (2001) 'Tumor growth inhibition by arsenic trioxide (As2O3) in the orthotopic metastasis model of androgen-independent prostate cancer', *Cancer Research*, 61(14), pp. 5432-5440.

Magaldi, T. G., Almstead, L. L., Bellone, S., Prevatt, E. G., Santin, A. D. and DiMaio, D. (2012) 'Primary human cervical carcinoma cells require human papillomavirus E6 and E7 expression for ongoing proliferation', *Virology*, 422(1), pp. 114-124.

Magarkar, A., Dhawan, V., Kallinteri, P., Viitala, T., Elmowafy, M., RÃ³g, T. and Bunker, A. (2014) 'Cholesterol level affects surface charge of lipid membranes in saline solution', *Scientific reports*, 4, pp. 5005.

Malam, Y., Loizidou, M. and Seifalian, A. M. (2009) 'Liposomes and nanoparticles: nanosized vehicles for drug delivery in cancer', *Trends in pharmacological sciences*, 30(11), pp. 592-599.

Mammen, M., Choi, S. K. and Whitesides, G. M. (1998) 'Polyvalent interactions in biological systems: implications for design and use of multivalent ligands and inhibitors', *Angewandte Chemie International Edition,* 37(20), pp. 2754-2794.

Mansur, C. P. and Androphy, E. J. (1993) 'Cellular transformation by papillomavirus oncoproteins', *Biochimica et Biophysica Acta (BBA)-Reviews on Cancer,* 1155(3), pp. 323-345.

Mathias, C. J., Wang, S., Waters, D. J., Turek, J. J., Low, P. S. and Green, M. A. (1998) 'Indium-111-DTPA-folate as a potential folate receptor-targeted radiopharmaceutical', *Journal of Nuclear Medicine,* 39(9), pp. 1579.

Matsumura, Y. and Maeda, H. (1986) 'A new concept for macromolecular therapeutics in cancer chemotherapy: mechanism of tumoritropic accumulation of proteins and the antitumor agent smancs', *Cancer research,* 46(12 Part 1), pp. 6387-6392.

Mc Carthy, D. J., Malhotra, M., O'Mahony, A. M., Cryan, J. F. and O'Driscoll, C. M. (2015) 'Nanoparticles and the blood-brain barrier: advancing from in-vitro models towards therapeutic significance', *Pharmaceutical research,* 32(4), pp. 1161-1185.

McCloughlin, E. C. (2016) *Protein Kinase LKB1 regulates MRP2/ABCC11 and Bile Excretion in vivo. A translational study linking Neonatal Jaundice & Adult onset Hepatocellular carcinoma.* Trinity College, University of Dublin.

McConville, C. (2015) 'The use of localised vaginal drug delivery as part of a neoadjuvant chemotherapy strategy in the treatment of cervical cancer', *Gynecol. Obstet. Res. Open. J,* 2(1), pp. 26-28.

McGlennen, R. C. (2000) 'Human papillomavirus oncogenesis', *Clinics in laboratory medicine,* 20(2), pp. 383-406.

Meng, Z. Q. and Meng, N. Y. (2000) 'Effects of arsenic on blast transformation and DNA synthesis of human blood lymphocytes', *Chemosphere,* 41(1-2), pp. 115-119.

Miller, C. R., Bondurant, B., McLean, S. D., McGovern, K. A. and O'Brien, D. F. (1998) 'Liposome- cell interactions in vitro: effect of liposome surface charge on the binding and endocytosis of conventional and sterically stabilized liposomes', *Biochemistry,* 37(37), pp. 12875-12883.

Miller, W. H., Schipper, H. M., Lee, J. S., Singer, J. and Waxman, S. (2002) 'Mechanisms of action of arsenic trioxide', *Cancer research,* 62(14), pp. 3893-3903.

Moore, D. H., Blessing, J. A., McQuellon, R. P., Thaler, H. T., Cella, D., Benda, J., Miller, D. S., Olt, G., King, S. and Boggess, J. F. (2004) 'Phase III study of cisplatin with or without paclitaxel in stage IVB, recurrent, or persistent squamous cell carcinoma of the cervix: a gynecologic oncology group study', *Journal of clinical oncology,* 22(15), pp. 3113-3119.

Morikawa, T., Wanibuchi, H., Morimura, K., Ogawa, M. and Fukushima, S. (2000) 'Promotion of skin carcinogenesis by dimethylarsinic acid in keratin (K6)/ODC transgenic mice', *Japanese journal of cancer research,* 91(6), pp. 579-581.

Mosqueira, V. C. F., Legrand, P., Gulik, A., Bourdon, O., Gref, R., Labarre, D. and Barratt, G. (2001) 'Relationship between complement activation, cellular uptake and surface physicochemical aspects of novel PEG-modified nanocapsules', *Biomaterials,* 22(22), pp. 2967-2979.

Muderspach, L. I., Blessing, J. A., Levenback, C. and Moore, J. L. (2001) 'A Phase II study of topotecan in patients with squamous cell carcinoma of the cervix: a gynecologic oncology group study', *Gynecologic oncology,* 81(2), pp. 213-215.

Munoz, N., Bosch, F. X., De Sanjose, S., Herrero, R., Castellsague, X., Shah, K. V., Snijders, P. J. F. and Meijer, C. J. L. M. (2003) 'Epidemiologic classification of human papillomavirus types associated with cervical cancer', *New England Journal of Medicine,* 348(6), pp. 518-527.

Munoz, N., Bosch, F. X., De Sanjose, S., Tafur, L., Izarzugaza, I., Gili, M., Viladiu, P., Navarro, C., Martos, C. and Ascunce, N. (1992) 'The causal link between human papillomavirus and invasive cervical cancer: a populationâ€□based caseâ€□control study in Colombia and Spain', *International journal of cancer*, 52(5), pp. 743-749.

Munoz, N., Castellsague, X., de Gonzalez, A. B. and Gissmann, L. (2006) 'HPV in the etiology of human cancer', *Vaccine*, 24, pp. S1-S10.

Murgo, A. J. (2001) 'Clinical trials of arsenic trioxide in hematologic and solid tumors: overview of the National Cancer Institute Cooperative Research and Development Studies', *The Oncologist*, 6(Supplement 2), pp. 22-28.

Narisawa-Saito, M. and Kiyono, T. (2007) 'Basic mechanisms of high-risk human papillomavirus-induced carcinogenesis: Roles of E6 and E7 proteins', *Cancer science*, 98(10), pp. 1505-1511.

NeufCoeur, P. E., Arafa, M., Delvenne, P. and Saussez, S. (2009) 'Involvement of human papillomavirus in upper aero-digestive tracts cancers', *Bulletin du cancer*, 96(10), pp. 941-950.

Nevins, J. R. (1998) 'Toward an understanding of the functional complexity of the E2F and retinoblastoma families', *Cell growth and differentiation*, 9(8), pp. 585.

Nguyen, M. L., Nguyen, M. M., Lee, D., Griep, A. E. and Lambert, P. F. (2003) 'The PDZ ligand domain of the human papillomavirus type 16 E6 protein is required for E6's induction of epithelial hyperplasia in vivo', *Journal of virology*, 77(12), pp. 6957-6964.

Ni, J., Chen, G., Shen, Z., Li, X., Liu, H., Huang, Y., Fang, Z., Chen, S., Wang, Z. and Chen, L. (1997) 'Pharmacokinetics of intravenous arsenic trioxide in the treatment of acute promyelocytic leukemia', *Zhonghua xue ye xue za zhi= Zhonghua xueyexue zazhi*, 18(5), pp. 250-253.

Ni, S., Stephenson, S. M. and Lee, R. J. (2002) 'Folate receptor targeted delivery of liposomal daunorubicin into tumor cells', *Anticancer research*, 22(4), pp. 2131-2135.

Nukolova, N. V., Oberoi, H. S., Cohen, S. M., Kabanov, A. V. and Bronich, T. K. (2011) 'Folate-decorated nanogels for targeted therapy of ovarian cancer', *Biomaterials*, 32(23), pp. 5417-5426.

Ohguchi, Y., Kawano, K., Hattori, Y. and Maitani, Y. (2008) 'Selective delivery of folate-PEG-linked, nanoemulsion-loaded aclacinomycin A to KB nasopharyngeal cells and xenograft: Effect of chain length and amount of folate-PEG linker', *Journal of drug targeting*, 16(9), pp. 660-667.

Ordikhani, F., Erdem Arslan, M., Marcelo, R., Sahin, I., Grigsby, P., Schwarz, J. K. and Azab, A. K. (2016) 'Drug delivery approaches for the treatment of cervical cancer', *Pharmaceutics*, 8(3), pp. 23.

Orive, G., Hernandez, R. M., GascÃ³n, A. R. Ì. g., DomÄ±Ì • nguez-Gil, A. and Pedraz, J. L. (2003) 'Drug delivery in biotechnology: present and future', *Current opinion in biotechnology*, 14(6), pp. 659-664.

Pan, X. Q., Wang, H. and Lee, R. J. (2002) 'Boron delivery to a murine lung carcinoma using folate receptor-targeted liposomes', *Anticancer research*, 22(3), pp. 1629-1633.

Pan, X. Q., Wang, H., Shukla, S., Sekido, M., Adams, D. M., Tjarks, W., Barth, R. F. and Lee, R. J. (2002) 'Boron-containing folate receptor-targeted liposomes as potential delivery agents for neutron capture therapy', *Bioconjugate chemistry*, 13(3), pp. 435-442.

Pan, X. Q., Zheng, X., Shi, G., Wang, H., Ratnam, M. and Lee, R. J. (2002) 'Strategy for the treatment of acute myelogenous leukemia based on folate receptor -targeted liposomal doxorubicin combined with receptor induction using all-trans retinoic acid', *Blood*, 100(2), pp. 594-602.

Park, W. and Na, K. (2015) 'Advances in the synthesis and application of nanoparticles for drug delivery', *Wiley Interdisciplinary Reviews: Nanomedicine and Nanobiotechnology,* 7(4), pp. 494-508.

Park, W. H., Cho, Y. H., Jung, C. W., Park, J. O., Kim, K., Im, Y. H., Lee, M. H., Kang, W. K. and Park, K. (2003) 'Arsenic trioxide inhibits the growth of A498 renal cell carcinoma cells via cell cycle arrest or apoptosis', *Biochemical and biophysical research communications,* 300(1), pp. 230-235.

Patrick, T. A., Kranz, D. M., Van Dyke, T. A. and Roy, E. J. (1997) 'Folate receptors as potential therapeutic targets in choroid plexus tumors of SV40 transgenic mice', *Journal of neuro-oncology,* 32(2), pp. 111-123.

Paul, M. (2003) 'Introduction to Immunocytochemistry', *Journal of Microscopy,* 211(2), pp. 188-188.

Pavey, K. D. and Olliff, C. J. (1999) 'SPR analysis of the total reduction of protein adsorption to surfaces coated with mixtures of long-and short-chain polyethylene oxide block copolymers', *Biomaterials,* 20(9), pp. 885-890.

Pawar, P. V., Domb, A. J. and Kumar, N. (2014) 'Systemic Targeting Systems-EPR Effect, Ligand Targeting Systems', *Focal Controlled Drug Delivery*: Springer, pp. 61-91.

Pecora, R. (2000) 'Dynamic light scattering measurement of nanometer particles in liquids', *Journal of nanoparticle research,* 2(2), pp. 123-131.

Peer, D., Karp, J. M., Hong, S., Farokhzad, O. C., Margalit, R. and Langer, R. (2007) 'Nanocarriers as an emerging platform for cancer therapy', *Nature nanotechnology,* 2(12), pp. 751.

Peng, Z. H., Sima, M., Salama, M. E., Kopečková, P. and Kopeček, J. (2013) 'Spacer length impacts the efficacy of targeted docetaxel conjugates in prostate-specific membrane antigen expressing prostate cancer', *Journal of drug targeting,* 21(10), pp. 968-980.

Peralta-Zaragoza, O., Bermudez-Morales, V. H., Perez-Plasencia, C., Salazar-Leon, J., Gomez-Ceron, C. and Madrid-Marina, V. (2012) 'Targeted treatments for cervical cancer: a review', *OncoTargets and therapy,* 5, pp. 315.

Platanias, L. C. (2009) 'Biological responses to arsenic compounds', *Journal of Biological Chemistry,* 284(28), pp. 18583-18587.

Porter, A. G. and Janicke, R. U. (1999) 'Emerging roles of caspase-3 in apoptosis', *Cell death and differentiation,* 6(2), pp. 99.

Qualls, M. M. and Thompson, D. H. (2001) 'Chloroaluminum phthalocyanine tetrasulfonate delivered via acid- labile diplasmenylcholine- • folate liposomes: Intracellular localization and synergistic phototoxicity', *International journal of cancer,* 93(3), pp. 384-392.

Rainov, N. G. and Soling, A. (2005) 'Technology evaluation: TransMID, KS Biomedix/Nycomed/Sosei/PharmaEngine', *Current opinion in molecular therapeutics,* 7(5), pp. 483-492.

Reddy, J. A., Abburi, C., Hofland, H., Howard, S. J., Vlahov, I., Wils, P. and Leamon, C. P. (2002) 'Folate-targeted, cationic liposome-mediated gene transfer into disseminated peritoneal tumors', *Gene therapy,* 9(22), pp. 1542.

Reddy, J. A., Allagadda, V. M. and Leamon, C. P. (2005) 'Targeting therapeutic and imaging agents to folate receptor positive tumors', *Current pharmaceutical biotechnology,* 6(2), pp. 131-150.

Regimbald, L. H., Pilarski, L. M., Longenecker, B. M., Reddish, M. A., Zimmermann, G. and Hugh, J. C. (1996) 'The breast mucin MUC1 as a novel adhesion ligand for endothelial intercellular adhesion molecule 1 in breast cancer', *Cancer research,* 56(18), pp. 4244-4249.

Reisinger, V. and Eichacker, L. A. (2007) 'How to Analyze Protein Complexes by 2D Blue Native SDS-PAGE', *PROTEOMICS,* 7(1), pp. 6-16.

Remmink, A. J., Walboomers, J. M. M., Helmerhorst, T. J. M., Voorhorst, F. J., Rozendaal, L., Risse, E. K. J., Meijer, C. J. L. M. and Kenemans, P. (1995) 'The presence of persistent high-risk HPV genotypes in dysplastic cervical lesions is associated with progressive disease: natural history up to 36 months', *International Journal of Cancer,* 61(3), pp. 306-311.

Rezaaiyaan, R., Hieftje, G. M., Anderson, H., Kaiser, H. and Meddings, B. (1982) 'Design and Construction of a Low-Flow, Low-Power Torch for Inductively Coupled Plasma Spectrometry', *Applied Spectroscopy,* 36(6), pp. 627-631.

Riccardi, C. and Nicoletti, I. (2006) 'Analysis of apoptosis by propidium iodide staining and flow cytometry', *Nature protocols,* 1(3), pp. 1458-1461.

Rimm, D. L., Koslov, E. R., Kebriaei, P., Cianci, C. D. and Morrow, J. S. (1995) 'Alpha 1 (E)-catenin is an actin-binding and-bundling protein mediating the attachment of F-actin to the membrane adhesion complex', *Proceedings of the National Academy of Sciences,* 92(19), pp. 8813-8817.

Ross, J. F., Wang, H., Behm, F. G., Mathew, P., Wu, M., Booth, R. and Ratnam, M. (1999) 'Folate receptor type Î² is a neutrophilic lineage marker and is differentially expressed in myeloid leukemia', *Cancer: Interdisciplinary International Journal of the American Cancer Society,* 85(2), pp. 348-357.

Saengkrit, N., Saesoo, S., Srinuanchai, W., Phunpee, S. and Ruktanonchai, U. R. (2014) 'Influence of curcumin-loaded cationic liposome on anticancer activity for cervical cancer therapy', *Colloids and Surfaces B: Biointerfaces,* 114, pp. 349-356.

Sage, J., Miller, A. L., PÃ©rez-Mancera, P. A., Wysocki, J. M. and Jacks, T. (2003) 'Acute mutation of retinoblastoma gene function is sufficient for cell cycle re-entry', *Nature,* 424(6945), pp. 223.

Sahoo, S. K., Misra, R. and Parveen, S. (2017) 'Nanoparticles: a boon to drug delivery, therapeutics, diagnostics and imaging', *Nanomedicine in Cancer*: Pan Stanford, pp. 73-124.

Saini, J., Bansal, V., Chandra, A., Madan, J., Jain, U. K., Chandra, R. and Jain, S. M. (2014) 'Bleomycin sulphate loaded nanostructured lipid particles augment oral bioavailability, cytotoxicity and apoptosis in cervical cancer cells', *Colloids and Surfaces B: Biointerfaces,* 118, pp. 101-110.

Salvati, A., Pitek, A. S., Monopoli, M. P., Prapainop, K., Bombelli, F. B., Hristov, D. R., Kelly, P. M., Ã…berg, C., Mahon, E. and Dawson, K. A. (2013) 'Transferrin-functionalized nanoparticles lose their targeting capabilities when a biomolecule corona adsorbs on the surface', *Nature nanotechnology,* 8(2), pp. 137.

Sapra, P. and Allen, T. M. (2003) 'Ligand-targeted liposomal anticancer drugs', *Progress in lipid research,* 42(5), pp. 439-462.

Saul, J. M., Annapragada, A., Natarajan, J. V. and Bellamkonda, R. V. (2003) 'Controlled targeting of liposomal doxorubicin via the folate receptor in vitro', *Journal of Controlled Release,* 92(1-2), pp. 49-67.

Schiffman, M., Castle, P. E., Jeronimo, J., Rodriguez, A. C. and Wacholder, S. (2007) 'Human papillomavirus and cervical cancer', *The Lancet,* 370(9590), pp. 890-907.

Schiffman, M., Wentzensen, N., Wacholder, S., Kinney, W., Gage, J. C. and Castle, P. E. (2011) 'Human papillomavirus testing in the prevention of cervical cancer', *Journal of the National Cancer Institute,* 103(5), pp. 368-383.

Schmitz, K. S. and Phillies, G. D. J. (1991) 'An introduction to dynamic light scattering by macromolecules', *Physics Today,* 44, pp. 66.

Semple, S. C., Chonn, A. and Cullis, P. R. (1998) 'Interactions of liposomes and lipid-based carrier systems with blood proteins: Relation to clearance behaviour in vivo', *Advanced drug delivery reviews,* 32(1-2), pp. 3-17.

Sercombe, L., Veerati, T., Moheimani, F., Wu, S. Y., Sood, A. K. and Hua, S. (2015) 'Advances and challenges of liposome assisted drug delivery', *Frontiers in pharmacology,* 6, pp. 286.

Shapiro, H. M. and Darzynkiewicz, Z. (1995) 'Practical Flow Cytometry (3rd edn)', *Trends in Cell Biology,* 5(9), pp. 372.

Shen, S., Li, X.-F., Cullen, W. R., Weinfeld, M. and Le, X. C. (2013) 'Arsenic binding to proteins', *Chemical reviews,* 113(10), pp. 7769-7792.

Shen, Z.-X., Chen, G.-Q., Ni, J.-H., Li, X.-S., Xiong, S.-M., Qiu, Q.-Y., Zhu, J., Tang, W., Sun, G.-L. and Yang, K.-Q. (1997) 'Use of arsenic trioxide (As2O3) in the treatment of acute promyelocytic leukemia (APL): II. Clinical efficacy and pharmacokinetics in relapsed patients', *Blood,* 89(9), pp. 3354-3360.

Shi, J., Votruba, A. R., Farokhzad, O. C. and Langer, R. (2010) 'Nanotechnology in drug delivery and tissue engineering: from discovery to applications', *Nano letters,* 10(9), pp. 3223-3230.

Shi, J., Xiao, Z., Kamaly, N. and Farokhzad, O. C. (2011) 'Self-assembled targeted nanoparticles: evolution of technologies and bench to bedside translation', *Accounts of chemical research,* 44(10), pp. 1123-1134.

Shukla, S., Bharti, A. C., Mahata, S., Hussain, S., Kumar, R., Hedau, S. and Das, B. C. (2009) 'Infection of human papillomaviruses in cancers of different human organ sites', *Indian Journal of Medical Research,* 130(3), pp. 222.

Siegel, B. A., Dehdashti, F., Mutch, D. G., Podoloff, D. A., Wendt, R., Sutton, G. P., Burt, R. W., Ellis, P. R., Mathias, C. J. and Green, M. A. (2003) 'Evaluation of 111In-DTPA-folate as a receptor-targeted diagnostic agent for ovarian cancer: initial clinical results', *Journal of nuclear medicine: official publication, Society of Nuclear Medicine,* 44(5), pp. 700-707.

Singh, M. (1999) 'Transferrin as a targeting ligand for liposomes and anticancer drugs', *Current pharmaceutical design,* 5(6), pp. 443-452.

Smith, J. S., Green, J., De Gonzalez, A. B., Appleby, P., Peto, J., Plummer, M., Franceschi, S. and Beral, V. (2003) 'Cervical cancer and use of hormonal contraceptives: a systematic review', *The Lancet,* 361(9364), pp. 1159-1167.

Soenen, S. J. H., Brisson, A. R. and De Cuyper, M. (2009) 'Addressing the problem of cationic lipid-mediated toxicity: the magnetoliposome model', *Biomaterials,* 30(22), pp. 3691-3701.

Soliman, P. T., Slomovitz, B. M. and Wolf, J. K. (2004) 'Mechanisms of cervical cancer', *Drug Discovery Today: Disease Mechanisms,* 1(2), pp. 253-258.

Soo-Jong Um, S.-Y. L., Eun-Joo Kim, Jin Myoung, Sung-Eun Namkoong, Jong-Sup Park (2002) 'Down-regulation of human papillomavirus E6/E7 oncogene by arsenic trioxide in cervical carcinoma cells', *Cancer Letters,* 181(1), pp. 11-22.

Stephenson, S. M., Low, P. S. and Lee, R. J. (2004) 'Folate receptor-mediated targeting of liposomal drugs to cancer cells', *Methods in enzymology,* 387, pp. 33.

Strebhardt, K. and Ullrich, A. (2008) 'Paul Ehrlich's magic bullet concept: 100 years of progress', *Nature Reviews Cancer,* 8(6), pp. 473.

Sudimack, J. and Lee, R. J. (2000) 'Targeted drug delivery via the folate receptor', *Advanced drug delivery reviews,* 41(2), pp. 147-162.

Sutcliffe, S., Viscidi, R. P., Till, C., Goodman, P. J., Hoque, A. M., Hsing, A. W., Thompson, I. M., Zenilman, J. M., De Marzo, A. M. and Platz, E. A. (2010) 'Human papillomavirus types 16, 18, and 31 serostatus and prostate cancer risk in the Prostate Cancer Prevention Trial', *Cancer Epidemiology and Prevention Biomarkers,* 19(2), pp. 614-618.

Swindell, E. P., Hankins, P. L., Chen, H., Miodragovic, D. U. and O'Halloran, T. V. (2013) 'Anticancer activity of small-molecule and nanoparticulate arsenic (III) complexes', *Inorganic chemistry,* 52(21), pp. 12292-12304.

Talekar, M., Kendall, J., Denny, W. and Garg, S. (2011) 'Targeting of nanoparticles in cancer: drug delivery and diagnostics', *Anti-Cancer Drugs,* 22(10), pp. 949-962.

Thomas, G. M. 1999. Improved treatment for cervical cancer-concurrent chemotherapy and radiotherapy. Mass Medical Soc.

Thomas, M., Laura, R., Hepner, K., Guccione, E., Sawyers, C., Lasky, L. and Banks, L. (2002) 'Oncogenic human papillomavirus E6 proteins target the MAGI-2 and MAGI-3 proteins for degradation', *Oncogene,* 21(33), pp. 5088.

Thomas, R. (2013) *Practical guide to ICP-MS: a tutorial for beginners.* CRC press.

Tommasino, M. (2013) *Papillomaviruses in human cancer: the role of E6 and E7 oncoproteins.* Springer Science & Business Media.

Torchilin, V. P. (2000) 'Drug targeting', *European Journal of Pharmaceutical Sciences,* 11, pp. S81-S91.

Torchilin, V. P. (2006) 'Multifunctional nanocarriers', *Advanced drug delivery reviews,* 58(14), pp. 1532-1555.

Torchilin, V. P. (2010) 'Passive and active drug targeting: drug delivery to tumors as an example', *Drug delivery*: Springer, pp. 3-53.

Trimarchi, J. M. and Lees, J. A. (2002) 'Transcription: sibling rivalry in the E2F family', *Nature reviews Molecular cell biology,* 3(1), pp. 11.

Um, S.-J., Lee, S.-Y., Kim, E.-J., Myoung, J., Namkoong, S.-E. and Park, J.-S. (2002) 'Down-regulation of human papillomavirus E6/E7 oncogene by arsenic trioxide in cervical carcinoma cells', *Cancer letters,* 181(1), pp. 11-22.

Valencia, P. M., Hanewich-Hollatz, M. H., Gao, W., Karim, F., Langer, R., Karnik, R. and Farokhzad, O. C. (2011) 'Effects of ligands with different water solubilities on self-assembly and properties of targeted nanoparticles', *Biomaterials,* 32(26), pp. 6226-6233.

van Heerde, W. L., Robert-Offerman, S., Dumont, E., Hofstra, L., Doevendans, P. A., Smits, J. F., Daemen, M. J. A. P. and Reutelingsperger, C. P. (2000) 'Markers of apoptosis in cardiovascular tissues: focus on Annexin V', *Cardiovascular research,* 45(3), pp. 549-559.

Van Oss, C. J. (1975) *Phagocytic engulfment and cell adhesiveness as cellular surface phenomena.* Dekker.

Van Sluis, R., Bhujwalla, Z. M., Raghunand, N., Ballesteros, P., Alvarez, J., CerdÃ¡n, S. n., Galons, J. P. and Gillies, R. J. (1999) 'In vivo imaging of extracellular pH using 1H MRSI', *Magnetic Resonance in Medicine: An Official Journal of the International Society for Magnetic Resonance in Medicine,* 41(4), pp. 743-750.

Vermes, I., Haanen, C., Steffens-Nakken, H. and Reutellingsperger, C. (1995) 'A novel assay for apoptosis flow cytometric detection of phosphatidylserine expression on early apoptotic cells using fluorescein labelled annexin V', *Journal of immunological methods,* 184(1), pp. 39-51.

Vladimir, P. Z., Ekaterina, I. G., Evgeny, V. S., Jin-Woo, K., Nikolay Grigorievich, K. and Valery Viktorovich, T. 'Photoacoustic flow cytometry: principle and application for real-time detection of circulating single nanoparticles, pathogens, and contrast dyes in vivo'. SPIE, 14.

Vleminckx, K., Vakaet Jr, L., Mareel, M., Fiers, W. and Van Roy, F. (1991) 'Genetic manipulation of E-cadherin expression by epithelial tumor cells reveals an invasion suppressor role', *Cell*, 66(1), pp. 107-119.

Vonarbourg, A., Passirani, C., Saulnier, P. and Benoit, J.-P. (2006) 'Parameters influencing the stealthiness of colloidal drug delivery systems', *Biomaterials*, 27(24), pp. 4356-4373.

Walboomers, J. M. M., Jacobs, M. V., Manos, M. M., Bosch, F. X., Kummer, J. A., Shah, K. V., Snijders, P. J. F., Peto, J., Meijer, C. J. L. M. and MuÃ±oz, N. (1999) 'Human papillomavirus is a necessary cause of invasive cervical cancer worldwide', *The Journal of pathology*, 189(1), pp. 12-19.

Wang, M. and Thanou, M. (2010) 'Targeting nanoparticles to cancer', *Pharmacological Research*, 62(2), pp. 90-99.

Wang, S., Lee, R. J., Cauchon, G., Gorenstein, D. G. and Low, P. S. (1995) 'Delivery of antisense oligodeoxyribonucleotides against the human epidermal growth factor receptor into cultured KB cells with liposomes conjugated to folate via polyethylene glycol', *Proceedings of the National Academy of Sciences*, 92(8), pp. 3318-3322.

Wang, S., Luo, J., Lantrip, D. A., Waters, D. J., Mathias, C. J., Green, M. A., Fuchs, P. L. and Low, P. S. (1997) 'Design and Synthesis of [111In] DTPAâˆ' Folate for Use as a Tumor-Targeted Radiopharmaceutical', *Bioconjugate chemistry*, 8(5), pp. 673-679.

Wang, X., Jiang, F., Mu, J., Ye, X., Si, L., Ning, S., Li, Z. and Li, Y. (2014) 'Arsenic trioxide attenuates the invasion potential of human liver cancer cells through the demethylation-activated microRNA-491', *Toxicology letters*, 227(2), pp. 75-83.

Wang, X., Li, D., Ghali, L., Xia, R., Munoz, L. P., Garelick, H., Bell, C. and Wen, X. (2016) 'Therapeutic potential of delivering arsenic trioxide into HPV-infected cervical cancer cells using liposomal nanotechnology', *Nanoscale research letters*, 11(1), pp. 94.

Wang, X., Shen, Y., Zhao, Y., Li, Z., Gou, H., Cao, D., Yang, Y., Qiu, M., Li, Q. and Liu, J. (2015) 'Adjuvant intensity-modulated radiotherapy (IMRT) with concurrent paclitaxel and cisplatin in cervical cancer patients with high risk factors: a phase II trial', *European Journal of Surgical Oncology (EJSO)*, 41(8), pp. 1082-1088.

Wang, Z.-Y. and Chen, Z. (2008) 'Acute promyelocytic leukemia: from highly fatal to highly curable', *Blood*, 111(5), pp. 2505-2515.

Waxman, S. and Anderson, K. C. (2001) 'History of the development of arsenic derivatives in cancer therapy', *The oncologist*, 6(Supplement 2), pp. 3-10.

Weissleder, R., Kelly, K., Sun, E. Y., Shtatland, T. and Josephson, L. (2005) 'Cell-specific targeting of nanoparticles by multivalent attachment of small molecules', *Nature biotechnology*, 23(11), pp. 1418.

Wen, X., Li, D., Zhang, Y., Liu, S., Ghali, L. and Iles, R. K. (2012) 'Arsenic trioxide induces cervical cancer apoptosis, but specifically targets human papillomavirus-infected cell populations', *Anti-cancer drugs*, 23(3), pp. 280-287.

Werner, M. E., Karve, S., Sukumar, R., Cummings, N. D., Copp, J. A., Chen, R. C., Zhang, T. and Wang, A. Z. (2011) 'Folate-targeted nanoparticle delivery of chemo-and radiotherapeutics for the treatment of ovarian cancer peritoneal metastasis', *Biomaterials*, 32(33), pp. 8548-8554.

Werness, B. A., Levine, A. J. and Howley, P. M. (1990) 'Association of human papillomavirus types 16 and 18 E6 proteins with p53', *Science*, 248(4951), pp. 76-79.

Wu, J. and Chu, C.-C. (2013) 'Water insoluble cationic poly (ester amide) s: synthesis, characterization and applications', *Journal of Materials Chemistry B*, 1(3), pp. 353-360.

Wyllie, A. H. (1997) 'Apoptosis: an overview', *British Medical Bulletin*, 53(3), pp. 451-465.

Yang, H.-C., Fu, H.-L., Lin, Y.-F. and Rosen, B. P. (2012) 'Pathways of arsenic uptake and efflux', *Current topics in membranes*: Elsevier, pp. 325-358.

Yim, E.-K. and Park, J.-S. (2005) 'The Role of HPV E6 and E7 Oncoproteins in HPV-associated Cervical Carcinogenesis', *Cancer Research and Treatment : Official Journal of Korean Cancer Association*, 37(6), pp. 319-324.

Yu, B. O., Tai, H. C., Xue, W., Lee, L. J. and Lee, R. J. (2010) 'Receptor-targeted nanocarriers for therapeutic delivery to cancer', *Molecular membrane biology*, 27(7), pp. 286-298.

Yu, J., Qian, H., Li, Y., Wang, Y., Zhang, X., Liang, X., Fu, M. and Lin, C. (2007) 'Arsenic trioxide (As2O3) reduces the invasive and metastatic properties of cervical cancer cells in vitro and in vivo', *Gynecologic oncology*, 106(2), pp. 400-406.

Yu, J., Qian, H., Li, Y., Wang, Y., Zhang, X., Liang, X., Fu, M. and Lin, C. (2007) 'Therapeutic effect of arsenic trioxide (As2O3) on cervical cancer in vitro and in vivo through apoptosis induction', *Cancer biology & therapy*, 6(4), pp. 580-586.

Yu Nie, L. J., Ding, H., Xie, L., Li, L., He, B., Wu, Y. and Gu, Z. (2012) 'Cholesterol derivatives based charged liposomes for doxorubicin delivery: preparation, in vitro and in vivo characterization', *Theranostics*, 2(11), pp. 1092.

Zamboni, W. C., Torchilin, V., Patri, A. K., Hrkach, J., Stern, S., Lee, R., Nel, A., Panaro, N. J. and Grodzinski, P. (2012) 'Best practices in cancer nanotechnology: perspective from NCI nanotechnology alliance', *Clinical cancer research*, 18(12), pp. 3229-41.

Zekri, A., Ghaffari, S. H., Yousefi, M., Ghanizadeh-Vesali, S., Mojarrad, M., Alimoghaddam, K. and Ghavamzadeh, A. (2013) 'Autocrine human growth hormone increases sensitivity of mammary carcinoma cell to arsenic trioxide-induced apoptosis', *Molecular and cellular endocrinology*, 377(1-2), pp. 84-92.

Zhang, C., Zhao, L., Dong, Y., Zhang, X., Lin, J. and Chen, Z. (2010) 'Folate-mediated poly (3-hydroxybutyrate-co-3-hydroxyoctanoate) nanoparticles for targeting drug delivery', *European Journal of Pharmaceutics and Biopharmaceutics*, 76(1), pp. 10-16.

Zhang, P. (1996) 'Arsenic trioxide treated 72 cases of acute promyelocytic leukemia', *Chin J Hematol.*, 17, pp. 58-62.

Zhang, Z., Jia, J., Lai, Y., Ma, Y., Weng, J. and Sun, L. (2010) 'Conjugating folic acid to gold nanoparticles through glutathione for targeting and detecting cancer cells', *Bioorganic & medicinal chemistry*, 18(15), pp. 5528-5534.

Zhao, S., Zhang, X., Zhang, J., Zhang, J., Zou, H., Liu, Y., Dong, X. and Sun, X. (2008) 'Intravenous administration of arsenic trioxide encapsulated in liposomes inhibits the growth of C6 gliomas in rat brains', *Journal of Chemotherapy*, 20(2), pp. 253-262.

Zhao, X. B. and Lee, R. J. (2004) 'Tumor-selective targeted delivery of genes and antisense oligodeoxyribonucleotides via the folate receptor', *Advanced drug delivery reviews*, 56(8), pp. 1193-1204.

Zheng, J., Deng, Y.-P., Lin, C., Fu, M., Xiao, P.-G. and Wu, M. (1999) 'Arsenic trioxide induces apoptosis of HPV16 DNA- • immortalized human cervical epithelial cells and selectively inhibits viral gene expression', *International journal of cancer*, 82(2), pp. 286-292.

Zhou, C., Boggess, J. F., Bae-Jump, V. and Gehrig, P. A. (2007) 'Induction of apoptosis and inhibition of telomerase activity by arsenic trioxide (As2O3) in endometrial carcinoma cells', *Gynecologic oncology*, 105(1), pp. 218-222.

Zhou, W., Yuan, X., Wilson, A., Yang, L., Mokotoff, M., Pitt, B. and Li, S. (2002) 'Efficient intracellular delivery of oligonucleotides formulated in folate receptor-targeted lipid vesicles', *Bioconjugate chemistry*, 13(6), pp. 1220-1225.

Zhu, J., Chen, Z., Lallemand-Breitenbach, V. r. and de ThÃ©, H. (2002) 'How acute promyelocytic leukaemia revived arsenic', *Nature Reviews Cancer*, 2(9), pp. 705.

Copies of published work